A MULTI-CHANNEL EEG MINI-CAP FOR RECORDING AUDITORY BRAINSTEM RESPONSES IN CHINCHILLAS

by

Hannah Ginsberg

A Thesis

Submitted to the Faculty of Purdue University

In Partial Fulfillment of the Requirements for the degree of

Master of Science in Biomedical Engineering

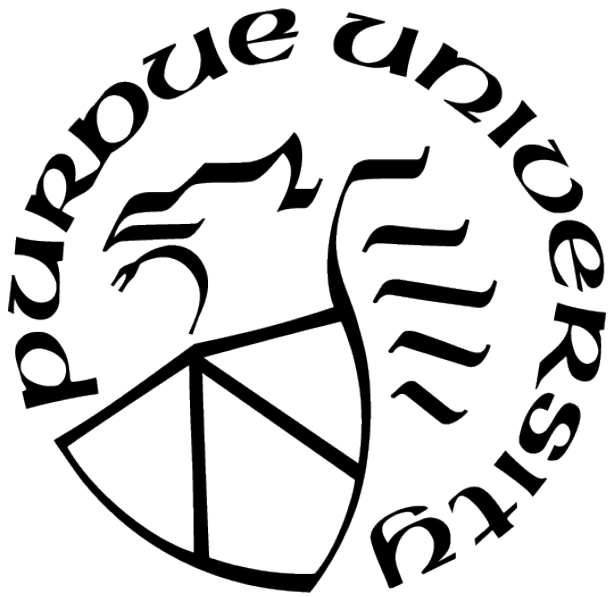

Weldon School of Biomedical Engineering

West Lafayette, Indiana

December 2020

THE PURDUE UNIVERSITY GRADUATE SCHOOL
STATEMENT OF COMMITTEE APPROVAL

Dr. Michael Heinz, Chair

Department of Speech, Language, and Hearing Sciences

Weldon School of Biomedical Engineering

Dr. Hari Bharadwaj

Department of Speech, Language, and Hearing Sciences

Weldon School of Biomedical Engineering

Dr. Jeffrey Lucas

Department of Biological Sciences

Approved by:

Dr. George R. Wodicka

To my family for their lifelong support.

ACKNOWLEDGMENTS

Thank you to Dr. Heinz for being a great advisor and mentor, for answering all of my questions, and for helping me progress and grow within lab these past three years.

Thank you to other my committee members, Dr. Bharadwaj and Dr. Lucas, for providing me with invaluable feedback throughout this process.

Thank you to the all the current and previous members of the Auditory Neurophysiology and Modeling Lab, especially Satya Parida and Caitlin Heffner for their help with this research. A special thank you to Rav Singh for helping me out with the data collection that made this thesis possible during COVID-19.

TABLE OF CONTENTS

LIST OF TABLES

LIST OF FIGURES

ABBREVIATIONS

ABR	Auditory Brainstem Response
AC	Auditory Cortex
AEP	Auditory Evoked Potential
AN	Auditory Nerve
ARHL	Age-Related Hearing Loss
BM	Basilar Membrane
CF	Characteristic Frequency
CHL	Conductive Hearing Loss
CN	Cochlear Nerve
CS	Cochlear Synaptopathy
DPOAE	Distortion Product Otoacoustic Emission
EEG	Electroencephalogram
HHL	Hidden Hearing Loss
IC	Inferior Colliculus
IHC	Inner Hair Cell
IP	Intraperitoneal
LL	Lateral Lemniscus
NIHL	Noise-Induced Hearing Loss
OAE	Otoacoustic Emission
OHC	Outer Hair Cell
SNHL	Sensorineural Hearing Loss
SOC	Superior Olivary Complex
SPL	Sound Pressure Level
SQ	Subcutaneous

ABSTRACT

According to the World Health Organization, disabling hearing loss affects nearly 466 million people worldwide. Sensorineural hearing loss (SNHL), which is characterized as damage to the inner ear (e.g., cochlear hair cells) and/or to the neural pathways connecting the inner ear and brain, accounts for 90% of all disabling hearing loss. One important clinical measure of SNHL is an auditory evoked potential called the auditory brainstem response (ABR). The ABR is a non-invasive measure of synchronous neural activity across the peripheral auditory pathway (auditory nerve to the midbrain), comprised of a series of multiple waves occurring within the first 10 milliseconds after stimulus onset. In humans, oftentimes ABRs are recorded using a high-density EEG electrode cap (e.g., with 32 channels). In our lab, a long-term goal is to establish and characterize reliable and efficient non-invasive measures of hearing loss in our pre-clinical chinchilla models of SNHL that can be directly related to human clinical measures. Thus, bridging the gap between chinchilla and human data collection by using analogous measures is imperative.

For this project, a 32-channel EEG electrode mini-cap for recording ABRs in chinchillas was studied. Firstly, the feasibility of this new method to record ABRs demonstrated. Secondly, the sources of bias and variability relevant to the mini cap were investigated. In this investigation, the ability of the mini cap to produce highly reliable, repeatable, reproducible, and valid ABRs was verified. Finally, the benefits of this new method, in comparison to our current approach using three subdermal electrodes, were characterized. It was found that ABR responses were comparable across channels both in magnitude and morphology when referenced to a tiptrode in the ipsilateral ear canal. Consequently, averaging across several channels led to a reduction in overall noise and the need for fewer repetitions (in comparison to the subdermal method) to obtain reliable response. Other methodological benefits of the mini cap included closer alignment with human ABR data collection, more efficient data collection, and capability for more in-depth data analyses, like source localization (e.g., in cortical responses). Future work will include collecting ABRs using the EEG mini-cap before and after noise exposure, as well as exploring the potential to leverage different chan-

nels to isolate brainstem and midbrain contributions to evoked responses from simultaneous recordings.

1. INTRODUCTION

1.1 Hearing loss is a global clinical problem

Hearing loss is a consequential clinical problem that affects millions of people around the world. In fact, according to the World Health Organization, approximately 466 million people worldwide experience disabling hearing loss, with children accounting for about 34 million of the total 466 million [1]. Those are the numbers as of the present day. By 2050, it is estimated that over 900 million people will have disabling hearing loss [1]. These numbers indicate that hearing loss is and will remain a healthcare problem of tremendous significance. Therefore, continued research and investigation into clinical diagnostics and assistive technology for hearing loss is imperative. In particular, clinical diagnostics are of utmost consequence because people with hearing loss benefit from early identification [1]. Therefore, this research will be focused on clinical diagnostics for hearing loss.

1.1.1 Types of hearing loss

Clinicians utilize different diagnostics to pinpoint the specific category of disabling hearing loss. There are three main categories of hearing loss: a conductive pathology, a sensorineural pathology, and a mixed pathology (i.e. a combination of both the conductive and sensorineural pathologies). If the sound is unable to transmit through the middle ear and reach the inner ear, a conductive hearing loss (CHL) will be diagnosed. If the sound is unable to transmit through the inner ear or the nerves from the ear to the brain, a sensorineural hearing loss (SNHL) will be diagnosed. SNHL is significantly more prevalent than CHL, accounting for about 90% of all cases of disabling hearing loss [2]–[4]. SNHL can be caused by a variety of risk factors, including aging, genetic mutations, noise exposure, ototoxic drug exposure, and chronic conditions [5]. The two leading causes of SNHL are aging and noise exposure. In fact, the leading cause of adult onset hearing loss is aging of the auditory system, often termed presbycusis or age-related hearing loss (ARHL) [5]. Approximately one in three people in the U.S. aged 65 to 74 have hearing loss, and above age 75, that increases to approximately one in every two people [6]. Noise exposure can result from a single exposure (e.g., a very loud sound blast) or from an extended exposure

(e.g., loud sounds over an extended period of time), resulting in damage to sensory hair cells [7]. Nearly one in four U.S. adults aged 20 to 69 have features in his or her hearing test indicative of noise-induced hearing loss (NIHL) in one or both ears [8]. Anatomically, SNHL is characterized as damage to the inner ear, more specifically to the cochlea or the neural pathways connecting the inner ear and the brain. The cochlea is the place where sound information is transformed from sound waves traveling along the basilar membrane (BM) to electrical signals sent to the brain via the auditory nerve (AN) to be processed. The normal function of certain anatomical structures within the cochlea is necessary for this process to occur adequately. Additionally, the associated anatomical structures along the ascending auditory pathway must be functioning normally.

1.2 Auditory system overview

The auditory system is comprised of three main parts and two main auditory pathways. Figure 1.1 portrays the three main parts of the ear. Each part contributes a specific, significant function that allows humans to hear a magnitude of sounds. The outer ear is composed of the pinna, the only visible part of the ear, and the auditory canal, which is the structure that transmits sound from the pinna to the eardrum. The middle ear is an air-filled, pressurized cavity between the outer ear and the inner ear containing the ossicles, a chain of the three smallest bones (i.e. malleus, incus, stapes) in the human body. The inner ear is composed of the cochlea, the auditory nerve, and the vestibular system (i.e. the balance mechanism).

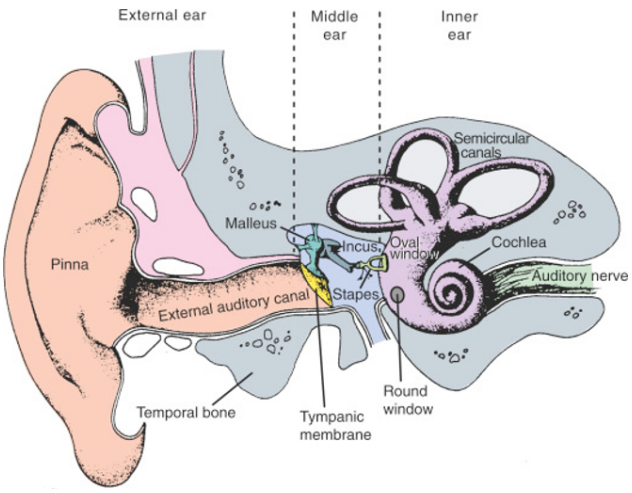

Figure 1.1. The anatomy of the human ear. The human ear consists of three main parts: the outer ear, the middle ear, and the inner ear [9].

Sound enters the outer ear as pressure waves. The eardrum (i.e. tympanic membrane) moves when sound hits it and these vibrations are sent into the middle ear where they are amplified via the ossicles and transferred to the oval window of the inner ear. The cochlea is a spiral-shaped, fluid-filled cavity that receives sound information in the form of mechanical vibrations from the middle ear (i.e. the oval window) and transforms these vibrations into neural signals sent via the auditory nerve to the brain. Figure 1.2 portrays the organ of Corti, the receptor organ located within the cochlea that allows for this auditory signal transduction. Both supporting cells and mechanosensory hair cells are embedded along the organ of Corti [10]. Related to this research, the mechanosensory hair cells that exist inside the organ of Corti are of utmost significance to SNHL. Respectively, a single row of inner hair cells (IHCs) and three rows of outer hair cells (OHCs) are separated by supporting cells along the organ of Corti [10]. Inside the cochlea, vibrations will transform into a traveling wave along the BM. At a certain place on the BM that is tuned to the characteristic frequency (CF) of the sound, these sensory hair cells will move back and forth, causing stereocilia deflection (i.e. bending). As stereocilia bend, the tips of the stereocilia open up, which causes chemicals to rush into the hair cell. As chemicals rush into the cell, the cell depolarizes, and this ultimately creates an electrical signal (i.e. an action potential) that is sent via the auditory nerve to the brain.

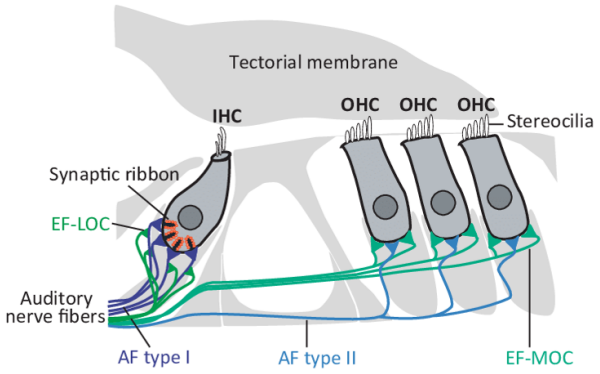

Figure 1.2. The anatomy of the human inner ear. An important structure in the inner ear, called the cochlea, contains two types of sensory cells: outer hair cells and inner hair cells. Inner hair cells encode sound information and send this information to directly innervated auditory nerve fibers [11].

1.2.1 The ascending auditory pathway

The auditory system is comprised of the peripheral auditory system and the central auditory system that together form the ascending auditory pathway. Figure 1.3 portrays the stages associated with the ascending auditory pathway. Auditory processing occurs in a series of analysis stages, beginning with the peripheral mechanisms that encode sounds and moving toward the central mechanisms in which sound processing, perception, and object recognition occur [12].

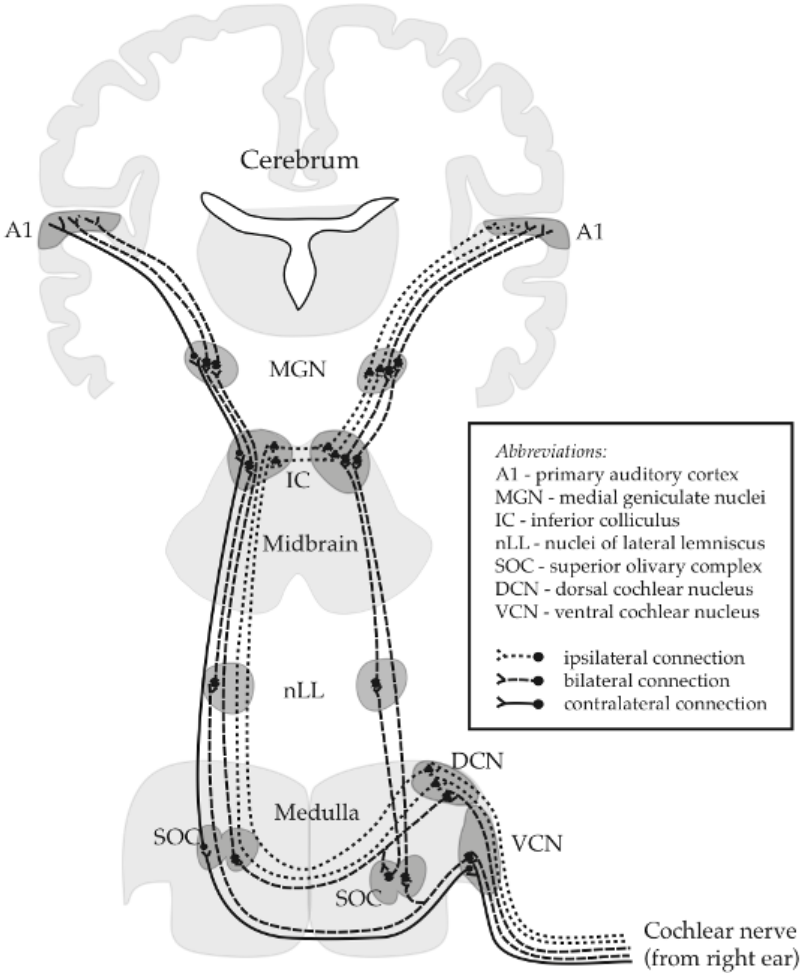

Figure 1.3. The ascending auditory pathway. This pathway begins at the auditory nerve and then travels through the brainstem and midbrain to reach the auditory cortex [13].

More specifically, IHCs act as mechanosensory transducers and convert mechanical energy into synaptic currents that will then drive the primary auditory neurons (i.e. ANFs) that synapse at their base [14]. These primary auditory afferent neurons that synapse with IHCs will respond to the glutamate released at the synapse by initiating and conducting an action potential to the cochlear nucleus [14]. Sound frequency, loudness, and temporal information are all encoded within these action potentials [14].

After the sound is encoded within the periphery, the auditory information is sent to the central auditory nuclei through the auditory nerve (AN) [15]. After the AN, the auditory information will travel up a series of nuclei towards the auditory cortex (AC), the place where auditory perception occurs [15]. The AN synapses with the cochlear nucleus (CN). From there, crossing fibers transmit the auditory information to the superior olivary complex (SOC). After the SOC, the auditory information will continue to ascend contralaterally and ipsilaterally towards the AC, crossing through the lateral lemniscus (LL) and the inferior colliculus (IC) of the midbrain. Finally, the auditory information will travel through the medial geniculate nucleus (MGN) to reach the centrally located AC. Altogether, each stage of this auditory pathway must be adequately functioning in order for the sound information to both effectively reach and be processed by the brain.

1.3 Chinchilla animal model

Animal models allow researchers to investigate what cannot be ethically investigated in humans, with the goal of converting each observation to progressing human knowledge. In humans, oftentimes behavioral and physiological measures can be performed, whereas anatomical measures are not possible. Consequently, in animals, anatomical measures can be performed and then directly related to human advancements. This is the indisputable advantage of utilizing an animal model in hearing research. In this research, chinchillas will be utilized as an animal model for noise-induced hearing loss.

Historically, chinchillas have been commonly used as an animal model for noise-induced hearing loss. In fact, the chinchilla animal model for NIHL has an been used in research for more than 50 years [16]. The chinchilla possesses behavioral, anatomical, and physiological characteristics that make it a favorable animal model for NIHL. As shown in Figure 1.4,

the chinchilla's hearing sensitivity and frequency range significantly overlap with humans [16]. Thus, unlike other rodent models (e.g., mice and rats), chinchillas are a particularly good rodent model to study perceptually relevant stimuli [16]. Besides the similar hearing sensitivity and frequency range, chinchillas share anatomical commonalities with humans as well, including a similar number of cochlear turns, a similar cochlear length, and a wide tympanic membrane [16]. Finally, previous research in chinchillas has established robust techniques to mimic the various types of hearing loss pathologies (e.g., CHL, NIHL, and ARHL) observed in humans [16]. For example, the anatomical, physiological, and behavioral effects of the two types of noise exposure (e.g., single loud blast or extended exposure) have been thoroughly investigated in chinchillas [16].

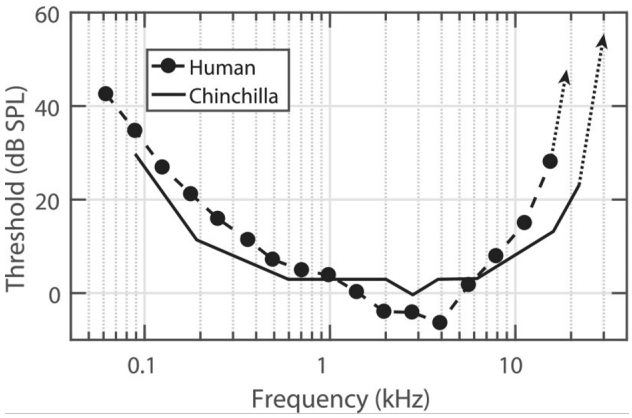

Figure 1.4. Chinchillas have similar hearing sensitivity to humans. Both the hearing sensitivity and frequency range of chinchillas significantly overlap with humans [16].

1.4 Cochlear synaptopathy

1.4.1 Audiograms provide limited information

In a noisy environment, a person with NIHL may find it difficult to understand speech. If a hearing loss is suspected, clinical audiometry is performed by an audiologist [17]. Pure-tone audiometry is a measure of how well a person is able to hear sounds at different pitches (i.e. frequency, Hertz) and volumes (i.e. intensity, decibels) [17]. During a behavioral audiogram, the minimum sound level (i.e. intensity) at which a person can hear a sound

at a range of frequencies is determined. The results of the audiogram indicate whether a patient has hearing loss and, if so, the associated severity of it (e.g., mild, moderate, severe, etc.). For example, a person with NIHL may show an elevated threshold at a few selected high frequencies (e.g., 3, 4, and 6 kHz) but show normal thresholds at all other frequencies tested. This may appear on the resulting audiogram as an audiometric notch (i.e. dip) at those few selected high frequencies. Previous studies have used audiometric notches as evidence suggesting the existence of NIHL in humans [8]. These audiometric notches can affect a person's ability to hear and consequentially understand high-pitched soft speech sounds that correspond with the notch frequencies [8].

1.4.2 The cocktail party problem

The cocktail party problem is the phenomenon concerning when a person frequently struggles understanding speech in a noisy environment in which there are multiple sound sources [18]–[20]. The essence of the cocktail party problem was encapsulated by the seemingly straightforward question: "How do we recognize what one person is saying when others are speaking at the same time?" [18]. Investigating this phenomenon has been a core goal within the hearing research field for several decades [18], [20]. Previous studies have indicated that cochlear synaptopathy could potentially be related to the cocktail party problem [21].

1.4.3 Anatomy of cochlear synaptopathy

Cochlear synaptopathy (CS) is defined as the loss of nerve connections (i.e. synapses) between the sensory inner hair cells and the auditory nerve fibers that launch the transmission of sound information up the ascending auditory pathway towards the brain. This pathology is more covert, and notably more insidious, than the typical overt NIHL pathology involving the evident damage of sensory hair cells after noise-exposure [22]. When these synapses become damaged, they are in-effect silencing the auditory nerve fibers that are responsible for transmitting sound information to the brain. Since the first stage of the pathway for transmitting sound information to the brain is effectively damaged, it makes sense that

this neural silencing alters auditory information processing [22]. Anatomically, however, the inner sensory cells are not damaged, and thus, this pathology does not appear as the normal threshold elevation in clinical audiograms. In fact, this cochlear synaptopathy pathology can be widespread in ears with intact hair cell populations and normal behavioral audiograms [22]. It has been shown that behavior detection thresholds for tones are minimally changed until neural loss exceeds about 80-90% [23]. Therefore, this pathology is often entirely hidden on the behavioral audiogram, hence the term "hidden hearing loss" (HHL) is often used interchangeably [24]. The auditory profile of cochlear synaptopathy, characterized by suprathreshold deficits in the presence of audiometrically normal hearing, has long been recognized and continues to be thoroughly investigated in the hearing science field [25].

1.4.4 Previous models of cochlear synaptopathy

Cochlear synaptopathy has been thoroughly investigated in both animal models and in humans. In multiple mammalian species, anatomical verification has been obtained, showing that before overt hearing loss (i.e. damage to sensory cells) can be resolved in an audiogram, there is a more insidious and likely more prevalent process taking place that involves synaptic damage between IHCs and a subset of cochlear nerve fibers [22]. In a mouse model, noise exposure that caused a temporary threshold shift produced a rapid loss of as many as 40-60% of the ANF synapses within 24 hours post-exposure, causing irreversible degeneration of these ANFs [21], [26]. Figure 1.5 displays this rapid loss of synaptic ribbons.

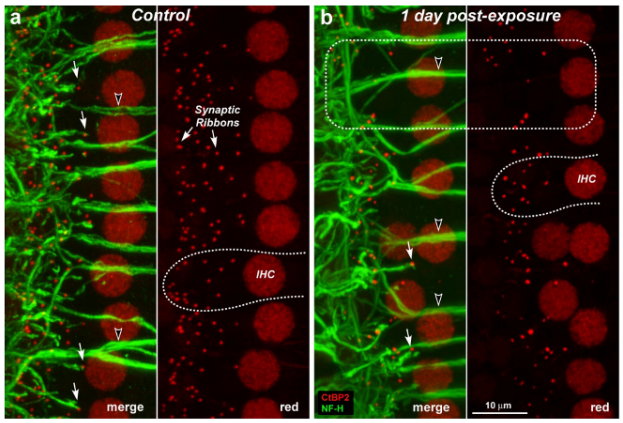

Figure 1.5. Anatomical depiction of cochlear synaptopathy. Noise exposure that produces a temporary threshold shift (TTS) and does not damage the sensory hair cells can produce a rapid loss of as many as 40-60% of the ANF synapses (i.e. synaptic ribbons) within 24h post-exposure [26]. However, after a TTS noise exposure, hair cells mantain normal function and the effect on cochlear function is negligible.

A temporary threshold shift (TTS) is defined as a sound exposure to an intense sound that generates acute changes in hearing sensitivity that recover over time, whereas, for a permanent threshold shift (PTS), hearing sensitivity does not recover to pre-exposure levels and remains over time [27]. Besides the rapid synaptic damage after a noise exposure causing a reversible threshold elevation, there is also an irreversible yet delayed and more progressive loss of cochlear neurons (i.e. spiral ganglion cells) after noise exposure, lasting from a few months to a few years [21], [28]. In a mouse model, it has been shown that high-threshold ANFs with lower spontaneous rates are, in fact, preferentially damaged, suggesting that the ability to process suprathreshold sounds could be significantly affected [29], [30]. Besides the mouse model, the cochlear synaptopathy pathology has been anatomically validated in guinea pigs [28], primates [31], and chinchillas [32], [33].

Additionally, neuronal counts conducted on post-mortem human temporal bones suggest that despite a near-normal hair cell population, cochlear synaptopathy and the degeneration of cochlear nerve peripheral axons may be a significant feature of presbycusis [34]. In humans, a growing number of studies suggest that cochlear synaptopathy causes hearing problems despite normal cochlear function. In particular, it has been shown that patients with a

normal audiogram differ in their ability to use fine temporal cues [25], [35] and spatial selection attention [36]–[38], both possibly indicative of potential consequences of cochlear synaptopathy in humans.

1.5 Auditory brainstem responses

We currently have no recognized clinical diagnostic measure of cochlear synaptopathy in humans. Thus, the overarching goal of this research, and of many others in the hearing science field, is to investigate and explore various biomarkers that have the potential to become clinical measures of cochlear synaptopathy in humans. Relevant to this research, features of the auditory brainstem response (ABR) will be studied as a possible biomarker of cochlear synaptopathy. The ABR is an auditory evoked potential originating from electrical activity in the ascending auditory pathway in response to a stimulus. The ABR is used in clinic as a measure of auditory sensitivity. Another measure used in this research to evaluate auditory sensitivity is the distortion-product otoacoustic emission (DPOAE). DPOAEs occur when two tones having different frequencies (f1 and f2) and different intensity (i.e. loudness) levels are introduced into the ear simultaneously and an emission response, known as the cubic distortion product (2*f1-f2), is recorded from the ear canal. In this research and in many clinical settings, DPOAEs are measured to assess OHC function. Since CS particularly involves IHCs, ANFs, and the synaptic connections between them, DPOAEs act as a control measure in order to ensure normal OHC function. DPOAEs provide information related to the peripheral auditory system only. This is in contrast to ABRs, which provide information related to the entire ascending auditory pathway.

The ABR is an auditory evoked potential extracted from electrical activity in the brain recorded via electrodes placed on the scalp [39]. The far-field recording consists of a series of five to six vertex-positive peaks within 10 milliseconds of stimulus onset [40]. Each wave corresponds to the neuronal activity of a distinct structure within the ascending auditory pathway. Figure 1.6 portrays the alignment of ABR waveform morphology and each corresponding structure in the ascending auditory pathway. Wave-I is generated in the proximal part of the auditory nerve whereas wave-II is generated in the cochlear nucleus. Wave-III is initiated in the superior olivary complex (SOC) of the lower brainstem. Finally, wave-IV

and wave-V are generated within the upper brainstem, in the lateral lemniscus (LL) and inferior colliculus (IC) respectively.

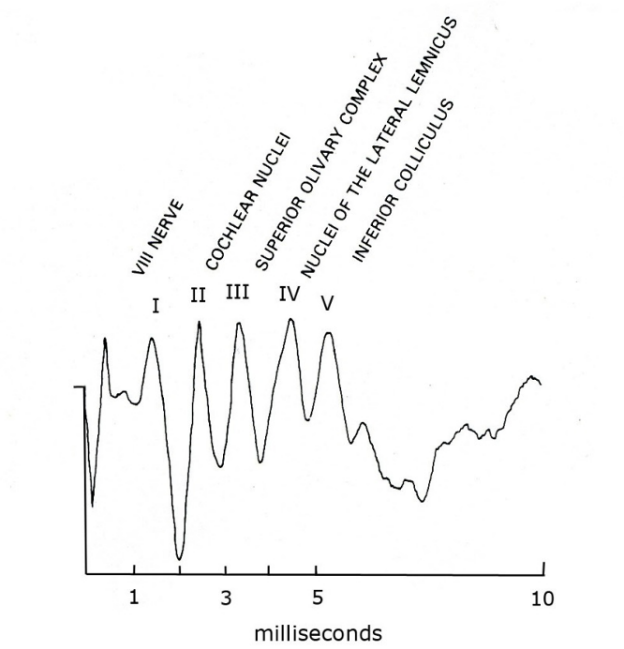

Figure 1.6. The corresponding brain structure to each wave of the auditory brainstem response (ABR). The ABR is an auditory evoked potential originating from different anatomical sources along the ascending auditory pathway. Wave-I corresponds to the auditory nerve, wave-II corresponds to the cochlear nucleus, wave-III corresponds to the superior olivary complex, wave-IV corresponds to the lateral lemniscus, and finally wave-V corresponds to the inferior colliculus [41].

1.5.1 ABRs in clinic

Clinically, ABRs are utilized as an assessment of hearing function. As mentioned, clinical audiometry is routinely performed by an audiologist if a hearing loss is suspected. However, since audiometry is a behavioral hearing assessment, it requires that the patient be cognizant and attentive. For most scenarios, these prerequisites are satisfied. However, it can be very difficult to conduct a behavioral hearing assessment on infants, patients with complicated medical conditions, and patients who are unable to cooperate for the test [42].

ABRs, therefore, have a wide range of clinical applications, including intraoperative monitoring, retro cochlear pathology screening, and newborn hearing screening [43]. For example, physicians may ask for an assessment of hearing function during a surgery when the patient is under general anesthesia [42]. Additionally, studies have shown that the ABR test is a reliable and objective method to estimate an infant's hearing sensitivity [44]–[48]. Therefore, in these cases, ABR tests are frequently performed to estimate hearing thresholds. Accordingly, ABRs are commonly used as a clinical assessment to detect hearing loss.

1.5.2 ABR clinical electrode configuration

The typical clinical electrode configuration for humans is a 1-channel ABR that utilizes three electrodes: an active electrode (i.e. Cz) placed on the high forehead, a ground electrode placed on earlobe of the contralateral ear, and a reference electrode placed on the earlobe of the ipsilateral ear [49]. If the microphone is in the right ear, the reference electrode will be placed on the right ear and the ground electrode will be placed on the left ear. Another configuration useful for when sound needs to be played interchangeably between both ears incorporates four electrodes and is called the 2-channel ABR. In this configuration, the ground electrode is placed on the low forehead, the active scalp electrode is placed similarly on the high forehead, and two reference electrodes are placed on each earlobe [49]. This configuration makes it simpler to switch between ears during data collection. Figure 1.7 portrays both of these configurations: the 3-electrode, 1-channel configuration and the 4-electrode, 2-channel configuration.

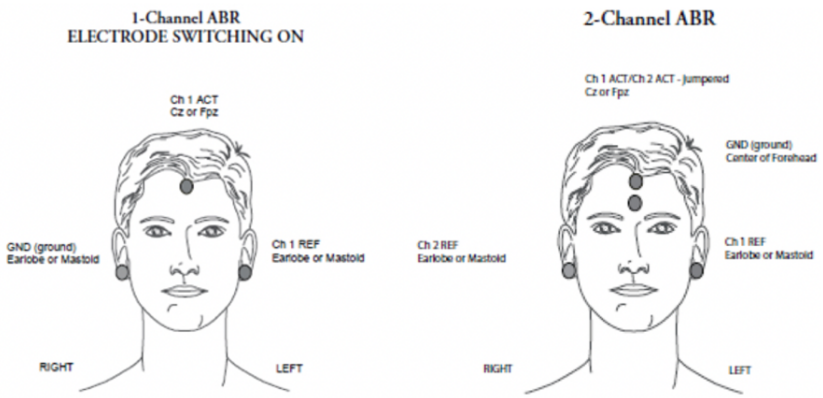

Figure 1.7. Two typical electrode configurations for human ABR data collection in clinic [49]. The 1-channel configuration utilizes one reference electrode placed on the earlobe of the ipsilateral ear. The 2-channel configuration utilizes two reference electrodes, one placed on each earlobe, making it more simple to switch between collecting responses from both ears.

1.5.3 ABR thresholds to evaluate hearing function

To evaluate hearing function in clinic, often an ABR threshold will be determined. The value of the ABR threshold provides direct insight into the hearing function of the patient. For all stimuli, ABR threshold is defined as the lowest level at which a response was observed [50]. Often, an intensity series (i.e. "waterfall") will be collected for a certain frequency (i.e. click or tone burst). This intensity series involves collecting an ABR response at multiple levels based on descending increments from a high level (e.g., 90 dBSPL) down to a low level (e.g., 10 dBSPL). Figure 1.8 portrays an ABR waterfall in which responses are collected in 10-dBSPL increments from 10 dBSPL to 90 dBSPL. A previous study showed that tone evoked ABR thresholds for normal hearing patients are typically 10 to 20 dB nHL, equating to about 5 to 15 dB higher than pure-tone audiometry [51].

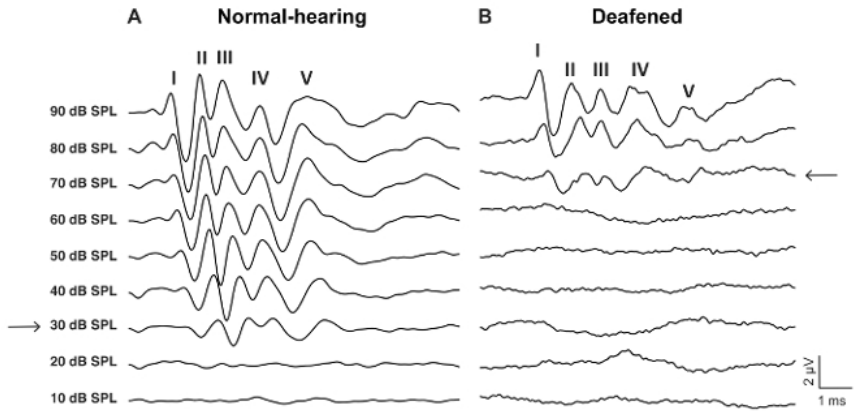

Figure 1.8. A typical ABR waterfall collected [52]. For an ABR waterfall, an ABR response at several sound pressure levels is collected. Threshold is then defined as the minimum sound pressure level at which there is an observable ABR response. For the deafened, hearing loss waterfall, threshold is higher than for the normal hearing waterfall.

1.5.4 ABRs in research

Since the ABR provides tremendous insight into the ascending auditory pathway, it is an advantageous measure used commonly in the diagnosis and localization of pathologies affecting these pathways to the brain [53]. ABR thresholds are frequently used in research as well. In fact, the ABR is one of the most widely used auditory evoked potentials for determining thresholds [54]. Besides the benefit of hearing loss diagnosis, ABR thresholds are suitable as a CS biomarker. A temporary increase in threshold after a TTS noise exposure correlates to IHC damage and loss of ANF fibers, both indicators of CS. Since each ABR wave characterizes a certain stage of the ascending auditory pathway, studying the waveform morphology before and after noise exposure can be valuable. Each wave amplitude provides insight into the number of neurons firing at the wave's anatomical source, and each wave latency provides insight into the speed of transmission along the auditory pathway relevant to the wave's anatomical source. Therefore, differences in wave amplitudes and latencies directly characterize the effects of noise exposure at different stages along the ascending auditory pathway.

ABRs are collected regularly in both animal and human auditory research. In animals, wave-I can be robustly and reliably measured. A previous study in a mouse model demonstrated that as a consequence of the rapid synaptic loss after a TTS noise exposure, there was a permanent amplitude reduction of ABR wave-I [26]. In chinchillas, noise exposure resulted in a decrease in both wave-I amplitude and wave-I latency, correlated with a decrease in ANF frequency selectivity [55]. However, wave-I can be difficult to measure in humans, limiting its clinical use [56]. In humans, wave-V is significantly more pronounced than wave-I [56]. In fact, wave-V latency has been shown to robustly predict perceptual temporal sensitivity at low stimulus levels and in background noise, suggesting it could be used to clinically diagnose CS in humans [56]. Besides wave-I amplitude and wave-V latency, an additional CS metric is the wave-V/wave-I amplitude ratio [57]. In one study, tinnitus patients with normal audiograms showed an enhanced wave-V/wave-I ratio [24]. The wave-V/wave-I ratio might be able to differentiate the deficits originating from OHC dysfunction from CS in listeners with a mixed hearing loss [57].

1.6 The human EEG electrode cap to record ABRs

Oftentimes a high-density electroencephalogram (EEG) electrode cap system is utilized in human ABR data collection [56]. Neuroscientists routinely use EEG to record event related potentials (e.g., ABRs) and investigate the underlying neural processes [58]. The benefits of using an EEG system include its high level of temporal precision, affordability, and ease of maintenance, all of which are significant both for research and clinical purposes [58], [59]. In humans, the cap is commonly arranged on the patient's head in accordance to the 10-20 system. The 10-20 system is an internationally recognized system that describes the location of electrodes placed directly on the scalp based on the human head anatomy [60]. This standardized system is based on the relationship between the location of each electrode and the underlying area of the cerebral cortex [60]. Contrastingly, in animal models, ABRs are typically recorded using subdermal needle electrodes placed in distinct locations subdermally under the skin. Commonly, one subdermal electrode will be placed near the skull vertex in addition to two other electrodes: the reference and ground subdermal needle electrodes. In rodent models, the reference and ground subdermal electrodes are typically

placed ventrolaterally to the right and left external pinna [26], [61]. In chinchillas, the vertex electrode (non inverting) is placed subdermally between the bullae at the dorsal midline, the reference electrode (inverting) is placed posterior to the right pinna, and the ground electrode (common ground) is placed at the bridge of the nose [55]. Since the objective of using an animal model is to have a high degree of valid extrapolation to humans, there is a need to align methods when possible between animals and humans in order to promote this extrapolation [62].

1.7 The small animal EEG mini cap to record ABRs

The EEG mini cap allows for non-invasive multi-channel EEG scalp recordings in small animals. The use of highly dense arrays of EEG electrodes on the human scalp is well-accepted and of common practice. Previous research has suggested that high-quality EEG recordings in animal species (e.g., mice and rats) is not possible due to the signal generated by the underlying cortex being too weak [63]. In small animals, there are a limited number of synchronized pyramidal neurons and the potential for a high level of noise due to the contamination of electrocardiogram artifacts [63]. Therefore, in animals, high-quality EEG scalp recordings is a relatively more recent technological development. This mini cap was initially described and developed to simultaneously record EEG and fMRI [64]. Initially, this MRI-compatible high-density electrode cap was designed to simultaneously record somatosensory event-related potential EEG responses and fMRI in response to forepaw stimulation in Wistar rats [64]. Prior to this mini cap, only simultaneous recordings of epicranial EEG from a multi-channel electrode array distributed across a mouse's head was described [65]. For epicranial EEG recordings, the electrode array directly contacts the surface of the animal's skull [65]. Thus, this is often an invasive procedure and involves retracting the animal's skin overlying the skull [65]. This mini cap is a significant technological breakthrough since it allows for non-invasive scalp EEG recordings that can be directly compared to non-invasive scalp EEG recordings in humans. This mini cap resolves two considerable problems of multi-channel EEG scalp recordings in small animals: the size of the animal's head and the relative distance between electrodes and brain tissues [64]. This research applies this mini cap to record auditory evoked potentials in chinchillas. A visualization of a 64-channel human EEG

high-density electrode cap in comparison to the 32-channel small animal EEG mini cap used in this research is shown in Figure 1.9.

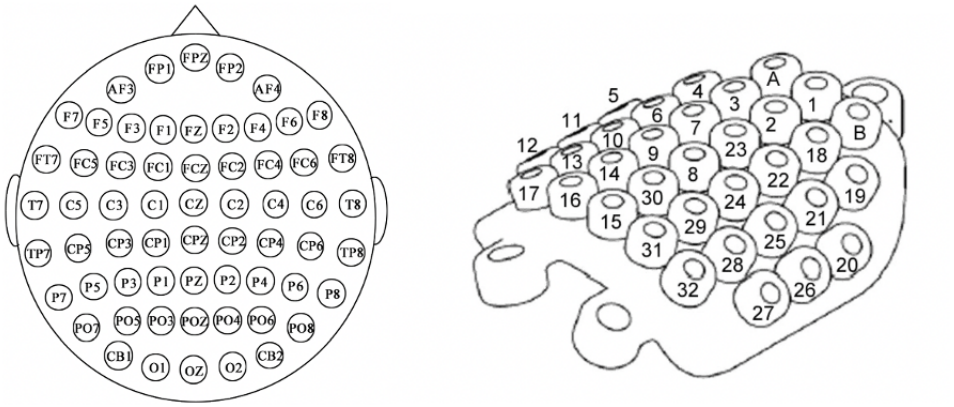

Figure 1.9. Left: A human EEG cap. Right: The small-animal EEG mini cap. A human EEG cap can consist of 32, 64 (shown, left), 128, or 256 channels. The small-animal EEG mini cap used in this research (shown, right) consists of 32 channels.

1.8 Overview of thesis research

In this research, we will advance the ABR measures in our chinchilla animal model to thoroughly align our ABR methods with those clinically performed in humans. With this alignment in methods, we expect enhanced resemblance for direct comparisons between chinchilla and human data, conceivably resulting in research advancements in our chinchilla animal model that can be prominently applied clinically to humans.

1.8.1 Research questions

In this study, a 32-channel EEG mini cap will be implemented for recording ABRs in chinchillas. A three-step methodology will be executed to evaluate the EEG mini cap as an acceptable method to measure auditory event related potentials in chinchillas. Initially, the feasibility of the EEG mini-cap and its capability to adequately record scalp ABR responses in chinchillas will be investigated. Subsequently, the reliability, repeatability, reproducibility,

and validity of this new EEG mini cap method, in comparison to the established subdermal needle electrode method, will be studied. By quantifying the reliability, repeatability, reproducibility, and validity of the mini cap, the variability inherent to the mini cap method can be directly compared to the variability inherent to the subdermal needle method. Finally, the methodological benefits of collecting ABRs using the EEG mini cap will be clearly characterized and compared to the subdermal needle method.

2. METHODS

2.1 Data collection

Five adult male chinchillas weighing between 400 to 700 g were used, two for the initial feasibility study and three for the detailed test/retest study. All experiments were conducted in an electrically shielded, double-walled sound-attenuating chamber (Industrial Acoustics Company, Bronx, NY, USA). Anesthesia was induced with xylazine (2-3 mg/kg SQ) followed by ketamine (30-40 mg/kg SQ). Once the animal descended deeper under anesthesia, the animal was placed in a stereotaxic device on a regulated heating pad, eye ointment was applied, a rectal probe was inserted to monitor body temperature, and a PulseOx sensor was attached to the animal's hind paw to monitor both oxygen and heart rate. To reverse the sedative effects of xylazine, atipamezole (0.4-0.5 mg/kg IP) was utilized. Lactated Ringers solution was provided to the animal (6 cc, SQ) at the beginning and end of the experiment to stimulate recovery. All procedures were approved by the Purdue Animal Care and Use Committee. A detailed procedure for the data collection procedure used in this research is included in *Appendix B*.

2.1.1 Stimulus creation

For all experiments, the stimulus was presented into the right ear of the animal. Acoustic stimuli were created using custom Matlab software to control Tucker-Davis-Technology (TDT) System 3 hardware (i.e. RP2 Real-Time Processor). At the start of each experiment, the stimulus level was calibrated using a probe tube microphone (ER 10B+ Low Noise Mic System, Etymotic Research, Elk Grove Village, IL, USA) inserted into the ipsilateral ear canal along with two transducers (ER-2 earphones, Etymotic Research, Elk Grove Village, IL, USA). For the initial feasibility study, both click and tone burst stimuli (e.g., 4kHz) were utilized. For the detailed test/retest study, only 4 kHz tone bursts were utilized. Acoustic bursts consisted of a 5 millisecond (ms) duration with 0.5 ms linear onset and offset ramps, equating to 20 repetitions per second. Overall, for each condition (i.e. a single frequency/level combination), 1000 repetitions were collected, 500 repetitions of positive polarity and 500 repetitions of negative polarity. All repetitions were averaged together

to generate the single ABR response. For each ABR stimulus frequency, 10 dBSPL increments between 0 dBSPL and 80 dBSPL were first collected. Additional 5 dBSPL increments were recorded if deemed necessary to better characterize threshold. The ABR threshold was visually estimated as the lowest SPL at which a response was identified (see Figure 1.8).

2.1.2 Subdermal method for electrophysiology

For previous data collection and initial experiments in this study using subdermal needle electrodes, ADC data acquisition was completed using custom Matlab software controlling Tucker-Davis Technology (TDT) System 3 hardware. Responses were recorded using the same probe tube microphone and transducers used for calibration. As shown in Figure 2.1, needle electrodes were inserted sub dermally at the dorsal midline between the bullae (vertex), underneath the ear (mastoid), and the bridge of the nose (common ground) [55]. Prior to collecting data, adequate placement of the three subdermal electrodes was ensured by reviewing the ABR waveform morphology. If the response seemed distorted, all three needle electrodes would be removed and replaced since, using the subdermal methodology, there is no technique in place to determine which of the three needles was causing the distortion. The recorded responses from the three subdermal electrodes were amplified 20,000 times and band-pass filtered from 0.3 to 3kHz (World Precision Instruments model ISO-80, Sarasota, FL, USA; Stanford Research Systems model SR560, Sunnyvale, CA, USA), and then each response was digitally sampled at 12.207 kHz (TDT model RX8 Multi I/O Processor, Alachua, FL, USA). All trials were saved as processed, filtered responses respectively.

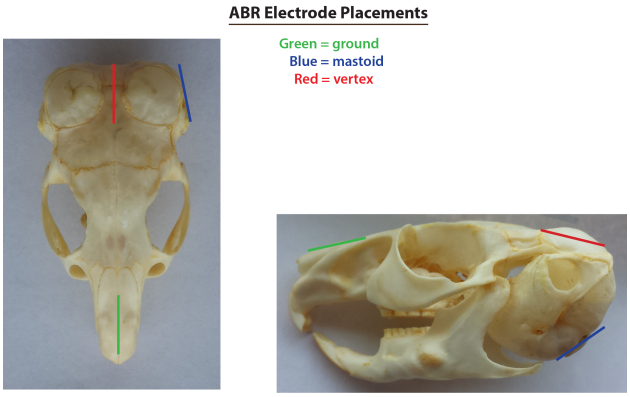

Figure 2.1. Placement of three subdermal needle electrodes. The vertex needle electrode is placed sub dermally at the dorsal midline between the bullae, the mastoid needle electrode is placed underneath the ear, and the ground needle electrode is placed on the bridge of the nose.

2.1.3 EEG mini cap for electrophysiology

For data collection using the EEG mini cap, an EEG signal for each active electrode was acquired using a high-resolution biopotential measurement system (Biosemi Active II system, Amsterdam, Netherlands). Overall, thirty-two active Ag/AgCl electrodes were included with 10 mm spacing between each. Figure 2.2 portrays the schematic diagram of each electrode. Firstly, each electrode contained an inner tube containing a silver wire and conductive EEG paste that could be moved perpendicularly to the head to ensure effective scalp contact. This movement allowed for greater flexibility between head anatomy since the horizontal position of the electrode could be customized to align with the head size and shape of each animal. Secondly, each electrode also contained an external sliding tube fixed to the plastic basement of the mini cap.

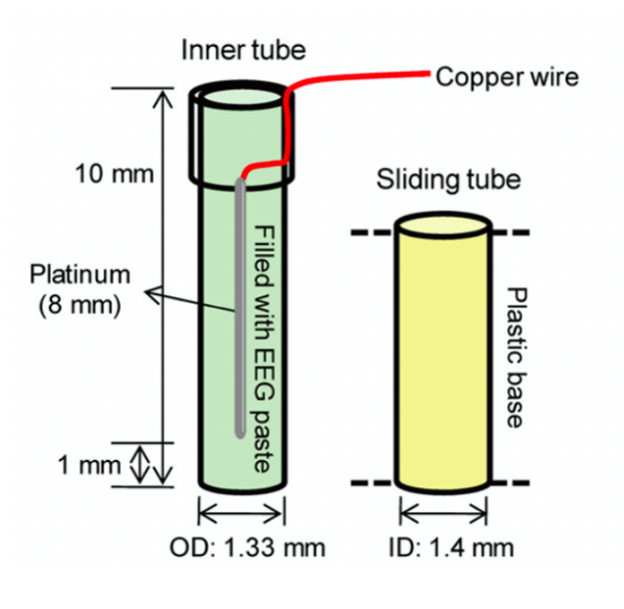

Figure 2.2. Schematic of inner tube and sliding tube for each channel of mini cap [64]. The electrode paste is filled into the inner tube, which moves perpendicularly within the sliding tube to ensure effective scalp contact.

Prior to the experiment, conductive electrode paste (2:1 v/v dilution, Elefix paste and saline) was inserted into each channel, filling from the bottom to ensure no air bubbles. Afterwards, the animal was prepared before placing the mini cap on the head. The tympanic bullae were located on the chinchilla's head and then the mini cap was placed in front of the two bullae. Figure 2.3 illustrates the relative location where the mini cap was placed in relation to the chinchilla skull.

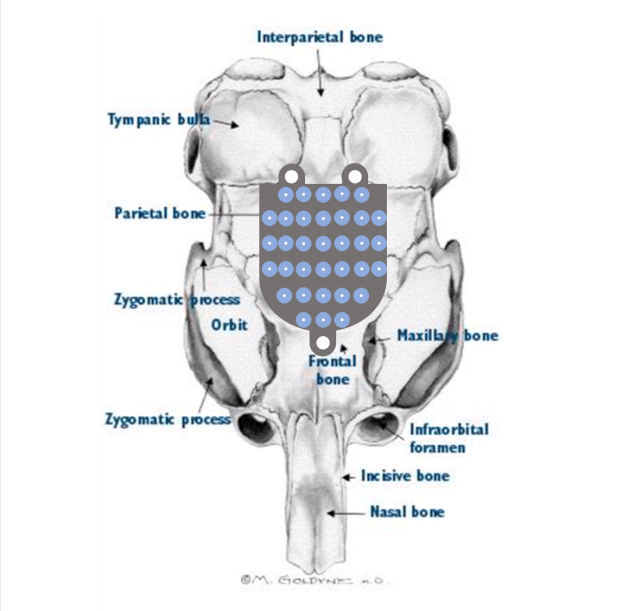

Figure 2.3. Mini cap placement on the chinchilla skull, adapted from [66]. The two bullae were located on the scalp and the mini cap was placed closely in front of the two bullae.

This scalp location was first shaved with an electronic razor and then Nair Hair Removal lotion was placed on the scalp to ensure a clean area. Following this, the area was wiped with isopropyl alcohol to remove any excess debris and to stimulate the blood vessels. Finally, a saline soaked cloth was placed over the exposed scalp until the mini cap was ready to be placed. A customized device was designed and built to more effectively secure the mini cap to the head, utilizing a flexible elastic band that was positioned to hold the cap securely once it was placed onto the exposed scalp. Figure 2.4 displays the final experimental setup in which the mini cap is securely positioned onto the exposed scalp using the customized device.

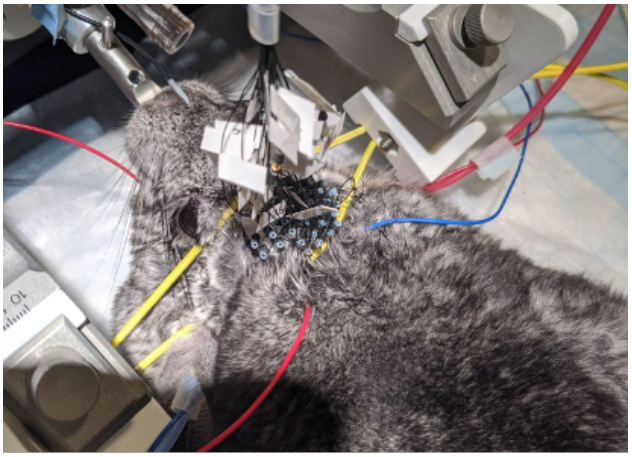

Figure 2.4. Final experimental setup of EEG mini cap data collection. A gold-foiled tiptrode (not pictured) is placed into each ear canal for referencing purposes. Three subdermal needle electrodes (see black, blue, and red subdermal electrodes) are also placed in order to simultaneously record subdermal ABR responses. The elastic band (see yellow band) holds the mini cap in place and only is placed above, not around, the chinchilla head.

2.1.4 External channels

Besides the recording of each active electrode, the biopotential measurement system allows for recording of up to eight external (i.e. "EXG") channels. In this experimental design, five external channels were utilized (see Table 2.1). EXG1 and EXG2 were two 10mm gold-foiled tiptrodes placed into the ear canal of both the ipsilateral and contralateral ear. Two key benefits arise from using gold-foiled tiptrodes. First, sound is played via the tiptrode inside the ipsilateral ear instead of the microphone. At the same time, the electrophysiological response from both ears was recorded via the measurement system. These tiptrode responses from both ears can act as the reference channel depending on which ear the stimulus is played into. Likewise, the convenience of these external channels allows for simultaneous subdermal recordings using the three subdermal needle electrodes mentioned in the subdermal approach. Thus, both mini cap and subdermal ABR responses can be collected at the same time using this setup. This increased efficiency of concurrent mini cap and subdermal recordings is one significant methodical benefit of using the EEG mini cap. The mini cap is placed onto the exposed scalp after placing the two gold-foiled tiptrodes and the three subdermal needle electrodes.

Table 2.1. External Channels.

External Channel	Experimental Correlate
EXG1	Right ipsilateral gold-foiled tiptrode
EXG2	Left contralateral gold-foiled tiptrode
EXG3	Mastoid subdermal needle electrode
EXG4	Vertex subdermal needle electrode
EXG5	Ground subdermal needle electrode

2.1.5 Data acquisition

Data were acquired from each channel (i.e. 32 active electrodes, 5 EXG channels) using Actiview software (Biosemi, Amsterdam, Netherlands), digitally sampled at 16.384 kHz. In the Biosemi system, two active electrodes replace the typical ground electrodes used by other EEG amplifiers [67]. The Common Mode Sense (CMS) active electrode acted as the recording reference whereas the Driven Right Leg (DRL) active electrode served as ground [68], [69]. These two active electrodes formed a feedback loop that drove the average potential of the subject (i.e. common mode voltage) close to the reference voltage. This feedback loop provides an additional benefit of reducing the common-mode powerline 50 Hz noise across channel inputs.

Adequate placement of the cap was ensured by reviewing channel offset values and channel signal quality. A solid blue CM in Range LED on the Biosemi box indicates whether the CMS/DRL electrodes are adequately connected to the subject and whether any fault conditions are detected. Electrode offsets were maintained at ±40 milliVolts. An electrode offset represents the quality of the electrode connection between each electrode and the scalp. If a few or more electrodes appeared noisy, they would be adjusted to ensure proper scalp contact and/or additional paste would be inserted into the channel. If a channel still had a high offset, it would be recorded and accounted for in post processing. Signal quality is inspected and if a noisy channel remained noisy, often appearing as evident powerline 50 Hz noise, it was similarly recorded and accounted for in post processing. Figure 2.5 portrays a visualization of data collection from a mini cap experiment: a screen to view signal quality of each channel, a screen to view EXG signal quality, a screen to view offsets of all channels, and finally a screen to view the ABR response. Throughout the experiment, offsets and

signal quality were consistently monitored. After the experiment, the mini cap was cleaned using saltwater.

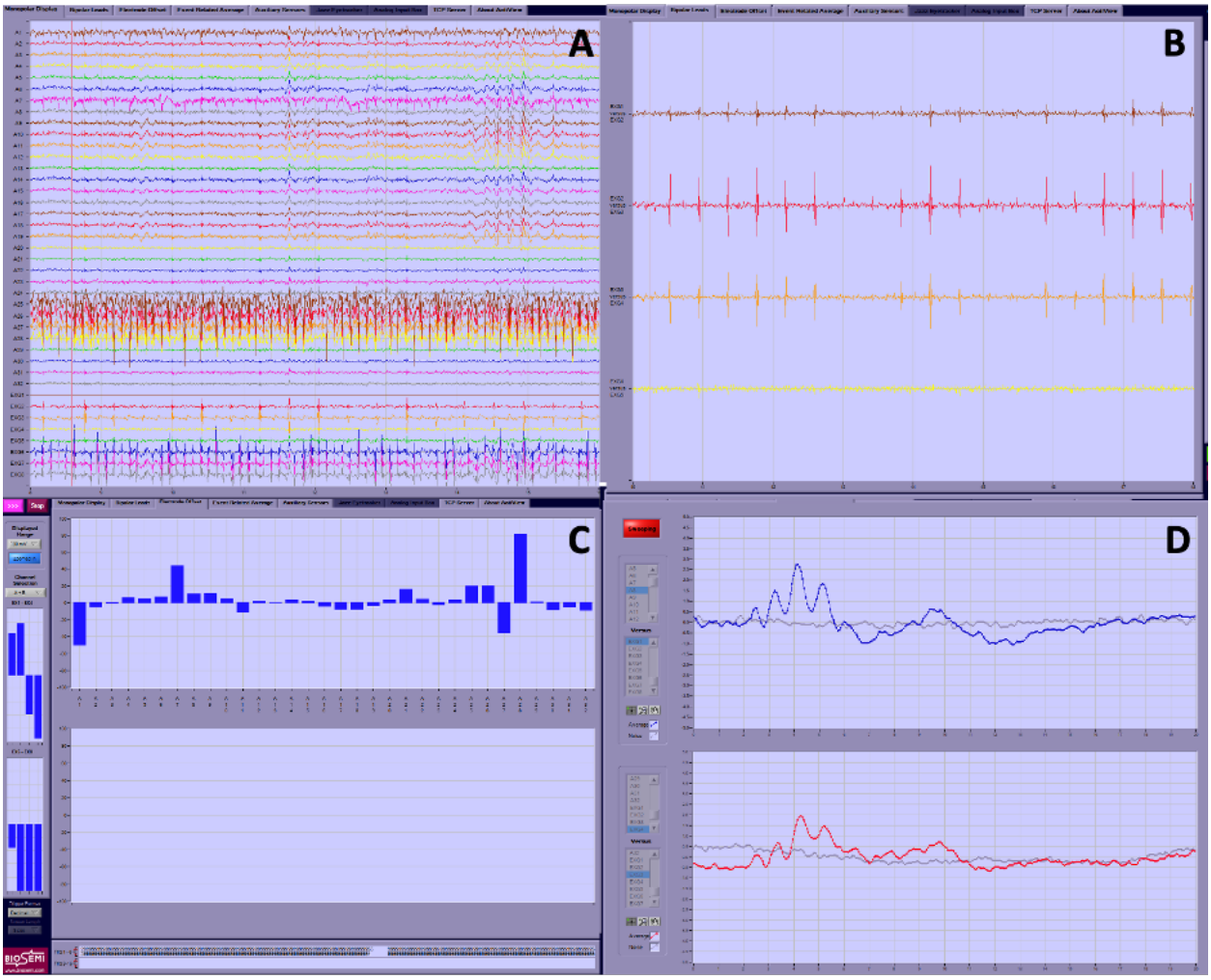

Figure 2.5. Mini cap data collection illustration. (A) Monopolar display showing signal quality of the 32 channels and 5 EXG channels. (B) Display showing the EXG channel quality of the two tiptrodes and the three subdermal needle electrodes. (C) Visualization of electrode offsets for each channel; ideally, offsets are maintained within a 40 millivolt range. (D) ABR visualization during data collection.

Triggers from the TDT System 3 hardware created during stimulus generation were sent to the ActiView software, allowing for documentation of stimulus onset. Each trigger corresponds to each instance a stimulus was presented into the ipsilateral ear. These trigger markers allowed for epoching, a procedure in which specific time-windows are captured from the continuous time signal and aligned according to the stimulus. In order to collect an

auditory evoked potential, multiple repetitions must be collected and averaged to produce a reliable single response. Accordingly, each epoch corresponds to a single repetition, and averaging across multiple epochs produces a reliable ABR response. During data collection, filtering and epoching was completed on the raw data for visualization purposes. However, the saved data were the raw, non-epoched, non-filtered continuous time signals only. Processing of the data required repeating the filtering, epoching, and averaging steps. This differs from the subdermal methods, in which the processed responses were saved. Overall, this was another significant methodical benefit since it provided undoubtedly more flexibility in data processing and data analysis.

2.1.6 Otoacoustic emissions

Distortion-product otoacoustic emissions (DPOAEs) were collected after initial calibration as a non-invasive control measure to ensure adequate cochlear function for each animal. Similar to the calibration procedure, a microphone (Etymotic, ER-10B) and two transducers (Etymotic, ER-2) were inserted into the right ear canal to concurrently present acoustic stimuli and record the DPOAE response. Paired tone stimulus frequencies, f1 and f2, over 5 repetitions at a level of 75 dBSPL were presented into the ear canal with a frequency ratio of 1.2 f2/f1. A total of 27 stimulus combinations, composed of 1 second duration followed by 1 second silent inter stimulus interval, were collected with f2 values increasing in logarithmic steps from 0.5 kHz to 12 kHz. For each frequency, the SPL of the emission at the distortion product frequency of 2f1-f2 was determined. The quintessential cubic distortion product response is portrayed in Figure 2.6.

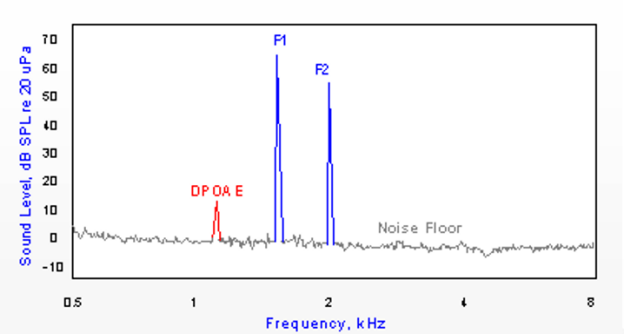

Figure 2.6. DPOAEs are the cubic distortion product in response to two primary tones (f1 and f2) [70]. In this experimental design, DPOAEs were used as a control measure to ensure normal cochlear function.

2.2 Data analysis

During data collection, data were saved into a 24-bit BDF file format. These data were an entirely raw, unprocessed, continuous time signal with trigger markers indicating when a stimulus was played into the ear. Thus, post processing was required to recreate the response visualized during data collection. Overall, this allowed for greater flexibility and greater opportunity for additional post processing of the responses themselves. The following three main analyses were conducted on the collected data: threshold determination, correlation analyses, and peak-picking. Each will be described in detail in the following paragraphs. For a step-by-step description of the data analysis performed, refer to *Appendix C*.

2.2.1 Post processing

Data processing was performed using the mne-python toolbox [71] combined with self-written software in Matlab (The Mathworks, Inc, Natick, Massachusetts) and Python. Figure 2.7 illustrates the post processing procedure that was followed. To summarize, after the data were loaded into mne-python, they were referenced, filtered, epoched, and averaged in order to produce the single ABR response. Replicating the subdermal response specifically required referencing to the ground subdermal electrode placed subdermally on the animal's nose. The mini cap response utilized the gold-foiled tiptrode placed in the ear canal of the ipsilateral right ear as the reference. After referencing accordingly, the raw data were high-pass filtered

at a cutoff of 300 Hz and a low-pass filtered at a cutoff of 3000 Hz. An additional 60 Hz notch filter was included to remove any remnants of line noise from the signal. The EEG signal was divided into epochs lasting 19 milliseconds, starting from 4 milliseconds before stimulus onset until 15 milliseconds after stimulus onset. A baseline correction from 2 millisecond before stimulus onset to stimulus onset was applied and subtracted from the entire epoch. To replicate the subdermal response, the epochs across the vertex subdermal EXG channel and the mastoid subdermal EXG channel were averaged and subtracted from each other. Before averaging across channels to obtain the mini cap response, bad channels were identified and removed. Bad channels were identified using a deviation criterion, which is a metric to detect differences in amplitude across channels included in the PREP pipeline [72]. This well-established method calculates a robust z score of the robust standard deviation for each channel, replacing the mean by the median and the standard deviation by the robust standard deviation (i.e. 0.7413 times the interquartile range) [72]. If a channel had a robust z score greater than 2.0, it was designated as a bad channel and not included in further analyses. After only good channels remained, they were averaged together and demeaned once more to ensure no DC shift to obtain the final mini cap ABR response.

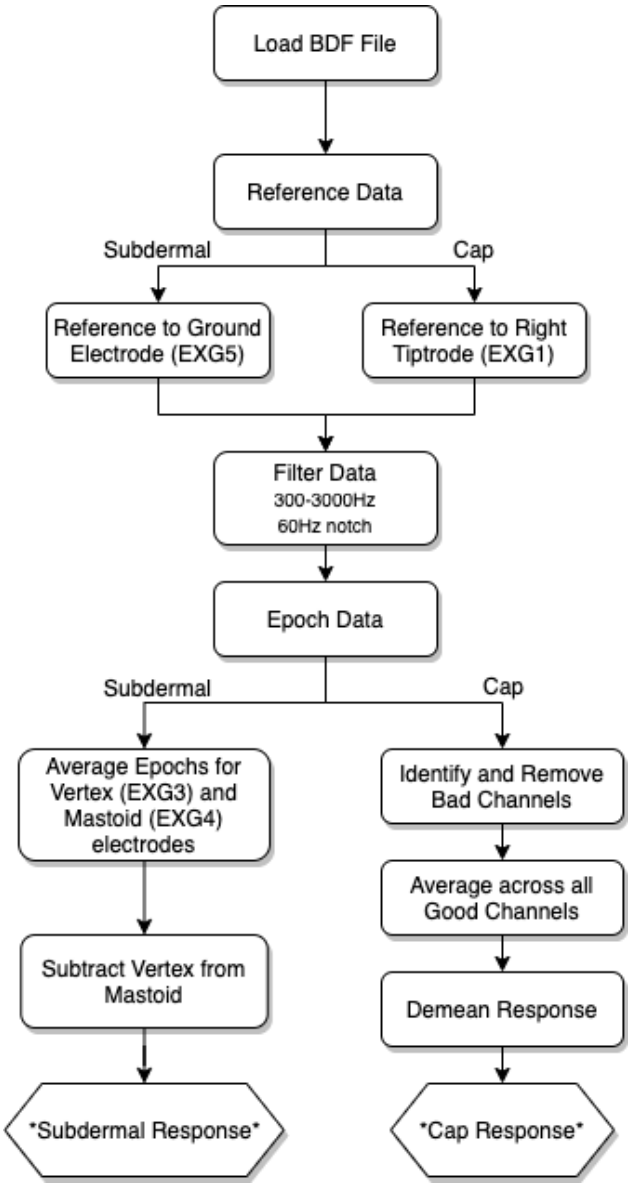

Figure 2.7. Process utilized for post processing. Data for both subdermal and mini cap responses are referenced, filtered, and epoched, and then averaged accordingly. After identifying and removing bad channels, the good channels were averaged together to produce the final mini cap response.

2.2.2 Threshold definition

To quantify threshold for the intensity waterfall for each frequency, the response at each level within the waterfall was subdivided into two windows: a signal window and a noise window. Figure 2.8 visually depicts these two windows. The signal window was defined as the response between 2 to 8 milliseconds after stimulus onset. The noise window was defined as the response from 4 milliseconds before stimulus onset up to 2 milliseconds after stimulus onset. In proceeding paragraphs, if the signal or noise window is mentioned, this definition of the signal and noise window is pertinent.

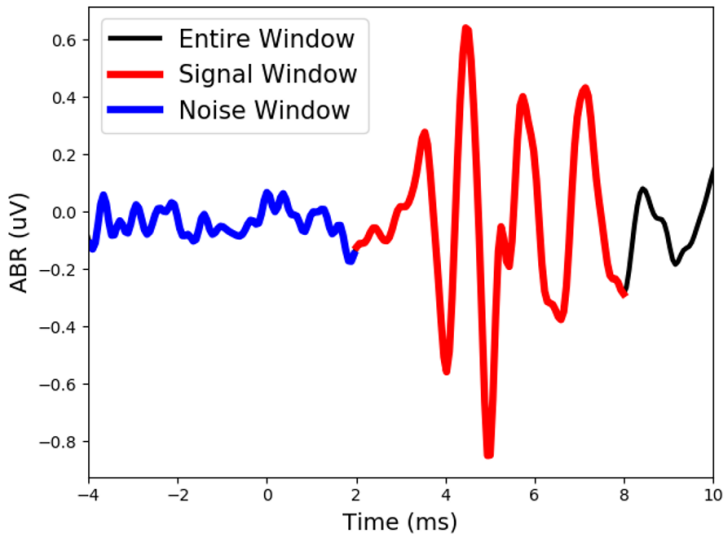

Figure 2.8. Definition of signal and noise window of ABR response. The signal window was defined as the response within 2 to 8 milliseconds. The noise window was defined as the response within -4 to 2 milliseconds, with 0 milliseconds representing the stimulus onset.

The peak-to-peak amplitude, defined as the maximum amplitude subtracted from the minimum amplitude, was determined for both the signal window and the noise window for each level collected. In order to define threshold, a noise criterion value was quantified as the mean of the noise floor plus two standard deviations of the noise across levels. From here, the noise criterion would intersect the signal peak-to-peak line at a specific point. To ensure a more straightforward comparison between waterfalls, the level experimentally collected that was closest to this intersection point would be labeled as the threshold of

the waterfall. Figure 2.9 illustrates the resultant figure of this thresholding procedure, with threshold defined accordingly as 10 dBSPL.

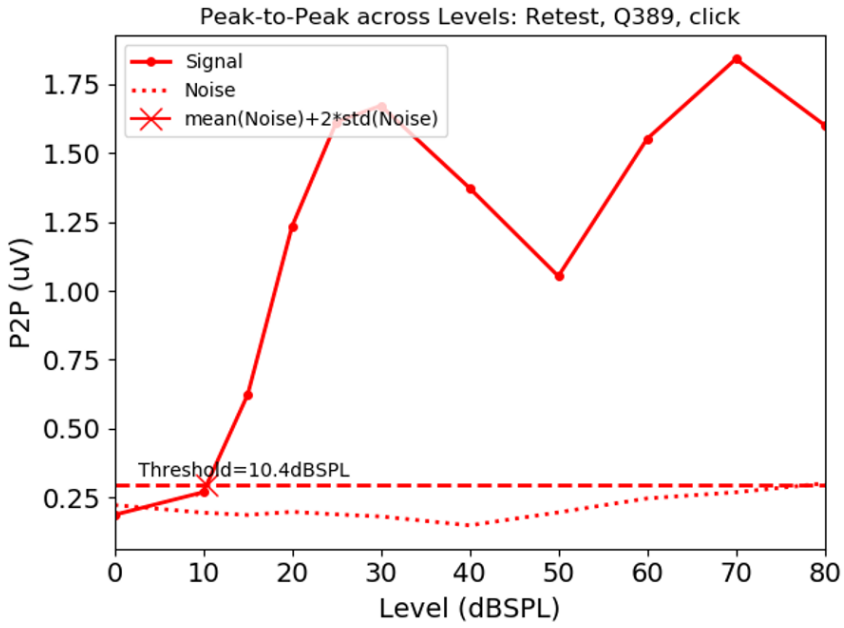

Figure 2.9. Threshold determination procedure. The maximum amplitude and the minimum amplitude in both the signal and noise window for each level of a waterfall were identified. These values were subtracted from one another to obtain a peak-to-peak (P2P) amplitude. The solid line displays the P2P amplitude for the signal window across levels. The dotted line displays the P2P amplitude for the noise window across levels. To determine threshold, the average of the noise floor plus two standard deviations resulted in a horizontal line that intersected the signal solid line at a specific point (i.e. exact threshold). To allow for simpler comparisons, the threshold was rounded to the closest level experimentally collected. In this example, threshold was defined as 10 dBSPL.

2.2.3 Correlation analysis

Cross-correlation, a well-established signal processing technique, was utilized to quantify the similarity between two responses. This was specifically used to compare equitable responses (i.e. same frequency, same level) and to eventually quantify the variability, or difference, between the two equitable responses. The cross-correlation coefficient was calculated for the signal window of each response (i.e. 2 to 8 milliseconds). No delay was included into

this calculation between two ABRs collected using the mini cap methodology due to the two responses being of equivalent level and frequency. For each correlation analysis, a correlation threshold was defined and if the cross-correlation coefficient matched or exceeded this threshold, those two responses were deemed to have acceptable correlation. Table 2.2 illustrates the resulting interpretation of a correlation coefficient according to the cross-correlation coefficient value. In correlation analyses pertinent to this research, the correlation threshold was set at 0.70, indicating a high positive correlation between the two responses. Since the objective was to have equivalent responses exhibit high positive correlation to one another, and a correlation value greater than 0.7 indicates high positive correlation, the 0.70 criterion was chosen accordingly. According to the interpretation, a correlation coefficient greater than 0.7 signified that the two waveform exhibited highly correlated, and thus highly equivalent, morphologies.

Table 2.2. Correlation interpretation.

Correlation Value	Interpretation
0.9-1.0	Very high positive correlation
0.7-0.9	High positive correlation
0.5-0.7	Moderate positive correlation
0.3-0.5	Low positive correlation
.00-0.3	Negligible correlation

2.2.4 Peak picking

Finally, peak-picking was performed on ABR responses in order to characterize the different CS biomarkers. Both the wave amplitude and wave latency were quantified. As a measure of cochlear synaptopathy, the amplitude and latency of wave-I and wave-V were computed. Amplitude was defined as the peak amplitude relative to the subsequent trough amplitude [73]. Latency was measured as timing of the the peak amplitude relative to the stimulus onset time [73]. A visualization of the peak-picking necessary to compute these metrics is shown in Figure 2.10. To obtain a more reliable value of each metric, peak and trough amplitudes and latencies were averaged across the highest levels (e.g., 60, 70, and 80 dBSPL) from a single waterfall. Additionally, the wave-V/wave-I ratio, another common CS

metric, was computed. In order to characterize any potential between-channel differences in the mini cap responses, peak-picking was conducted on the other ABR waves (i.e. waves 2-4) for each channel and compared directly to one another.

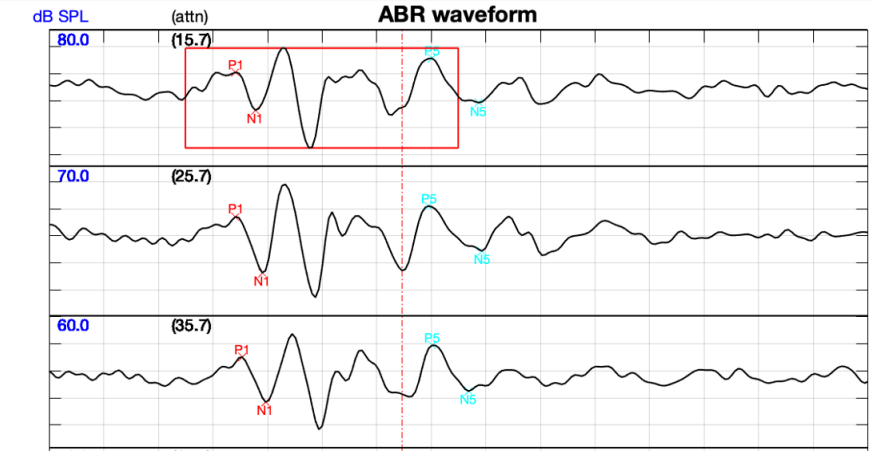

Figure 2.10. Peak-picking completed in order to quantify CS metrics. The peak and trough of Wave-I and wave-V are identified for the top three sound pressure levels (i.e. 60, 70, and 80 dBSPL). The vertical red dashed line was placed 3 millisecond (ms) after the average of all wave-I peak amplitudes in order to allow for simpler identification of the wave-V peak. To increase consistency, the wave-V peak was defined as the closest subsequent peak after 3 ms, closest to the vertical red-dashed line. In peak-picking, The trough of wave-V can often be difficult to differentiate as well, so the red-dashed line is helpful for visualization. Common CS metrics include the amplitude and latency of wave-I and wave-V before and after noise exposure.

3. RESULTS

3.1 Subdermal needle method variability

The subdermal needle method routinely used for recording ABRs is inherently variable. This variability primarily originates from electrode placement. As mentioned, for this technique, three subdermal needle electrodes are placed in designated spots around the chinchilla skull. The vertex electrode is placed between the two bullae, the mastoid electrode is placed underneath the ear, and the ground electrode is placed on the bridge of the nose. The ground electrode placed on the noise and vertex electrode placed between the two bullae are often easily placed because there are visual landmarks for both. However for the mastoid electrode, it can be challenging to confidently place this electrode in the identical location each experiment because there is no clear visual landmark. It has been found that, with regard to electrode placement, there is more robust intra-rater reliability (i.e. across a single experimenter) than inter-rater reliability (i.e. across multiple experimenters). Figure 3.1 illustrates this inherent variability emerging from electrode placement. In a single experiment, four experimenters placed the three subdermal needle electrodes and ABR responses were recorded according to each experimenter's electrode placement. As apparent in Figure 3.1, there is considerable variability in waveform morphology as a result of each experimenter placing the three subdermal electrodes. In this example, it appears as if the waveform morphology is consistent between two groups of two experimenters each. However, between the two groups of two experimenters, there is noticeable variability between the waveforms. Changes in waveform morphology appear to influence the wave amplitudes more than the wave latencies. However, wave amplitudes, specifically for wave-I and wave-V, are two primary measures of CS, so the fact that these appear to differ between different experimenters would significantly impact the end results.

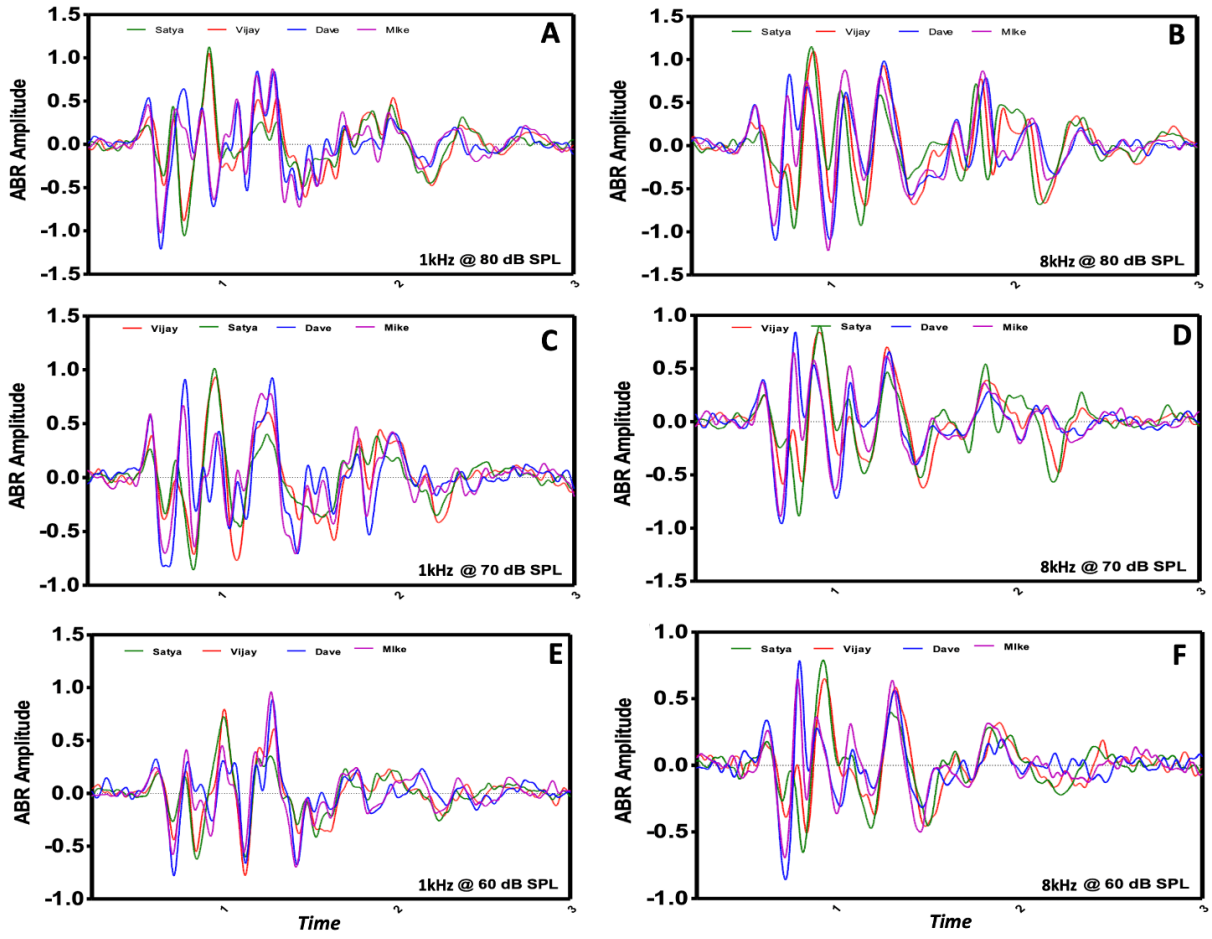

Figure 3.1. Inherent variability of electrode placement in subdermal method. During a single experiment, four experimenters placed the three subdermal needle electrodes. Responses at three levels (60, 70, 80 dBSPL) for two different frequencies (1kHz, 8 kHz) for each experimenter were recorded. There is significant differences in waveform morphology across the four experimenters for each frequency/level combination shown. This result verifies that there is inherent variability in the subdermal method as a result of electrode placement.

A fundamental objective of the mini cap is to reduce this inherent variability from electrode placement. The only placement required for the mini cap procedure is the placement of the singular mini cap in its desired location in front of the two bullae. The placement of the mini cap is more straightforward because the landmarks (i.e. in front of the two bullae) are easier to visualize and confirm than the landmarks for the subdermal electrodes, especially for the mastoid electrode in which visual confirmation is not possible. Additionally,

the size of the mini cap in relation to the size of the scalp is similar, so there is not as much variation with mini cap placement compared to subdermal needle placement. Since channels are averaged together for the mini cap, slight differences in mini cap placement would be less apparent in the final response. In summary, reducing the inherent variability due to electrode placement was a primary objective of introducing this new mini cap method. For this reason, the variability of the mini cap method will be acutely studied.

3.2 Feasibility of EEG mini cap to record ABRs

Initially, the feasibility of the EEG mini cap was investigated. The three main goals of this initial feasibility study were the following: (1) ensure the mini cap could record ABR responses in chinchillas; (2) confirm that the EEG responses across channels were satisfactory with regard to signal quality and offsets; and (3) establish and finalize the methodology that would allow for adequate EEG data to be collected using the mini cap.

3.2.1 Initial feasibility experiments

A significant portion of the initial experiment was spent finalizing the appropriate procedure in order to ensure effective contact of the mini cap to the chinchilla's head. For the first experiment, an electronic razor was used to remove the fur and loose rubber bands were used in attempt to secure the cap to the chinchilla's head. As seen in Figure 3.2, the resulting EEG response collected during the first experiment was exceedingly noisy and no clear ABR response was recognized. There was significant 60 Hz line noise visually apparent in the response. In order to successfully record ABRs in the second experiment, multiple issues were resolved between the first and second experiment. Firstly, to reduce 60 Hz line noise, the CMS/DRL wire was wrapped around the other cables that attached the mini cap to the hardware, effectively minimizing the magnetic interference pickup. Secondly, in addition to the electronic razor, Nair hair removal lotion was utilized to more effectively remove the fur from the spot in which the mini cap was placed. The electronic razor was effective at removing the vast majority of the fur but there still remained a layer of fur on the skin after shaving that must be removed. Nair hair removal lotion was quite effective at removing this

remaining layer of fur, resulting in a hairless spot. Lastly, rubber bands were not effective at sufficiently securing the mini cap to the chinchilla's head. It is important that the cap is tightly held onto the chinchilla's head in order to provide the required scalp contact for each electrode on the mini cap. A customized device, further detailed in the next paragraph, was developed to secure the mini cap to the head. Altogether, by implementing these three methodological improvements during the second experiment, an unambiguous ABR response of satisfactory signal quality was observed (see Figure 3.2).

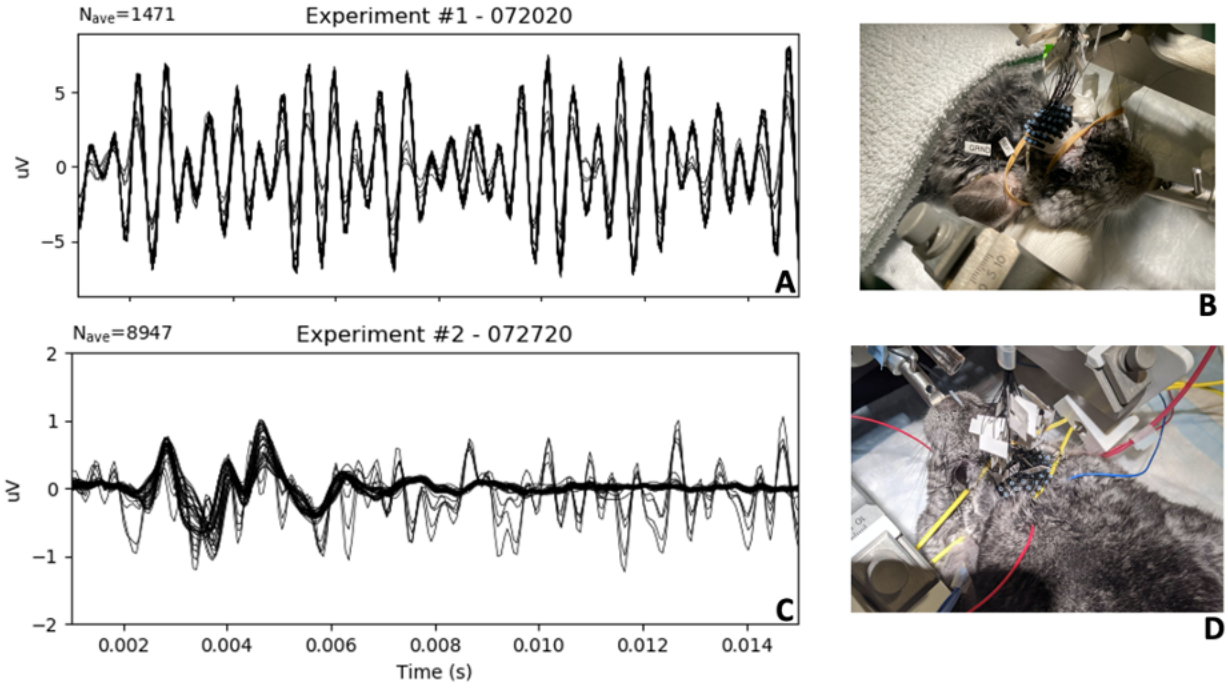

Figure 3.2. Improvements made between the first two experiments to obtain a convincing ABR using the mini cap. The signal quality of the first experiment (see A) is considerably noisy whereas, in the second experiment (see C), a clear ABR response is observable. Three methodological improvements allowed for this noticeable improvement in signal quality. First, the cap was more properly secured to the head during the second experiment (see D) using a customized device (see Figure 3.3) than the first experiment (see B). Secondly, the fur was more effectively removed from the scalp in the second experiment (not shown). Thirdly, interweaving the cables reduced line noise (not shown).

The 3D printed customized device was designed to solve this issue of effectively securing the mini cap to the chinchilla's head. This device utilized an elastic band that is placed over

the front and back of the mini cap, crossing over the top of the chinchilla's head, and was attached and tightened with the screw on the opposite side (see Figure 3.3). One benefit of this device was that securing the mini cap did not require placing anything around the chinchilla's head, which averted the initial concern of placing anything too tight around the chinchilla's head. A second benefit was that this device could be customized and tightened accordingly to each animal. This flexibility allowed for the mini cap to be securely placed on both smaller and larger chinchillas.

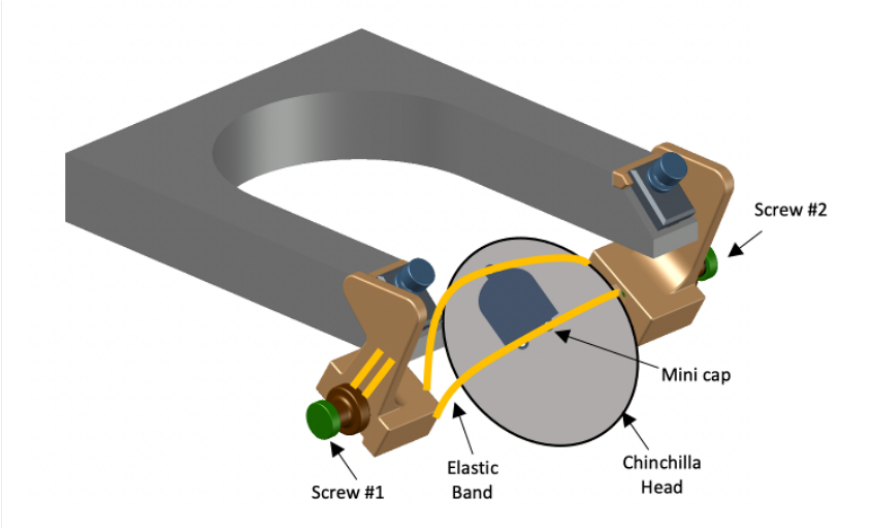

Figure 3.3. Custom-built device used to effectively secure mini cap to chinchilla head. An elastic band wrapped around the top of the chinchilla's head, tightly holding the mini cap in place. First, the elastic band was tightened to one side using screw #1. Then, the band was placed to hold the mini cap using the top and bottom extrusions of the mini cap, and tightened accordingly on the other side using screw #2. This customizable design allowed for flexibility with chinchilla head size. Additionally, since this design only involved placing an elastic band on the top of the head, it avoided wrapping anything tight around the chinchilla's head (e.g., a rubber band).

3.2.2 Identification of noisy channels

It was not uncommon for a few channels to appear noisy during data collection. There are a few reasons as to why this was occurring. A noisy electrode could indicate inadequate scalp contact or that more paste needed to be added to the electrode inner tube. Scalp

contact was improved by sliding the electrode tube downward in the scaffold to ensure firm contact with the scalp. High 60 Hz noise suggested that the impedance at the reference and ground was faulty. Broadband electrode noise suggested that the electrode was contaminated with stray ions. Finally, a slow drift suggested a poor contact between an electrode and the body of the animal. Low-frequency instability also suggested an aged electrode from which too much chloride had been lost.

As mentioned during post-processing, bad channels were identified using a thresholding procedure. However, during experiments, bad channels were visually identified by signal quality and/or faulty offsets. Based on this visual identification, and confirmed in post-processing, certain channels on the mini cap were frequently labeled bad channels. Figure 3.4 visually illustrates the effect of including these bad channels (e.g., often channels 25-28) in the averaged response used. One potential rationale for why certain channels were consistently noisy across data sets is because the shape of the mini cap might not comprehensively align with the chinchilla head anatomy. The mini cap was designed according to the Wistar rat head anatomy. Differences in the head anatomy of the Wistar rat and the chinchilla could potentially account for this certain region of the mini cap (e.g., channels 25-28) appearing consistently more noisy than other regions of the mini cap. Another potential rationale may be that the noisy channels were contaminated with stray ions due to handling. Overall, including bad channels in the averaged response added unnecessary noise. Therefore, only good channels were included in the averaged responses utilized in subsequent analyses.

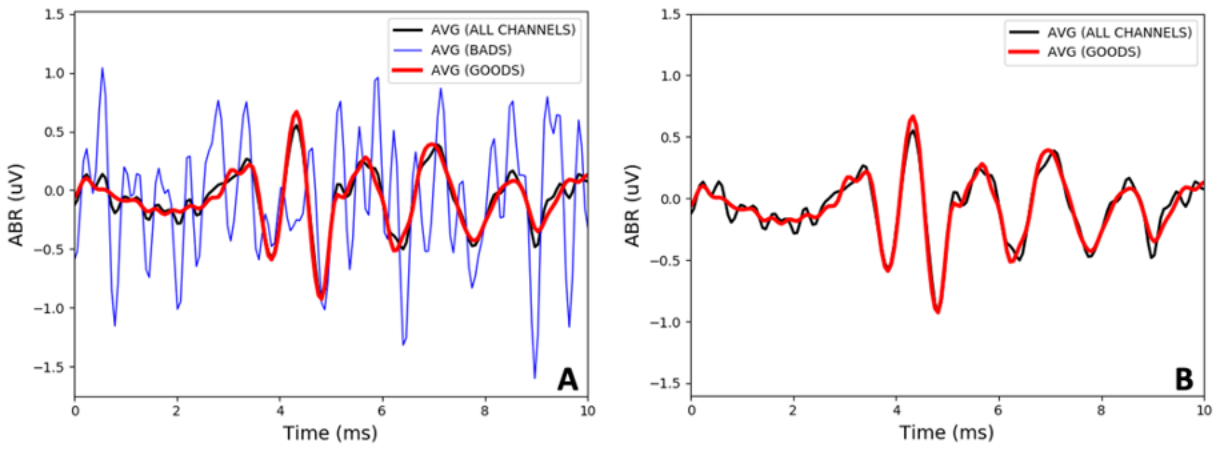

Figure 3.4. Effect of including and removing bad channels from averaged response. Bad channels were identified using a z-score deviation criterion and removed before averaging (see A for average of all, good, and bad channels separately). Since bad channels only added noise to the response (see B), only good channels were averaged together to produce the final ABR response.

3.2.3 Replicated subdermal response from simultaneous data collection

During each experiment, three subdermal needle electrodes (i.e. vertex, mastoid, ground) were placed accordingly in addition to the mini cap. These three electrodes were recorded as external EXG channels. Replicating the subdermal response while simultaneously recording EEG responses from the mini cap was achievable and is a significant methodological benefit of using the mini cap, as shown in Figure 3.5. In Figure 3.5, the waveform labeled as goods was the average of all good channels. Additional EXG channels (i.e. up to eight) allowed for other measures as well. In this experimental design, two additional external channels were the two gold-foiled tiptrodes placed into the ear canal of each ear. Overall, this process of replicating the subdermal response with the three external channels was feasible and advantageous.

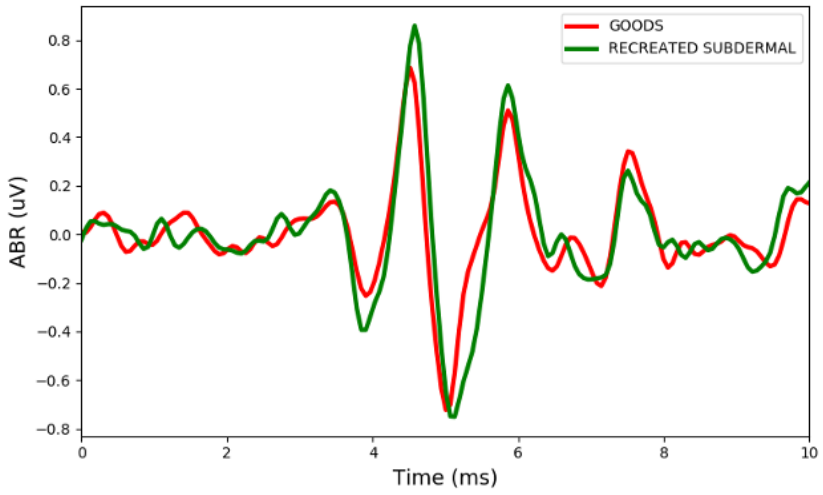

Figure 3.5. Simultaneous data collection of mini cap and subdermal responses. Using three EXG channels, a replicated subdermal response was simultaneously collected along with the mini cap response. Here, the cap response (see red, average of good channels) and subdermal response (see green) were recorded concurrently.

3.2.4 Significance of a clean reference channel

Choosing an adequate reference electrode was of utmost importance. An EEG electrode only yields information about the difference of electrical activity between two positions on the head [74]. Thus, the resulting EEG signal is the difference between the raw continuous time signal of that particular electrode and the reference electrode. If the reference electrode contains a high level of noise, it will contaminate every other electrode with the same noise artifact. This means that even if each individual channel is noise-free, referencing to a noisy reference channel will introduce the noise into the other channels. In this experimental setup where sound was played only into the right ear, the reference channel was chosen to be a gold-foiled tiptrode placed into the right ipsilateral ear canal of the chinchilla. It is recommended that the position of the reference electrode be an electrically neutral position away from the electrodes in which the main effects are expected [75]. Oftentimes mastoids are chosen as reference electrodes because while they are close in distance to the electrodes, they record less signal from the brain [75]. In this setup, the ipsilateral tiptrode meets this same criterion. The ipsilateral tiptrode was close in distance to the electrodes (i.e. placed in the ear

canal) and recorded less signal from the brain. Figure 3.6 shows an example of how a noisy reference electrode (i.e. EXG1) can affect the overall ABR response by introducing noise into all electrical channels. Referencing to the left contralateral tiptrode (i.e. EXG2), which did not contain the high level of noise seen in the ipsilateral tiptrode, resulted in a cleaner, more prominent ABR response. This example demonstrates the importance of ensuring that the reference electrode is not noisy during data collection. Before starting each experiment, it is imperative to replace the two tiptrodes. In this example, the high level of noise in the right tiptrode was caused by a reused tiptrode from the previous experiment. One benefit of this methodology, however, is that if hypothetically the reference channel is noisy, a different reference channel (e.g., EXG2) can easily be utilized in processing of the data instead of the noisy reference channel.

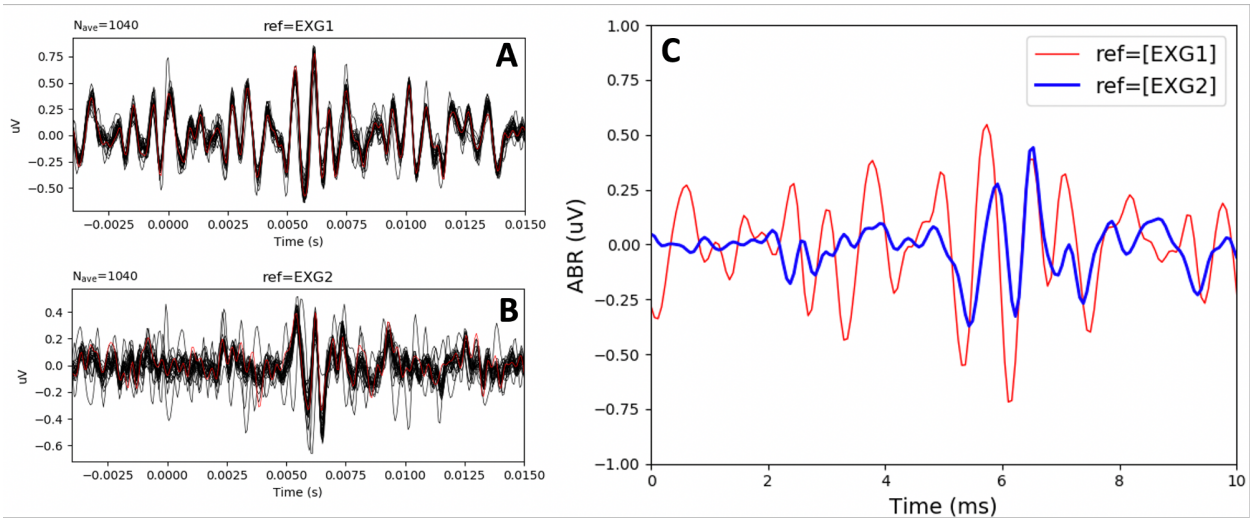

Figure 3.6. Importance of a clean reference channel. During this experiment, EXG1 was significantly noisy (see A) compared to EXG2 (see B). EXG1 is typically used as the reference channel. Referencing to a noisy EXG1 led to a noisy, indistinguishable ABR response whereas referencing to a clean EXG2 led to a convincing ABR response (see C). Thus, ensuring a clean reference channel was crucial to obtain accurate ABRs.

3.2.5 First animal results

After finalizing the procedure and demonstrating the feasibility of the cap to record ABR responses, a single animal was studied to demonstrate the feasibility of the mini cap to collect

ABR waterfalls across two days. Overall, two full waterfalls of two frequencies (4kHz and click) were collected on one day and then a second day one week after the first day. This was the initial test/retest study to examine the feasibility of the mini cap across days. Ideally, the thresholds would be the same across two days. Here, a 5 dBSPL criterion range was set in which a 5 dBSPL threshold difference between the two days was permitted. For all threshold comparisons in this research, the 5 dBSPL criterion will be utilized. Figure 3.7 shows the threshold figures for both frequencies across both days. For both frequencies, thresholds were within the 5 dBSPL range of one another, and, thus, deemed acceptable. Therefore, this first animal confirmed initial feasibility of the mini cap's ability to produce equivalent thresholds across two days. Since the mini cap was replaced between two days, this result also confirmed that the mini cap was capable of producing equivalent thresholds after introducing the variability associated with removing and replacing the mini cap. To summarize, these initial experiments demonstrated the feasibility of the mini cap to record clear ABR responses with equivalent intensity waterfalls in chinchillas across multiple days. After initial troubleshooting, the methodology described that allowed for this was resolved and will be applied in the ensuing experiments discussed.

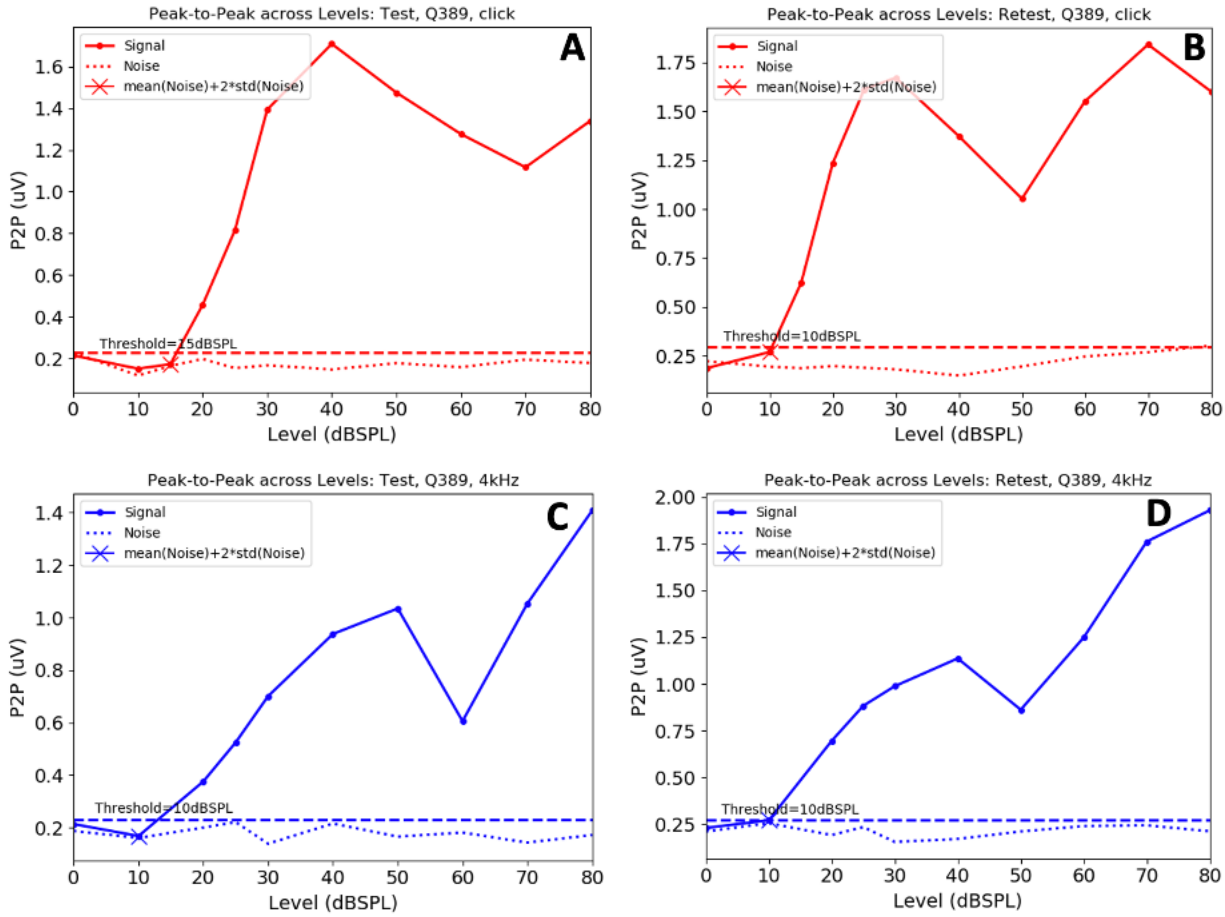

Figure 3.7. Initial test/retest feasibility results. For the first animal, both the click thresholds and the P2P waveforms between the test experiment (15 dBSPL, see A) and the retest experiment (10 dBSPL, see B) were highly comparable. Additionally, the 4kHz thresholds and P2P waveforms between the test experiment (10 dBSPL, see C) and the retest experiment (10 dBSPL, see D) were significantly equivalent. This result confirmed the feasibility for the mini cap to produce robust thresholds and ABR responses across levels across two days.

3.3 Sources of bias and variability

The second aim of this research investigated the sources of bias and variability inherent to the mini cap to determine whether each of these sources was significant or insignificant with regard to the mini cap's capability to record ABRs in chinchillas. To characterize this, the reliability, repeatability, reproducibility, and validity of the mini cap were quantified. Since this is a new method, it was essential to examine and understand to what extent, if

any, variability affected the mini cap. In general terms, variability refers to the spread of the data. Investigating the different forms of variability of a new method is recommended to thoroughly understand the advantages and disadvantages of the new method to perform its desired function. In fact, the first step in the scientific method is to quantify the amount of variability in the data [76]. In this case, the variability of the method itself to produce robust, invariable data (i.e. ABR waveforms) was characterized.

3.3.1 Reliability, repeatability, and reproducibility of the mini cap

Examining the reliability, repeatability, reproducibility, and validity of the mini cap provided direct insight into the variability of mini cap as a method to record ABRs in chinchillas. Each provided insight into a potential different form of variability. In the following descriptions, the measurand refers to the measured quantity, which, in this case, is the animal. The instrument refers to the mini cap used to record the response.

Reliability refers to the consistency of the measure [77]. There are three main types of consistency: across day (i.e. test-retest reliability), across items (i.e. internal consistency), and across experimenters (i.e. inter-rater reliability) [77]. High test-retest reliability indicates the method is consistent across time. High internal consistency indicates the method is consistent across multiple measures within a single experiment. High inter-rater reliability indicates the method is consistent across difference experimenters. Reliability measures require the same measurand and the same instrument. Repeatability refers to the closeness of agreement between results of successive measurements of the same measurand carried out under the same conditions [78]. Thus, repeatability measures require the same experimenter, the same experiment (i.e. day), the same instrument, and the same measurand. Studying repeatability is significant because it is important to ensure that the mini cap can successively record comparable ABRs within a single experiment. Reproducibility refers to closeness of the agreement between the results of measurements of the same measurand carried out under changed conditions of measurement [78]. Similarly, studying repeatability is crucial because it is imperative to ensure that the mini cap can successively record comparable ABRs in different experiments on different days.

3.3.2 Identification of five potential sources of variability

Overall, five potential sources of variability were identified and studied. Table 3.1 shows the classification of reliability, repeatability, and reproducibility, and specifically what must remain consistent and what can be altered for each. For each comparison, only one source of variability was altered. This allowed for direct insight into that specific form of variability. Changing two sources of variability at once cannot provide information on each source of variability individually, only a combination of both sources. Consistency across the additional experimental components were maintained as well. Across a single experiment, both the tiptrodes and the subdermal needle electrodes remained consistent, unless poor signal quality and/or offsets were recognized during the experiment. Additionally, a single experimenter placed the tiptrodes and the subdermal needle electrodes across all experiments in order to minimize the variability of these two experimental components.

Table 3.1. Five potential sources of variability for the mini cap.

Term	Reliability	Repeatability	Reproducibility
Remains consistent	Same measurand Same instrument	Same measurand Same experimenter Same instrument Same day	Same measurand
Can be changed	Repetition over a short period of time (**X-Time**) Removing and replacing cap (**X-Cap Removal**) Different experimenter (**X-Experimenter**) Different day (**X-Day**)	Repetition over a short period of time (**X-Time**) Removing and replacing cap (**X-Cap Removal**)	Different experimenter (**X-Experimenter**) Different instrument (**X-Cap**) Different day (**X-Day**)

The variability associated with repeating measures over a short period of time was evaluated, labeled accordingly as X-Time. For this, a subsequent measure was collected right after collecting the first measure. Quantifying X-Time variability provided information about the reliability and repeatability of the mini cap. Next, the variability produced by removing and replacing the mini cap (i.e. the instrument) was examined, identified as X-Cap Removal. Experimentally, after the first measure was collected, the same experimenter removed and replaced the mini cap, injecting any additional paste if they deemed it necessary to do so.

Here, X-Cap Removal similarly portrayed the reliability and repeatability of the mini cap. Thirdly, the variability associated with different experimenters placing the mini cap, designated as X-Experimenter, was investigated to evaluate reliability and reproducibility. After the first experimenter placed the mini cap, the second experimenter removed and replaced the mini cap, again injecting any additional paste if they deemed it necessary to do so. The variability from using a different instrument, in this case a second mini cap, was additionally studied. This was labeled as X-Cap and illustrated the reproducibility of the mini cap. For X-Cap, the same methodology was utilized in preparation of both mini caps, as previously described, and the same experimenter placed each mini cap. Finally, the fundamental test-retest, across-day variability was inspected by collecting data on one day and then collecting data one week later after the animal was fully recovered from any potential lasting anesthesia effects. For this X-Day variability, the same experimenter and the same instrument (i.e. mini cap) were maintained. By quantifying X-Day variability, the reliability and reproducibility of the mini cap was evaluated. Overall, characterizing each source of variability provided additional insight into the comprehensive reliability, repeatability, and reproducibility of the mini cap to record ABRs.

3.3.3 Test/Retest experimental design

To reiterate, five forms of variability were explored: X-Time, X-Cap Removal, X-Experimenter, X-Cap, and X-Day. To research this, a detailed test/retest paradigm study was designed. In this design, E1 will refer to experimenter #1 and E2 will refer to experimenter #2. After an original 4 kHz waterfall was collected, a subsequent replicate 4 kHz waterfall would be collected (i.e. X-Time) and this replicate waterfall was labeled Replicate #1. After the first two waterfalls were collected, the same experimenter would replace the mini cap and a third waterfall was collected. This third waterfall was called Replicate #2. For X-Cap variability, a similar design was performed, except only experimenter #1 would place and remove either the first mini cap or the second mini cap. The ambition was to collect a total of six 4 kHz waterfalls for each experiment. For the first design, these six waterfalls, all collected with the first mini cap, were the following: E1-Original, E1-Replicate #1, E1-Replicate #2, E2-Original, E2-Replicate #1, and E2-Replicate #2. For the second design, X-Cap variability

was examined and the following waterfalls, all collected by experimenter #1, were collected: Cap #1-Original, Cap #1-Replicate #1, Cap #1-Replicate #2, Cap #2-Original, Cap #2-Replicate #1, and Cap #2-Replicate #2. According to time constraints, collecting all six waterfalls during a single experiment was not always feasible. However, as many waterfalls, up to the total of six waterfalls, that could be collected within each experiment were collected and then analyzed. Figure 3.8 portrays these two experimental designs.

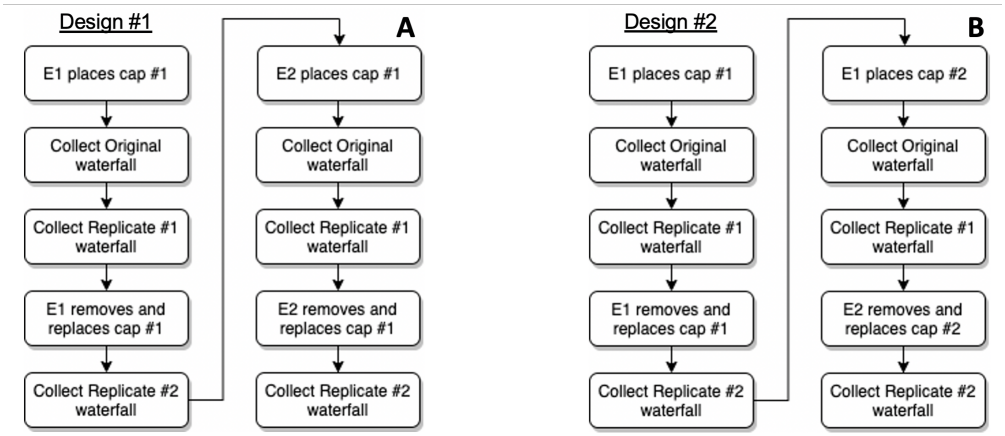

Figure 3.8. Two experimental designs utilized to assess the five sources of variability. The X-Experimenter design (see Design #1, A) required two experimenters and one mini-cap, and three waterfalls per experimenter were collected during a single experiment. The X-Cap design (see Design #2, B) required one experimenter and two mini-caps, and three waterfalls per mini cap were collected during a single experiment.

3.3.4 Test/Retest data collection

Overall, three animals were tested using this paradigm. A total of 30 waterfalls were collected (see Table 3.2). Four experiments followed the first experimental design (i.e. X-Experimenter) and two experiments followed the second experimental design (X-Cap). For the third animal, an additional replicate #3 (i.e. across time after replicate #2, not replacing the cap) was collected during the test experiment. Also, in the retest experiment of the third animal, an additional experimenter comparison was collected with the first cap (i.e. Cap #1-E2-Original). From the waterfalls collected across all three animals, each source of variability was fully characterized and quantified.

Table 3.2. Number of waterfalls collected for each animal.

Animal Number	Animal	Test	Retest
1	Q365	E1-Original	CAP1-E1-Original
		E1-Replicate #1	CAP1-E1-Replicate #1
		E1-Replicate #2	CAP2-E1-Original
		E2-Original	CAP2-E1-Replicate #1
2	Q383	E1-Original	E1-Original
		E1-Replicate #1	E1-Replicate #1
		E1-Replicate #2	E1-Replicate #2
		E2-Original	E2-Original
			E2-Replicate #1
			E2-Replicate #2
3	Q394	E1-Original	CAP1-E1-Original
		E1-Replicate #1	CAP1-E1-Replicate #1
		E1-Replicate #2	CAP1-E1-Replicate #2
		E1-Replicate #3	CAP1-E2-Original
		E2-Original	CAP2-E1-Original
		E2-Replicate #2	CAP2-E1-Replicate #1

3.3.5 Threshold comparisons

Thresholds were calculated for each waterfall following the thresholding procedure detailed in the *Methods* section. As previously mentioned, the ideal difference between thresholds of waterfalls collected within a single day and across days was set as a 5 dBSPL range. Thresholds that fall within the 5 dBSPL criterion indicated that the the introduction of the different sources of variability that each waterfall represented did not significantly affect the thresholds. Since thresholds are commonly used as indicators of hearing loss before and after noise exposure, it is important that the mini cap produces robust thresholds.

Thresholds for animal #1

For the first animal, thresholds were mainly within the 5 dBSPL range both within a single day and across both days. Figure 3.9 and Table 3.3 portray these results. This was indicative that each of the five sources of variability did not affect the thresholds for both the test and retest experiments for the first animal.

Table 3.3. Animal #1 mini cap thresholds.

Experiment	Waterfall	Cap Threshold (dBSPL)
Test	E1-Original	20
	E1-Replicate #1	15
	E1-Replicate #2	10
	E2-Original	10
Retest	CAP1-E1-Original	10
	CAP1-E1-Replicate #1	10
	CAP2-E1-Original	10
	CAP2-E1-Replicate #1	10

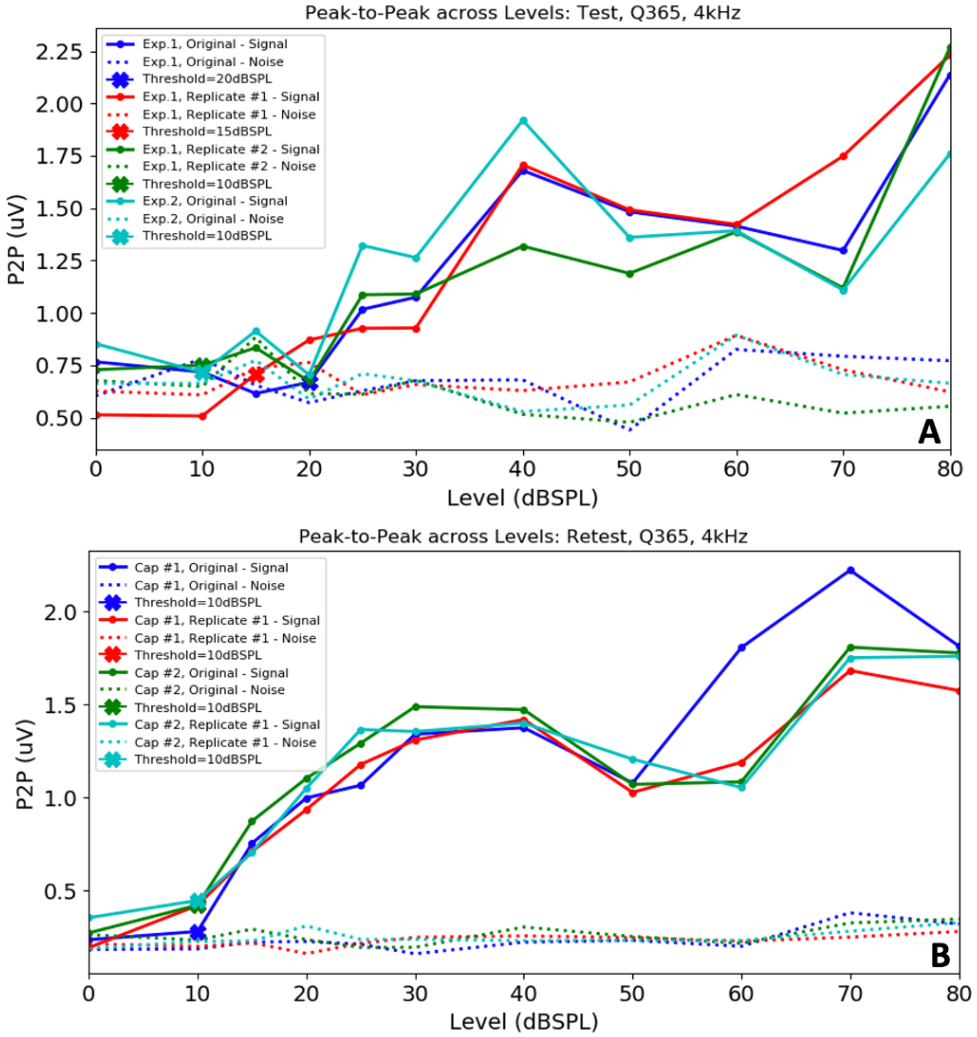

Figure 3.9. Mini cap thresholds for Animal #1. Between the test experiment (see A) and the retest experiment (see B), thresholds were mainly within the 5-dBSPL range criterion for animal #1 (see Table 3.3 for exact thresholds).

Thresholds for animal #2

Similarly, for the second animal, almost all thresholds were within the 5 dBSPL range, both within a single day and across both days (see Figure 3.10, Table 3.4). These results, similar to for the first animal, were promising and indicative that the mini cap can produce robust thresholds within a single day and across multiple days.

Table 3.4. Animal #2 mini cap thresholds.

Experiment	Waterfall	Cap Threshold (dBSPL)
Test	E1-Original	15
	E1-Replicate #1	20
	E1-Replicate #2	10
	E2-Original	10
Retest	E1-Original	25
	E1-Replicate #1	25
	E1-Replicate #2	20
	E2-Original	10
	E2-Replicate #1	15
	E2-Replicate #2	20

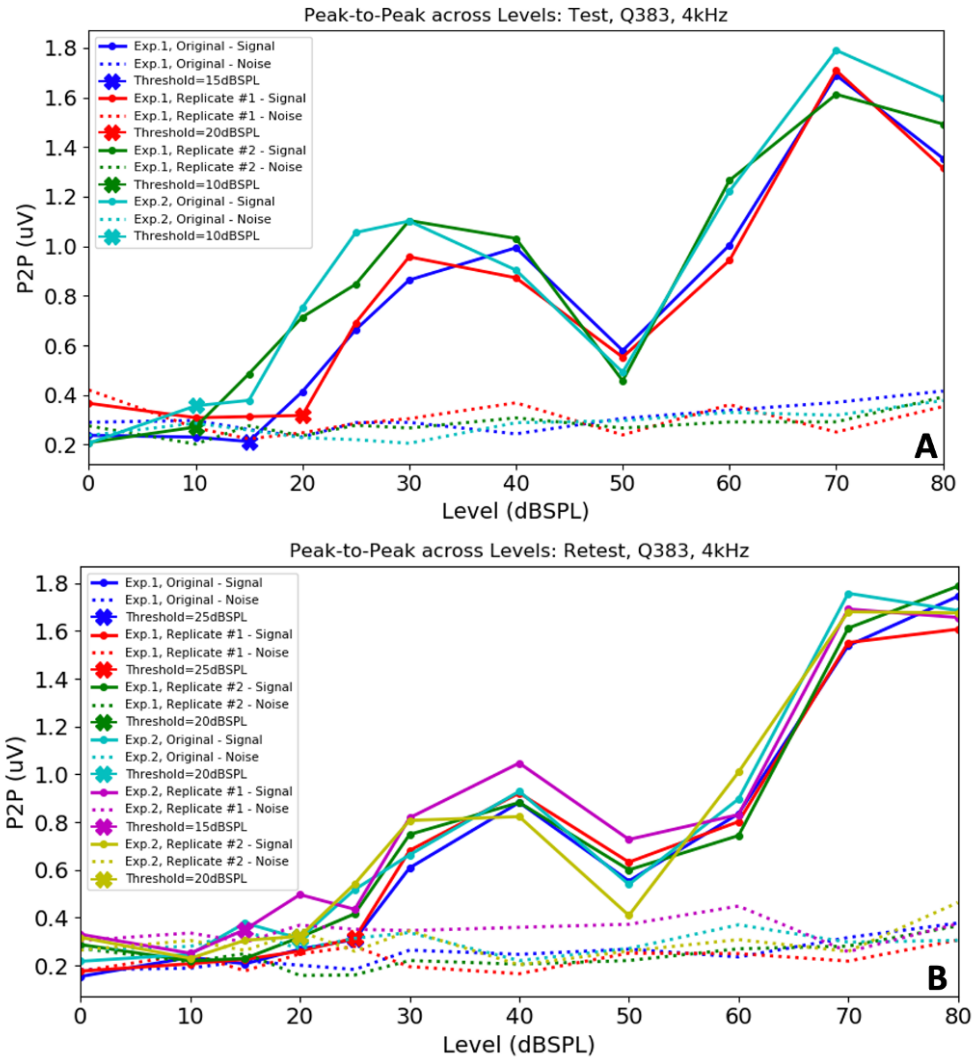

Figure 3.10. Mini cap thresholds for Animal #2. Between the test experiment (see A) and the retest experiment (see B), thresholds were mostly within the 5-dBSPL range criterion for animal #2 (see Table 3.4 for exact thresholds).

Thresholds for animal #3

Finally, for the third animal, every threshold met the 5 dBSPL criterion (see Figure 3.11 and Table 3.5). Thus, for all three animals, the vast majority of the thresholds met the 5 dBSPL threshold criterion. These results across all three animals suggest that the five different sources of variability did not significantly affect thresholds. The fact that the mini cap produced robust thresholds, even as the different potential sources of variability were

introduced, is encouraging. This result is a positive indicator that the mini cap produces reliable, repeatable, and reproducible thresholds.

Table 3.5. Animal #3 mini cap thresholds.

Experiment	Waterfall	Cap Threshold (dBSPL)
Test	E1-Original	10
	E1-Replicate #1	10
	E1-Replicate #2	10
	E1-Replicate #3	10
	E2-Original	10
	E2-Replicate #2	10
Retest	CAP1-E1-Original	15
	CAP1-E1-Replicate #1	15
	CAP1-E1-Replicate #2	10
	CAP1-E2-Original	15
	CAP2-E1-Original	15
	CAP2-E1-Replicate #1	10

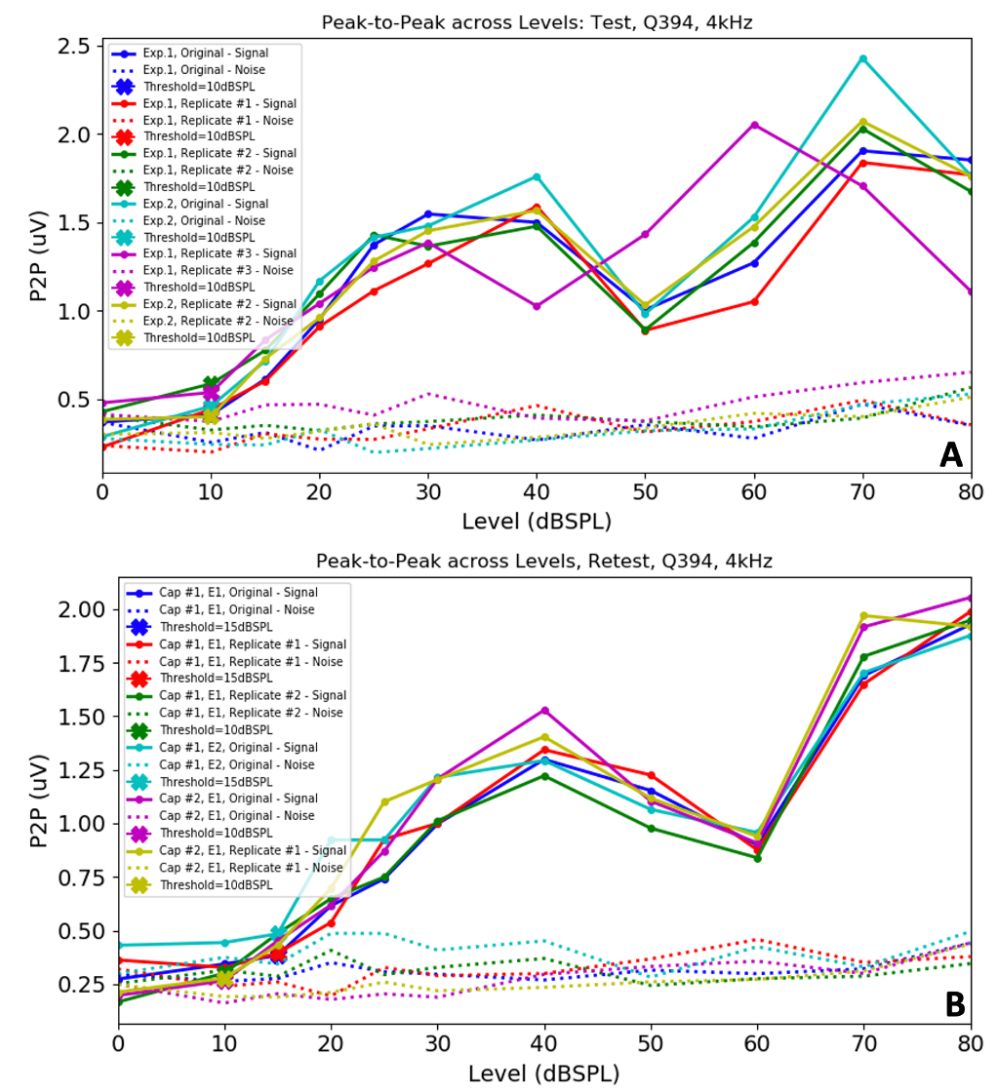

Figure 3.11. Mini cap thresholds for Animal #3. Between the test experiment (see A) and the retest experiment (see B), thresholds were all within the 5-dBSPL range criterion (see Table 3.5 for exact thresholds)

3.3.6 Waveform comparisons

In order to quantify each source of variability, the correlation between two equivalent waveforms (i.e. same frequency, same level) from two waterfalls was computed. These comparisons were then quantified accordingly to assess the effect of each source of variability. For example, to compare X-Time variability, the original waveform was cross correlated to the second waveform collected subsequently (i.e. Replicate #1) for both experimenters.

Table 3.6 shows the breakdown of the possible comparisons for each source of variability according to the ideal experimental designs (see Figure 3.8). It is important to note that the actual number of comparisons depended on which waterfalls were actually collected during the experiment. If all six waterfalls were collected according to each design, then the number of comparisons would be equivalent to the total number of listed possible comparisons. Also, it is necessary to reiterate that for each comparison, only one distinct source of variability was modified while all other sources of variability remained consistent. This was significant in order to understand the impact of each individual source of variability and not a combined impact of multiple sources of variability. For the future correlation figures, each correlation bar will be color coded according to the source of variability it represents (see *Color Code* in Table 3.6).

Table 3.6. Total comparisons representative of each source of variability.

Source of Variability	Color Code	Possible Comparisons	Total Comparisons
X-Time	Red	E1-Original versus E1-Replicate #1 E2-Original versus E1-Replicate #1	2
X-Cap Removal	Blue	E1-Original versus E1-Replicate #2 E1-Replicate #1 versus E1-Replicate #2 E2-Original versus E2-Replicate #1 E2-Replicate #1 versus E2-Replicate #2	4
X-Experimenter	Green	E1-Original versus E2-Original E1-Original versus E2-Replicate #1 E1-Original versus E2-Replicate #2 E1-Replicate #1 versus E2-Original E1-Replicate #1 versus E2-Replicate #1 E1-Replicate #1 versus E2-Replicate #2 E1-Replicate #2 versus E2-Original E1-Replicate #2 versus E2-Replicate #1 E1-Replicate #2 versus E2-Replicate #2	9
X-Cap	Orange	CAP1-Original versus CAP2-Original CAP1-Original versus CAP2-Replicate #1 CAP1-Original versus CAP2-Replicate #2 CAP1-Replicate #1 versus CAP2-Original CAP1-Replicate #1 versus CAP2-Replicate #1 CAP1-Replicate #1 versus CAP2-Replicate #2 CAP1-Replicate #2 versus CAP2-Original CAP1-Replicate #2 versus CAP2-Replicate #1 CAP1-Replicate #2 versus CAP2-Replicate #2	9
X-Day	Teal	Day1-E1-Original versus Day2-E1-Original Day1-E1-Original versus Day2-E1-Replicate #1 Day1-E1-Original versus Day2-E1-Replicate #2 Day1-E1-Replicate #1 versus Day2-E1-Original Day1-E1-Replicate #1 versus Day2-E1-Replicate #1 Day1-E1-Replicate #1 versus Day2-E1-Replicate #2 Day1-E1-Replicate #2 versus Day2-E1-Original Day1-E1-Replicate #2 versus Day2-E1-Replicate #1 Day1-E1-Replicate #2 versus Day2-E1-Replicate #2 Day1-E2-Original versus Day2-E2-Original Day1-E2-Original versus Day2-E2-Replicate #1 Day1-E2-Original versus Day2-E2-Replicate #2 Day1-E2-Replicate #1 versus Day2-E2-Original Day1-E2-Replicate #1 versus Day2-E2-Replicate #1 Day1-E2-Replicate #1 versus Day2-E2-Replicate #2 Day1-E2-Replicate #2 versus Day2-E2-Original Day1-E2-Replicate #2 versus Day2-E2-Replicate #1 Day1-E2-Replicate #2 versus Day2-E2-Replicate #2	18

3.3.7 Correlation analysis, between-cap

The cross-correlation coefficient for each comparison was computed. Specifically, the signal window (i.e. 2 to 8 milliseconds) of one waveform was cross correlated with the signal window of the second waveform. For example, as shown in Figure 3.12, the only X-Time comparison would be the correlation of the signal window of the E1-Original waveform and the signal window of the E1-Replicate #1 equivalent-in-level waveform. No delay was introduced into the correlation calculations due to the same methodological setup between both waveforms. The coefficients ranged from 0 to 1, with 1 indicating two identical waveforms. If the cross-correlation coefficient for a certain comparison was above 0.7, then the two waveforms within that comparison were deemed adequately correlated. If the two waveforms were deemed adequately correlated that would indicate that the particular source of variability the comparison was representing did not evidently influence the waveform morphology. This, in turn, would suggest that the particular source of variability represented by the comparison was minimal.

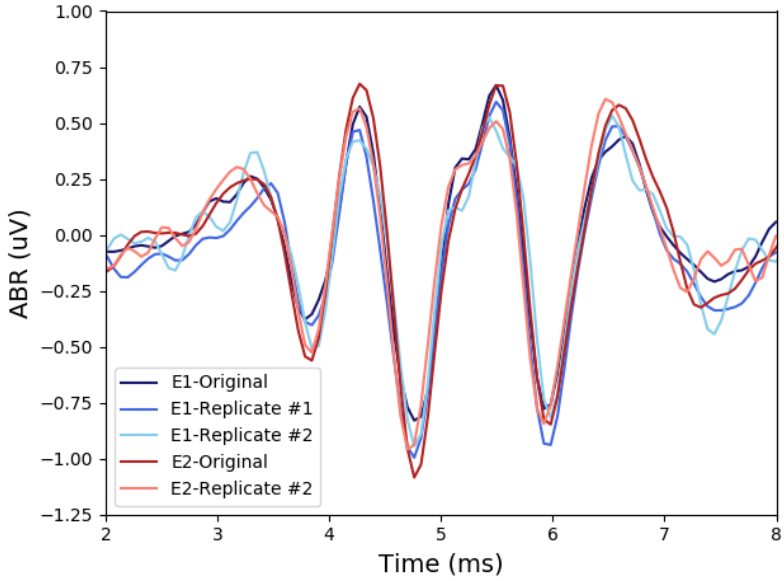

Figure 3.12. Signal window of 60 dBSPL response from each waterfall collected during a single experiment. To quantify each source of variability, responses representing each source of variability were compared directly to one another. For example, the single X-Time comparison that can be made in this example is directly comparing and correlating E1-Original to E1-Replicate #1.

3.3.8 Correlation results

Correlation results for X-Time, X-Removal, X-Cap, and X-Experimenter

For each experiment, the correlation results for a near-threshold level (i.e. 40 dBSPL) and a suprathreshold level (i.e. 80 dBSPL) will be presented. For the correlation results of all levels in each experiment, refer to *Appendix A*. These plots will be color-coded according to the color code referred to in Table 3.6.

For animal #1, the correlation results for animal #1 are shown in Figure 3.13 (test) and Figure 3.14 (retest). A total of six comparisons could be made for the test experiment. T Overall, all six comparisons clearly exceeded the correlation threshold. For the retest experiment, six comparisons were completed. All comparisons were highly correlated. In general, these initial results from the first animal were promising but required more data to gain a more comprehensive understanding.

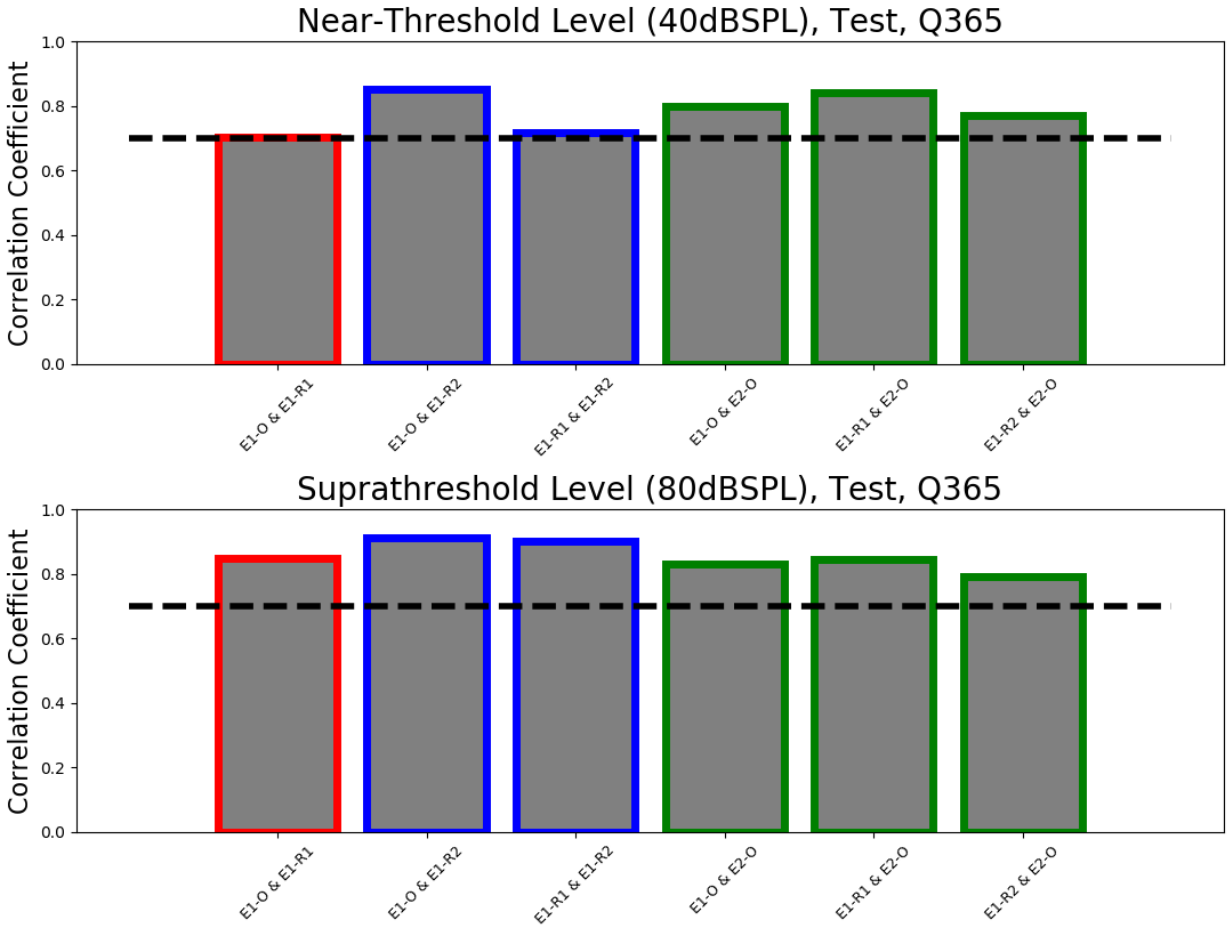

Figure 3.13. Correlation results from animal #1, test experiment. All six comparisons for both levels shown exceeded the correlation criterion, indicating the effect of X-Time, X-Removal, and X-Experimenter variability was minimal for this experiment.

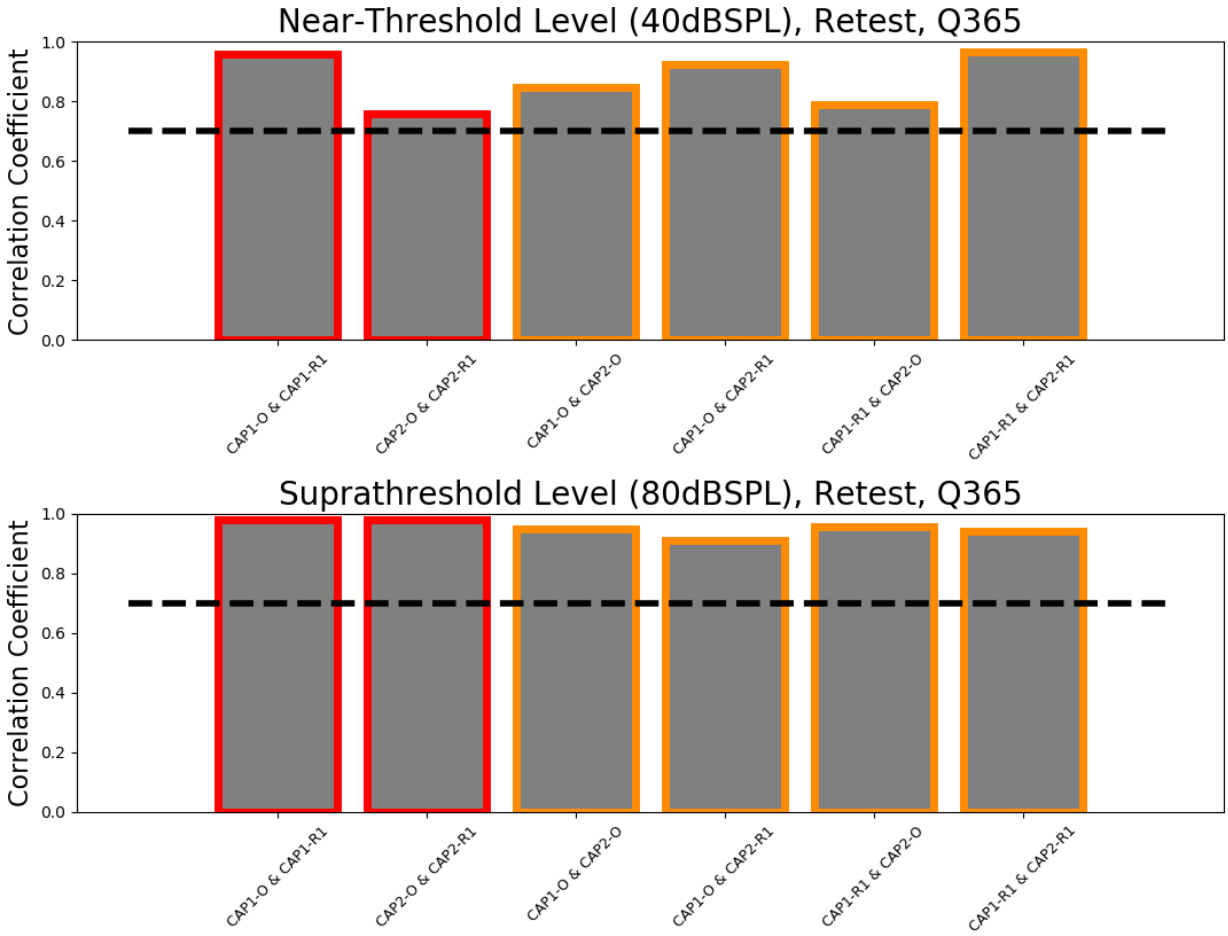

Figure 3.14. Correlation results from animal #1, retest experiment. All six comparisons for both levels shown exceeded the correlation criterion, indicating the effect of X-Time and X-Cap variability was minimal for this experiment.

For animal #2, all comparisons for the test experiment and all comparisons for the retest experiment met the correlation criterion. Visually, the correlation results for a near-threshold level and a suprathreshold level are portrayed in Figures 3.15 and 3.16. These results further demonstrate that across time, across cap removal, and across experimenter, the mini cap produces repeatable and reproducible ABRs.

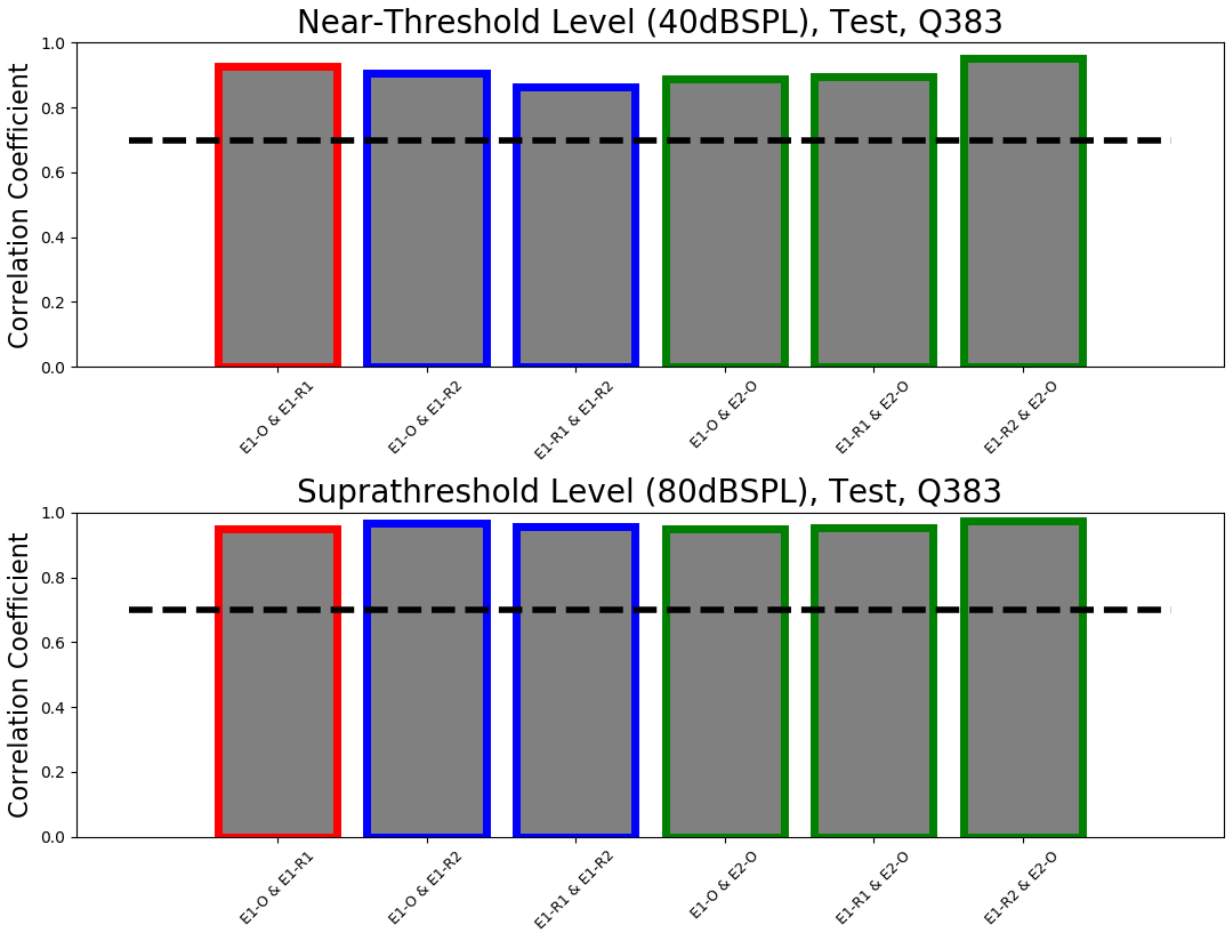

Figure 3.15. Correlation results from animal #2, test experiment. All six comparisons for both levels shown exceeded the correlation criterion, indicating the effect of X-Time, X-Removal, and X-Experimenter variability was minimal for this experiment.

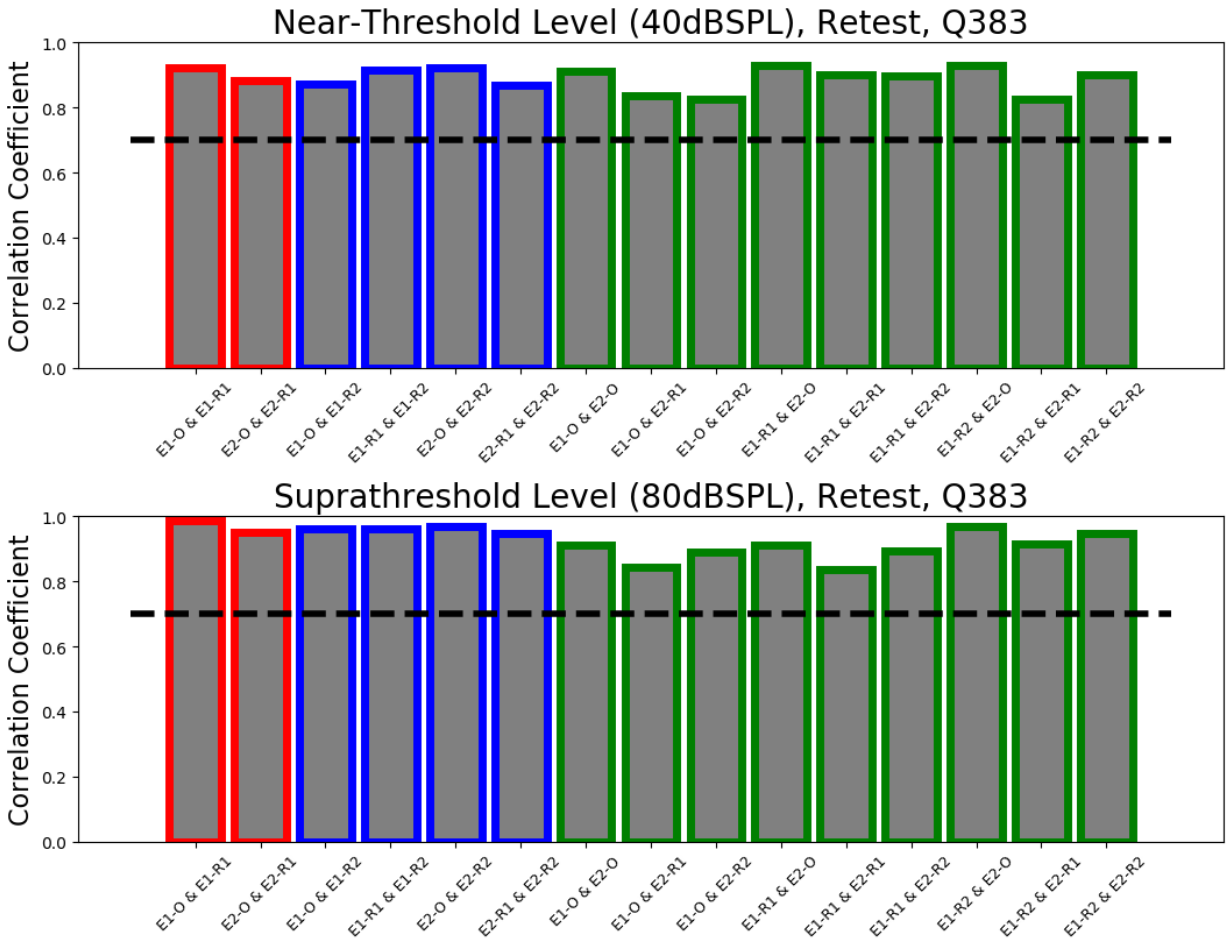

Figure 3.16. Correlation results from animal #2, retest experiment. All fifteen comparisons for both levels shown exceeded the correlation criterion, indicating the effect of X-Time, X-Removal, and X-Experimenter variability was minimal for this experiment.

For animal #3, all comparisons in both the test and retest experiment clearly exceeded threshold (see Figures 3.17 and 3.18). This high correlation consistency across all three animals indicates that the mini cap does produce ABRs that are highly repeatable, reproducible, and reliable. Overall, this suggests that X-Time, X-Removal, X-Experimenter, and X-Cap variability are insignificant and the mini cap is capable of producing consistent ABRs across each of these methodological variations.

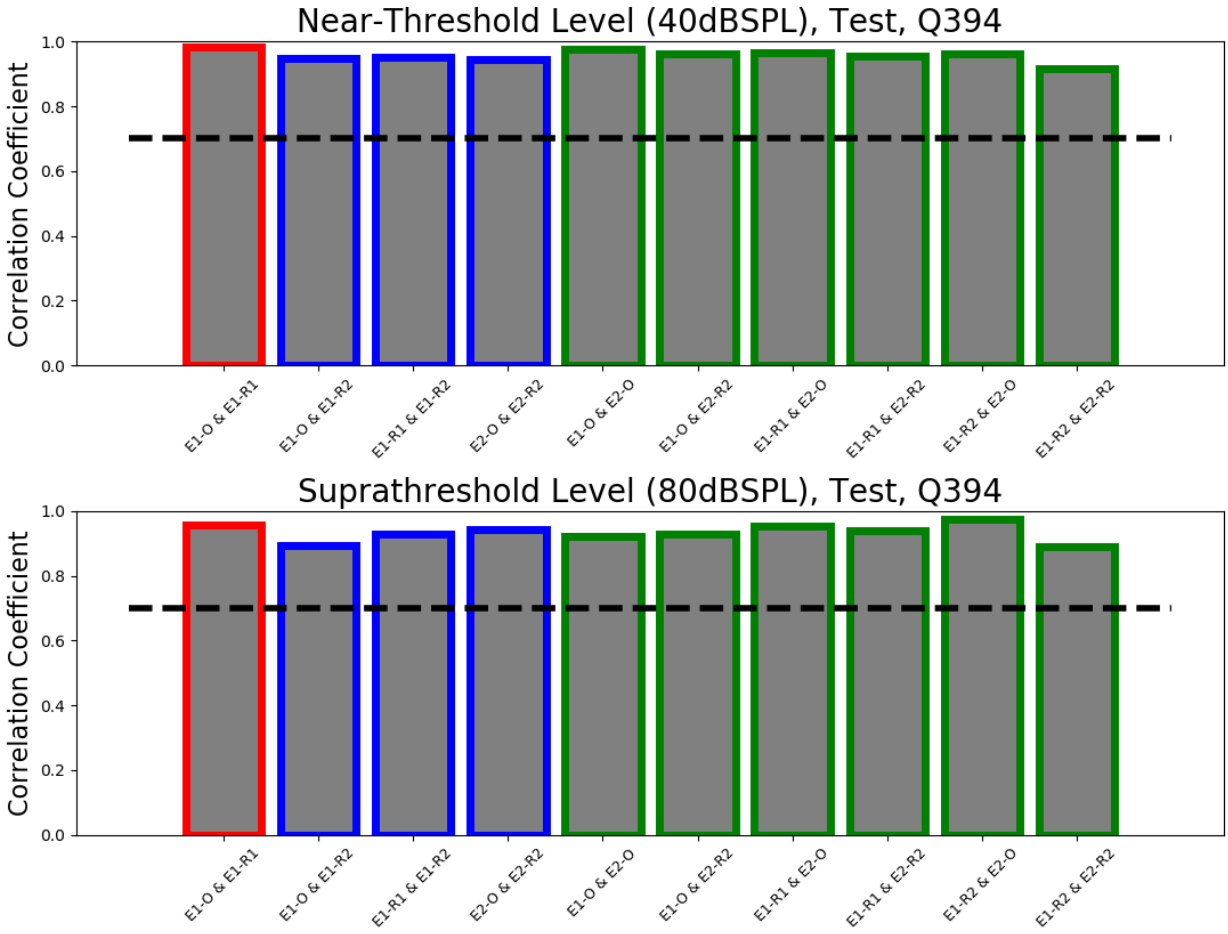

Figure 3.17. Correlation results from animal #3, test experiment. All ten comparisons for both levels shown exceeded the correlation criterion, indicating the effect of X-Time, X-Removal, and X-Experimenter variability was minimal for this experiment.

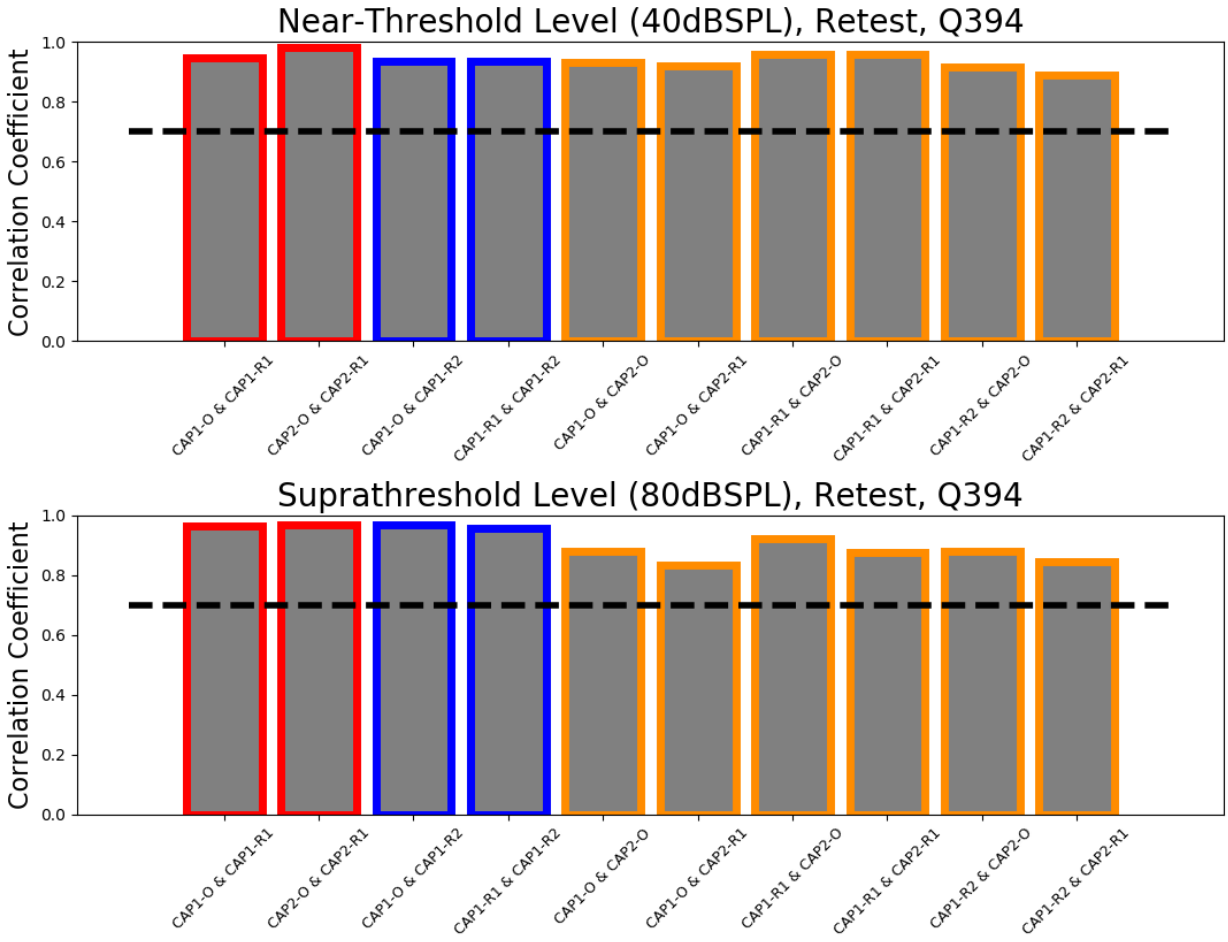

Figure 3.18. Correlation results from animal #3, retest experiment. All ten comparisons for both levels shown exceeded the correlation criterion, indicating the effect of X-Time, X-Removal, and X-Cap variability was minimal for this experiment.

Correlation results for X-Day

Next, the variability from using the cap on the test day versus the retest day will be described for each of the three animals. Across a single comparison, the mini cap (i.e. cap #1 or cap #2) used and the experimenter remained consistent. Thus, these results are representative of only variability associated with using the cap on two different days.

For animal #1, the variability associated with X-Day was minimal. All six comparisons clearly exceeded the correlation threshold for the suprathreshold level although two comparisons did not meet threshold for the near threshold level, as shown in Figure 3.19. However, these two comparisons were still notably positively correlated (e.g., greater than 0.5), so this was still indicative of convincingly correlated waveforms. Thus, in general for animal #1, it appeared that the mini cap provided reliable and reproducible waveforms across two days.

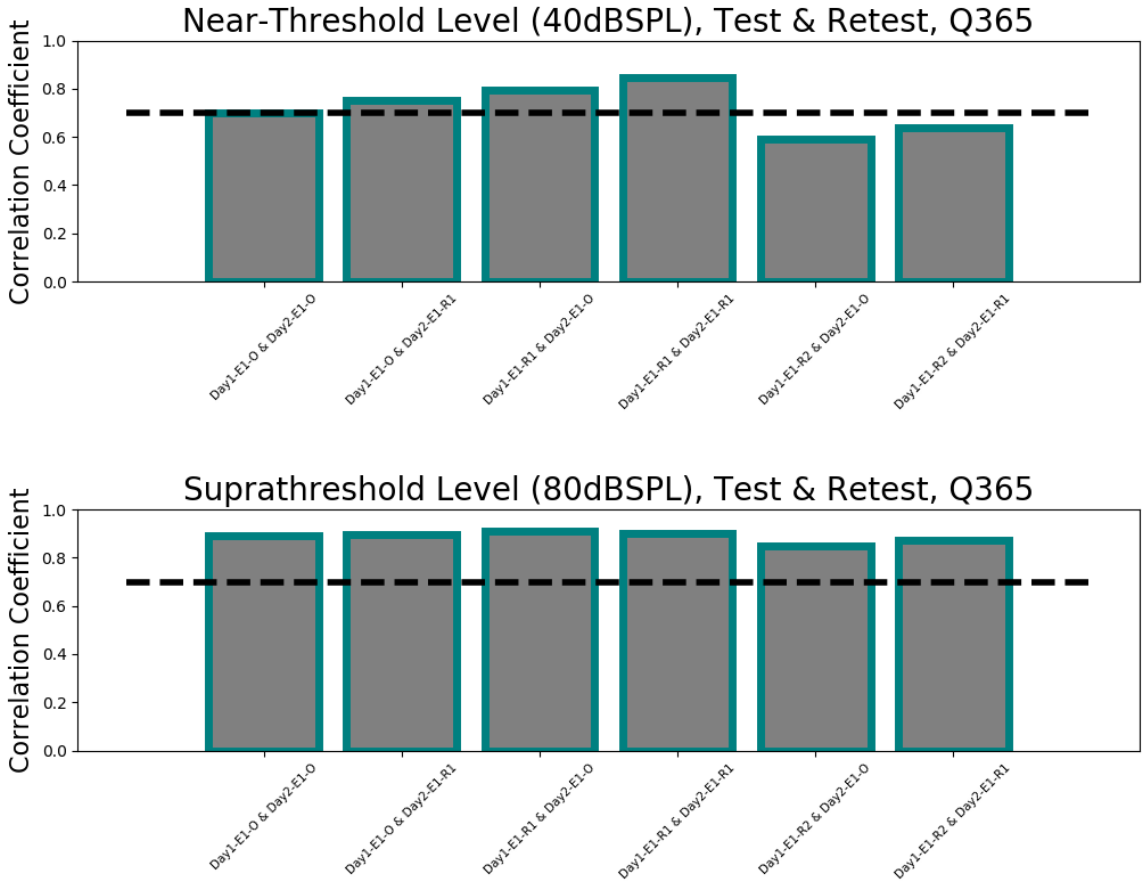

Figure 3.19. Correlation results from X-Day comparisons, animal #1. All six comparisons exceeded the correlation criterion for the suprathreshold level whereas four out of six comparisons met criterion for the near-threshold level. This indicates that X-Day variability, overall, does not appear to impact mini cap ABR responses.

For animal #2, all twelve comparisons similarly met the correlation criterion for both the near threshold and suprathreshold level. The X-Day correlation values for animal #2 are shown in Figure 3.20. These animal #2 results imply that variability due to using the mini cap on two different days does not significantly influence waveform morphology. The mini cap remained repeatable and reproducible across two days.

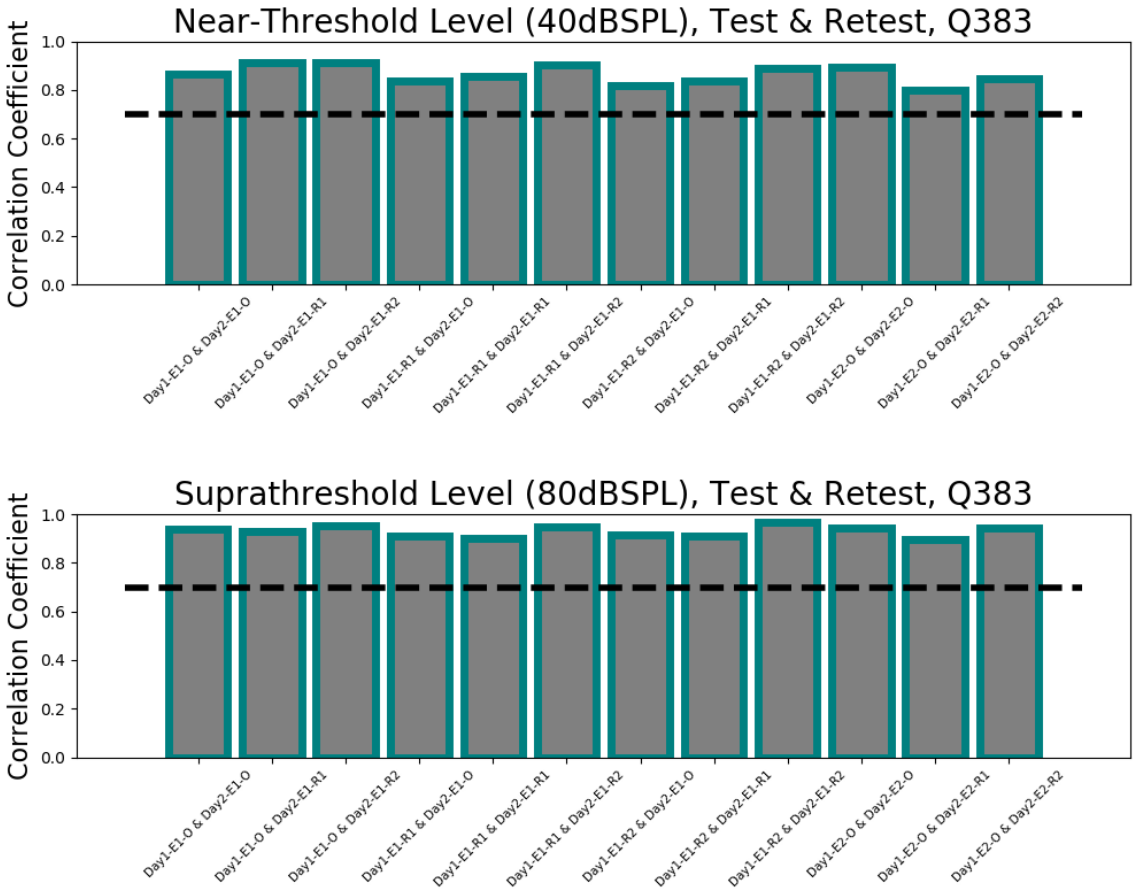

Figure 3.20. Correlation results from X-Day comparisons, animal #2. All twelve comparisons for both the near-threshold and suprathreshold levels exceeded the correlation criterion. This result aligns with the previous animal, suggesting X-Day variability is minimal for the mini cap.

Animal #3 follows the same trend as the previous two animals (see Figure 3.21). For both levels, the correlation for each comparison met the correlation criterion. Consistent across all three animals, the mini cap appears to deliver repeatable and reproducible ABRs across different days. Therefore, X-Day variability seems insignificant.

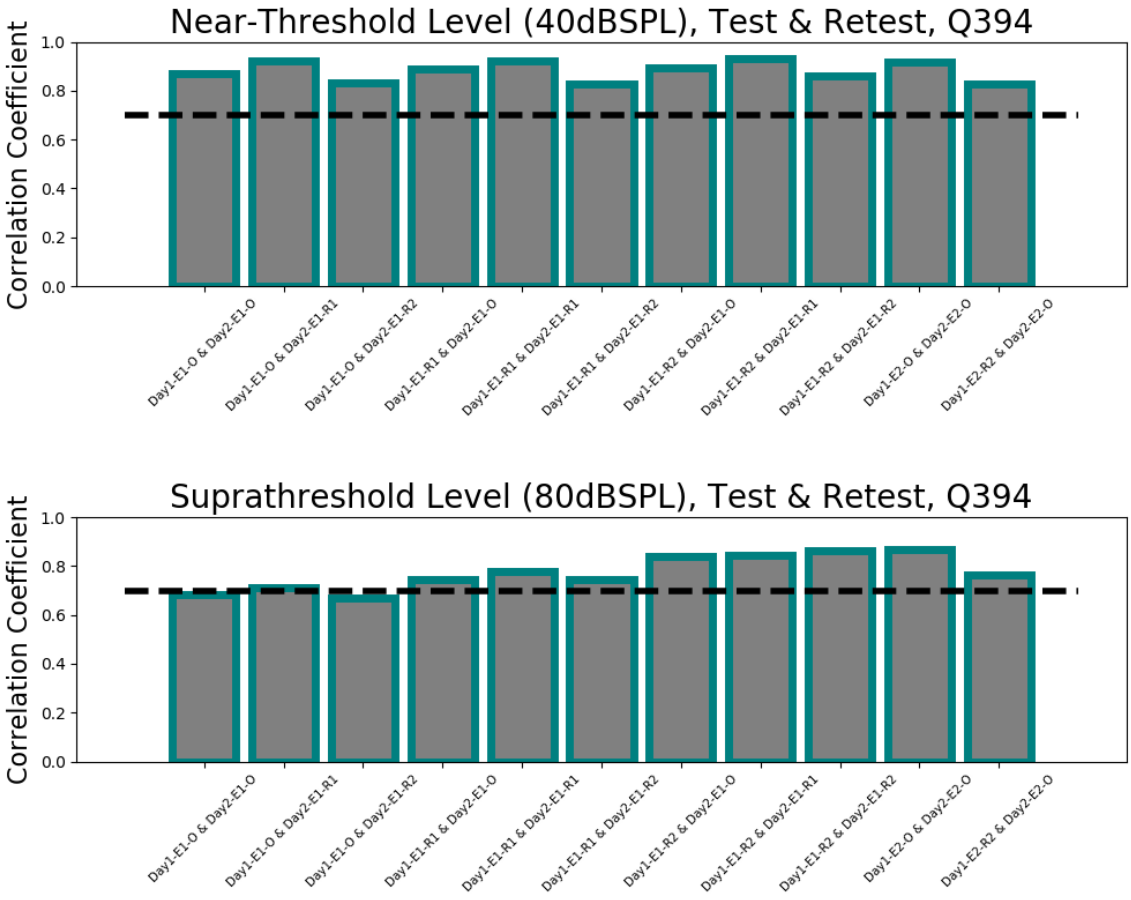

Figure 3.21. Correlation results from X-Day comparisons, animal #3. For both the near-threshold and suprathreshold levels, the correlation criterion was met for each comparison. The overall trend for all three animals demonstrates that, for the mini cap, X-Day variability is insignificant.

Correlation summary for five sources of variability

All comparisons were grouped together and a single average of the correlation for all comparisons representing each source of variability at each corresponding level was computed. The summary results are displayed in Figure 3.22. This analysis provides insight into the similarity in waveform morphology between the two waveforms in each comparison. At levels above threshold where there was a pronounced response (i.e. above 25-30 dBSPL), the correlation threshold was clearly met for all sources of variability. This is reasonable because as level increases, the response itself becomes more well-defined. It does appear

that X-Experimenter variability affected the correlation most notably followed by X-Day in comparison to the other three sources of variability. However, both X-Experimenter and X-Day overall results indicate the waveforms are still highly correlated, implying that X-Experimenter and X-Day variability do not significantly alter the waveform morphology of mini cap ABRs. Altogether, the five sources of variability described (i.e. X-Time, X-Cap Removal, X-Experimenter, X-Cap, and X-Day) did not significantly influence waveform morphology. In general, the sources of variability do not seem to affect the ability for the mini cap to produce reliable, repeatable, and reproducible ABRs. Thus, the mini cap does not seem to be susceptible to any new or additional forms of variability in comparison to the subdermal approach (i.e. the current gold standard), implying a robust methodology producing dependable ABRs from the mini cap.

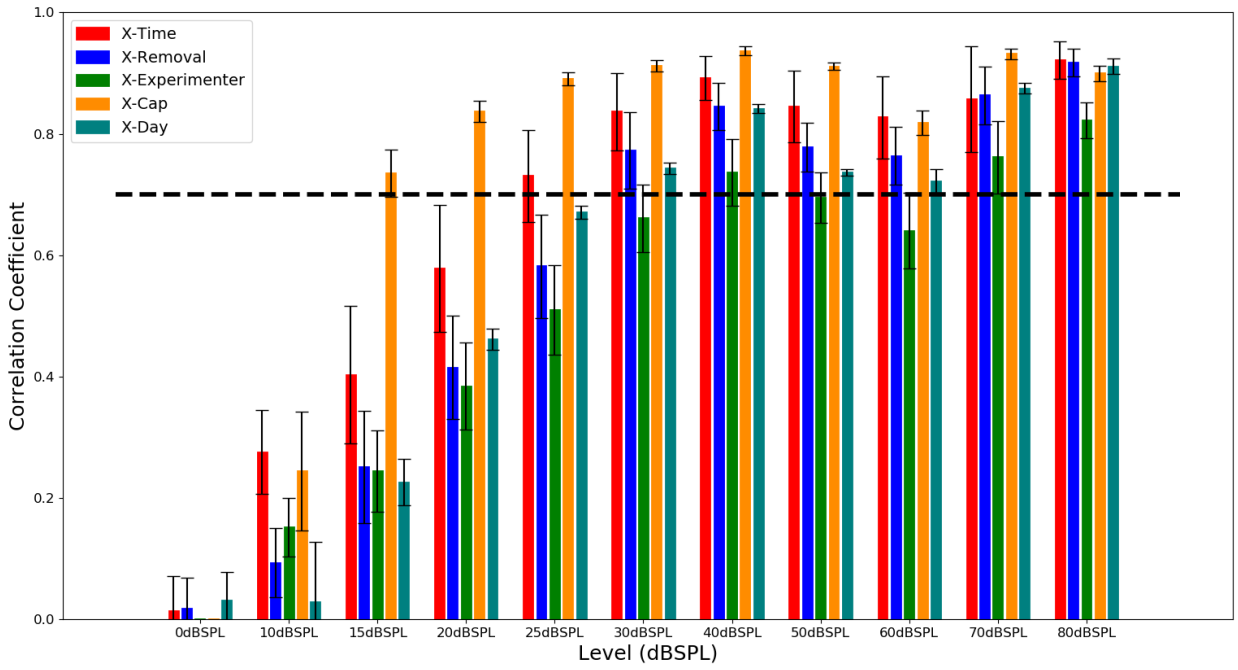

Figure 3.22. Summary of five sources of variability. For each source of variability, all comparisons for each level across all three animals were averaged together. Since at levels above threshold (i.e. 25-30 dBSPL) the average correlation coefficient was above the correlation criterion, it appears that all five sources of variability do not significantly affect the mini cap's ability to produce reliable, repeatable, and reproducible ABRs.

3.3.9 Correlation Analysis, cap versus subdermal

Since the mini cap methodology allows for simultaneous data collection of mini cap ABRs and replicated subdermal ABRs, the same comparisons that were described correlating two mini cap responses to one another were also implemented with the replicated subdermal responses. Therefore, a similar correlation analysis for the replicated subdermal responses was performed. Previously, the signal window of a mini cap response was cross correlated with the signal window of a different mini cap response. Instead, in this analysis, the signal window (i.e. 2 to 8 milliseconds) of one replicated subdermal waveform was cross correlated with the signal window of a second subdermal waveform.

Equivalent subdermal comparisons as shown in Table 3.6 were completed and compared directly to the resulting mini cap comparisons previously detailed. During a single experiment, the subdermal needle electrodes remained consistent and were not replaced, unless one was accidentally removed while placing the mini cap. This became apparent during an experiment because either the offsets of one of the EXG channels would drastically increase and/or the signal would suddenly become very noisy. Therefore, no additional forms of variability were added to the replicated subdermal response as they were for the mini cap response. Since within a single experiment the subdermal needles were not replaced, the comparisons for X-Removal, X-Experimenter, and X-Cap were theoretically equivalent to additional X-Time comparisons for subdermal responses.

Statistical testing was performed for between-cap and between-subdermal equivalent comparisons for each source of variability. More specifically, a paired two-way t-test was performed to compare the between-cap correlations and the between-subdermal comparisons for each level and each source of variability. Here, the null hypothesis states that there was no difference (i.e. for a specific level and source of variability) between the mean correlation of between-cap and the mean correlation of between-subdermal comparisons. If the null hypothesis was rejected (i.e. $p < 0.05$), visually shown with an asterisk, there was a statistical difference between the correlations of the two methodologies. Overall, for each source of variability, eleven t-tests were conducted for each of the eleven intensity levels.

Since the waveforms in each comparison were equivalent in methodology and, thus the delays, if any, should be equivalent, no delay was introduced into the correlation calculations. These results provided insight into the capability of each methodology to produce highly correlated ABR responses as different sources of variability are introduced. Figure 3.23 illustrates two level conditions and the corresponding cap and subdermal responses for both. As shown, cross correlating the two mini cap responses, shown in red, would signify the effect of X-Time variability for the mini cap methodology. Cross correlating the two subdermal responses, shown in green, would represent an equivalent X-Time comparison for the subdermal needle methodology.

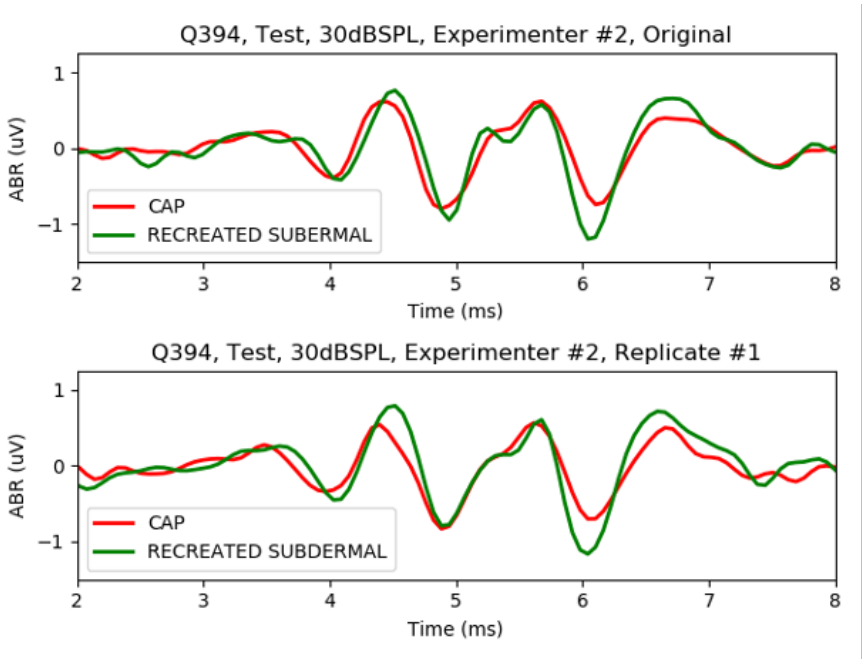

Figure 3.23. Cross correlation of two cap responses and two subdermal responses. An example from two waterfalls of a single experiment is depicted: E2-Original (see top) and E2-Replicate #1 (see bottom). Since subdermal responses were recorded concurrently to mini cap responses, equivalent comparisons can be performed for subdermal responses. Here, a single X-Time comparison can be performed: E2-Original versus E2-Replicate #1. The mini cap X-Time comparison involved cross correlating the signal window of the two red waveforms in the top and bottom plots. The subdermal X-Time comparison required cross correlating the signal window of the two green waveforms shown. The result was two correlation values, one representative of X-Time variability for the mini cap method and the other representative of X-Time variability for the subdermal method.

Out of the five total sources of variability studied, only two sources of variability, X-Time and X-Day, were truly representative of both cap and subdermal data collection. For both of these sources, the sources of variability introduced into the mini cap method and into the subdermal method were equivalent. Since neither the mini cap or subdermal needles were altered during the first original waterfall and the second replicate #1 waterfall, the resulting correlations from X-Time comparisons of between-cap responses and between-subdermal responses can be related to one another. Additionally, X-Day comparisons utilized a single waterfall from one day and a second waterfall from a different day. Thus, both mini cap and subdermal comparisons are portraying equivalent variability of performing the methodology on two separate days.

X-Time correlations, shown in Figure 3.24, were not statistically different for between-cap in comparison to between-subdermal comparisons. This suggests that both the mini cap and subdermal methods can produce reliable and repeatable ABRs within a short period of time under the same conditions. The X-Day correlation analysis (see Figure 3.25) suggests that the mini cap produces slightly less variable ABRs across two days than the subdermal procedure. In fact, at levels above 20 dBSPL (besides 60 dBSPL where the typical peak-to-peak notch appeared), the mini cap produced statistically greater mean correlation values across comparisons than the subdermal method. Thus, the mini cap provided more reliable and reproducible ABRs across two days than the subdermal method.

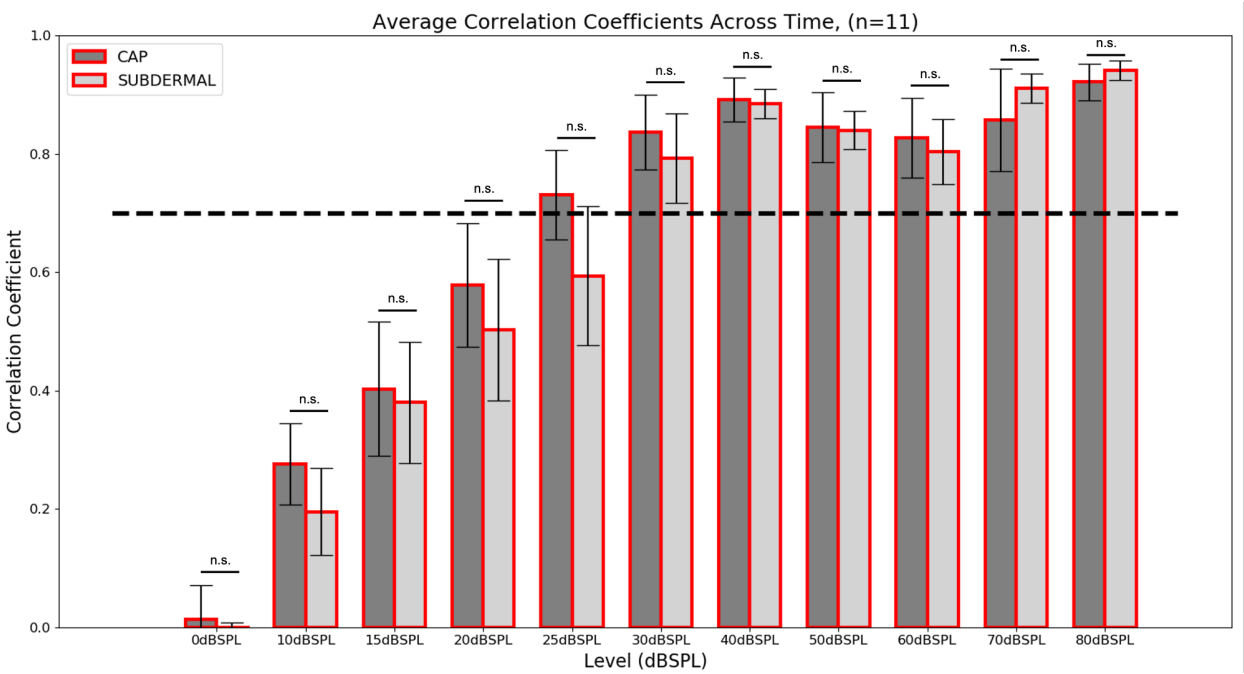

Figure 3.24. X-Time Summary Figure for between-cap and between-subdermal comparisons. X-Time comparisons for both between-cap and between-subdermal were statistically equivalent because in both cases the only changing element in each comparison was the time of data collection. These results indicate that, within a short period of time under the same conditions, both the mini cap and subdermal needles can produce reliable and repeatable responses.

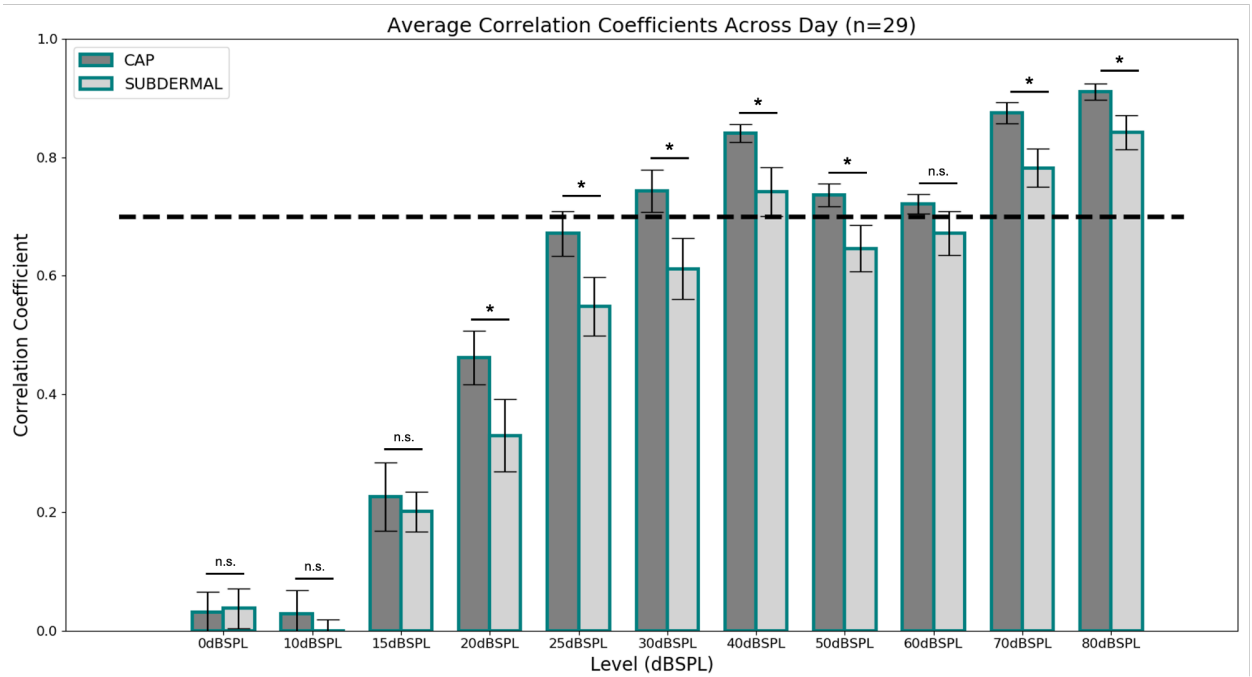

Figure 3.25. X-Day Summary Figure for between-cap and between-subdermal comparisons. Similar to X-Time variability, X-Day comparisons can be performed for both cap and subdermal responses. This is because for each day of the X-Day comparison, both the mini cap and subdermal needles were placed. This result suggests that the mini cap produces statistically less variable ABRs across two days than the subdermal method, suggesting greater X-Day reliability and reproducibility of the mini cap.

As previously described, the X-Removal, X-Experimenter, and X-Cap were only representative of variability introduced into the mini cap. The equivalent subdermal comparisons were technically additional X-Time comparisons since the only element changing for subdermal responses within a single experiment was time of data collection. Thus, the subdermal correlation comparisons for these three types of variability can be equated to a control measure. It is important to note that the mini cap comparisons involve changing or altering the mini cap response in a more significant way than, for example, in an X-Time comparison where the only changing element is time of data collection.

The summary figures for these three sources of variability are portrayed in Figures 3.26, 3.28, and 3.27. For X-Cap, the correlation was notably high at lower levels for between-cap in comparison to between-subdermal. A potential reason for this occurrence is, for the ten X-Cap comparisons, threshold for each waterfall was around 10 dBSPL. This means that the response at 15 dBSPL was more distinct than for the waterfalls with higher thresholds. Additionally, the X-Cap comparison had a small sample size in comparison to, for example X-Experimenter or X-Removal, so increasing the X-Cap sample size would be beneficial. With the comparisons completed, the X-Cap mini cap correlations were statistically greater than the theoretical equivalent X-Time subdermal correlations, indicating that using a different mini cap did not affect the resulting ABRs. For X-Removal, the mini cap correlations were slightly higher than the subdermal correlations for all levels above 30 dBSPL, although not statistically significant. Since the subdermal correlations were only representing X-Time variability and X-Removal variability involved removing and replacing the instrument, it is notable that the mini cap produced slightly higher correlated responses even when the greater variability of removing and replacing the cap was introduced. Finally, for X-Experimenter, the comparisons for the mini cap seemed considerably more equivalent to those of the subdermal method. Since having two experimenters place the instrument was a more drastic introduction of variability than repeating a measure over a short period of time, it is still encouraging that the X-Experimenter mini cap correlations here align well the subdermal correlations, again representing X-Time.

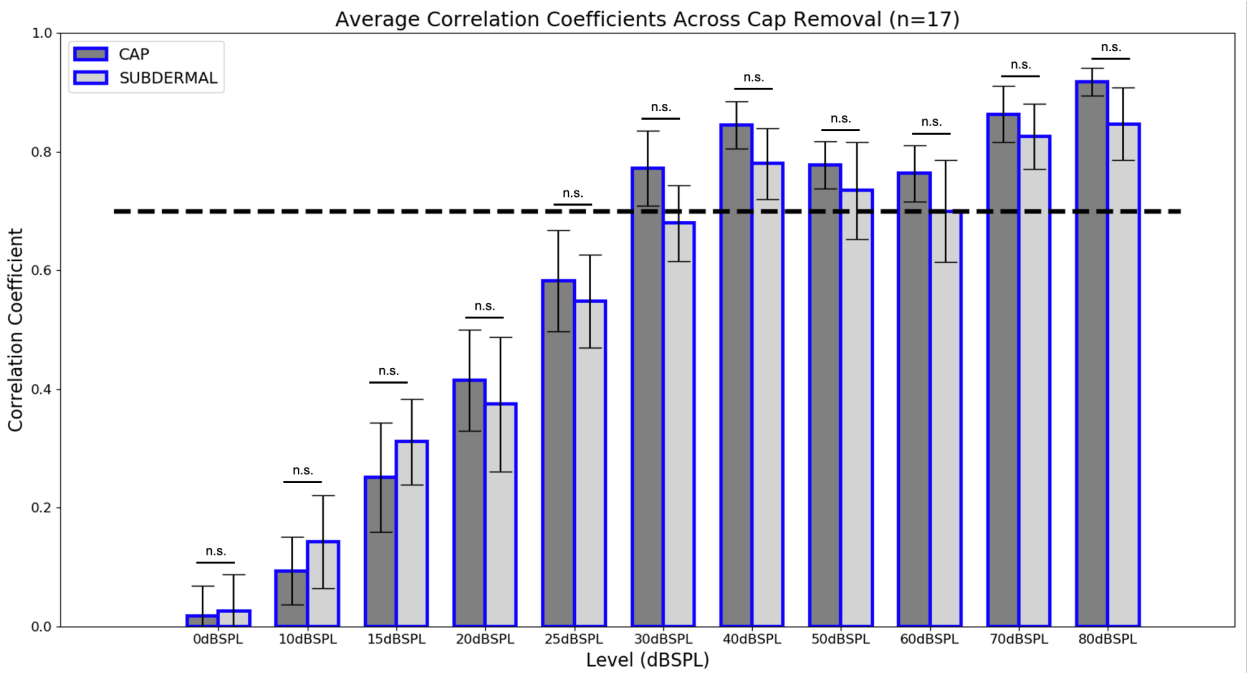

Figure 3.26. X-Removal Summary Figure for between-cap and between-subdermal comparisons. Since subdermal needle electrodes were not replaced within a single experiment, here, X-Removal variability was only relevant for cap responses and subdermal comparisons act as a control comparison. Statistically, the between-cap and between-subdermal comparisons were similar. However, since the cap correlation values appear slightly more correlated at levels above 30 dBSPL than the control subdermal correlations and are all above the correlation criterion, it appears that X-Removal variability is minimal for the mini cap.

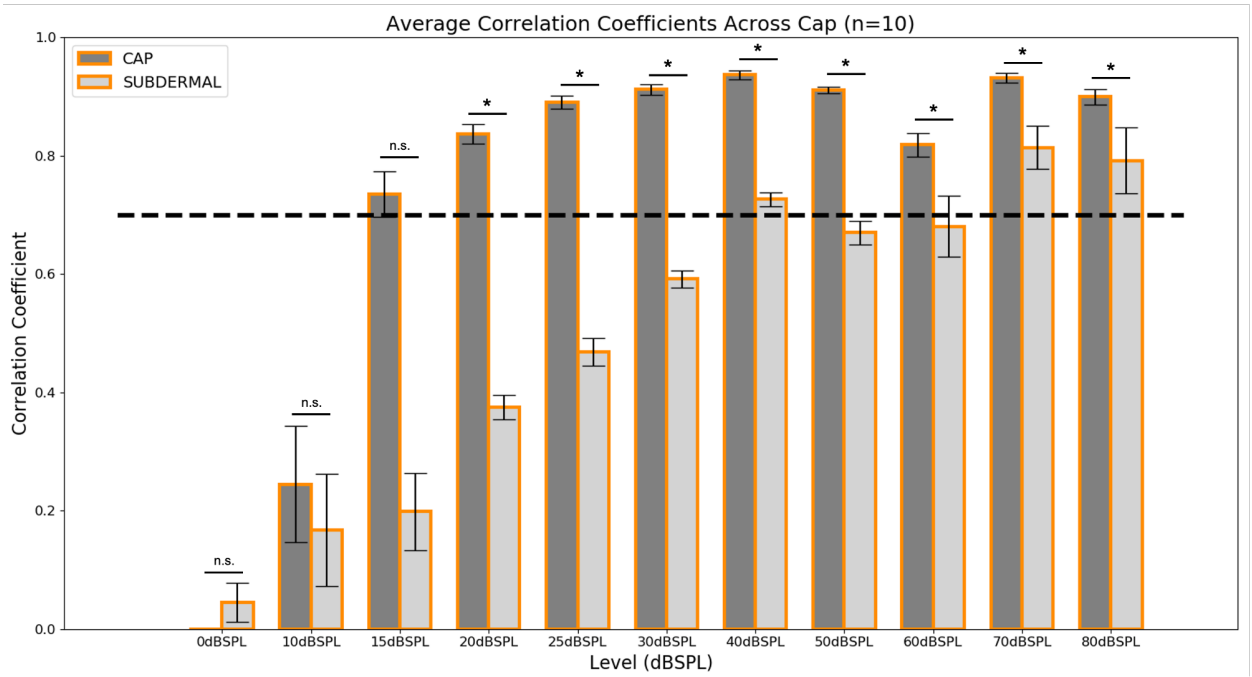

Figure 3.27. X-Cap Summary Figure for between-cap and between-subdermal comparisons. Again, subdermal comparisons here acted as a control comparison since subdermal needle electrodes were not replaced within a single experiment. X-Cap correlation values were statistically greater than the equivalent control subdermal comparisons. This strongly suggests that changing the mini cap does not impact the resulting mini cap ABR response.

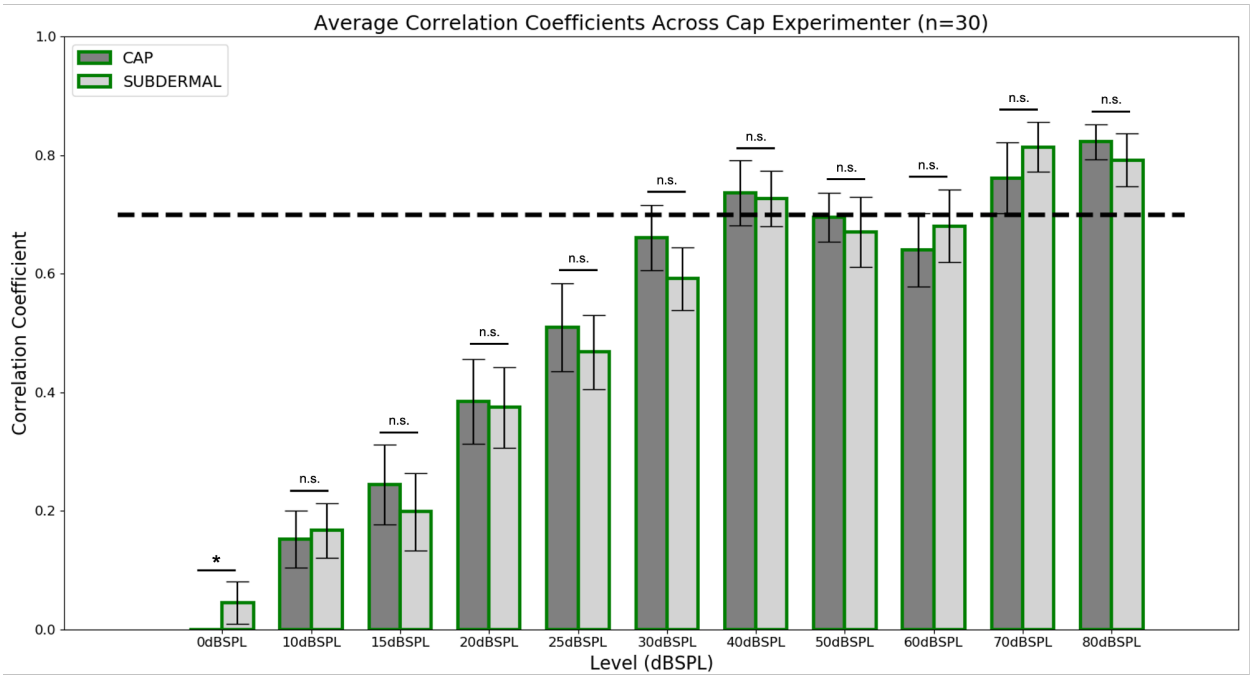

Figure 3.28. X-Experimenter Summary Figure for between-cap and between-subdermal comparisons. For X-Experimenter, the correlation values for mini cap and subdermal comparisons were more comparable and statistically equivalent. However, since the subdermal responses were acting as a control measure here, this suggests that having two experimenters place the mini cap produces equivalently correlated responses to collecting a repeat measure using the subdermal needles.

3.3.10 Validity of mini cap

Finally, validity refers to the extent to which the method truly measures what it is proposed to measure. A measure is deemed valid if it is both accurate and precise. Accuracy refers to the closeness of agreement between the measured quantity value and a true quantity value of the measurand [79]. Precision refers to the closeness of agreement between indications or measured quantity values obtained by replicate measurements on the same or similar objects under specified conditions [79]. Figure 3.29 shows a simple visualization of how precision and accuracy relate to one another and how they differ from each other. For both precision and accuracy, the experimental measures were compared to a certain gold standard measure. The gold standard for accuracy was the replicated subdermal needle response. For precision, the gold standard was the average response across all trials and across all good channels.

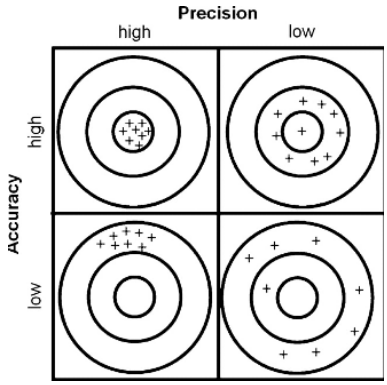

Figure 3.29. Validity Definition [80]. For a method to be considered valid, it must be both accurate and precise.

Accuracy of mini cap

Comparing the mini cap responses directly to replicated subdermal responses provides insight into whether the mini cap is providing accurate measures. This analysis will be separated into two parts: (1) threshold comparisons and (2) correlation analysis of mini cap versus subdermal responses. The design of this accuracy analysis is depicted in Figure 3.30. The gold standard was defined as the replicated subdermal response.

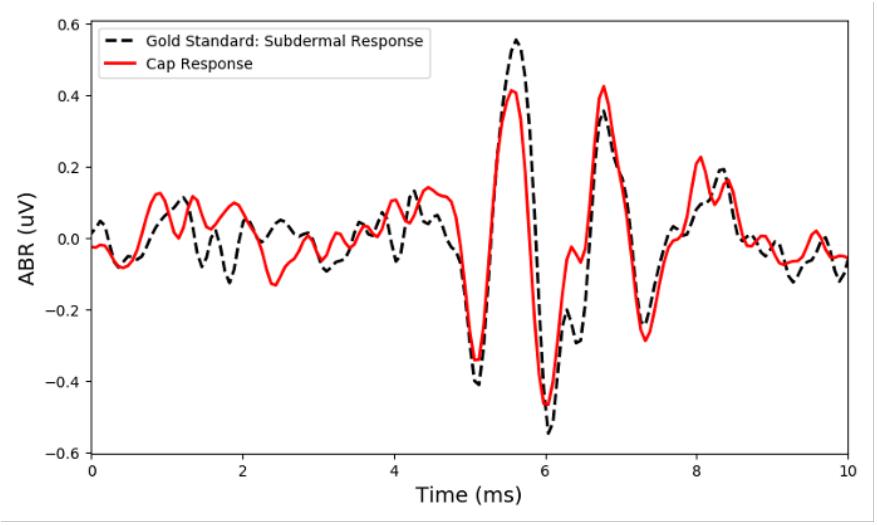

Figure 3.30. Visualization of cap response and gold standard to quantify accuracy. Here, the gold standard was the subdermal response because that is the traditional ABR methodology.

Since thresholds are a critical measure used to measure hearing loss, ensuring the mini cap provides accurate thresholds is of critical importance. To achieve this, the same threshold analysis as previously described was completed for the mini cap responses and then for the replicated subdermal responses. Thresholds for each mini cap and subdermal ABR waterfall were compared directly to one another. Consistent with previous comparisons, the objective was for the mini cap threshold and the subdermal threshold to meet the 5 dBSPL criterion. Since the subdermal threshold was considered the ”true” threshold, if the mini cap threshold was close in value to the subdermal threshold, the mini cap threshold would be considered accurate.

For the first animal, each threshold comparison indicates that the mini cap was producing accurate waterfalls. Except for one comparison, each mini cap threshold was within 5 dBSPL range of the subdermal threshold. Results are shown in Table 3.7 and Figure 3.31.

Table 3.7. Animal #1 mini cap and subdermal thresholds.

Experiment	Waterfall	Cap Threshold (dBSPL)	Subdermal Threshold (dBSPL)
Test	E1-Original	20	15
	E1-Replicate #1	15	20
	E1-Replicate #2	10	20
	E2-Original	10	15
Retest	CAP1-Original	10	10
	CAP1-Replicate #1	10	10
	CAP2-Original	10	10
	CAP2-Replicate #1	10	10

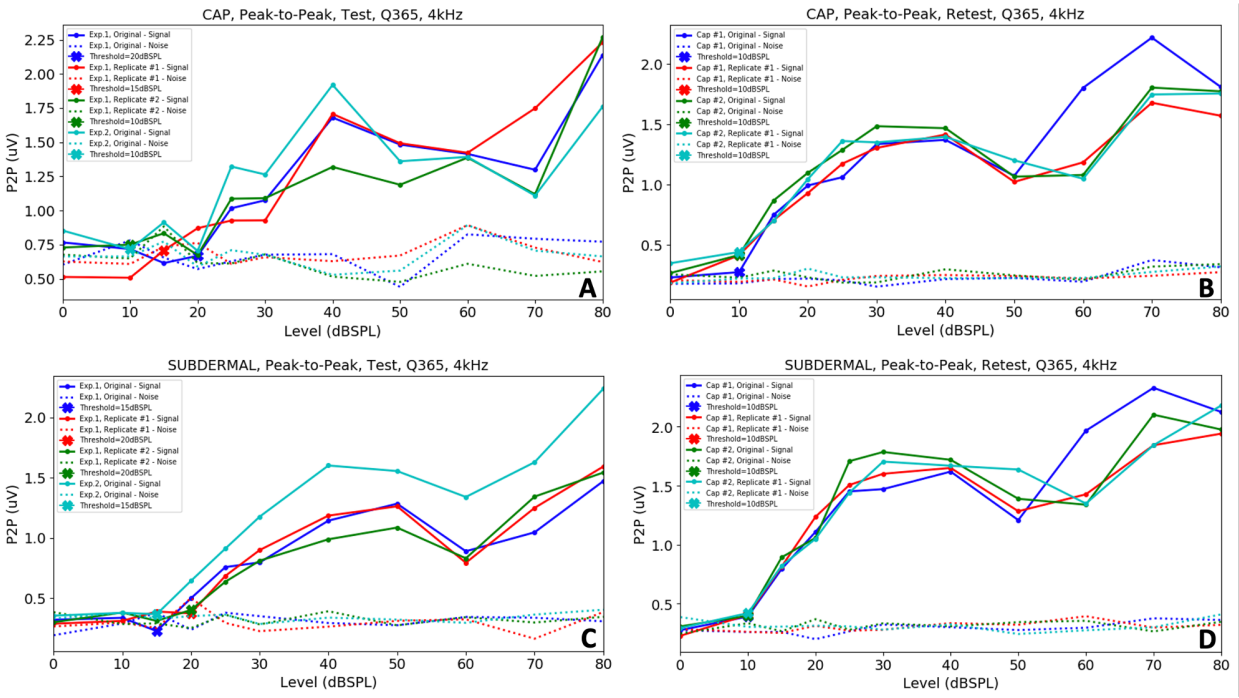

Figure 3.31. Mini cap and subdermal thresholds for Animal #1. Comparing thresholds from the mini cap (see A and C) to the "true" subdermal thresholds (see B and D) suggests that, for animal #1, the mini cap thresholds were accurate. See Table 3.7 for exact thresholds.

The second animal presented a similar finding. For the test experiment, all comparisons met threshold. Five out of six waterfalls during the retest experiment were consistent as well. However, with respect to the last waterfall (i.e. Exp. 2, Replicate #2) during the retest experiment, the vertex subdermal needle electrode was accidentally displaced during replacement of the mini cap and this was not realized until after the waterfall was collected. Thus, for this single comparison, the subdermal threshold was not applicable. Table 3.8 and Figure 3.32 illustrate these results for animal #2.

Table 3.8. Animal #2 mini cap and subdermal thresholds.

Experiment	Waterfall	Cap Threshold (dBSPL)	Subdermal Threshold (dBSPL)
Test	E1-Original	15	20
	E1-Replicate #1	20	20
	E1-Replicate #2	10	10
	E2-Original	10	15
Retest	E1-Original	25	20
	E1-Replicate #1	25	20
	E1-Replicate #2	20	20
	E2-Original	20	20
	E2-Replicate #1	15	20
	E2-Replicate #2	20	N/A

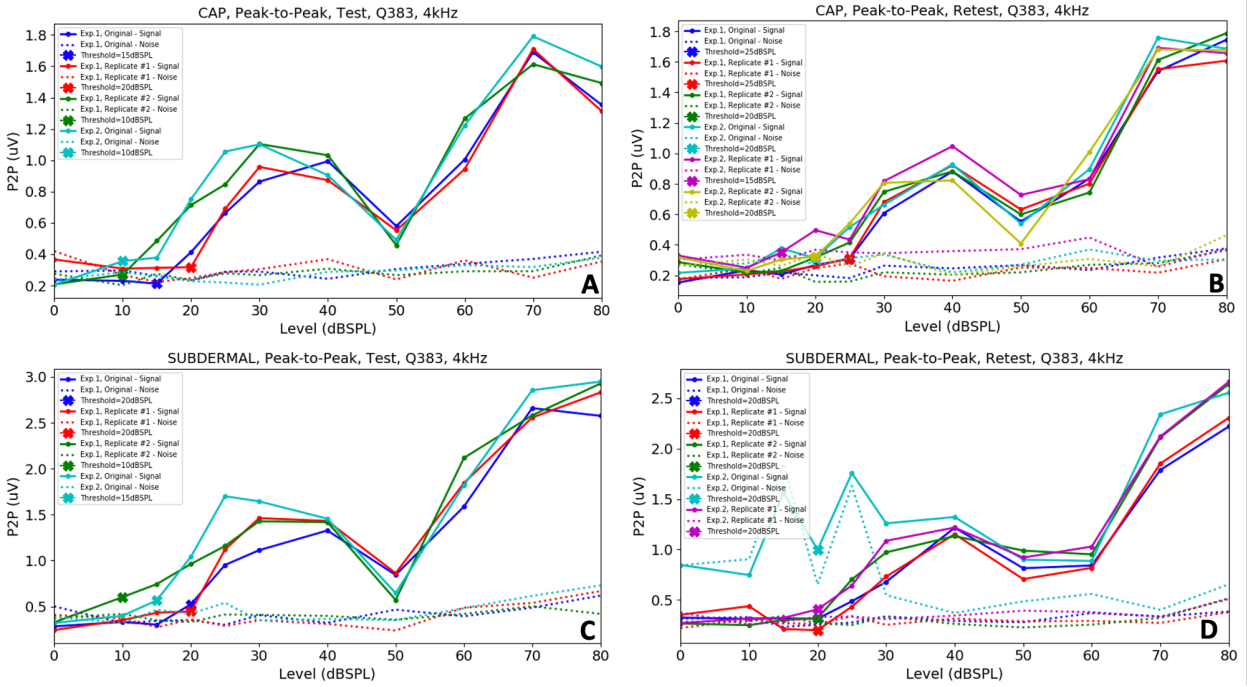

Figure 3.32. Mini cap and subdermal thresholds for Animal #2. The vertex subdermal needle accidentally was displaced during the Exp. 2, Replicate #2 waterfall, so no threshold could be determined for this waterfall. For Animal #2, mini cap thresholds (see A and C) aligned closely with subdermal thresholds (see B and D), again indicating accurate mini cap thresholds. Table 3.8 shows exact thresholds.

Finally, the third animal confirms the capability of the mini cap to produce accurate ABR thresholds. In comparison to the subdermal thresholds (i.e. the gold standard), the mini cap thresholds were considerably equivalent. For the entire waterfall collected for Cap #1-E2-Original and the last four levels collected for Cap #2-E1-Original, the mastoid electrode was misplaced, leading to noisy responses. Thus, no accurate threshold could be determined for these two waterfalls due to the magnitude of noise present in the subdermal response. The summary of this analysis is included in Table 3.9 and Figure 3.33.

Table 3.9. Animal #3 mini cap and subdermal thresholds.

Experiment	Waterfall	Cap Threshold (dBSPL)	Subdermal Threshold (dBSPL)
Test	E1-Original	10	10
	E1-Replicate #1	10	20
	E1-Replicate #2	10	10
	E2-Original	10	10
	E2-Replicate #1	10	20
	E2-Replicate #2	10	10
Retest	CAP1-E1-Original	10	15
	CAP1-E1-Replicate #1	15	10
	CAP1-E1-Replicate #2	10	15
	CAP1-E2-Original	15	N/A
	CAP2-E1-Original	10	60
	CAP2-E1-Replicate #1	10	15

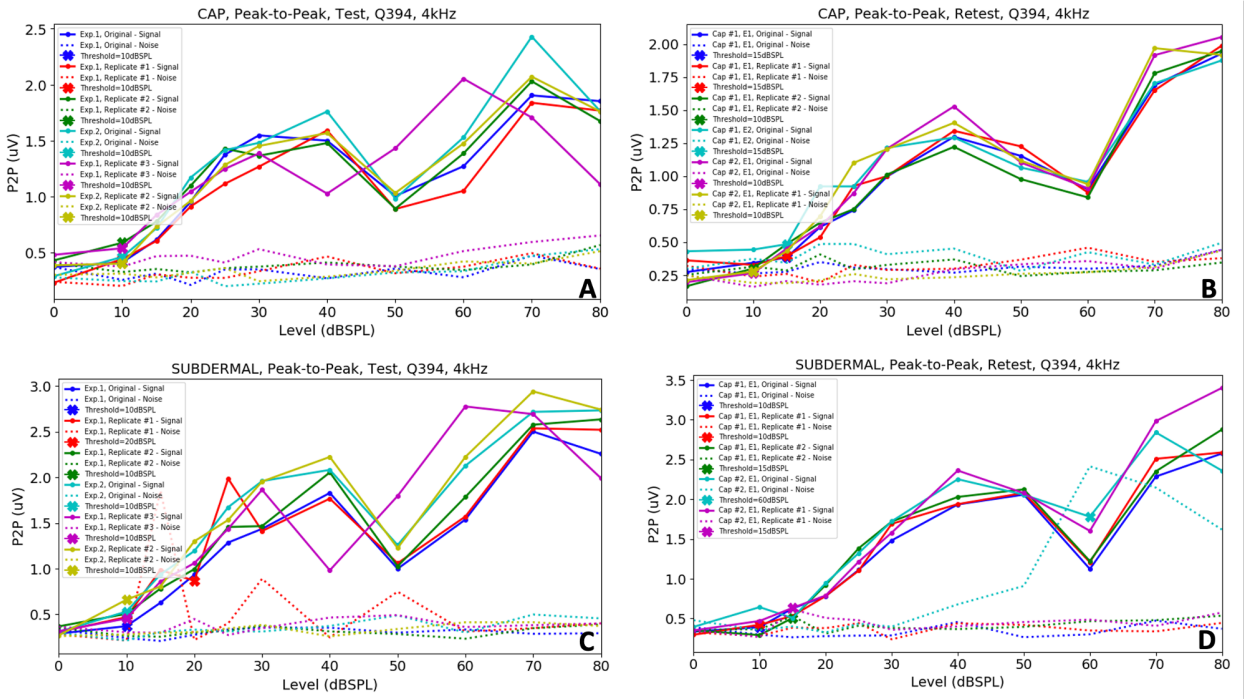

Figure 3.33. Mini cap and subdermal thresholds for Animal #3. The mastoid subdermal electrode was accidentally displaced during the Cap #1-E2-Original and Cap #2-E1-Original waterfalls, so subdermal thresholds were not determined for these two waterfalls. Animal #3 displays accurate mini cap thresholds (see A and C) as well, with the subdermal thresholds (see B and D) acting as the gold standard thresholds. Exact thresholds are shown in Table 3.9.

To further quantify whether the mini cap was accurate with regard to waveform morphology, a correlation analysis was performed. In this analysis, the signal window (i.e. 2 to 8 ms) of a mini cap response (i.e. average of good channels) was correlated to the signal window of the replicated subdermal response. The delay between the mini cap and subdermal responses was inspected and deemed minimal. Thus, the correlation function did not incorporate a delay between the cap response and the subdermal response.

Here, to avert any potential for variability affecting the correlation results, the only comparisons produced were representative of simultaneous data collection. This means that, for each waterfall collected, the mini cap response was directly correlated to the replicated subdermal response recorded concurrently. Theoretically, there should be no additional sources of variability present between these two responses since they were recorded simultaneously. A total of 31 waterfalls were collected across four animals, equating to a total of 31 comparisons. The three noisy subdermal waveforms due to a displaced subdermal needle electrode mentioned previously were not included in this analysis. Figure 3.34 portrays the average correlation value for each level across all 31 comparisons. Notably, the correlation of the mini cap to the equivalent subdermal response was compelling across all levels above 30 dB-SPL, aligning with the previous correlation results in which higher, more pronounced levels above threshold provoked greater correlation. Since the mini cap waveforms were highly correlated with the subdermal waveforms, and the subdermal waveforms, for this analysis, were considered the gold standard, the mini cap produced highly accurate ABRs.

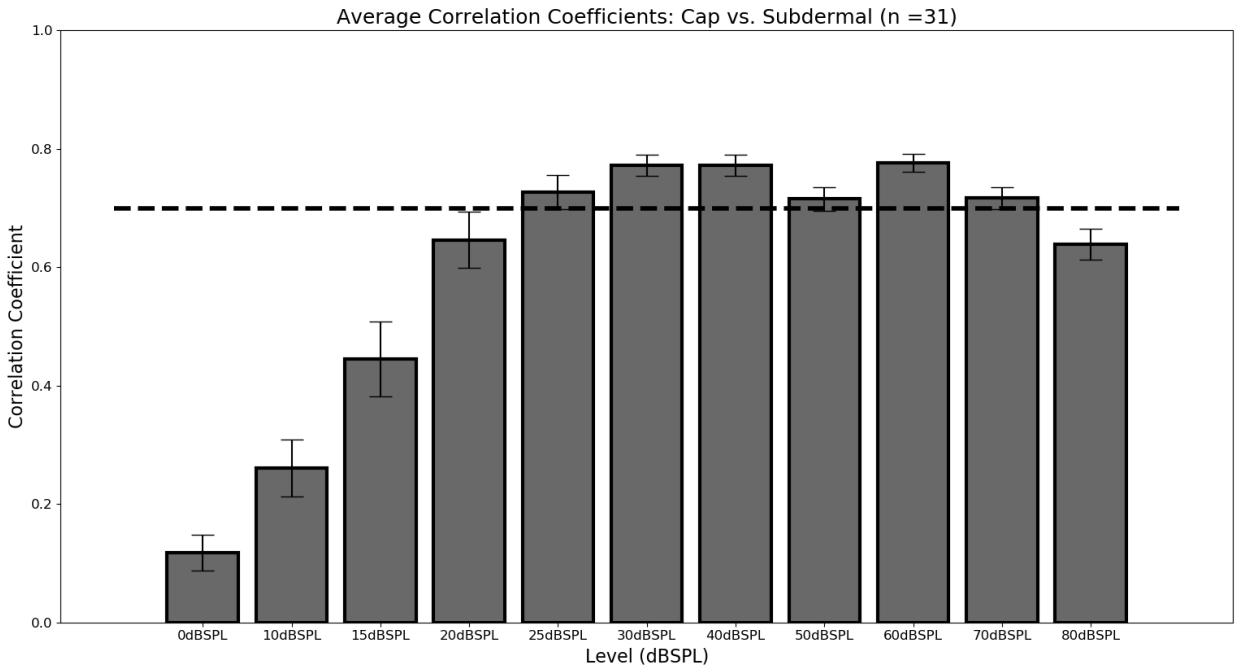

Figure 3.34. Cap versus subdermal correlation analysis results. Here, the signal window of a mini cap response was cross correlated with the signal window of the concurrent subdermal response. Only comparisons representative of simultaneous data collection were performed. It appears that at levels above 30 dBSPL, the cap response was highly correlated to the subdermal response. Therefore, since the subdermal response is the gold standard, it has been shown that the mini cap was producing accurate ABR responses.

Precision of mini cap

To determine the precision of the mini cap, a large data set was divided into theoretical replicate measurements. For a large data set with about 10,000 repetitions, the first 1000 repetitions were averaged together and compared to the average of the subsequent 1000 repetitions. This was completed for each grouping of 1000 repetitions. Figure 3.35 shows the resulting averaged waveform for each grouping of 1000 repetitions. It appears that each grouping of 1000 repetitions averaged together generated a highly comparable ABR to the gold standard (i.e. the average of all 10,000 repetitions). This suggests that the mini cap does produce precise ABRs since the measurand quantity values (i.e. averaged ABR waveform) obtained by replicate measurements (i.e. every 1000 repetitions) were notably similar to one another.

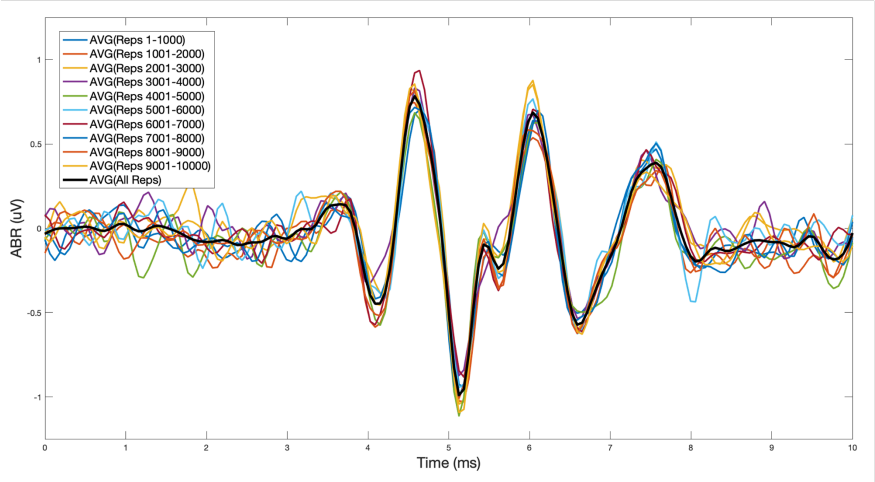

Figure 3.35. Precision quantification, averaging analysis. For a data set consisting of 10,000 repetitions, each subsequent subset of 1000 repetitions were averaged together. Visually, each response was highly comparable to the gold standard (i.e. average of all 10,000 repetitions). This confirms that the mini cap was producing highly precise ABR responses.

Next, a bootstrapping procedure was implemented to further quantify this precision. Instead of just grouping each subsequent 1000 repetitions and averaging, a random selection of 1000 repetitions from the larger data set (n=4500 repetitions) were averaged together. Overall, 20 boots (i.e. random selections) were executed. This random selection was performed without replacement since it is more representative of experimental data collection. Without replacement indicates a single repetition can only be included once within a single boot. Figure 3.36 shows the results of this bootstrapping procedure and the resulting correlation of each boot to the gold standard (i.e. average of all repetitions). The correlation results were impressively high, implying that each averaged boot was highly correlated to the gold standard. Altogether, these analyses suggest that the mini cap was able to produce highly similar ABRs within replicate measurements, indicating excellent precision.

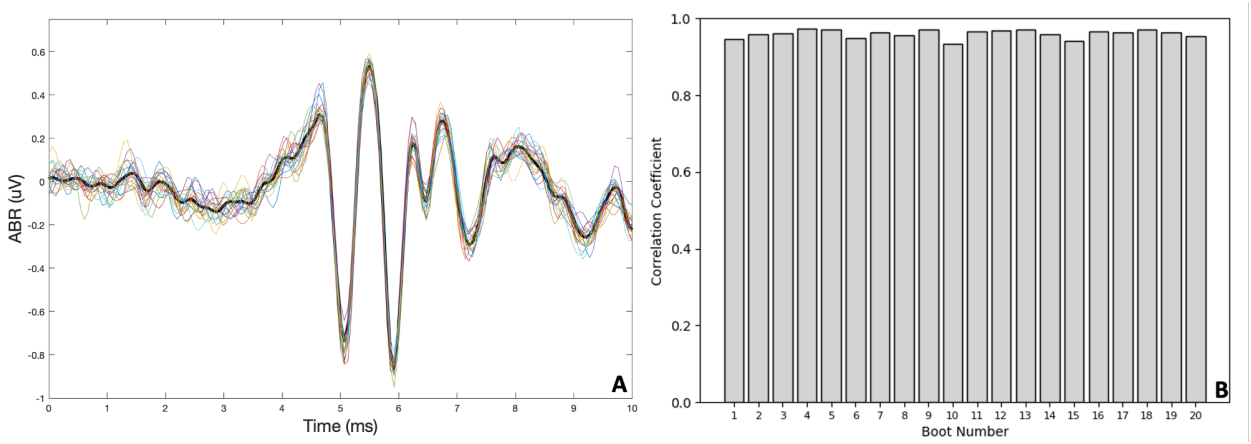

Figure 3.36. Precision quantification, bootstrapping analysis. Here, a random subset of 1000 repetitions was chosen from the larger data set and averaged together, representing a single bootstrap response. Overall, 20 boots were developed, resulting in 20 bootstrap responses (see A). The signal window of each bootstrap response was cross correlated with the signal window of the gold standard response (i.e. average of all repetitions) and the correlation values for each boot are shown (see B). All bootstrap responses were highly correlated to the gold standard response, once again confirming the mini cap was producing highly precise ABRs.

Validity summary

To summarize, the accuracy and precision of the mini cap's ability to produce ABRs has been confirmed. The mini cap generated markedly comparable thresholds and highly correlated responses to the subdermal responses (i.e. the gold standard), confirming accuracy. Additionally, the mini cap was able to generate remarkably precise responses. Since the mini cap was accurate and precise, the validity has, hence, been justified as well.

3.4 Benefits of the mini cap

3.4.1 Stimulus repetition analysis

The number of repetitions necessary to attain convincing responses for both the mini cap and subdermal was inspected. Firstly, the number of repetitions necessary for the mini cap to produce a similar response as the subdermal needles was investigated. Figure 3.37 shows the side-by-side comparison of how changing the number of repetitions affected the averaged

ABR response. In this example, for each repetition number, X, the first X repetitions of the total 1000 repetitions for the 50 dBSPL response shown were averaged together to produce the waveform in color. The black-colored waveforms indicate the average response across all 1000 repetitions (i.e. the gold standard). This visualization suggests that a comparable number of repetitions were needed for both the cap and subdermal to obtain a clear, not noisy response. For both mini cap and subdermal methodologies, it appears that about 500 repetitions were needed to attain a clear, not noisy response. It is encouraging that, based solely on visual determination, it appears an equivalent number of repetitions were necessary for both methodologies.

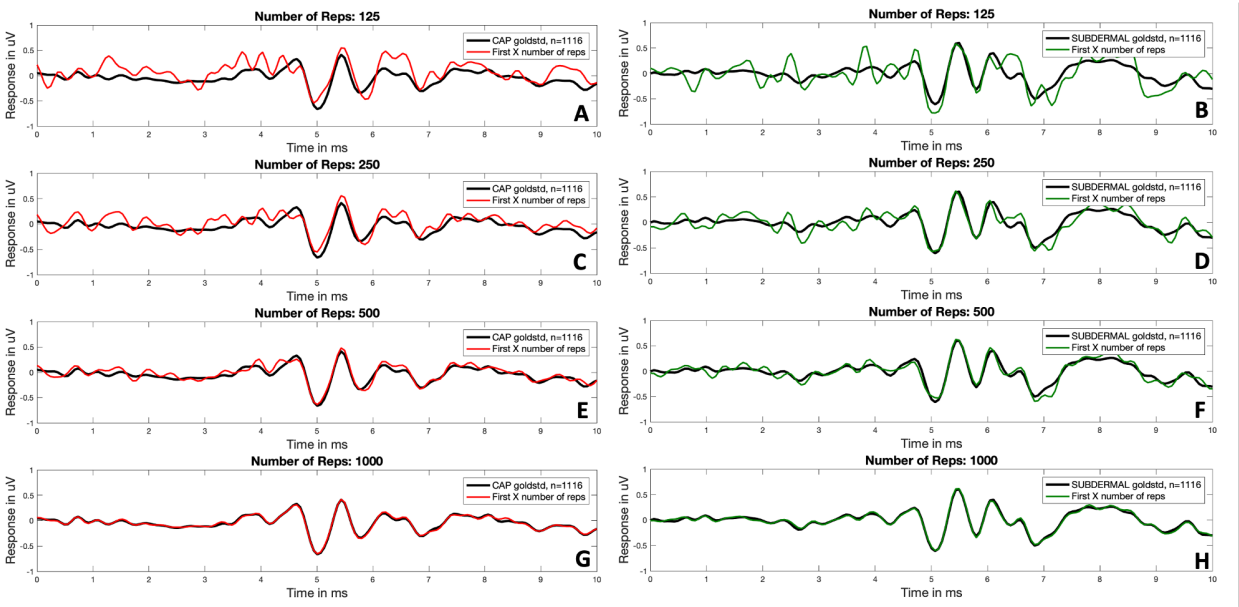

Figure 3.37. Repetition analysis, first X number of repetitions. Here, the first X number of repetitions from an entire data set were averaged together to visualize the total number of repetitions necessary to produce a convincing ABR response. Mini cap results (see A, C, E, and G) and subdermal results (see B, D, F, H) for different repetition numbers are shown. It appears that, at about 500 repetitions for both mini cap (see E) and subdermal (see F), the ABR response within the signal window aligns well with the gold standard (i.e. average of all repetitions). This suggests that about 500 repetitions were needed for both cap and subdermal to obtain a convincing ABR response.

Stimulus repetition bootstrapping

To further quantify this, a bootstrapping analysis was implemented. The goal of this analysis was to use a randomized number of repetitions instead of the first number of repetitions. The last analysis was relative to experimental data collection whereas this analysis is the more statistically-sound quantitative method. To complete this, a single boot consisted of a certain number of repetitions randomly selected from a large-repetition data set without replacement. All the repetitions within that single boot were averaged together and that was defined as a single boot response. Overall, 20 boots were introduced for a total of 20 boot responses for each chosen repetition number. For the mini cap, an additional step of averaging across all good channels was required to produce a single ABR response. This was performed for both the mini cap data and replicated subdermal data from a single experiment in which many repetitions were collected. Figure 3.38 and Figure 3.39 show the responses for four repetition numbers for the mini cap and the subdermal approach. Based solely on visualization of these responses, it appears that the mini cap produces slightly less noisy waveforms at fewer repetitions.

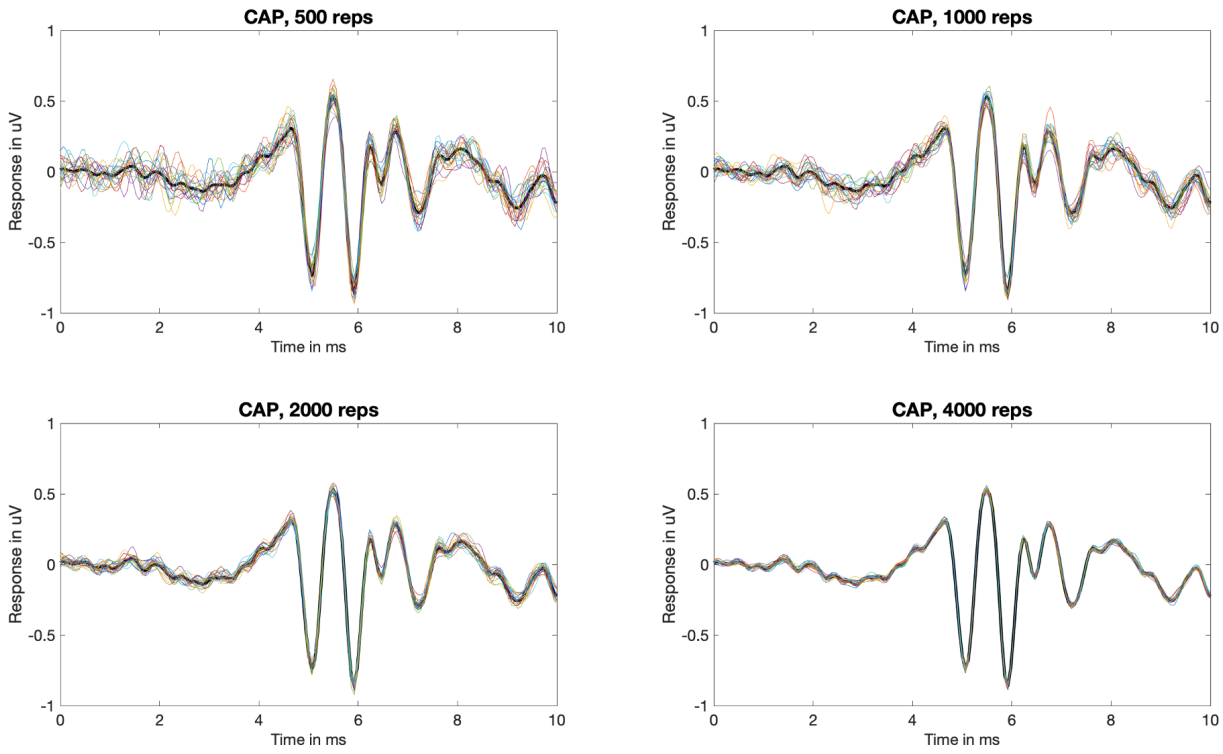

Figure 3.38. Bootstrapping stimulus repetitions, mini cap. For each repetition number, a subset of mini cap repetitions was randomly chosen and averaged together, producing a single bootstrap response (n=20 boots).

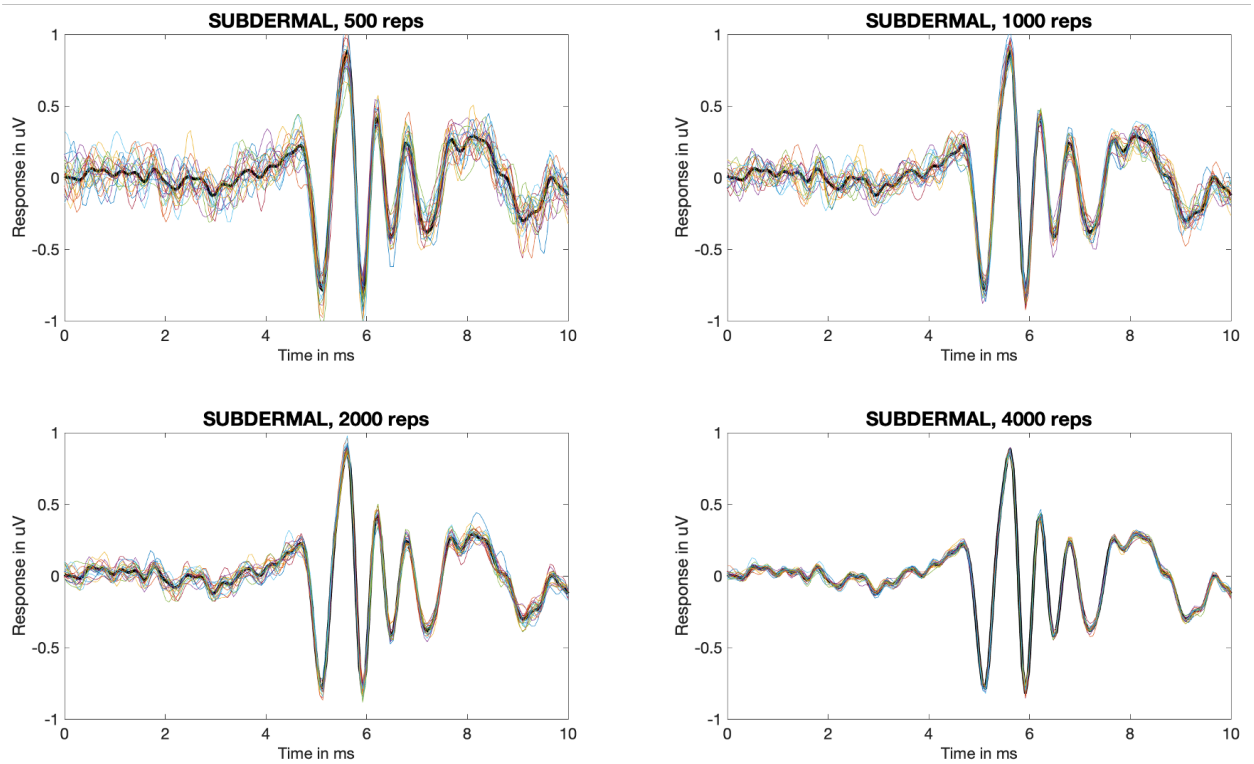

Figure 3.39. Bootstrapping stimulus repetitions, subdermal. For each repetition number, a subset of subdermal repetitions was randomly chosen and averaged together, producing a single bootstrap response (n=20 boots).

To further quantify this, an additional correlation analysis was performed. Each repetition number consisted of 20 boot responses. For each boot response, the signal window (i.e. 2 to 8 milliseconds) was cross correlated with the signal window of the gold standard (i.e. average across all repetitions). This would provide 20 correlation values and these would then be averaged together to obtain a single correlation for each number of repetitions. The correlation value for each associated number of repetitions represents the capability of that method to obtain satisfactory responses at different repetition amounts. Figure 3.40 illustrates the mini cap result from bootstrapping a data set. The dashed line is indicative of 1000 repetitions, the number of repetitions currently used for both methodologies. This result indicates that only a small number of repetitions (e.g., around 500 repetitions) are needed to obtain a highly correlated average response. At around 1000 repetitions, there is a plateau of correlation. This is indicative that additional repetitions after 1000 repetitions will not benefit or improve the correlation of the response significantly.

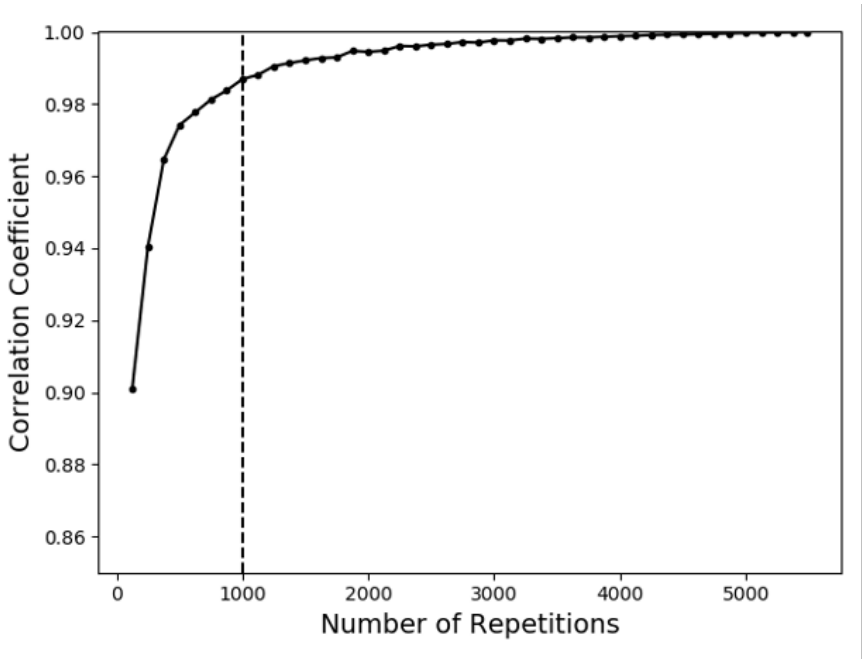

Figure 3.40. Correlation analysis from stimulus repetition bootstrapping, mini cap only. For each repetition number, the signal window of each bootstrap response was cross correlated with the signal window of the gold standard (i.e. average across all repetitions). This resulted in 20 correlation values that were then averaged together to obtain a single correlation value representative of that repetition number. Typically, 1000 repetitions were collected for a single level for the mini cap. This analysis depicts a correlation plateau at 1000 repetitions, indicating 1000 repetitions was adequate to attain a highly correlated mini cap ABR.

Subsequently, the same bootstrapping analysis was performed on subdermal repetitions. Figure 3.41 compares the mini cap and subdermal results from a single large-repetition data set. The mini cap required fewer repetitions to produce an equitably correlated response than the subdermal method. For the same number of repetitions, the mini cap method produced responses that were more correlated to the gold standard than the subdermal method. However, it appears to be only a slight improvement. Finally, for both mini cap and subdermal, at 1000 repetitions, a similar plateau effect occurs, suggesting that about 1000 repetitions were needed for both methods to produce ideal responses.

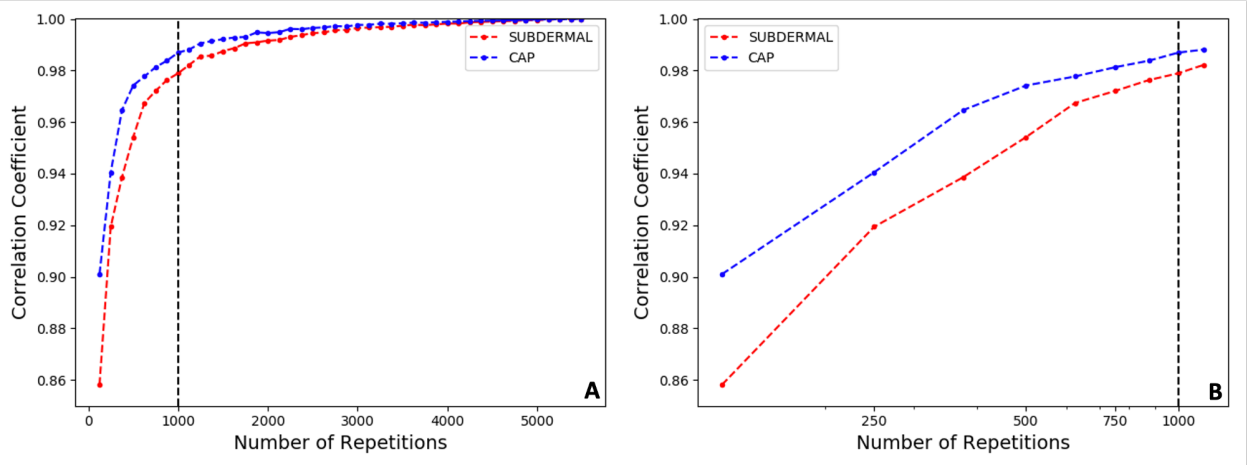

Figure 3.41. Correlation analysis from stimulus repetition bootstrapping, mini cap and subdermal. Here, the same process was performed for subdermal repetitions as described in caption of Figure 3.40. For both cap and subdermal responses, a similar 1000 repetition correlation plateau exists (see A, linear x-axis). However, notably, the mini cap required fewer repetitions to produce an equitably correlated response than the subdermal method (see B, logarithmic x-axis).

3.4.2 Mini cap channel analysis

Similarly, an analysis to quantify the number of channels necessary to produce a convincing ABR response was conducted for the 32-channel mini cap. For previous analyses, the average response of all good channels was deemed the mini cap response. However, the benefit of having these additional channels on the mini cap is significant to comprehend.

Topological maps of ABRs

Topological maps of the mini cap were created to compare and contrast the responses across different channels on the chinchilla skull. First, the channel layout specific to the mini cap was initialized, as shown in Figure 3.42. One important note is that the MRI used in this topological mapping is specific to the Wistar rat [64]. Eventually, the goal is to collect a chinchilla MRI, but, until then, this mapping is still beneficial since it is showing the mini cap placed onto the scalp of a rodent head model.

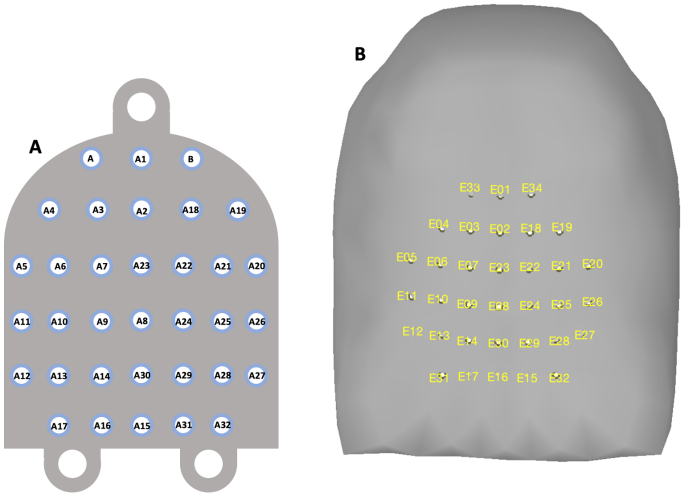

Figure 3.42. Topological map of mini cap layout. The mini cap layout (see A) was placed onto the scalp (see B) to visualize the topological map of mini cap ABR responses.

The topological map at different time points corresponding to noise (i.e. before onset of the response), certain peaks (i.e. P1, P2, and P5), and certain troughs (i.e. N1, N5) are shown in Figure 3.43. The two critical CS biomarkers, wave-I and wave-V, are depicted. The important takeaway of this analysis was that, for the ABR, all channels seem to be equivalently activated at the time locations shown. For example, at peak of wave-I, the magnitude response seems to be equivalent across all channels around the head. Therefore, for the ABR, between-channel differences on the mini cap seem minimal. Anatomically, this makes sense because the ABR reaches the brainstem, a source deep enough to cause similar contributions to each electrode.

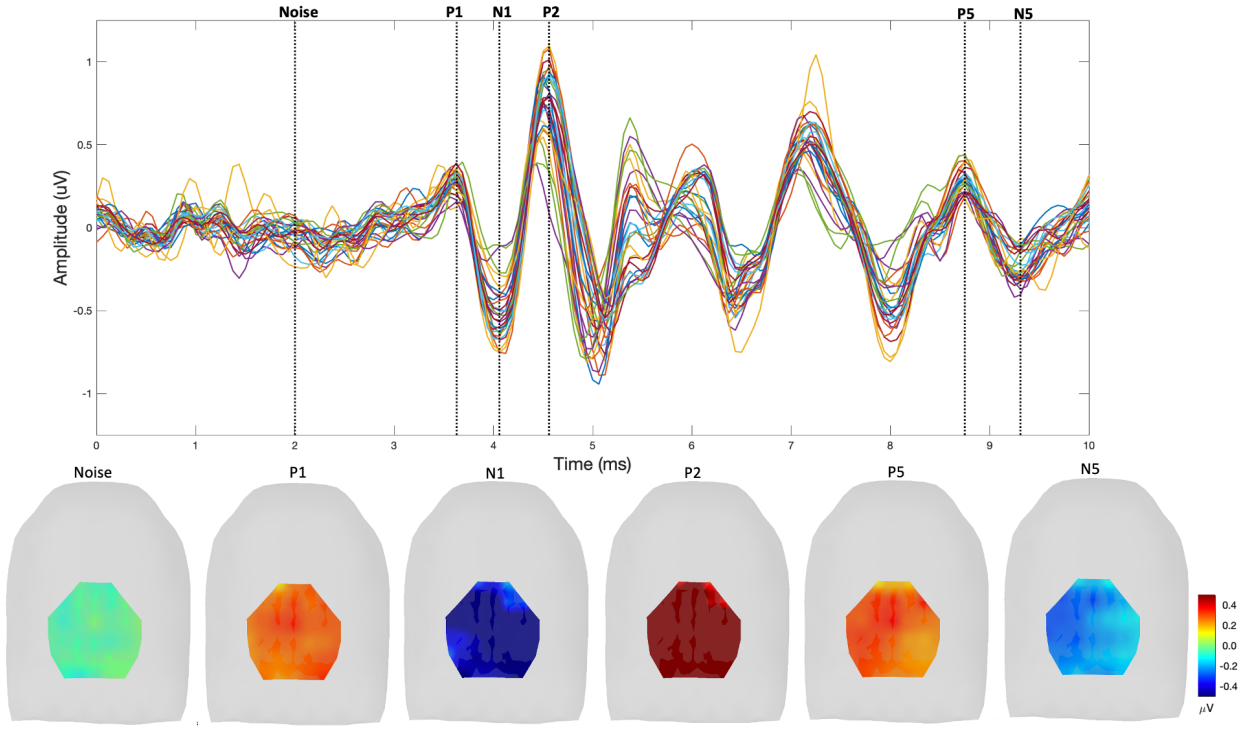

Figure 3.43. Topological mapping of an ABR response. At different time points, the topological map portraying the responses across different channels on the scalp is illustrated. For peaks and troughs of the ABR response, it appears that all electrodes across the scalp show similar magnitude responses. Here, since the ABR originates from a deep-seated source, between-channel differences are minimal.

Topological maps of cortical responses

In order to visualize the benefit of a multi-channel mini cap and identify between-channel differences, a cortical response to a 4 Hz amplitude-modulated SAM noise was measured in an awake chinchilla. The reference utilized was the average of all electrodes. The resulting response is portrayed in Figure 3.44, along with the topological maps at different time points in the response. It is apparent from this cortical measure that there were considerable between-channel differences. The onset response, in particular, was indicative of cortical activation. Responses from the cortex were dominating the responses since the cortex is closest to the electrodes on the scalp. Visually, the response magnitude at different time points varies across regions of the mini cap. Therefore, depending on where in the brain the auditory evoked potentials originate will alter whether there are noticeable between-channel differences or if all channels appear to follow the same response pattern. In this research, ABRs were principally studied and between-channel differences were minimal. However, this cortical response demonstrates that between-channel differences for the mini cap are achievable. For auditory evoked potentials in which channels differ in magnitude at certain time points, this mini cap will be of critical importance to implement.

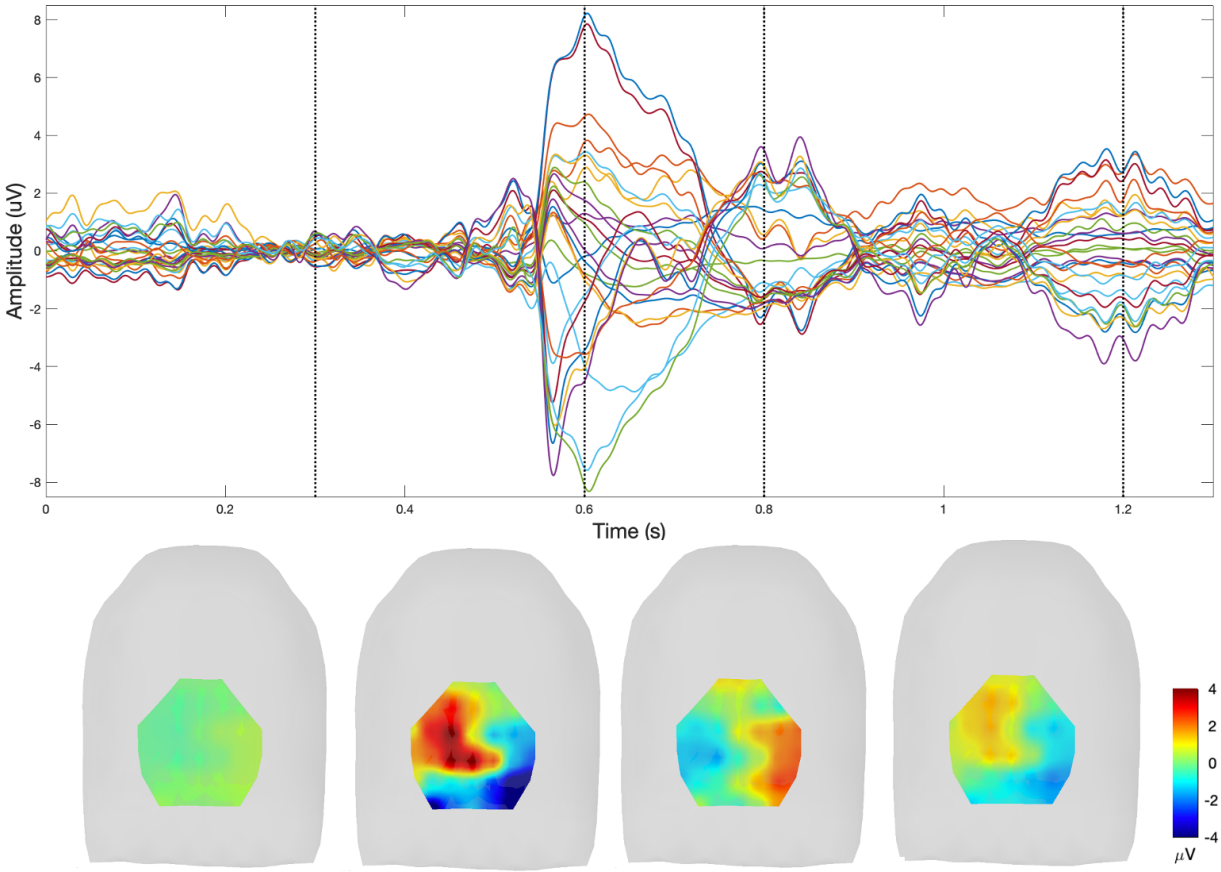

Figure 3.44. Topological mapping of a cortical response. Here, a 4 Hz amplitude-modulated SAM noise was the stimulus. Clear cortical activation is apparent, especially from the onset response. This cortical response confirms the capability of the mini cap to produce responses that possess large between-channel differences. The source of the response itself determines whether between-channel differences are significant or not.

Principal component analysis

Principal component analysis (PCA) is an established technique used for feature extraction and dimensionality reduction [81]. The goal of PCA is to represent the data of d dimensions in a lower dimension space, reducing the degrees of freedom and time complexities [81]. The chosen space is the space that best exhibits the sum-squared error variation [81]. PCA is a useful analysis for segmenting signals that originate from different sources when those sources are known ahead of time.

Computationally, the d-dimension mean vector and the associated covariance matrix are calculated for the full dataset [81]. Then, the eigenvectors and eigenvalues are computed and sorted from largest to smallest eigenvalue with the largest eigenvectors chosen [81]. The result is the representative dimensions that describe the inherent dimensionality of the subspace of the signal, with the additional dimensions representing noise [81]. The end result of PCA is a minimally dimensioned vector that represents the most significant features of the signal with the noise features removed. In EEG analyses, PCA is recommended to minimize the amount of data and computation time [82].

Here, PCA was implemented on ABR responses from the mini cap. The results are illustrated in Figure 3.45. Initially, all channels, including bad channels, were included. The reason bad channels were initially included was to determine whether this PCA approach could classify the ABR and the noise source separately, and thus, separate the noisy, bad channels into the noise source. However, including the bad channels led to inaccurate channel weighting as the bad channels were the most significantly weighted channels. For this, the source that was being most represented was the noise artifact (e.g., 60 Hz line noise) that was common between the bad channels. Thus, removing the bad channels initially using the z-score deviation criterion method previously described, was necessary. After removing the bad channels, PCA was performed again and the result was all channels being equitably weighted to one another. This means that each channel was originating from an equivalent source, which was previously justified using the topological maps (see Figure 3.43). Finally, the PCA-generated waveform was directly compared to the waveform from averaging across all good channels. These two waveforms were identical, implying that implementing PCA

does not significantly impact the resulting response. This result is reasonable because, again, all channels show an equivalent magnitude response across time. This also implies that, after removing the bad channels, the effect of noise seems similarly insignificant across all good channels. Altogether, PCA did not greatly benefit the processing of ABR responses. However, for auditory evoked potentials originating from different sources in the brain, this analysis could be very beneficial.

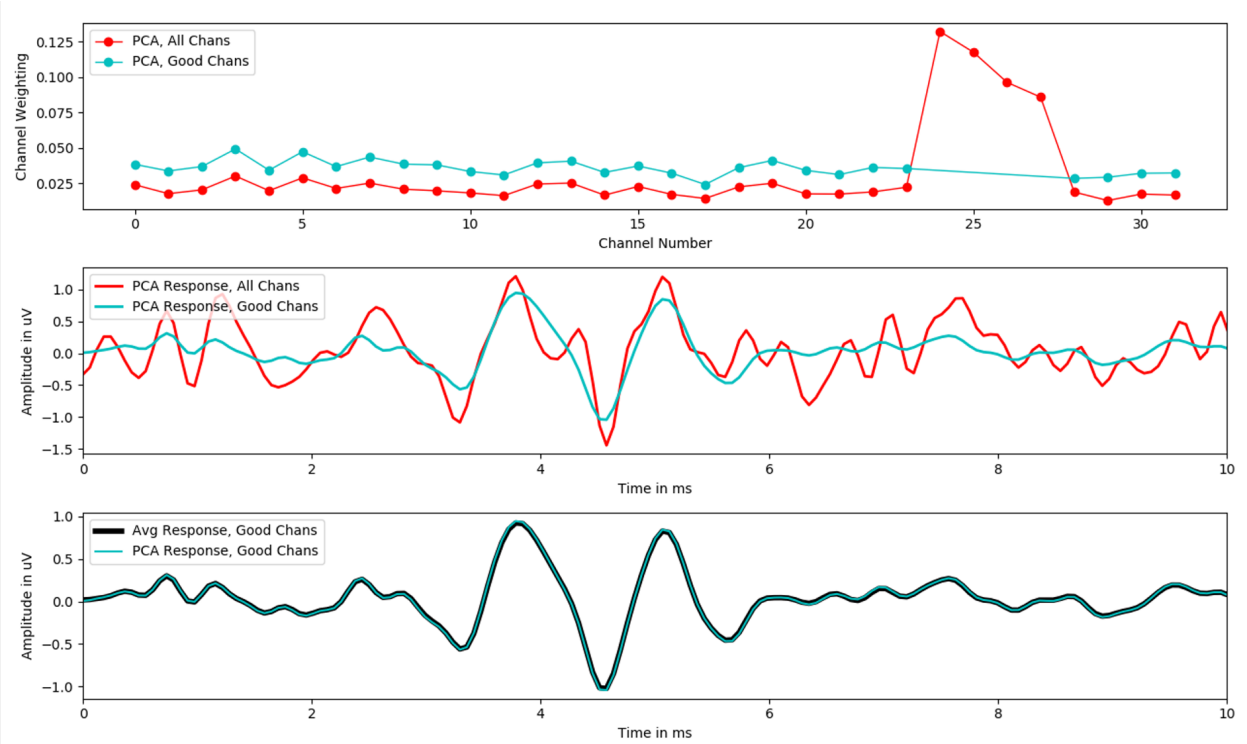

Figure 3.45. Principal component analysis (PCA) does not strongly mini cap impact ABRs. After removing bad channels, the PCA response is equivalent to the response of the average of all good channels. Since all channels are displaying equivalent magnitude ABR responses, implementing PCA does not seem to add any noticeable benefit.

Correlation between channels

The correlation between different channels across the mini cap was quantified. The signal window of each good channel was cross correlated with the signal window of the average across all good channels. Figure 3.46 shows the correlation results. This analysis

reiterates the concept that all channels are displaying equivalent response morphology and magnitude within the signal window. All channels are significantly correlated to the average response since they are originating from an equal deep-seated source within the brain, again substantiating the results from the ABR topological map (see Figure 3.43).

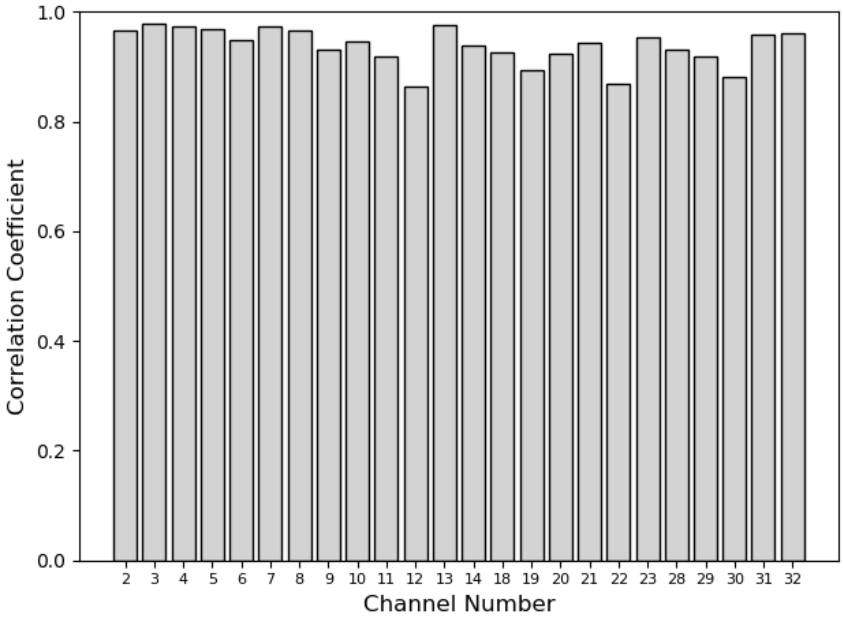

Figure 3.46. Each channel correlated to the average of all channels. The signal window of each channel was cross correlated with the signal window of the average of all good channels. All channels are highly correlated to the average response. This aligns with the fact that all channels are displaying equivalent ABR responses.

Channel bootstrapping

Although the mini cap contains 32 channels, since all channels are showing equivalent responses, all 32 channels are theoretically not needed to generate a convincing ABR response. To determine an estimate of the number of channels needed, a channel bootstrapping procedure was implemented. Here, a random set of channels from all good channels were chosen without replacement and averaged together. Then, this boot response was compared directly to the average response of all good channels (i.e. the gold standard). Similar to the repetition bootstrapping procedure, 20 boots for each number of channels created 20 unique boot

responses for each set of channel numbers. A visualization of this channel bootstrapping procedure is shown in Figure 3.47 for four different channel quantities. There appears to be slight morphology changes, specifically at waveform peaks (e.g., P3), for quantities of 3 and 5 channels. However, at about 10 channels, there is little apparent difference between any boot responses and the gold standard.

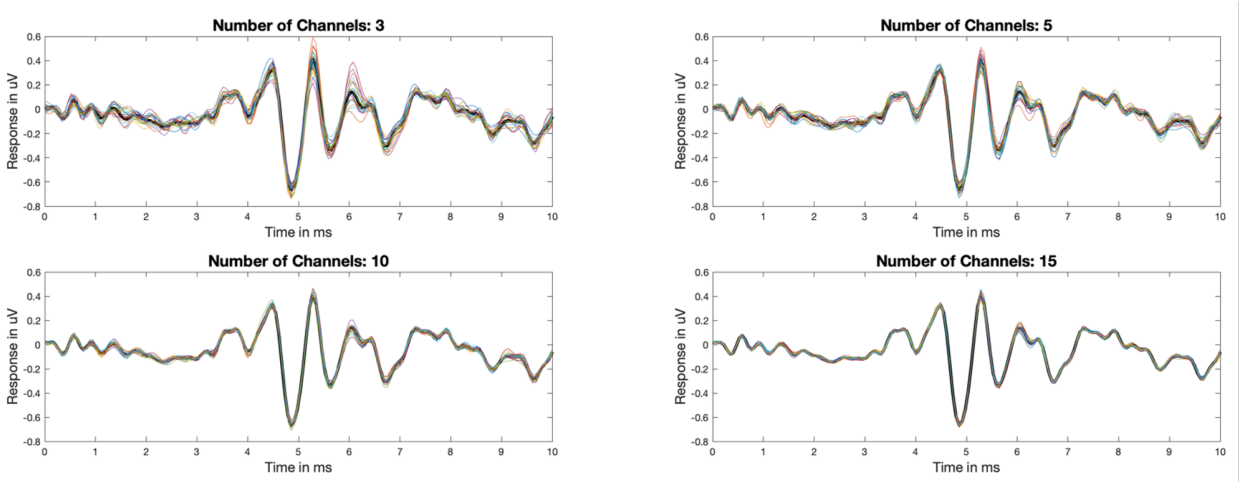

Figure 3.47. Bootstrapping channels, mini cap. For each channel number X, a random subset of X channels from all good channels were selected and averaged together to produce a bootstrap response (n=20 boots). This process was completed for different channel numbers.

An additional correlation analysis, similar to the one completed for the repetition bootstrapping analysis, was performed. In this analysis, for each quantity of channels, the signal window of each boot response was cross correlated with the signal window of the gold standard response (i.e. average across all good channels). The twenty correlation values for each quantity of channels were averaged together, and this value was representative of the correlation when incorporating that particular quantity of channels. Figure 3.48 portrays these correlation values across number of included channels. It appears that the correlation value displayed a plateau effect at about 4 channels. Therefore, this implies that only a few channels on the mini cap are necessary to produce a convincing ABR. The correlation plateau occurs at 4 channels, but prior to the plateau, the correlation strength indicates fewer than 4 channels results in a highly correlated response as well. These results align with the prevalent concept that since the channels are displaying equivalent ABR responses,

only a few channels are needed to obtain a highly correlated ABR. If a different auditory evoked potential was being measured, it is likely that more channels would be necessary to include to produce a robust response.

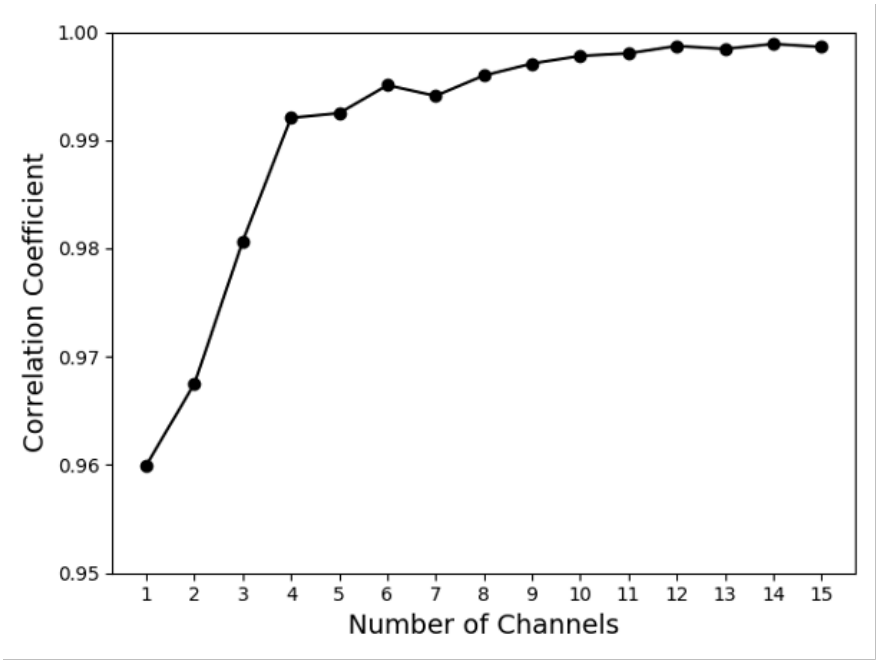

Figure 3.48. Correlation analysis from channel bootstrapping, mini cap. For each channel number, the signal window of each bootstrap response was cross correlated with the signal window of the gold standard (i.e. average across all good channels). This resulted in 20 correlation values that were then averaged together to obtain a single correlation value representative of that channel number. It appears that about four channels were needed to produce a highly correlated ABR response. However, fewer than four channels still produced a highly correlated ABR response since all channels were showing equivalent ABR responses.

Noise across channels

Averaging across 1000 repetitions and across all good channels leads to significant noise reduction in the resulting ABR response. As a technique, averaging is beneficial for reducing noise from a subset of repetitions or a subset of channels. Averaging across channels should reduce the noise within the final mini cap ABR response. This reduction in noise could

explain why the mini cap required fewer repetitions to generate an equivalently correlated response, as shown in Figure 3.41.

Further evaluation of how noise affects the multi-channel mini cap is important. Figure 3.49 displays the topological mapping for a 0 dBSPL response. Theoretically, this represents the noise condition. Visually, the channels differ in topology at different time points. This is expected because noise is random so there should not be any clear channel patterns. If there were clear channel patterns, that would indicate the noise was not random and an outside artifact was impacting the channels (e.g., 60 Hz power line interference). Additionally, the noise response was significantly smaller in magnitude than the ABR signal response, which is expected as well because high-level of noise indicates the potential for a common noise artifact.

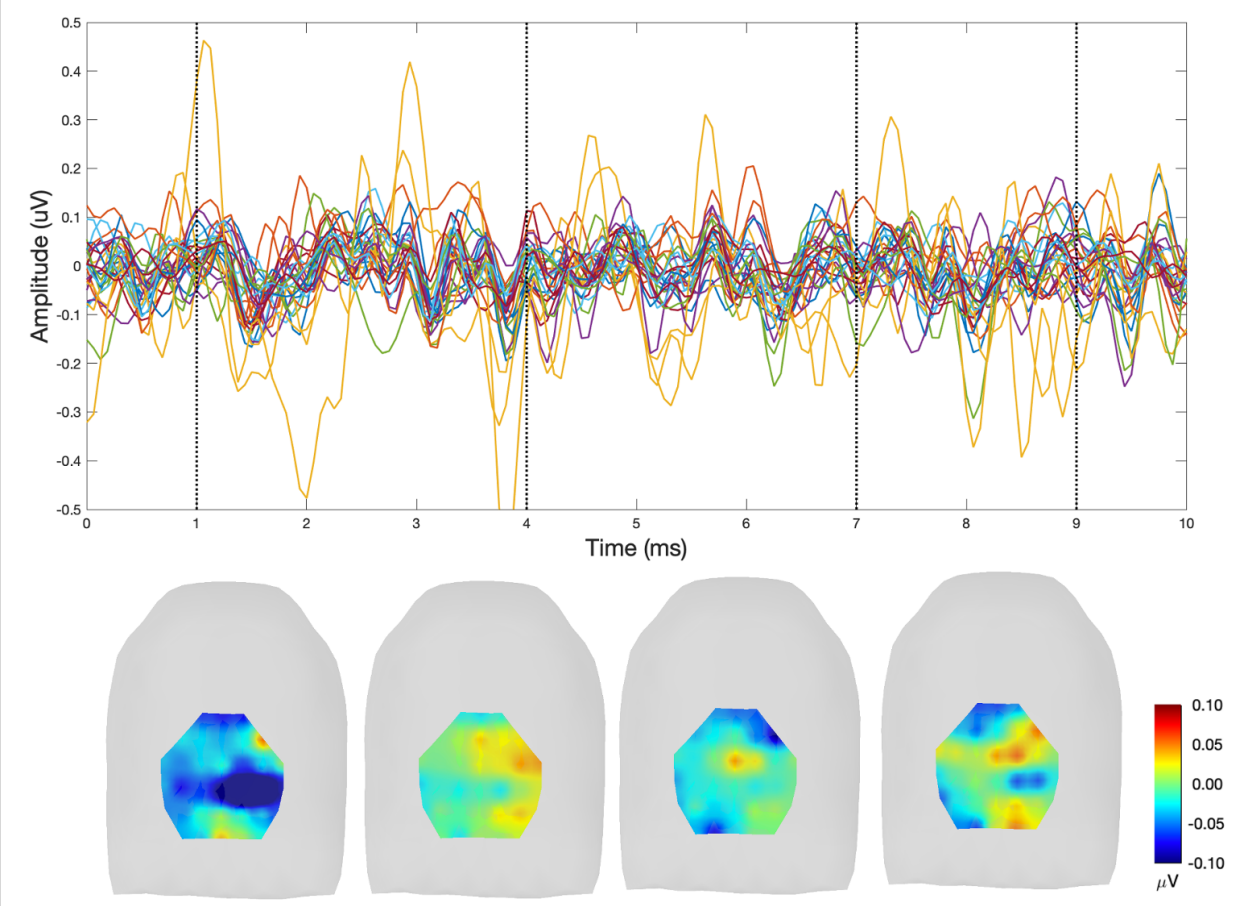

Figure 3.49. Topological mapping of noise. Responses to noise (i.e. 0 dBSPL response) appear to be random, which is expected from the random nature of noise. Averaging across all channels on the scalp reduces the noise in the final ABR response, which is a strong benefit using this multi-channel EEG cap to collect ABRs.

Noise correlated to noise should result in a low correlation due to the random nature of noise. In this analysis, the signal window of noise (i.e. 0 dBSPL response) for each good channel was cross correlated with the signal window of all good channels. The correlation for noise was significantly lower for this channel-by-channel correlation in comparison to the signal analysis, as expected (see Figure 3.50). The mean correlation across all channels was 0.52, which falls into the low positive correlation category. However, there does appear to be some noise commonalities between the channels. One potential source of this noise commonality could be due to referencing. Each channel was referenced to the right ipsilateral tiptrode, so this could theoretically introduce a common noise signal across all channels as

well. From experimental experience, the clean injection of paste and secure placement of the cap drastically reduced noise. The reduction and removal of noise among channels will continue to be investigated in future experiments.

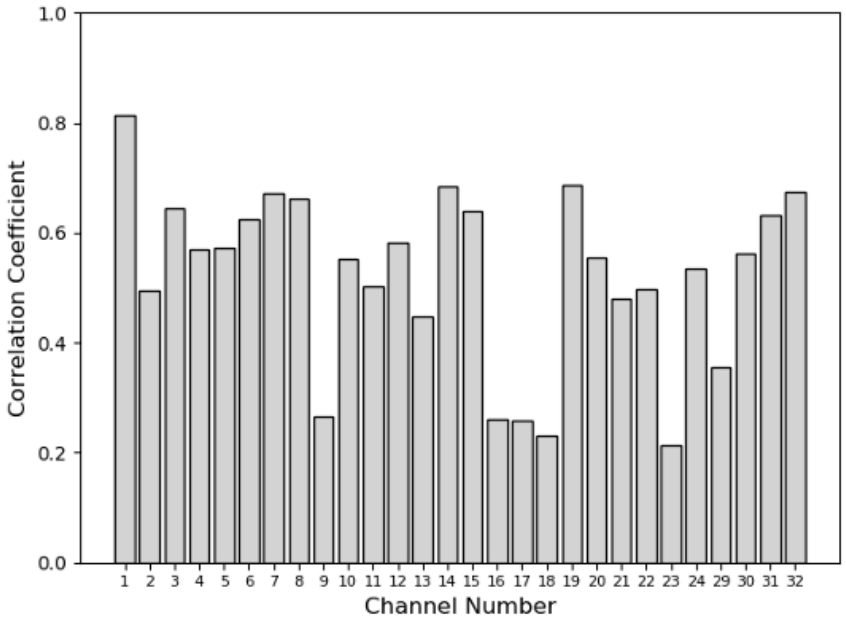

Figure 3.50. Each channel correlated to the average of all channels, noise. For a 0 dBSPL response representing the noise condition, the signal window of each channel was cross correlated with the signal window of the average of all good channels. Noise was significantly less correlated across channels; however, there does appear to be some noise commonalities. One potential source of this commonality could be due to referencing.

Channel patterns across regions of the mini cap

To further explore any potential for between-channel differences, the mini cap was divided into four quadrants. Figure 3.51 displays these regions of the cap. The center channel of the cap, A8, is comparable to channel Cz on the human cap. Altogether, there are four quadrants and two midlines that intersect the center channel. The two midlines are the LR-Line (i.e. left-to-right) and the Z-Line. The channel breakdown for each region is shown in Table 3.10. If consistent with previous analyses, there should not be any drastic differences between

regions of the cap because all channels were highly correlated to the average response across all channels.

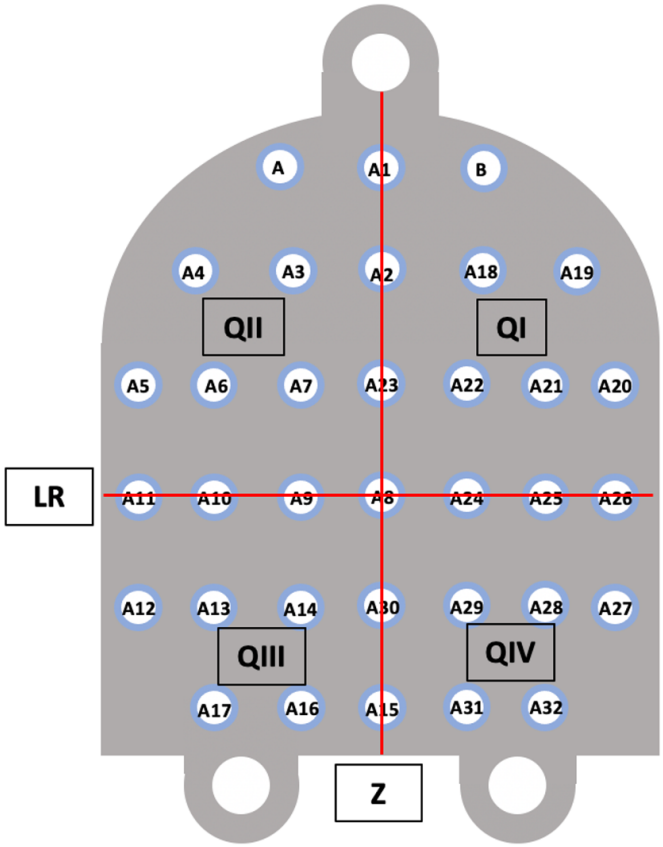

Figure 3.51. Mini cap divided into four quadrants. Channel A8 is equivalent to channel Cz (i.e. center of head) on the human EEG cap. In this analysis, channels in each quadrant were averaged together to determine if channel patterns exist.

Table 3.10. Channels in each of the four mini cap quadrants.

Quadrant	Area of Head	Channels
Z-Line	Midline	A1, A2, A23, A8, A30, A15
LR-Line	Midline	A11, A10, A9, A8, A24, A25, A26
Quadrant I	Front, Right	A18, A19, A20, A21, A22
Quadrant II	Front, Left	A3, A4, A5, A6, A7
Quadrant III	Back, Left	A12, A13, A14, A16, A17
Quadrant IV	Back, Right	A27, A28, A29, A31, A32

Although it was not expected for there to be drastic differences, based on visualization, the 60 dBSPL average waveform (shown in Figure 3.52) across different quadrants appeared to be have slightly different peak and trough amplitudes. In this example, quadrant-IV was not included because three of the five channels in quadrant-IV were identified as bad channels. Slight differences in peaks and troughs could lead to differences in wave amplitude and wave latency, which, as previously mentioned, are important biomarkers of CS. This, in turn, might signify differences in the number of neurons firing (i.e. the wave amplitude) and the speed of transmission (i.e. the wave latency) at different regions of the scalp.

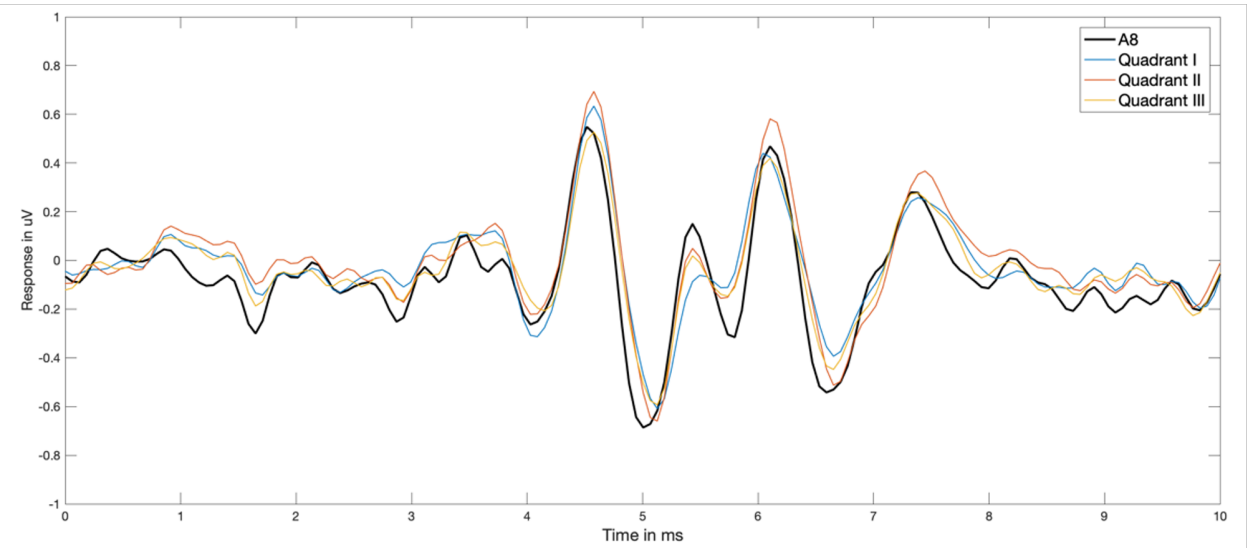

Figure 3.52. Visual confirmation of quadrant differences. In this quadrant analysis, specifically amplitudes and latencies of peaks and troughs will be quantified because it appears that across quadrants there could be differences in peaks and troughs that are commonly used as CS metrics.

Peak picking to identify channel patterns

Peak-picking for all five waves was performed for all good channels of a single data set (see Figure 3.53). Only suprathreshold levels (i.e. 60, 70, and 80 dBSPL) were used. Usually, as a CS biomarker, only peaks and troughs for wave-I and wave-V are identified. However, due to the slight amplitude differences in other waves shown in Figure 3.52, all five waves were identified for this analysis. Routinely, wave-I amplitude is defined as amplitude of P1

subtracted from the amplitude of N1 whereas wave-V amplitude is defined as amplitude of P5 subtracted from the amplitude of N5. The latency is defined as the time between stimulus onset and the wave peak (e.g., P1). After peak-picking was performed for the three suprathreshold levels, the peak and trough amplitudes and latencies were computed by averaging across the 70 dBSPL and 80 dBSPL intensity levels.

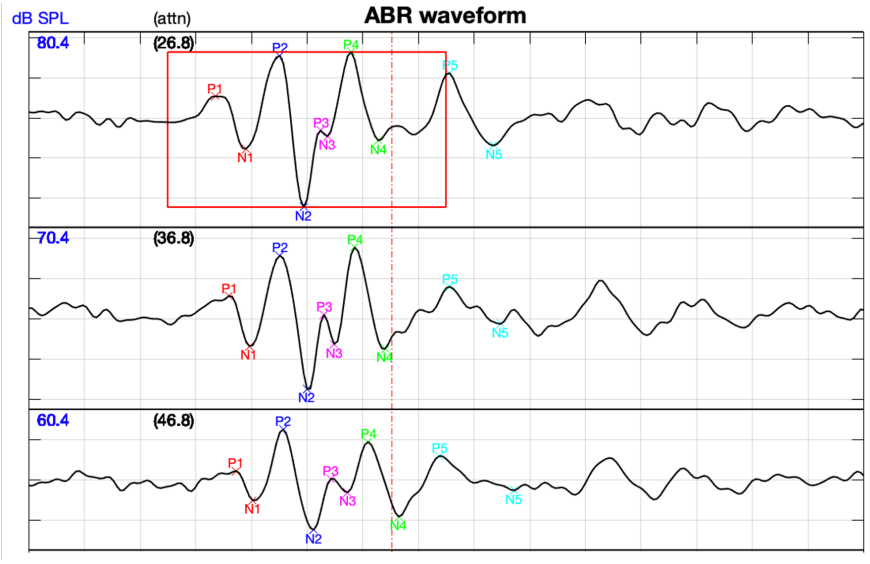

Figure 3.53. Peak picking of all five waves to identify quadrant patterns. P1-P5 and N1-N5 for the top three levels (i.e. 60, 70, and 80 dBSPL) were identified for all channels within a single waterfall. Final peaks, troughs, and wave amplitudes for each channel were averaged across the highest two levels. Similarly, this was also performed for latencies.

First, the channel-by-channel comparison of the measures for all waves is shown in Figure 3.54. The goal of this visualization is to see if any single channel is noticeably different than the other channels for each of the metrics. Generally, there does not appear to be any channels that are noticeably different in any of the measures. For wave amplitudes, there does appear to be an increase in wave-I and wave-III amplitude for the later channels (i.e. channels 20-32). Latencies for all fives waves are remarkably consistent across channels. The wave-I/wave-V ratio, used commonly as a CS biomarker, seems to trend higher for the later channels as well, which aligns with the increase in wave-I amplitude effect previously mentioned.

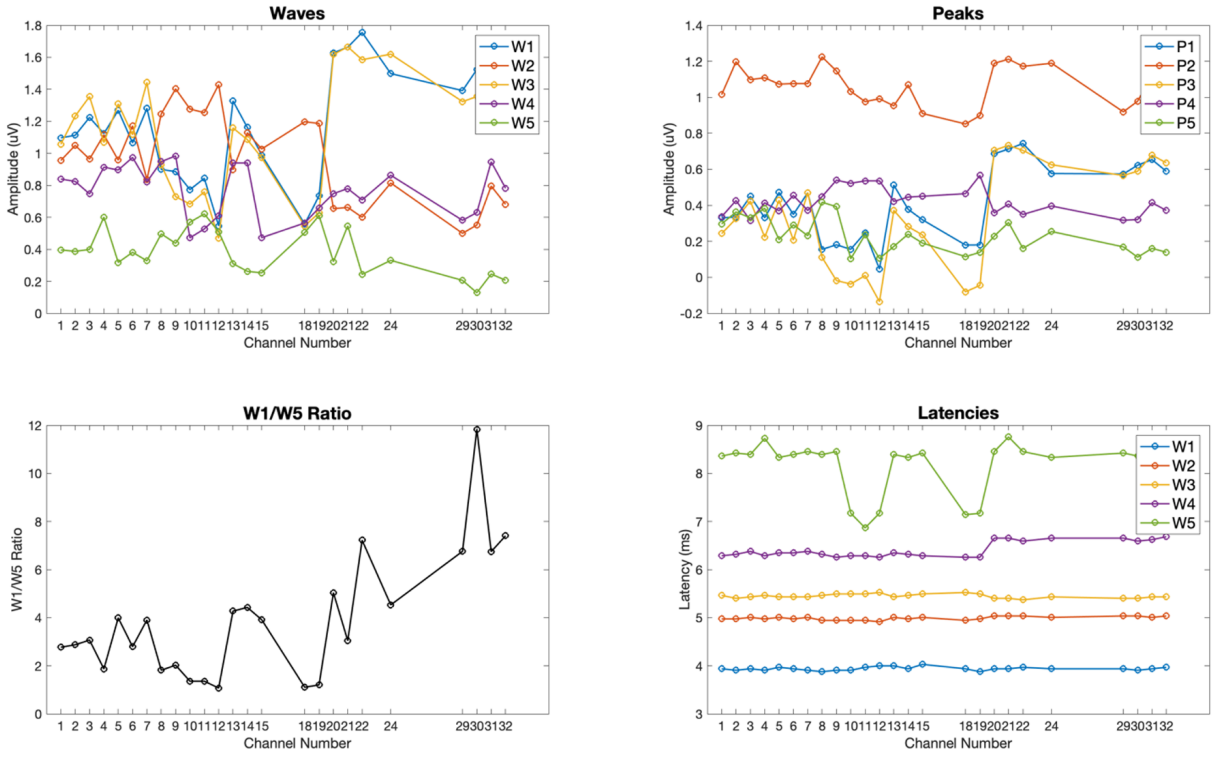

Figure 3.54. Peak-picking results across all channels. Wave amplitudes (top left), peak amplitudes (top right), latencies (bottom right) and wave-I/wave-V ratio (bottom left) are displayed across all channels. There does not appear to be strong patterns across any channels for any of the metrics. The only observable effect seems to be that wave-I and wave-III are of higher amplitude at later channels (see top left).

The regions of the mini cap previously mentioned were organized based on location. For this first test, the cap was divided into a front region and a back region, divided by the LR-line. The wave amplitudes and peak amplitudes for the front, in red, and the back, in blue, are indicated in Figure 3.55. There does not appear to be any noticeable differences in wave and peak amplitudes between the front and back region of the mini cap.

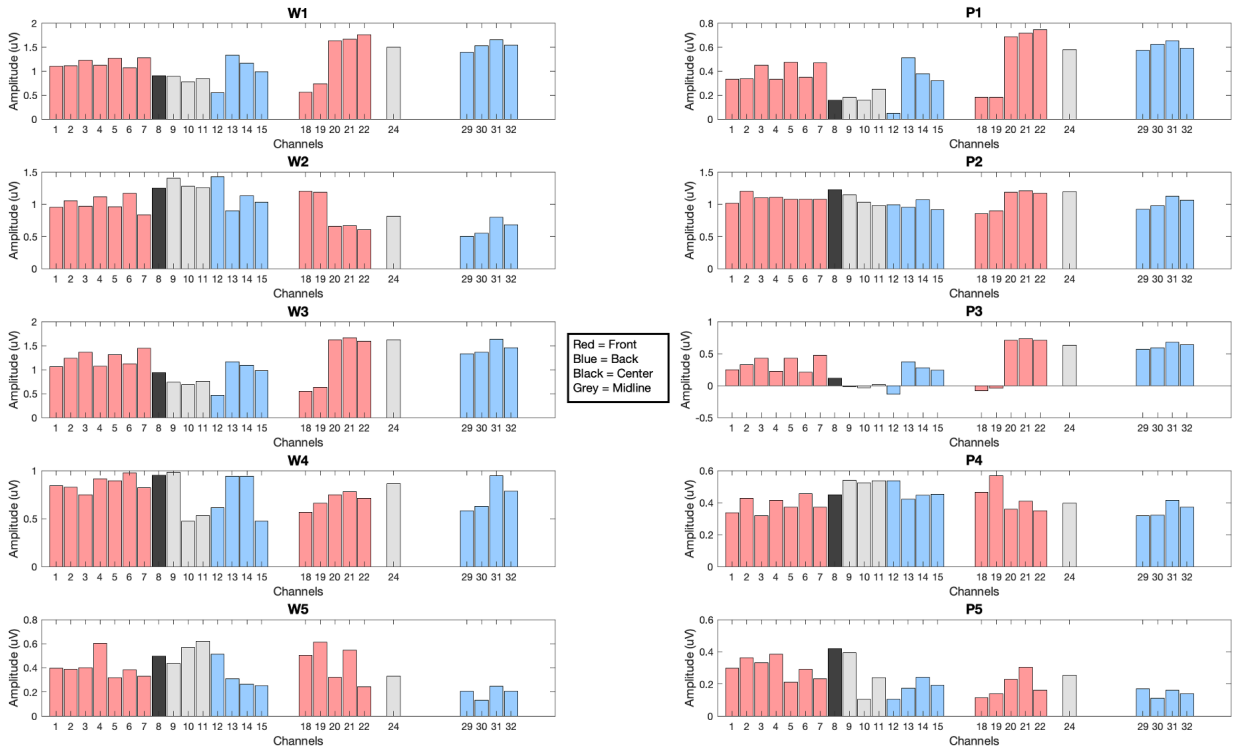

Figure 3.55. Peak-picking results, front versus back of cap. There does not appear to be any differences between the front (red) and back (blue) of the mini cap with regard to wave or peak amplitudes, aligning with the concept that all channels are exhibiting equivalent ABR responses.

Secondly, the mini cap was divided into the left and right region. The left region consisted of quadrant-II and quadrant-III. The right region included quadrant-I and quadrant-IV. The Z-line divided the left and right regions. Figure 3.56 shows these results for the left and right regions of the mini cap. Here, the right side of the mini cap seems to have slightly increased wave-I/peak-I and wave-III/peak-III in comparison to the left side of the mini cap. This confirms the previous result since the later channels showing an increased wave-I and wave-III amplitude are comprised in the right region of the mini cap.

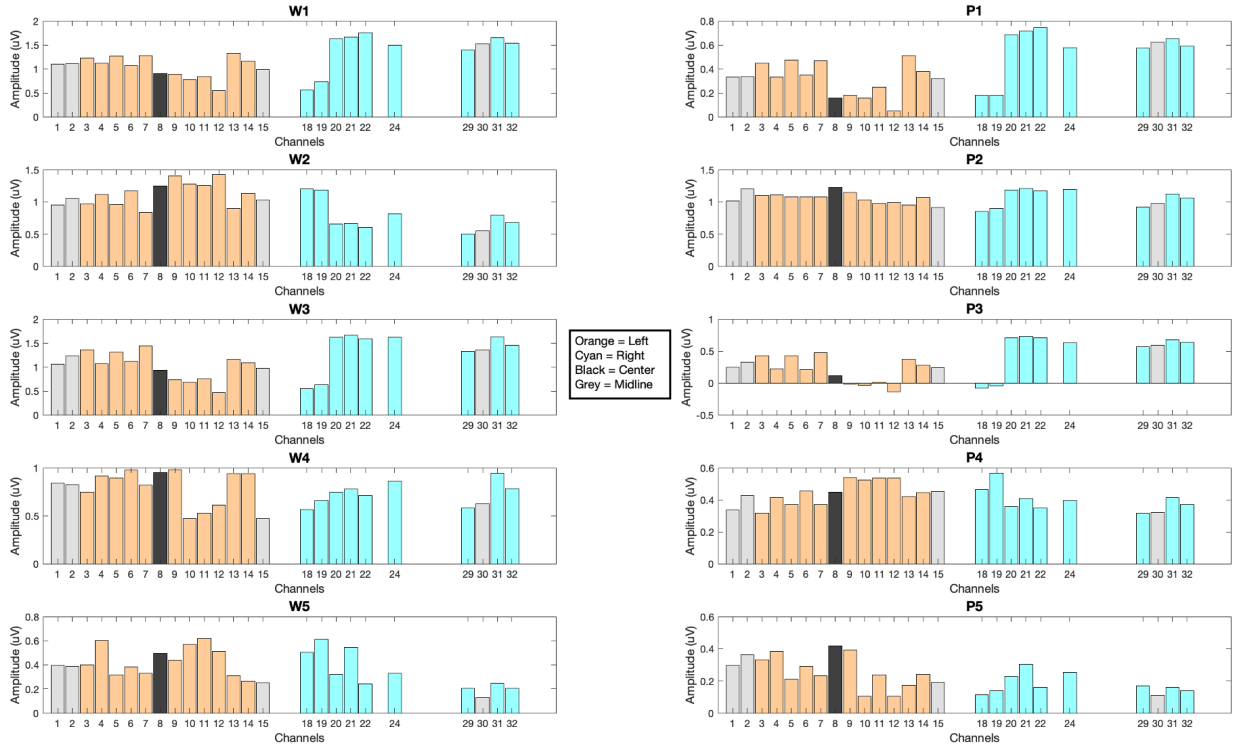

Figure 3.56. Peak-picking results, left versus right hemisphere of cap. The right hemisphere (cyan) seems to have slightly increase wave-I/peak-I and wave-III/peak-III in comparison to the left hemisphere (orange). This result needs to be confirmed with additional data sets.

Finally, the four quadrants of the mini cap were compared to one another directly. This representation is shown in Figure 3.57. To summarize, quadrant-III and quadrant-IV seem to show slight amplitude differences in wave-I and wave-III. Further analysis on additional data sets is necessary to confirm this result.

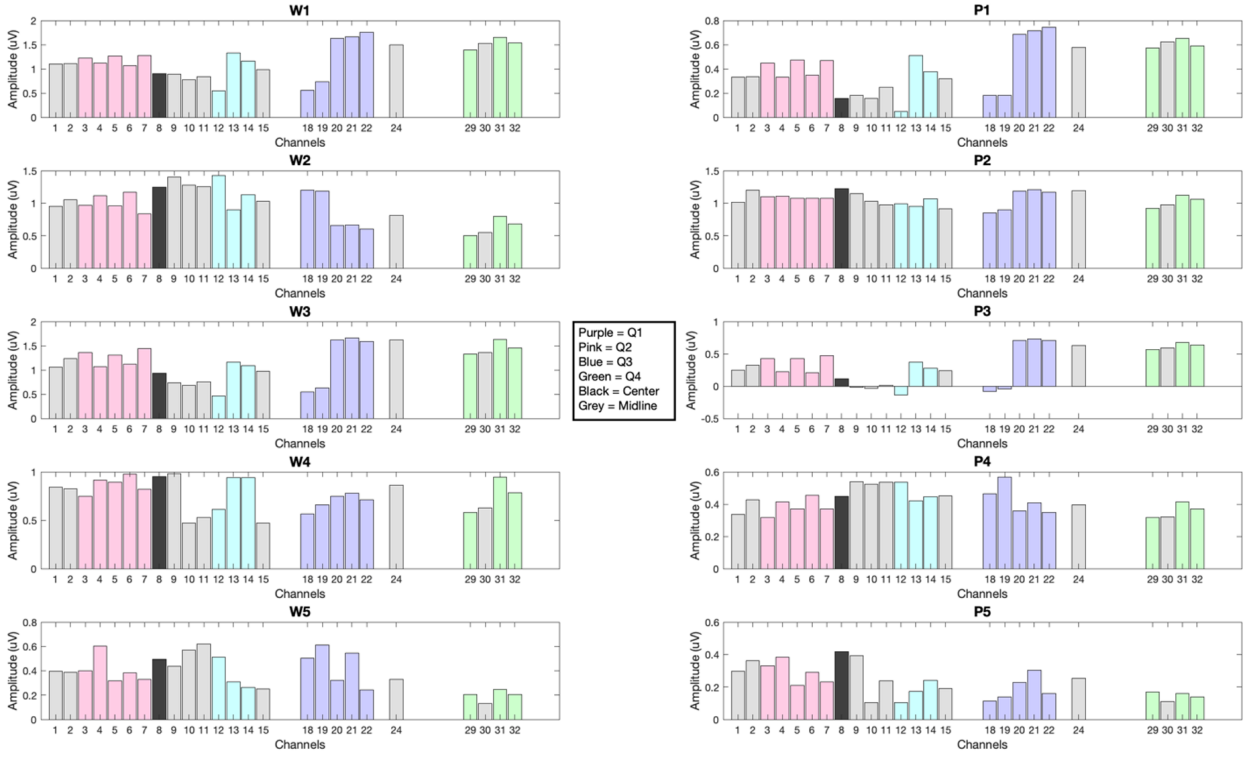

Figure 3.57. Peak-picking results, four quadrants of cap. The two quadrants on the right side, quadrant-III and quadrant-IV, present a slight amplitude difference in wave-I and wave-III, although this pattern still needs to be confirmed with additional data sets.

3.5 Effect of anesthesia

The sources of variability mentioned thus far comprise different methodological elements related to the mini cap that may or may not introduce variability into the measure. Besides the mini cap itself, it is significant to determine whether the anesthesia itself was affecting the measures to any magnitude. This variability would affect both the new mini cap method and the established subdermal method since the same anesthetic, xylazine followed by ketamine, is used. Previous research in rodents has demonstrated that residual ketamine and xylazine concentrations can still be present up to 3 to 5 days after administration [83]. To avert this, each retest experiment was completed one week after the test experiment. Instead, the objective of this analysis is to investigate whether there was any effect of anesthesia across experimental time during a single experiment.

To study this, a 40 dBSPL click response was collected about every 15-20 minutes during a single experiment. It was ensured that the first response and last response measured during each experiment with the mini cap were 40 dBSPL click responses. Theoretically, if anesthesia was altering the waveform morphology to any extent, observing waveforms collected at different experimental times would provide insight into the significance of such an occurrence. Figure 3.58 shows an example of a single data set collected following this methodology. Based solely on visual appearance, there does not appear to be any noticeable changes to waveform morphology across experimental time.

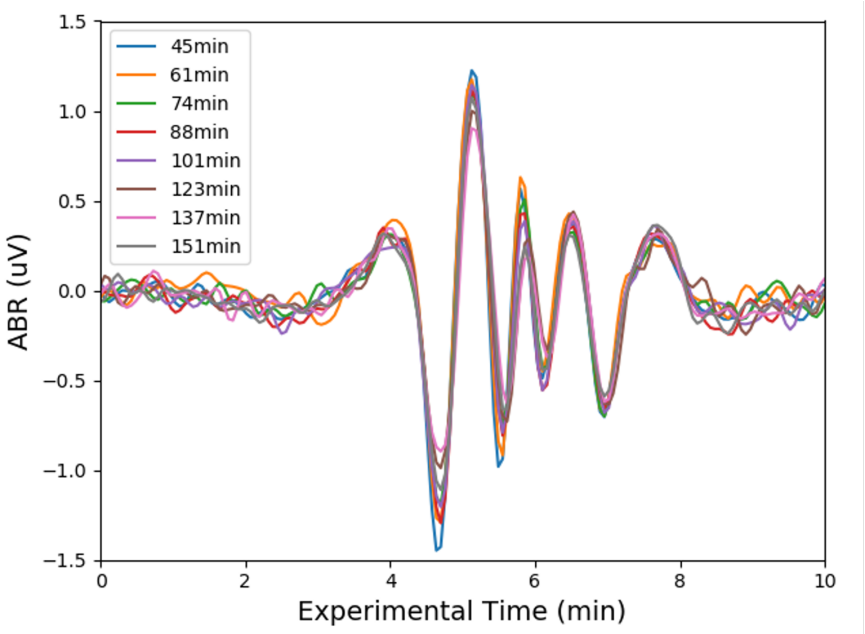

Figure 3.58. Several click responses were collected within a single experiment to determine the effect of anesthesia. About every 15-20 minutes within an experiment, a 40 dBSPL click response was collected. These responses were directly compared to one another to determine whether there was an effect of anesthesia.

3.5.1 Effect of anesthesia analysis

To further quantify this, a windowing procedure was performed in order to isolate the amplitudes and latencies of wave-I and wave-V of the ABR response. Wave-I and wave-V were chosen because they are routinely used as biomarkers for CS, so it is significant that

they remain consistent across experimental time. In detail, the peak and trough of both wave-I and wave-V were computed. Then, the overall amplitude of wave-I and wave-V were calculated by subtracting the peak from the subsequent trough. The latency of wave-I and wave-V were determined as the time of each peak relative to the stimulus onset time.

Overall, this analysis was performed for three experiments across two animals. The first two data sets depicted were from two different experiments on the first animal, and the third data set was from an experiment with a second animal. Across experimental time, the effect of anesthesia does not appear to noticeably affect either wave-I or wave-V amplitudes. For latencies, there still does not appear to be a strong effect across experimental time. The only data set that appears to have a slight increasing trend for wave-I and wave-V latency is data set #2. However, it is important to note the effect appears small in magnitude, in comparison to typical latency changes across level. In fact, the latency difference magnitude appears, at most, to be around 0.2 milliseconds for both wave-I and wave-V. Comparing back to a typical waterfall, as the intensity level increases, the latency of all ABR waves decrease, and this routinely results in about a 1 millisecond difference in latency for wave-I and wave-V when comparing the highest level and the level at threshold. Thus, this 0.2 millisecond slight difference does not appear to be large enough to indicate a significant effect of anesthesia. Figure 3.59 illustrates these findings. Therefore, these results indicate that anesthesia does not diminish or consistently alter the amplitudes or latencies of wave-I or wave-V, and, thus, the effect of anesthesia is minimal.

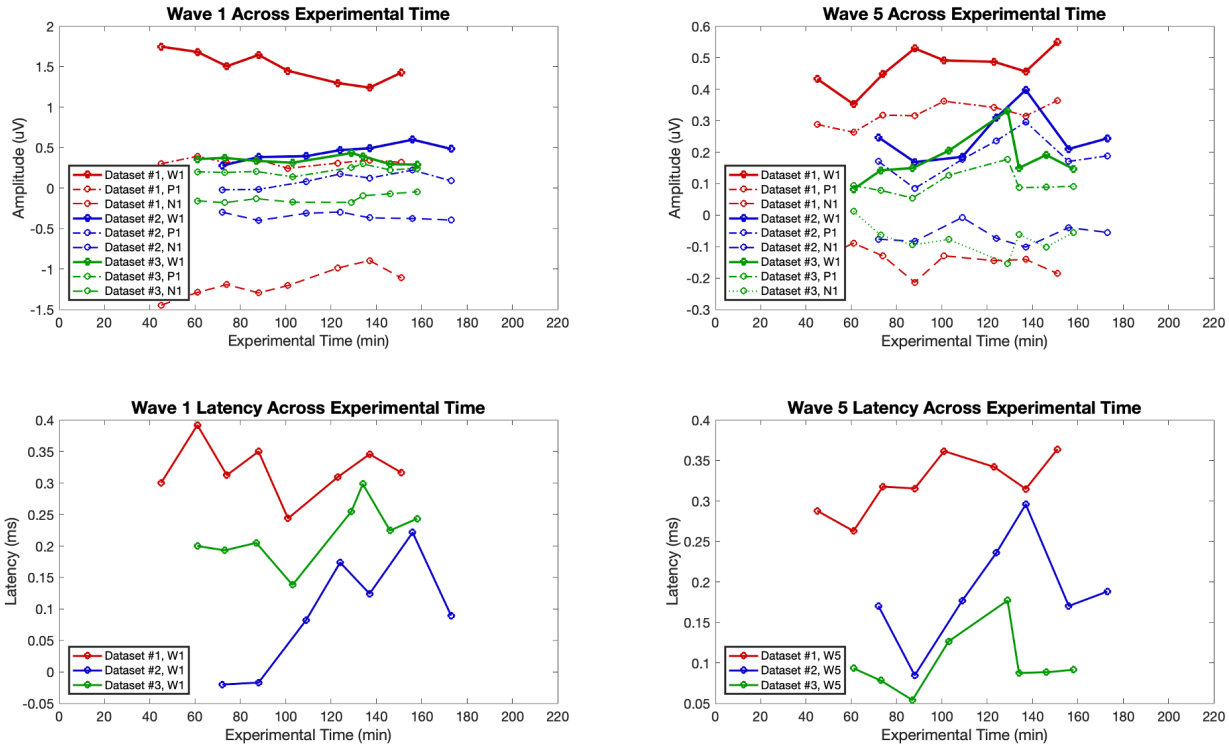

Figure 3.59. Wave-I and wave-V were identified in each waveform to quantify the effect of anesthesia. Across experimental time, there does not appear to any noticeable effects to amplitudes of wave-I or wave-V. Latencies, overall, also seem to be unaffected by anesthesia. Data set #2 appears to have a slight increasing latency trend across experimental time. However, in comparison to the typical latency differences between intensity levels, the magnitude of this trend in data set #2 does not appear significant. Altogether, this control measure confirms the effect of anesthesia is minimal.

4. DISCUSSION

4.1 Summary of mini cap variability

To quantify variability, the reliability, repeatability, reproducibility, and validity of the mini cap were characterized by identifying five potential sources of variability that could potentially affect the capability of the mini cap to produce robust ABRs. These five sources of variability were X-Time, X-Cap Removal, X-Experimenter, X-Cap, and X-Day. Firstly, the mini cap delivered reliable, repeatable, and reproducible thresholds, a frequently used ABR metric (see Tables 3.3, 3.4, and 3.5). Secondly, directly comparing and correlating the responses allowed for insight into the effect of introducing each source of variability on waveform morphology. Overall, at levels where the response was pronounced and well-defined (i.e. levels above 30 dBSPL), all five sources of variability did not significantly influence waveform morphology (see Figure 3.22). These threshold and correlation analyses suggest that the mini cap is not susceptible to the variability intrinsic to collecting replicate measurements within a short period of time, replacing the mini cap, having a different experimenter place the mini cap, collecting data with a different mini cap, or collecting data on two different days. The mini cap methodology to record ABRs in chinchillas is, thus, robust and dependable.

4.1.1 Summary of mini cap variability in comparison to subdermal needle variability

Direct comparisons between mini cap variability and subdermal needle variability were possible due to the simultaneous data collection capability within the mini cap methodology. Since within a single experiment the subdermal needle electrodes were not replaced, only comparisons for two out of the five sources of variability were applicable for both the mini cap and subdermal methods. To start with, X-Time represents the variability associated with replicate measurements without altering the mini cap or subdermal needles. Within a short period of time under the same conditions (i.e. X-Time), both methodologies produced robust ABRs (see Figure 3.24). This is reasonable since neither the mini cap or subdermal needles were being touched or altered in any way. Conversely, X-Day represents the variability

associated with replacing the mini cap and subdermal needle electrodes. As shown in Figure 3.25, the mini cap produced statistically less variable ABRs across two days in comparison to the subdermal method. Placing the mini cap does not appear to strongly effect the following ABR; however, placing the subdermal needles does appear to contribute to the variability of the method, confirming the inherent variability from electrode placement of the subdermal method (see Figure 3.1). Since the three other sources of variability (i.e. X-Removal, X-Cap, and X-Experimenter) represent introducing more significant methodological changes for the mini cap than the variability associated with collecting a replicate measurement under the same conditions for the subdermal needles (i.e since needles are not altered), it is compelling that the mini cap often produced statistically equivalent correlations than subdermal needles for these three sources of variability (see Figures 3.26, 3.27, and 3.28). In fact, for no variability condition was the mini cap variability greater than the subdermal variability, even when cap adjustments were made and needles adjustment were not made. Altogether, this implies that the mini cap, as a whole, produces less variable ABRs than the subdermal needles.

4.2 Summary of mini cap benefits

There are crucial benefits of collecting ABRs using the mini cap instead of using the three subdermal needle electrodes. One empirical benefit these results suggest is the need to collect fewer repetitions using the mini cap (see Figure 3.41). Since the ABR responses are roughly equal across all channels (see Figure 3.43), averaging across all channels will theoretically reduce the noise. Additionally, as mentioned in the previous section, these results indicate that the mini cap methodology produces less variable and more robust ABRs than the subdermal needle methodology (see Figure 3.25). The fact that all potential sources of variability have been quantified and deemed to have a minimal effect for the mini cap is already a striking benefit in comparison to the subdermal method that has not been equivalently quantified and has previously demonstrated considerable variability (see Figure 3.1). The previous two benefits are specific to collecting ABRs. However, there are significant benefits relevant to recording other evoked electrical potentials, like cortical potentials (see Figure 3.44), using the mini cap. For other more centrally evoked electrical potentials, each

channel may provide unique information for which using the mini cap will be especially useful (e.g., for source localization, as has been done in Wistar rats [64]).

4.3 Summary of mini cap limitations

There are a few limitations inherent to the mini cap methodology that should be discussed. As illustrated in Figure 3.4, there are consistently a few channels that are noisy and identified as bad channels. These bad channels are removed before averaging across all channels. Across several experiments, it appeared that a few channels (i.e. A25-A28) were consistently noisy. During the two experiments in which two different mini caps were used, it was confirmed that these same few bad channels appeared during data collection of both mini caps. Since there was consistency across both mini caps, it seems that the reason these few channels are frequently noisy is bigger than just an issue with the contamination of a few electrodes on a single mini cap. This mini cap was designed according to the head anatomy of a Wistar rat. Therefore, anatomical differences, specifically within that region of the mini cap (see quadrant-IV, Figure 3.57) between the chinchilla and the Wistar rat is one reasonable explanation as to why those few channels are consistently noisy across two mini caps. Thus, potential geometrical differences of the chinchilla head and the Wistar rat head, and the fact that this mini cap was designed according to the Wistar rat head, is one current limitation.

A few other limitations concern the experimental setup of the mini cap methodology. Since the head must be shaved in order to place the mini cap on a clean area of the scalp, the time to prepare the animal during an experiment is greater. The cost of the equipment to implement the mini cap methodology is also substantial. In fact, the mini cap costs around $1500, the ActiveTwo adapter cable for the mini cap costs around $1800, and the Biosemi ActiveTwo amplifier and buffer itself costs up to $32,000. Fortunately, the Actiview software used to analyze the multi-channel data from the BioSemi is free. Consequently, the mini cap is a methodology that requires a sizable early investment to introduce, but the numerous advantages for a wide range of evoked responses may make this investment worthwhile in the long run.

4.4 Future directions

4.4.1 Mini cap redesign

Redesigning the mini cap to be specific to the chinchilla anatomy would be ideal. However, for ABR responses, since bad channels are removed and all channels, showing equivalent responses, are averaged together, the current design of the mini cap is acceptable. If the electrically evoked potential recorded was instead a cortical measure where the capability to have channels portray unique information is necessary, utilizing a mini cap designed accordingly to the chinchilla anatomy would become more important. Although the current design is adequate for ABRs, moving forward and implementing different measures in which regions of the scalp exhibit different responses would require a mini cap redesign. The first step of this redesign would require obtaining an MRI of the chinchilla head. Then, a chinchilla brain atlas could be developed and the mini cap could be modified as necessary, as was done in the Wistar rat [64], [84], and is now provided by CorTech Solutions with the rat EEG mini cap.

4.4.2 Cortical measures and analyses

In order to visualize the capability of the mini cap to record an evoked response with significant between-channel differences, a cortical response was measured in an awake chinchilla (see Figure 3.44). To effectively record a spatially specific cortical response, using a high-density electrode cap is required. For the cortical response, there were unambiguous channel differences across the scalp since the response was originating from sources closer to the mini cap surface. Utilizing the mini cap allows for source localization, as validated in [64]. The feasibility of awake cortical measures has been verified here. Collecting more cortical data using the mini cap from additional animals will further refine the capability of the mini cap to record cortical activity.

Likewise, a prominent topic of current interest in the hearing science field is the central effects of cochlear synaptopathy. The capability of the mini cap to record awake cortical responses would make studying this in chinchillas thoroughly feasible. Finally, it is possible to use the up to eight external channels to measure responses from different sources around

the chinchilla head, while simultaneously recording with the mini cap. Similarly, by referencing to different channels on the mini cap, there is the potential to separate out different anatomical sources within a single response [85]. Analyses emphasizing a multitude of different anatomical sources would provide significantly more information. Overall, this mini cap methodology allows for the completion of far more specific and detailed awake cortical and efferent studies than would be possible using the subdermal needle methodology.

4.4.3 Animal & human translation

Most importantly, continuing to align the chinchilla mini cap methodology with the human cap methodology will allow for enhanced translation of animal findings to human clinical improvements. Here, the experimental design of chinchilla data collection was considerably aligned to that of humans. To advance this alignment further, one approach is to implement the more efficient ABR data collection procedure used in several humans labs [86]–[88]. In these types of efficient procedures, frequencies, levels, and ears in which the sound is played into are inter weaved together. Traditionally, only one ear receives the sound and each frequency and level combination requires starting and stopping data collection. This intertwining of stimuli conditions drastically improves the efficiency of data collection.

Besides continuing to improve the alignment of chinchilla and human ABR data collection, a crucial next step is to integrate the chinchilla mini cap results with the human cap results. Collecting ABRs using the mini cap before and after a TTS noise exposure, and then quantifying the typical CS metrics (e.g., wave-I amplitude, wave-V latency) will allow for direct comparison to human ABR metrics. In a previous study in which chinchilla CS metrics were directly compared to human CS metrics, one issue that emerged was there appeared to be larger variability in chinchilla ABRs than human ABRs [89]. Although thresholds were not noticeably affected, suprathreshold wave analyses (i.e. peak picking) were affected by this more considerable variability resulting from the subdermal needle methodology. Overall, this made comparisons between the chinchilla metrics and human metrics significantly more difficult. The objective moving forward is to perform a similar comparison between chinchillas and humans, but, instead, use the mini cap to record ABRs in chinchillas. Based on validation from the research presented here, the mini cap will reduce this variability and

allow for more straightforward comparisons to human metrics. The fundamental motivation behind this research is to use our chinchilla data to advance human clinical diagnostics and human clinical outcomes. The small animal EEG mini cap is a state-of-the-art development that boosts alignment between chinchilla ABR data and human ABR data, considerably moving the needle forward in our pursuit to achieve this valuable translation between our chinchillas discoveries and human clinical advancements.

5. CONCLUSION

Here, a multi-channel EEG mini cap was implemented and generated robust auditory brainstem responses in chinchillas. This mini cap met the critical need for an improved ABR methodology due to the inherent variability of the conventional subdermal needle methodology. Additionally, since in human auditory research multi-channel EEG caps are routinely used, employing this mini cap allowed for remarkably enhanced alignment in methodology between chinchillas and humans. Other methodological benefits of recording ABRs using the mini cap in comparison to the subdermal needle electrodes became clearly apparent during this study. For example, the opportunity to simultaneously collect both mini cap and subdermal ABRs using three external channels is only possible using the mini cap methodology.

In this study, first, the feasibility of the mini cap to record ABRs in chinchillas was validated. Utilizing the mini cap, high-quality EEG recordings of comparable magnitude as the subdermal recordings were recorded from the exterior scalp of a small animal (i.e. chinchilla). After validating the feasibility, a comprehensive paradigm to assess the sources of bias and variability inherent to the mini cap methodology was devised. In this, the reliability, repeatability, reproducibility, and validity of the mini cap was quantified. It was confirmed that the mini cap is able to produce highly reliable, repeatable, and reproducible ABRs across each conceivable source of variability. Correspondingly, the validity of the mini cap was substantiated by corroborating the accuracy and precision of the mini cap. The compelling benefits of employing the mini cap were subsequently identified. The ideal number of both repetitions and channels necessary to produce a highly correlated ABR response was computed. Since the ABR originates from a deep-seated source within the head, all channels display equivalent ABR responses when referenced to a tiptrode in the ear canal. However, averaging across several channels contributes noise reduction to the final response, which explains why the ideal number of repetitions quantified was fewer for the mini cap than the subdermal method.

Altogether, this thesis validates the minimal effect of variability within the mini cap methodology. Considering the substantial variability of the conventional subdermal needle methodology and the compelling benefits of the mini cap methodology, the mini

cap is proposed to emerge as the superior ABR methodology. Therefore, it is decidedly recommended to move forward recording ABRs in chinchillas using the mini cap methodology detailed in this research.

Animal 1, Test

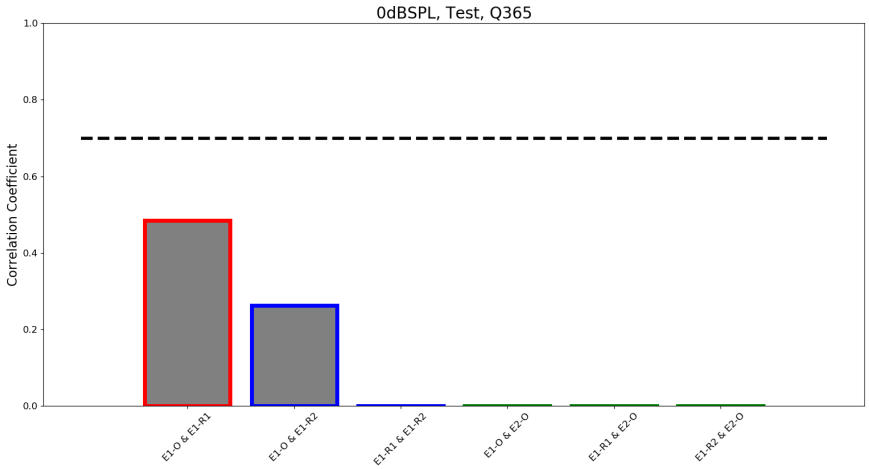

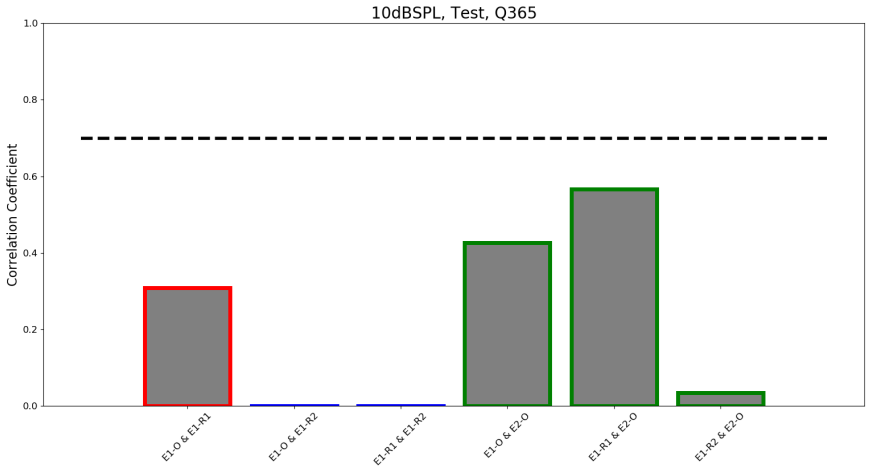

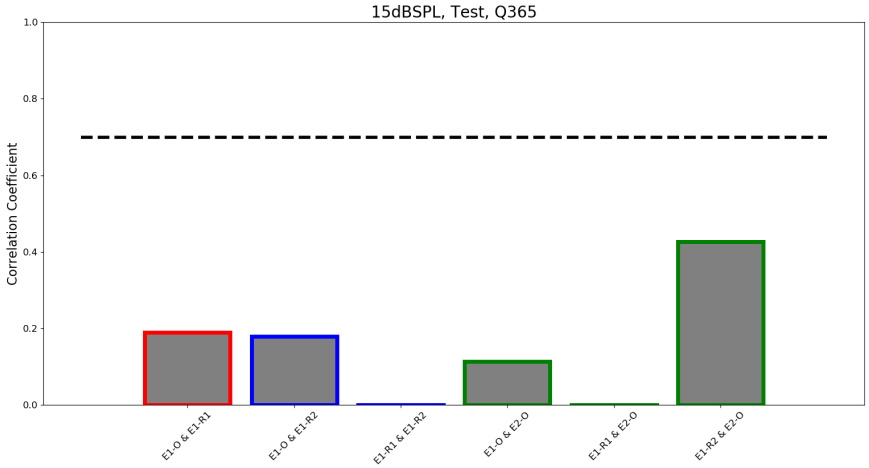
15dBSPL, Test, Q365
Correlation Coefficient
1.0
0.8
0.6
0.4
0.2
0.0
E1-O & E1-R1
E1-O & E1-R2
E1-R1 & E1-R2
E1-O & E2-O
E1-R1 & E2-O
E1-R2 & E2-O

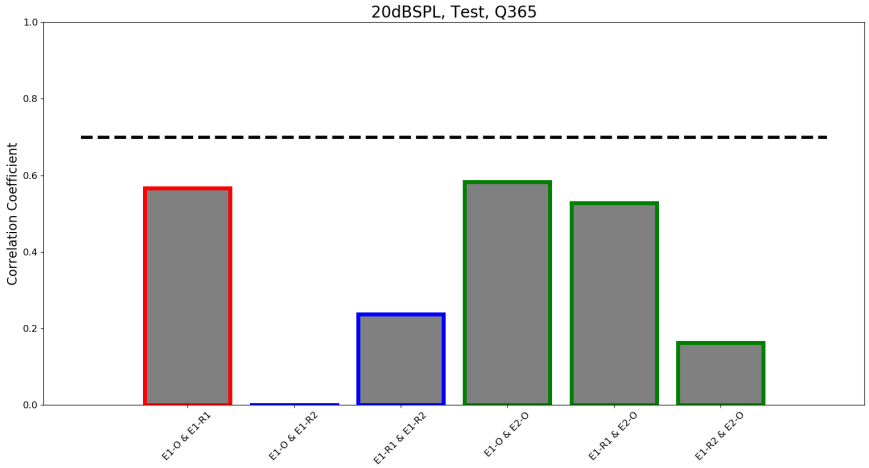
20dBSPL, Test, Q365
Correlation Coefficient
1.0
0.8
0.6
0.4
0.2
0.0
E1-O & E1-R1
E1-O & E1-R2
E1-R1 & E1-R2
E1-O & E2-O
E1-R1 & E2-O
E1-R2 & E2-O

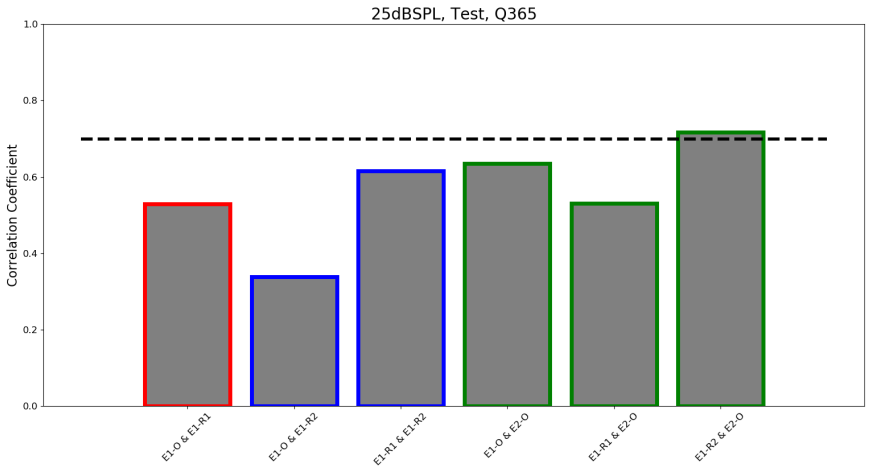
25dBSPL, Test, Q365
Correlation Coefficient
1.0
0.8
0.6
0.4
0.2
0.0
E1-O & E1-R1
E1-O & E1-R2
E1-R1 & E1-R2
E1-O & E2-O
E1-R1 & E2-O
E1-R2 & E2-O

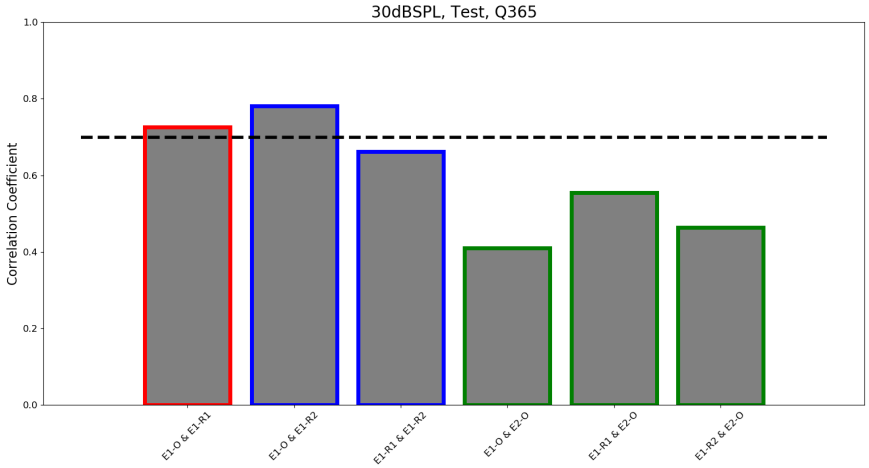
30dBSPL, Test, Q365
Correlation Coefficient
1.0
0.8
0.6
0.4
0.2
0.0
E1-O & E1-R1
E1-O & E1-R2
E1-R1 & E1-R2
E1-O & E2-O
E1-R1 & E2-O
E1-R2 & E2-O

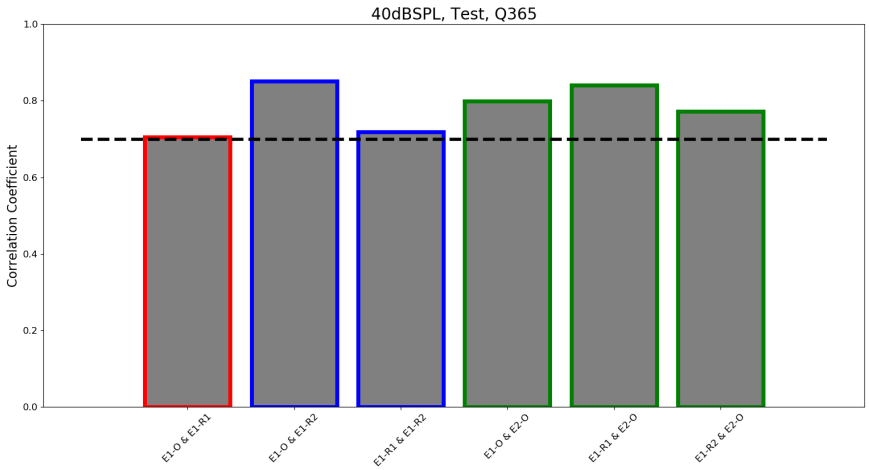
40dBSPL, Test, Q365
Correlation Coefficient
1.0
0.8
0.6
0.4
0.2
0.0
E1-O & E1-R1
E1-O & E1-R2
E1-R1 & E1-R2
E1-O & E2-O
E1-R1 & E2-O
E1-R2 & E2-O

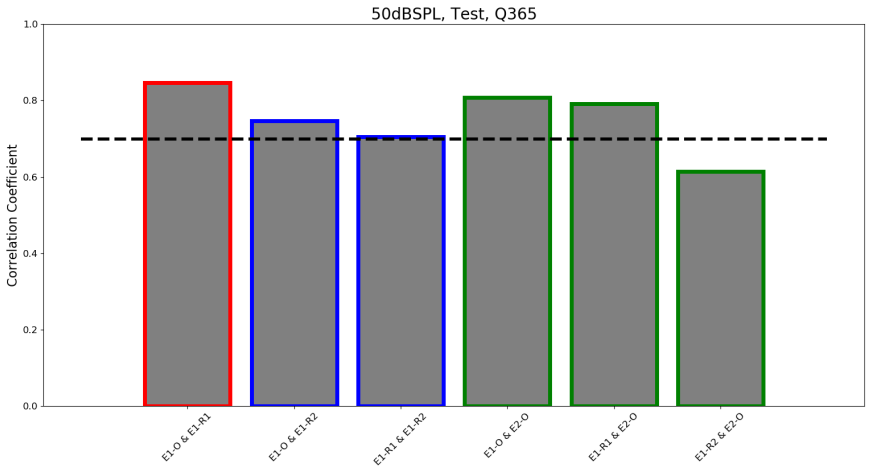
50dBSPL, Test, Q365
Correlation Coefficient
1.0
0.8
0.6
0.4
0.2
0.0
E1-O & E1-R1
E1-O & E1-R2
E1-R1 & E1-R2
E1-O & E2-O
E1-R1 & E2-O
E1-R2 & E2-O

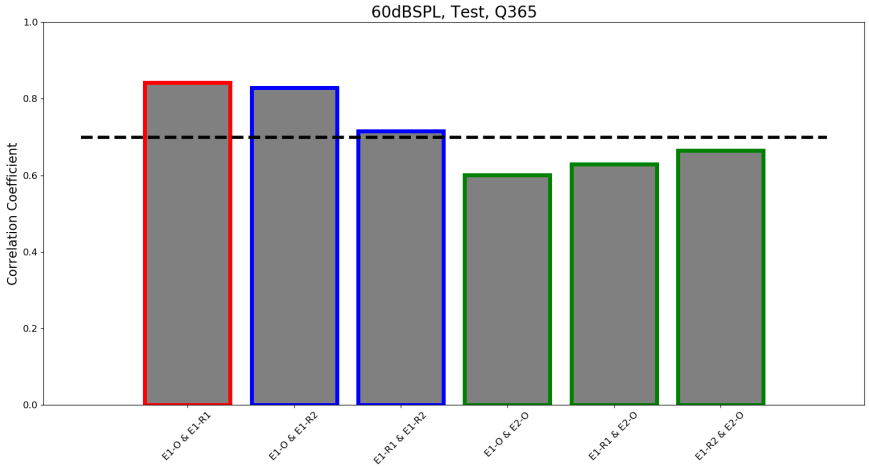
60dBSPL, Test, Q365
Correlation Coefficient
1.0
0.8
0.6
0.4
0.2
0.0
E1-O & E1-R1
E1-O & E1-R2
E1-R1 & E1-R2
E1-O & E2-O
E1-R1 & E2-O
E1-R2 & E2-O

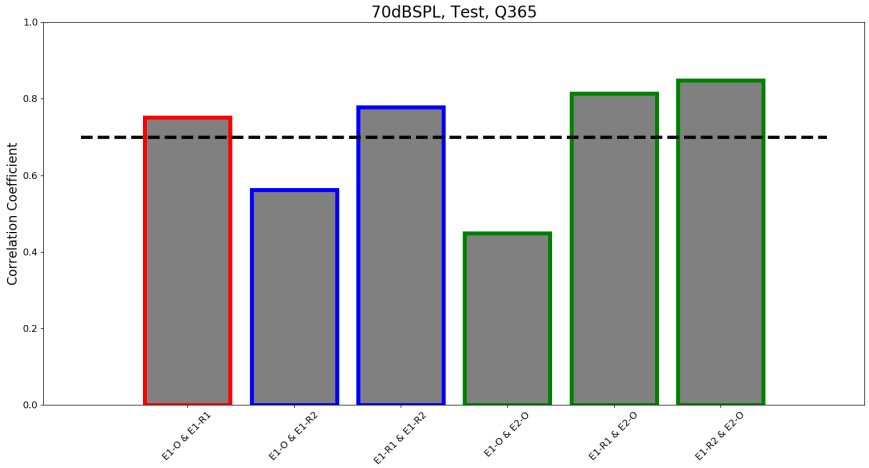
70dBSPL, Test, Q365
Correlation Coefficient
1.0
0.8
0.6
0.4
0.2
0.0
E1-O & E1-R1
E1-O & E1-R2
E1-R1 & E1-R2
E1-O & E2-O
E1-R1 & E2-O
E1-R2 & E2-O

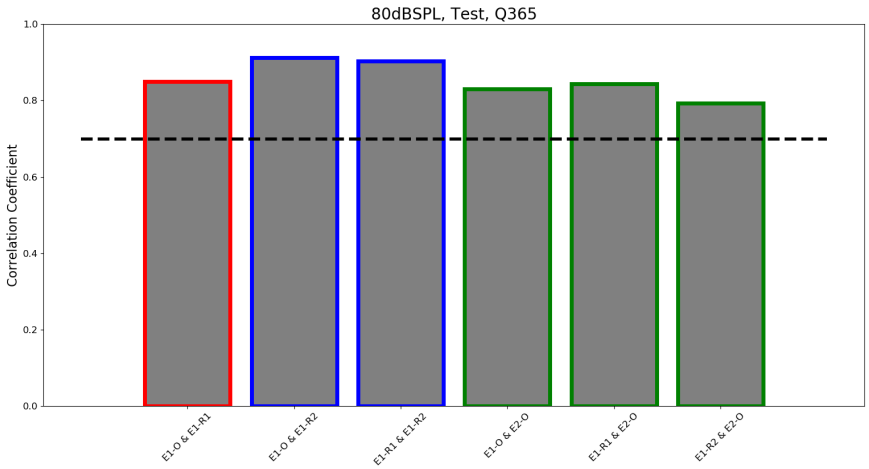
80dBSPL, Test, Q365
Correlation Coefficient
1.0
0.8
0.6
0.4
0.2
0.0
E1-O & E1-R1
E1-O & E1-R2
E1-R1 & E1-R2
E1-O & E2-O
E1-R1 & E2-O
E1-R2 & E2-O

Animal 1, Retest

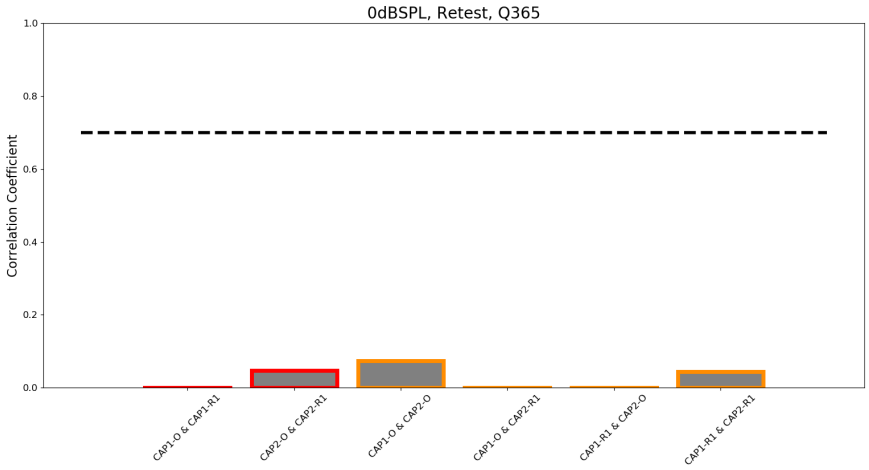

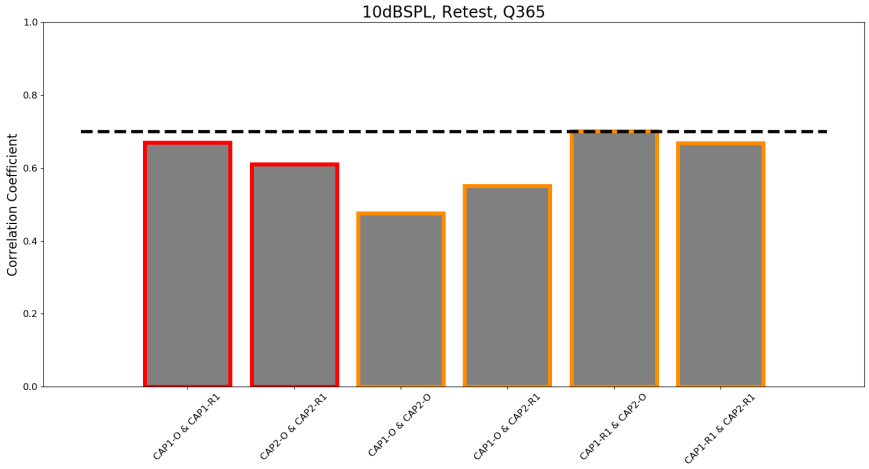

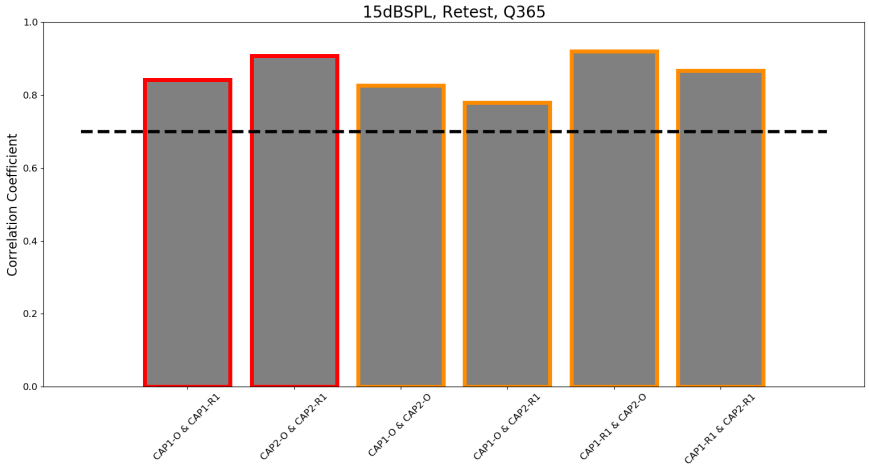
15dBSPL, Retest, Q365
Correlation Coefficient
1.0
0.8
0.6
0.4
0.2
0.0
CAP1-O & CAP1-R1
CAP2-O & CAP2-R1
CAP1-O & CAP2-O
CAP1-O & CAP2-R1
CAP1-R1 & CAP2-O
CAP1-R1 & CAP2-R1

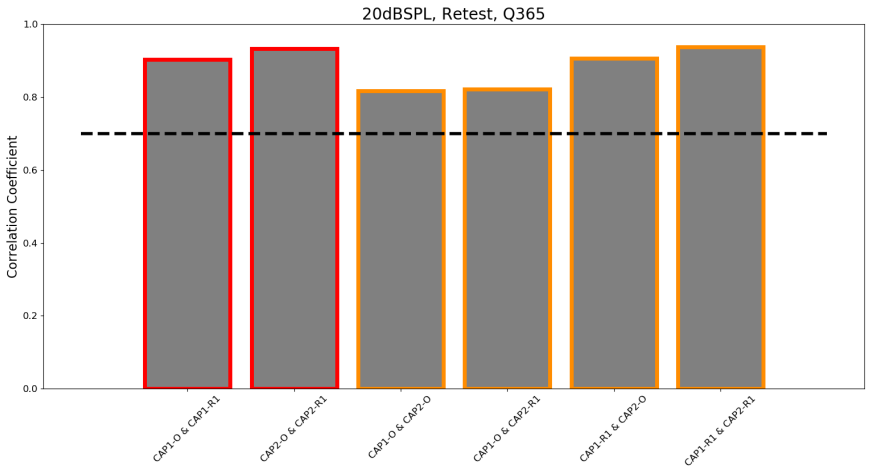
20dBSPL, Retest, Q365
Correlation Coefficient
1.0
0.8
0.6
0.4
0.2
0.0
CAP1-O & CAP1-R1
CAP2-O & CAP2-R1
CAP1-O & CAP2-O
CAP1-O & CAP2-R1
CAP1-R1 & CAP2-O
CAP1-R1 & CAP2-R1

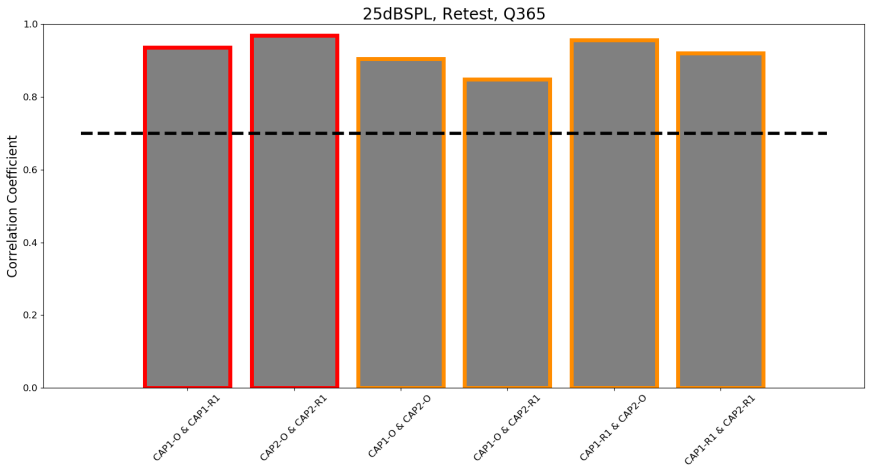
25dBSPL, Retest, Q365
Correlation Coefficient
1.0
0.8
0.6
0.4
0.2
0.0
CAP1-O & CAP1-R1
CAP2-O & CAP2-R1
CAP1-O & CAP2-O
CAP1-O & CAP2-R1
CAP1-R1 & CAP2-O
CAP1-R1 & CAP2-R1

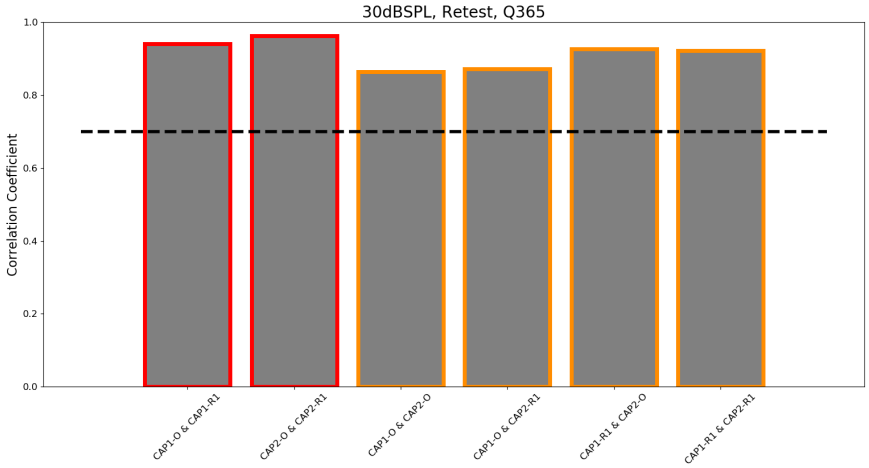
30dBSPL, Retest, Q365
Correlation Coefficient
1.0
0.8
0.6
0.4
0.2
0.0
CAP1-O & CAP1-R1
CAP2-O & CAP2-R1
CAP1-O & CAP2-O
CAP1-O & CAP2-R1
CAP1-R1 & CAP2-O
CAP1-R1 & CAP2-R1

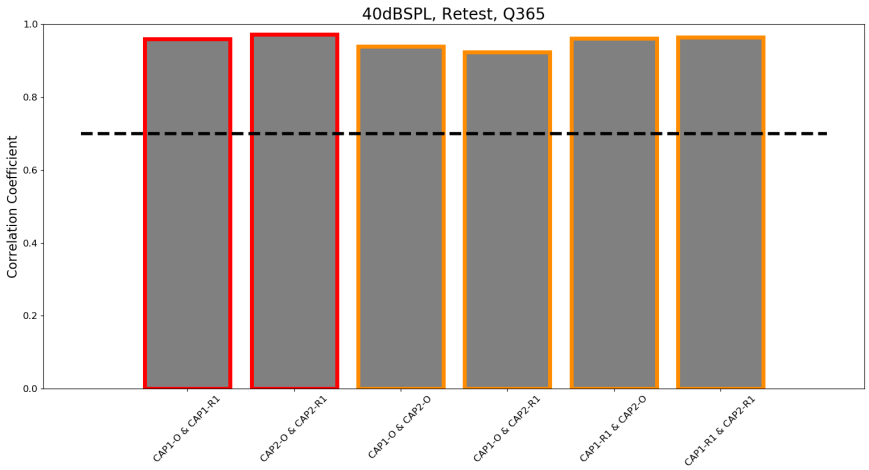
40dBSPL, Retest, Q365
Correlation Coefficient
1.0
0.8
0.6
0.4
0.2
0.0
CAP1-O & CAP1-R1
CAP2-O & CAP2-R1
CAP1-O & CAP2-O
CAP1-O & CAP2-R1
CAP1-R1 & CAP2-O
CAP1-R1 & CAP2-R1

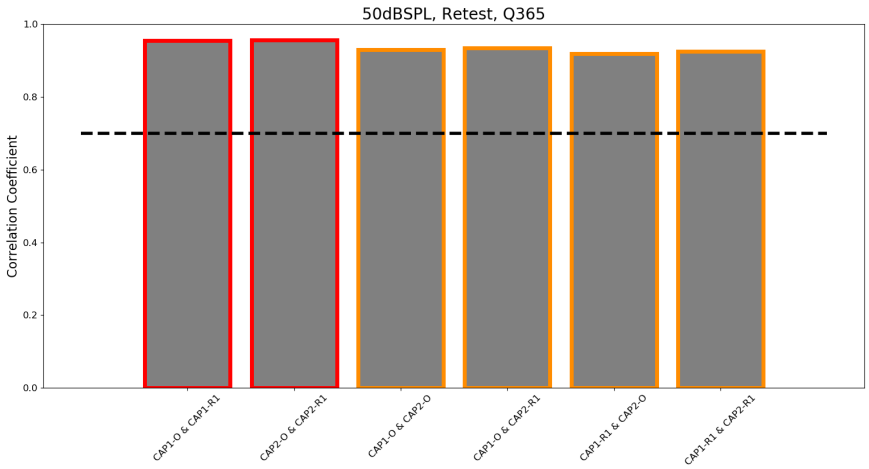
50dBSPL, Retest, Q365
Correlation Coefficient
1.0
0.8
0.6
0.4
0.2
0.0
CAP1-O & CAP1-R1
CAP2-O & CAP2-R1
CAP1-O & CAP2-O
CAP1-O & CAP2-R1
CAP1-R1 & CAP2-O
CAP1-R1 & CAP2-R1

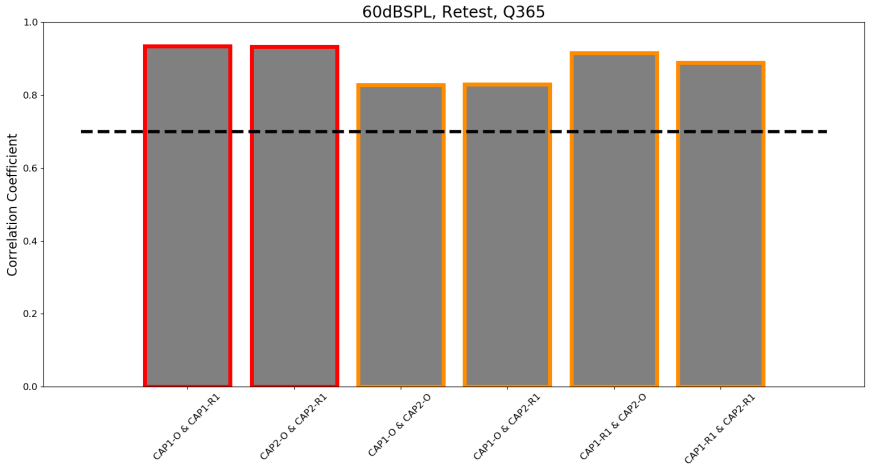
60dBSPL, Retest, Q365
Correlation Coefficient
1.0
0.8
0.6
0.4
0.2
0.0
CAP1-O & CAP1-R1
CAP2-O & CAP2-R1
CAP1-O & CAP2-O
CAP1-O & CAP2-R1
CAP1-R1 & CAP2-O
CAP1-R1 & CAP2-R1

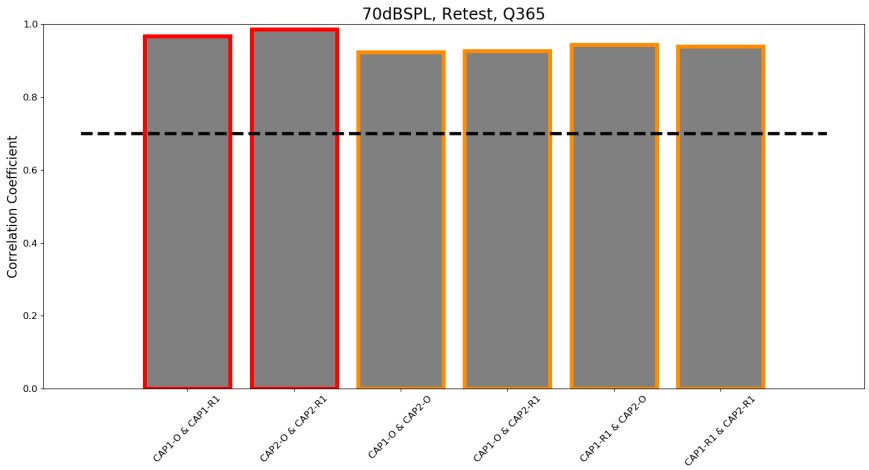
70dBSPL, Retest, Q365
Correlation Coefficient
1.0
0.8
0.6
0.4
0.2
0.0
CAP1-O & CAP1-R1
CAP2-O & CAP2-R1
CAP1-O & CAP2-O
CAP1-O & CAP2-R1
CAP1-R1 & CAP2-O
CAP1-R1 & CAP2-R1

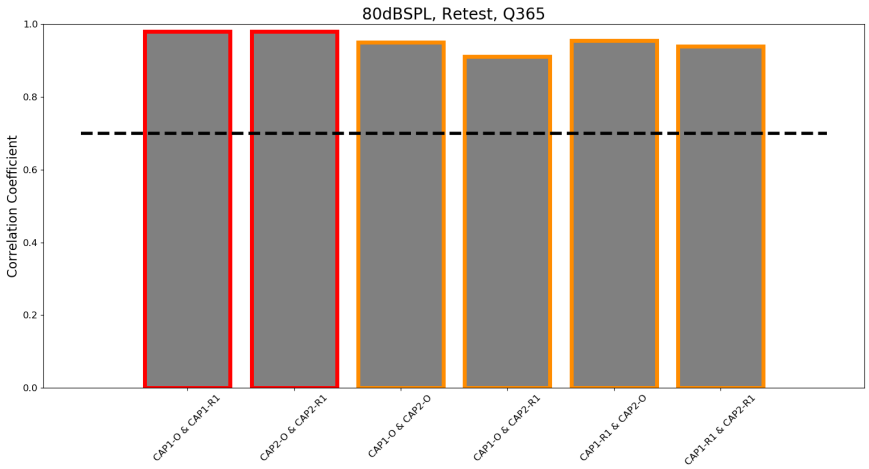
80dBSPL, Retest, Q365
Correlation Coefficient
1.0
0.8
0.6
0.4
0.2
0.0
CAP1-O & CAP1-R1
CAP2-O & CAP2-R1
CAP1-O & CAP2-O
CAP1-O & CAP2-R1
CAP1-R1 & CAP2-O
CAP1-R1 & CAP2-R1

Animal 2, Test

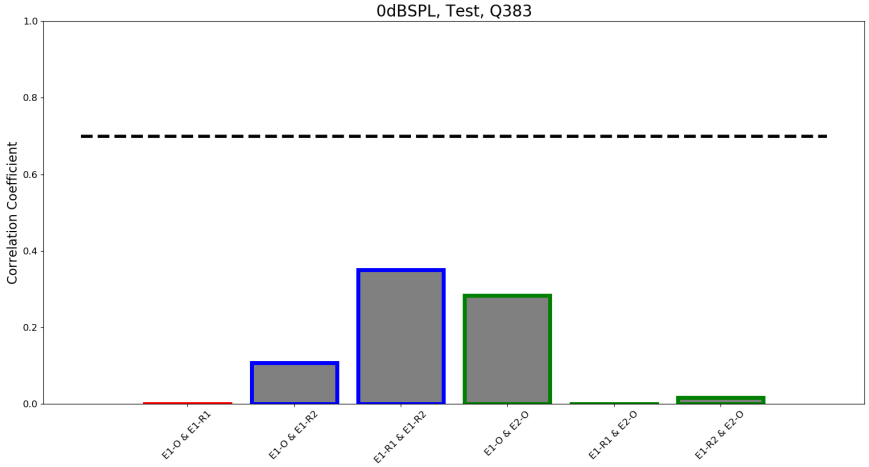

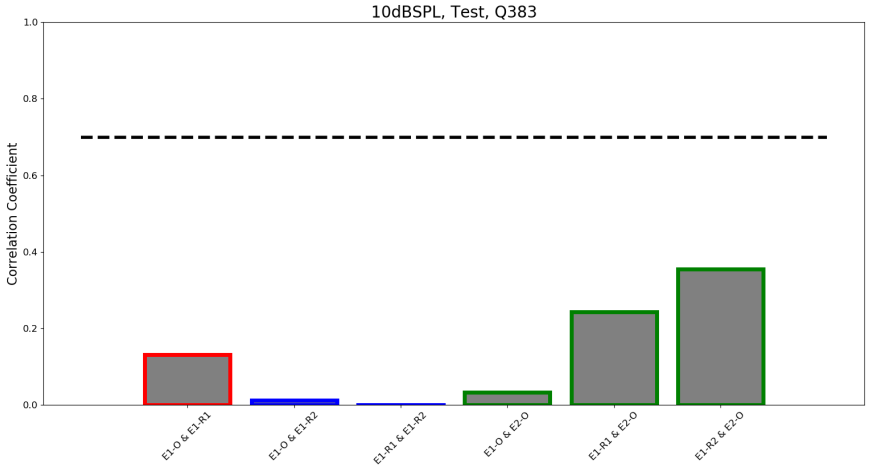

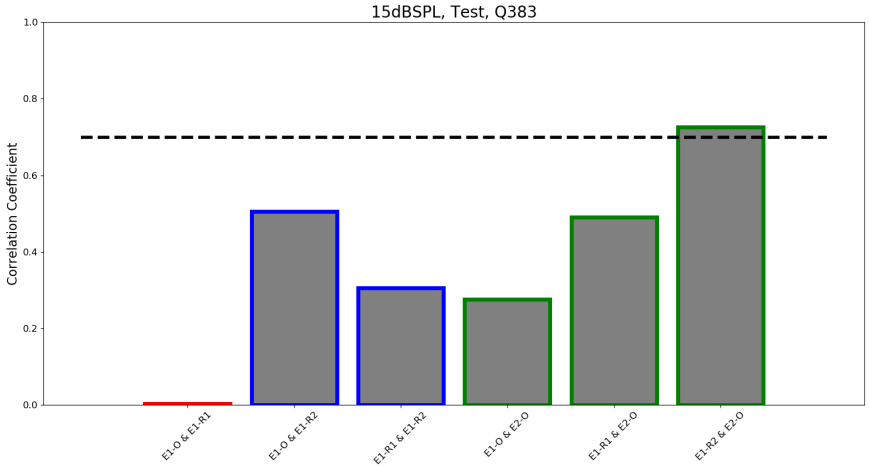
15dBSPL, Test, Q383
Correlation Coefficient
1.0
0.8
0.6
0.4
0.2
0.0
E1-O & E1-R1
E1-O & E1-R2
E1-R1 & E1-R2
E1-O & E2-O
E1-R1 & E2-O
E1-R2 & E2-O

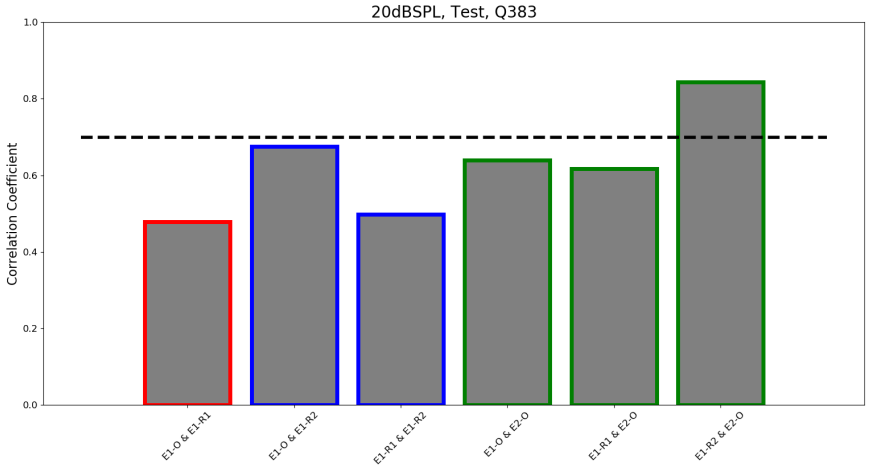
20dBSPL, Test, Q383
Correlation Coefficient
1.0
0.8
0.6
0.4
0.2
0.0
E1-O & E1-R1
E1-O & E1-R2
E1-R1 & E1-R2
E1-O & E2-O
E1-R1 & E2-O
E1-R2 & E2-O

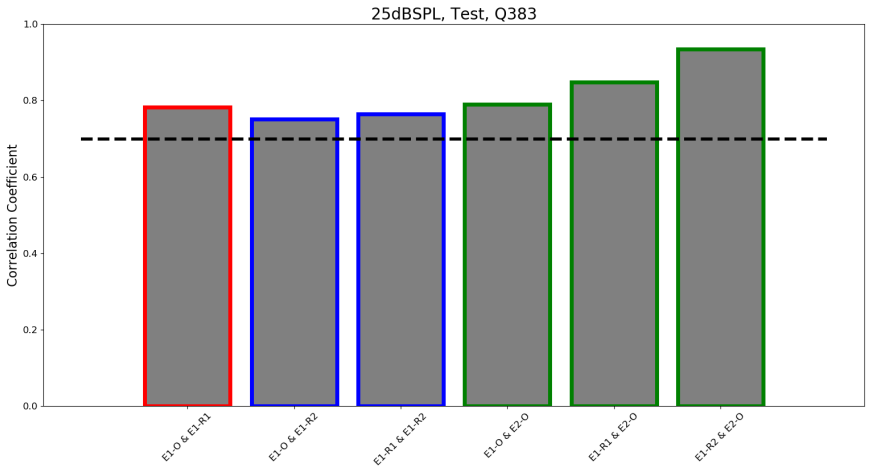
25dBSPL, Test, Q383
Correlation Coefficient
1.0
0.8
0.6
0.4
0.2
0.0
E1-O & E1-R1
E1-O & E1-R2
E1-R1 & E1-R2
E1-O & E2-O
E1-R1 & E2-O
E1-R2 & E2-O

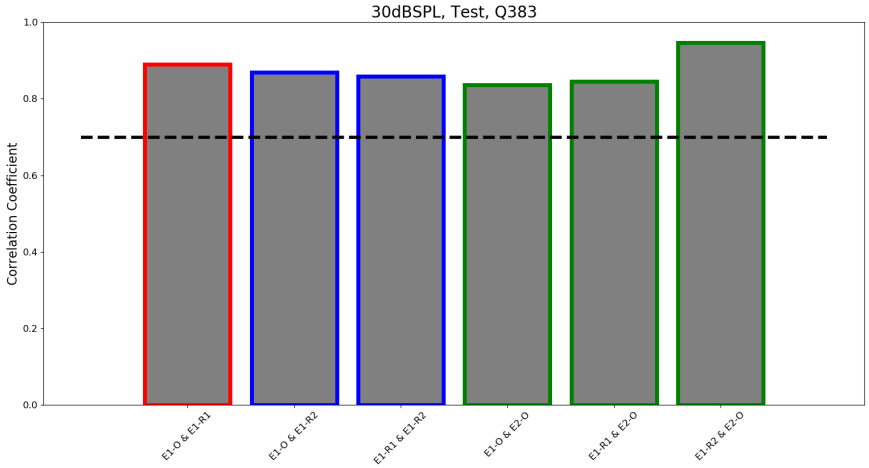
30dBSPL, Test, Q383
Correlation Coefficient
1.0
0.8
0.6
0.4
0.2
0.0
E1-O & E1-R1
E1-O & E1-R2
E1-R1 & E1-R2
E1-O & E2-O
E1-R1 & E2-O
E1-R2 & E2-O

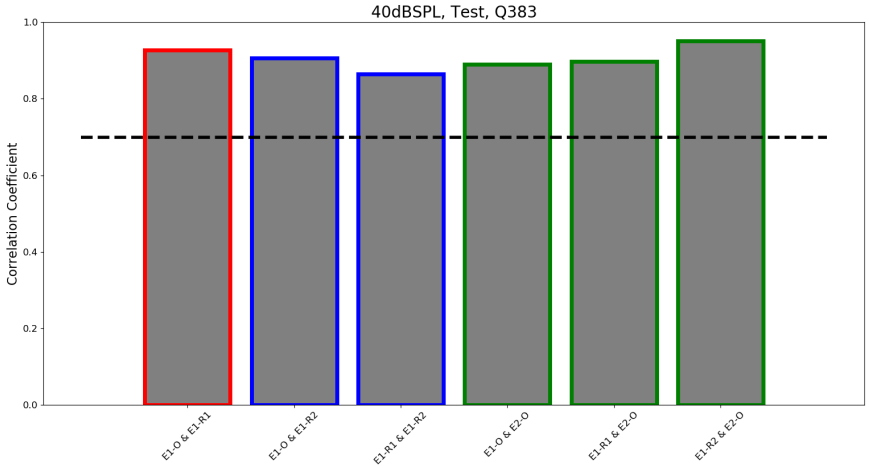
40dBSPL, Test, Q383
Correlation Coefficient
1.0
0.8
0.6
0.4
0.2
0.0
E1-O & E1-R1
E1-O & E1-R2
E1-R1 & E1-R2
E1-O & E2-O
E1-R1 & E2-O
E1-R2 & E2-O

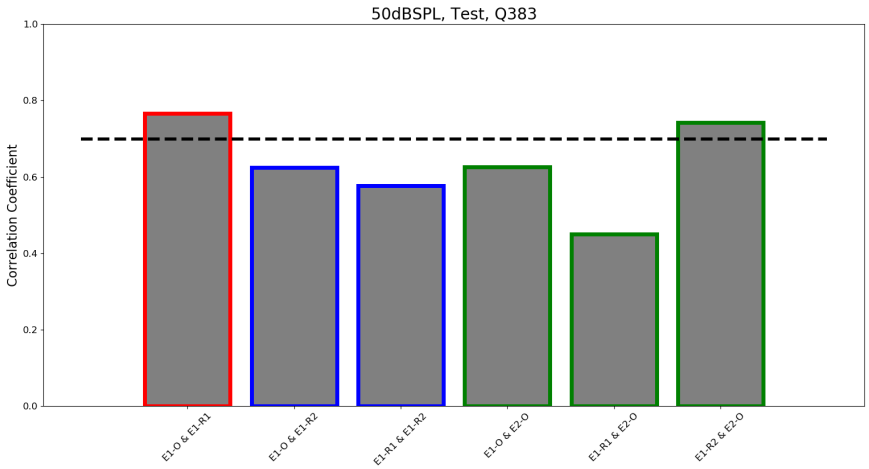
50dBSPL, Test, Q383
Correlation Coefficient
1.0
0.8
0.6
0.4
0.2
0.0
E1-O & E1-R1
E1-O & E1-R2
E1-R1 & E1-R2
E1-O & E2-O
E1-R1 & E2-O
E1-R2 & E2-O

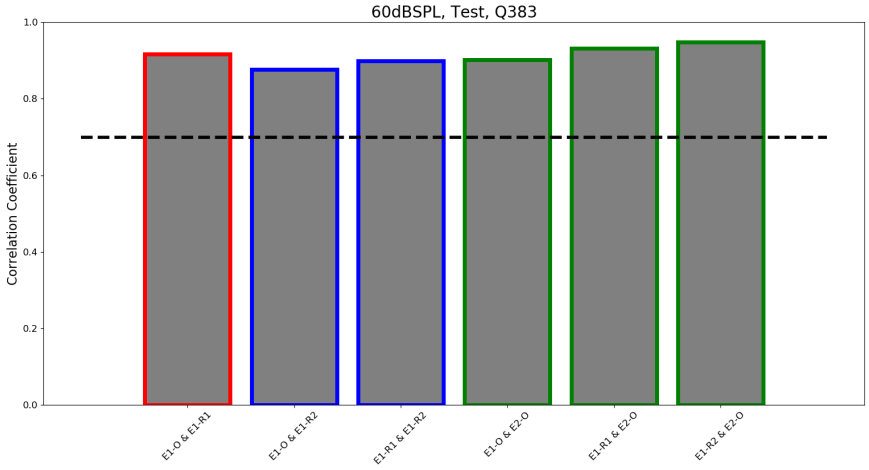
60dBSPL, Test, Q383
Correlation Coefficient
1.0
0.8
0.6
0.4
0.2
0.0
E1-O & E1-R1
E1-O & E1-R2
E1-R1 & E1-R2
E1-O & E2-O
E1-R1 & E2-O
E1-R2 & E2-O

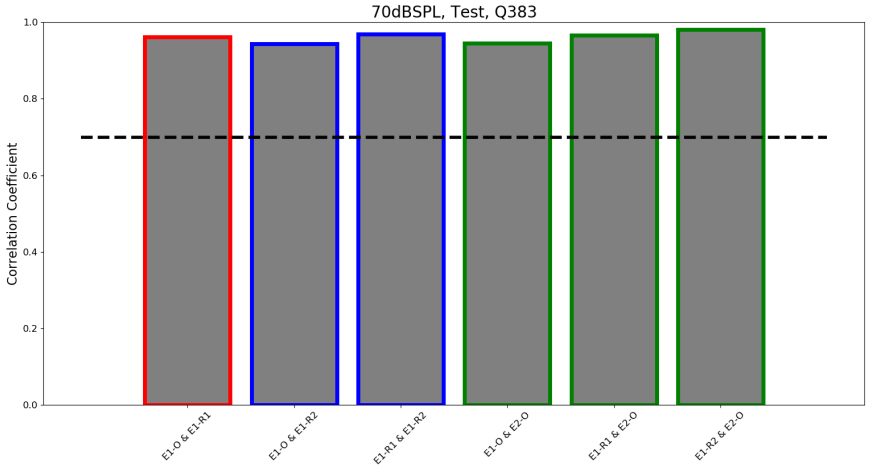
70dBSPL, Test, Q383
Correlation Coefficient
1.0
0.8
0.6
0.4
0.2
0.0
E1-O & E1-R1
E1-O & E1-R2
E1-R1 & E1-R2
E1-O & E2-O
E1-R1 & E2-O
E1-R2 & E2-O

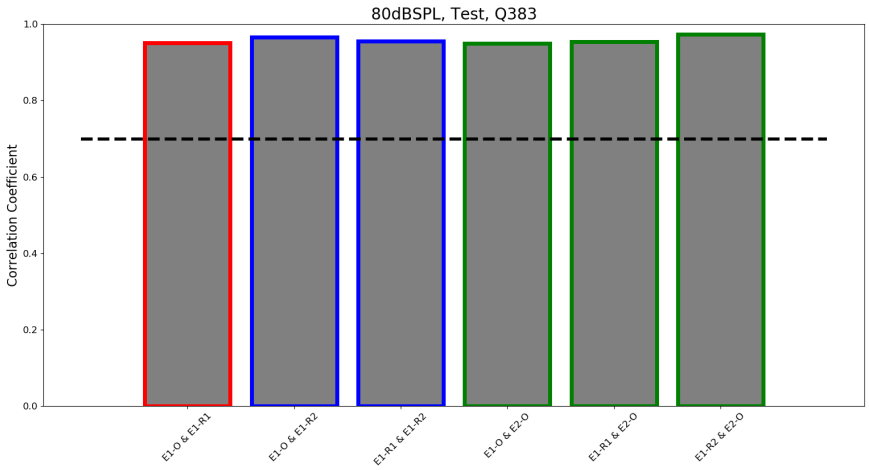
80dBSPL, Test, Q383
Correlation Coefficient
1.0
0.8
0.6
0.4
0.2
0.0
E1-O & E1-R1
E1-O & E1-R2
E1-R1 & E1-R2
E1-O & E2-O
E1-R1 & E2-O
E1-R2 & E2-O

Animal 2, Retest

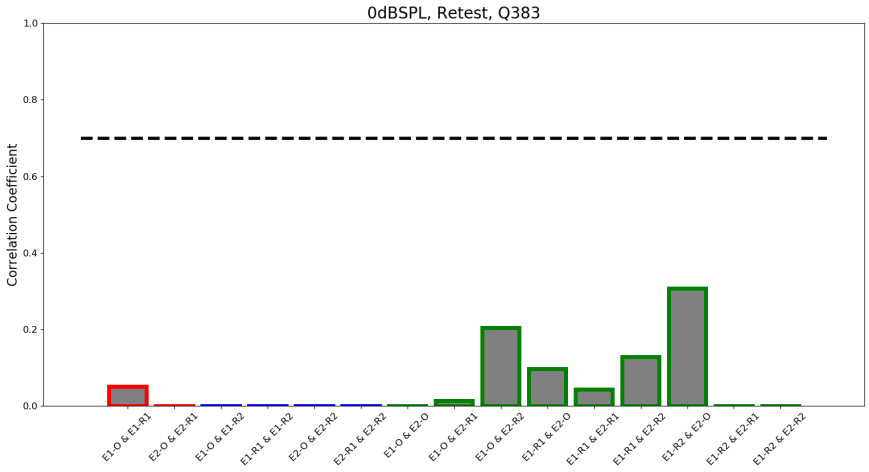

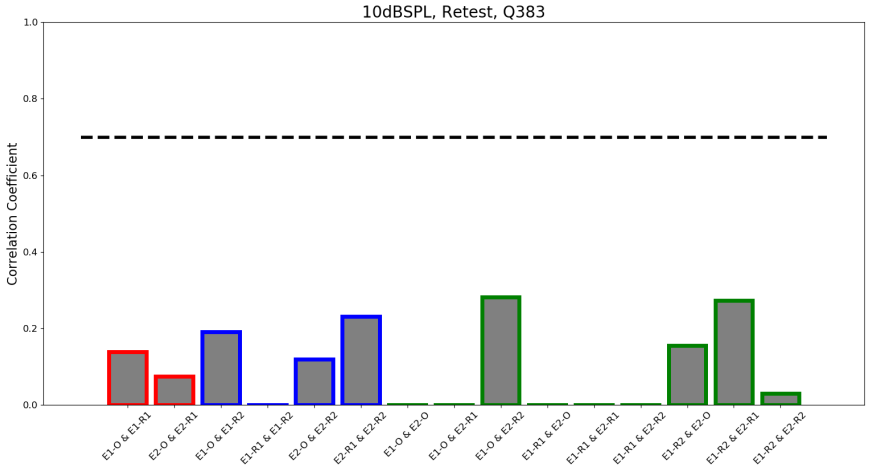

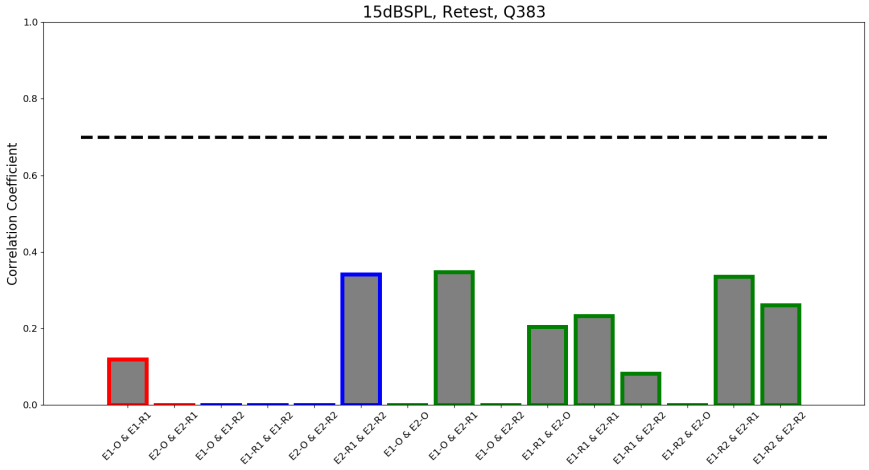
15dBSPL, Retest, Q383
Correlation Coefficient
1.0
0.8
0.6
0.4
0.2
0.0
E1-O & E1-R1
E2-O & E2-R1
E1-O & E1-R2
E1-R1 & E1-R2
E2-O & E2-R2
E2-R1 & E2-R2
E1-O & E2-O
E1-O & E2-R1
E1-O & E2-R2
E1-R1 & E2-O
E1-R1 & E2-R1
E1-R1 & E2-R2
E1-R2 & E2-O
E1-R2 & E2-R1
E1-R2 & E2-R2

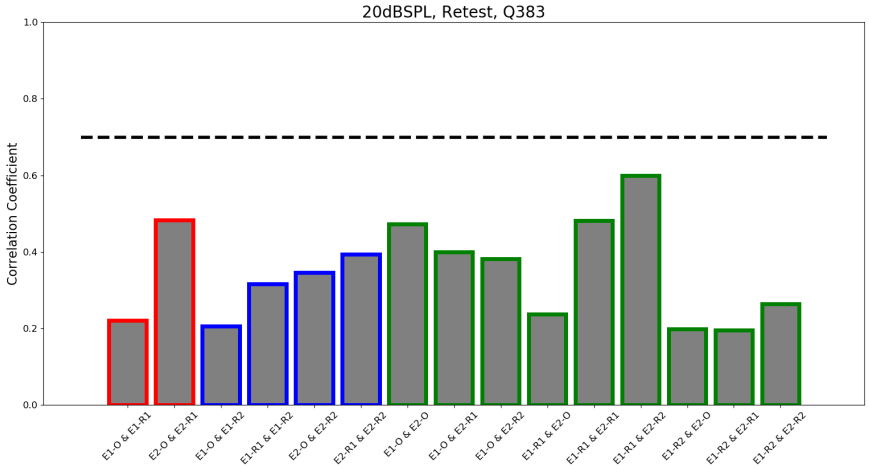
20dBSPL, Retest, Q383
Correlation Coefficient
1.0
0.8
0.6
0.4
0.2
0.0
E1-O & E1-R1
E2-O & E2-R1
E1-O & E1-R2
E1-R1 & E1-R2
E2-O & E2-R2
E2-R1 & E2-R2
E1-O & E2-O
E1-O & E2-R1
E1-O & E2-R2
E1-R1 & E2-O
E1-R1 & E2-R1
E1-R1 & E2-R2
E1-R2 & E2-O
E1-R2 & E2-R1
E1-R2 & E2-R2

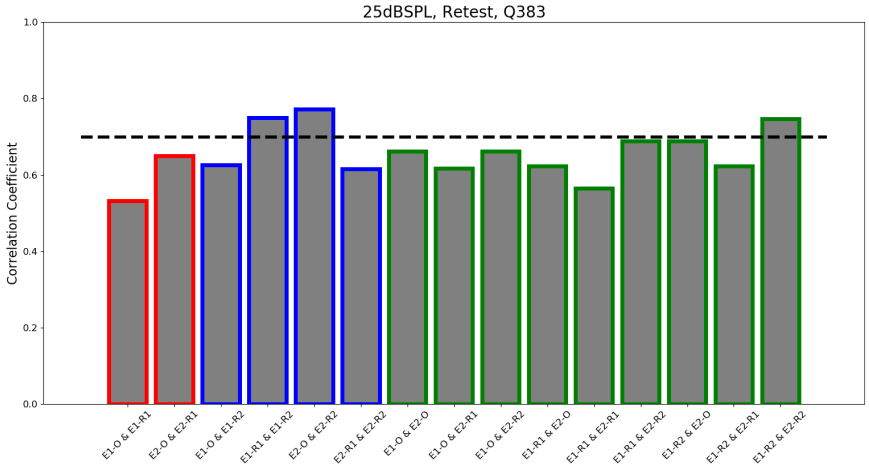
25dBSPL, Retest, Q383
Correlation Coefficient
1.0
0.8
0.6
0.4
0.2
0.0
E1-O & E1-R1
E2-O & E2-R1
E1-O & E1-R2
E1-R1 & E1-R2
E2-O & E2-R2
E2-R1 & E2-R2
E1-O & E2-O
E1-O & E2-R1
E1-O & E2-R2
E1-R1 & E2-O
E1-R1 & E2-R1
E1-R1 & E2-R2
E1-R2 & E2-O
E1-R2 & E2-R1
E1-R2 & E2-R2

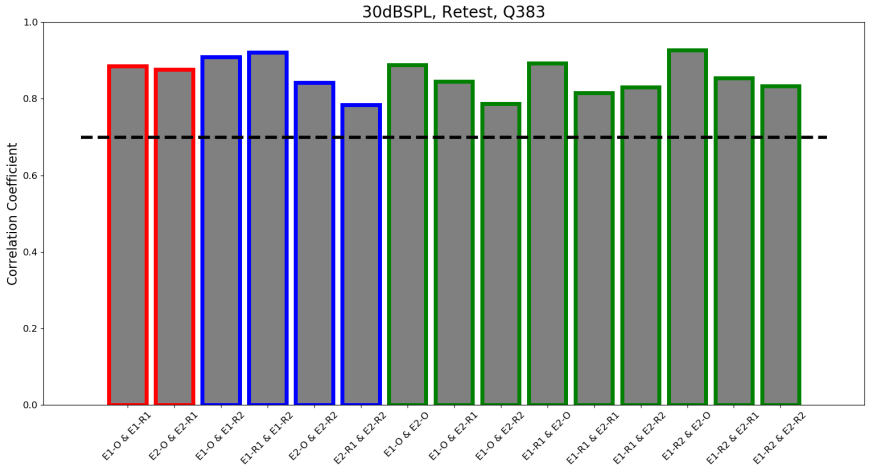
30dBSPL, Retest, Q383
Correlation Coefficient
1.0
0.8
0.6
0.4
0.2
0.0
E1-O & E1-R1
E2-O & E2-R1
E1-O & E1-R2
E1-R1 & E1-R2
E2-O & E2-R2
E2-R1 & E2-R2
E1-O & E2-O
E1-O & E2-R1
E1-O & E2-R2
E1-R1 & E2-O
E1-R1 & E2-R1
E1-R1 & E2-R2
E1-R2 & E2-O
E1-R2 & E2-R1
E1-R2 & E2-R2

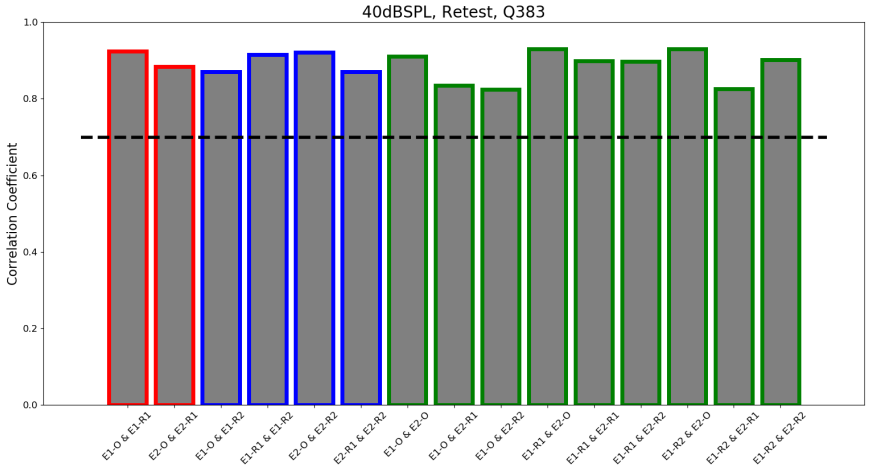
40dBSPL, Retest, Q383
Correlation Coefficient
1.0
0.8
0.6
0.4
0.2
0.0
E1-O & E1-R1
E2-O & E2-R1
E1-O & E1-R2
E1-R1 & E1-R2
E2-O & E2-R2
E2-R1 & E2-R2
E1-O & E2-O
E1-O & E2-R1
E1-O & E2-R2
E1-R1 & E2-O
E1-R1 & E2-R1
E1-R1 & E2-R2
E1-R2 & E2-O
E1-R2 & E2-R1
E1-R2 & E2-R2

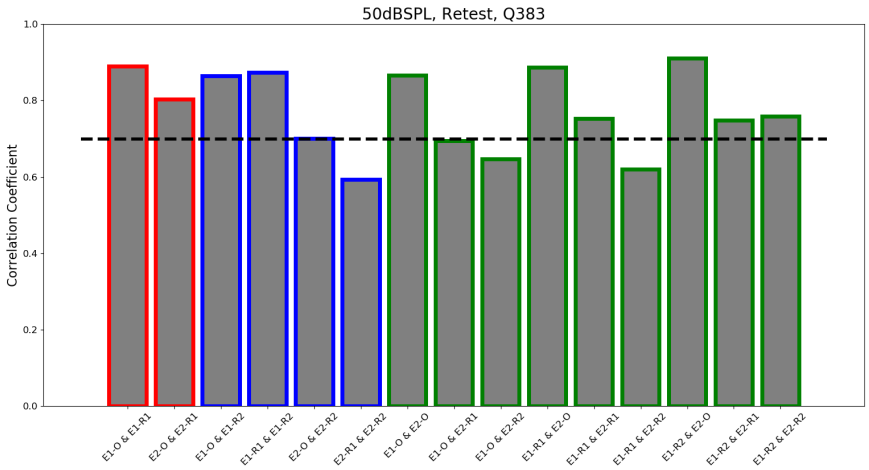
50dBSPL, Retest, Q383
Correlation Coefficient
1.0
0.8
0.6
0.4
0.2
0.0
E1-O & E1-R1
E2-O & E2-R1
E1-O & E1-R2
E1-R1 & E1-R2
E2-O & E2-R2
E2-R1 & E2-R2
E1-O & E2-O
E1-O & E2-R1
E1-O & E2-R2
E1-R1 & E2-O
E1-R1 & E2-R1
E1-R1 & E2-R2
E1-R2 & E2-O
E1-R2 & E2-R1
E1-R2 & E2-R2

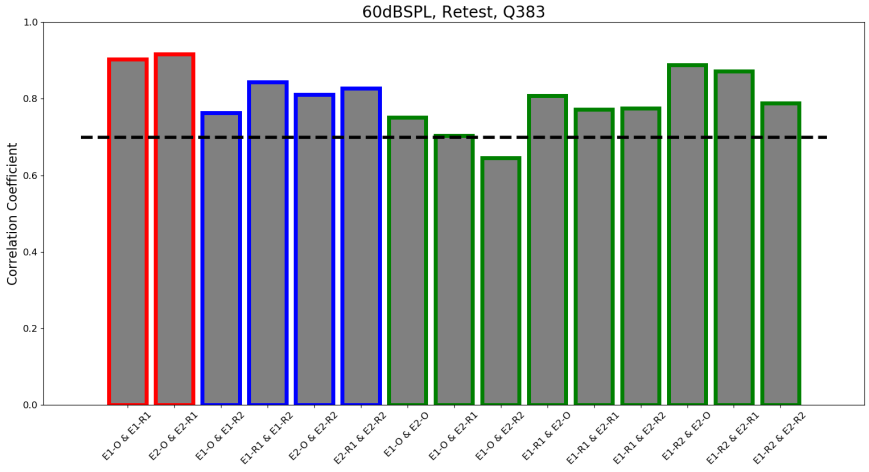
60dBSPL, Retest, Q383
Correlation Coefficient
1.0
0.8
0.6
0.4
0.2
0.0
E1-O & E1-R1
E2-O & E2-R1
E1-O & E1-R2
E1-R1 & E1-R2
E2-O & E2-R2
E2-R1 & E2-R2
E1-O & E2-O
E1-O & E2-R1
E1-O & E2-R2
E1-R1 & E2-O
E1-R1 & E2-R1
E1-R1 & E2-R2
E1-R2 & E2-O
E1-R2 & E2-R1
E1-R2 & E2-R2

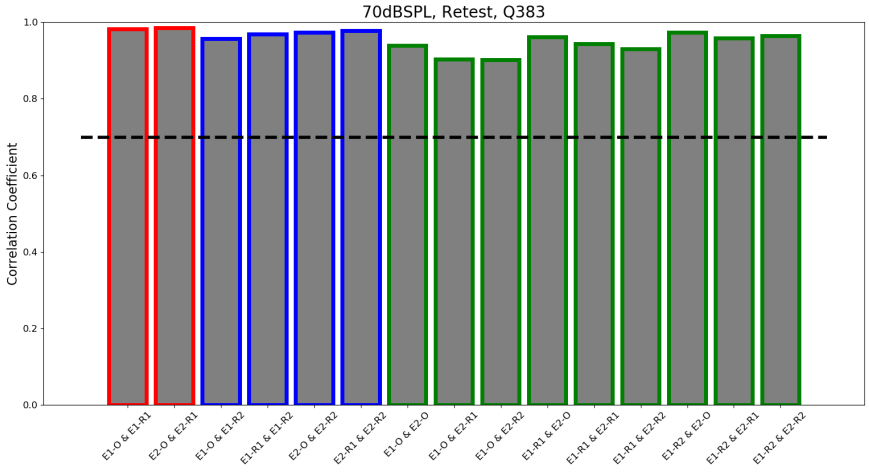
70dBSPL, Retest, Q383
Correlation Coefficient
1.0
0.8
0.6
0.4
0.2
0.0
E1-O & E1-R1
E2-O & E2-R1
E1-O & E1-R2
E1-R1 & E1-R2
E2-O & E2-R2
E2-R1 & E2-R2
E1-O & E2-O
E1-O & E2-R1
E1-O & E2-R2
E1-R1 & E2-O
E1-R1 & E2-R1
E1-R1 & E2-R2
E1-R2 & E2-O
E1-R2 & E2-R1
E1-R2 & E2-R2

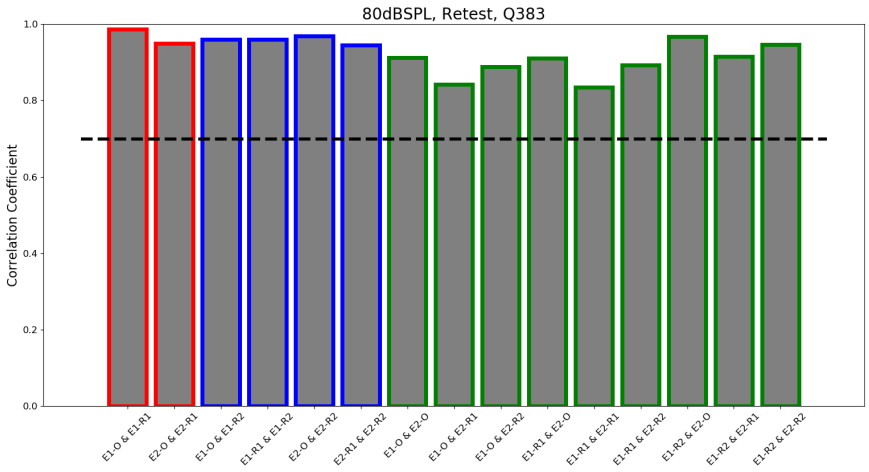
80dBSPL, Retest, Q383
Correlation Coefficient
1.0
0.8
0.6
0.4
0.2
0.0
E1-O & E1-R1
E2-O & E2-R1
E1-O & E1-R2
E1-R1 & E1-R2
E2-O & E2-R2
E2-R1 & E2-R2
E1-O & E2-O
E1-O & E2-R1
E1-O & E2-R2
E1-R1 & E2-O
E1-R1 & E2-R1
E1-R1 & E2-R2
E1-R2 & E2-O
E1-R2 & E2-R1
E1-R2 & E2-R2

Animal 3, Test

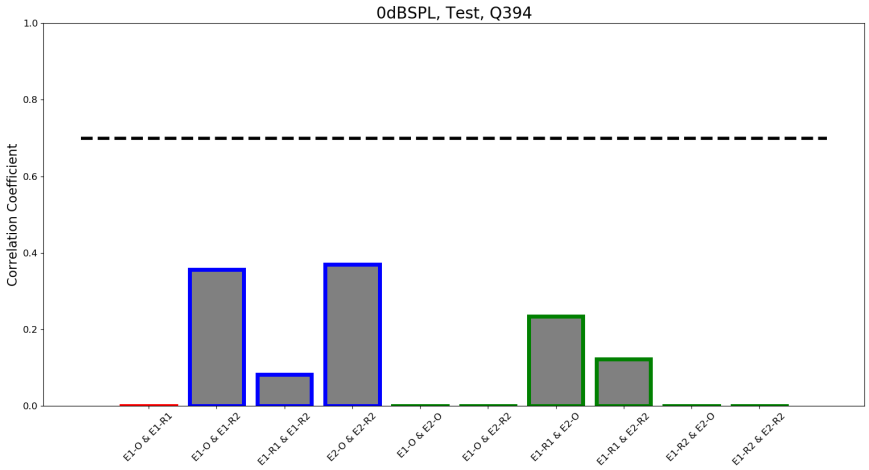

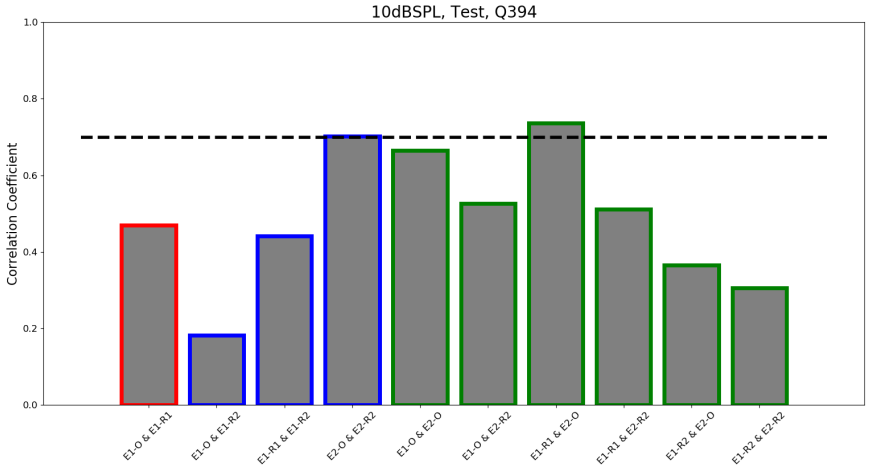

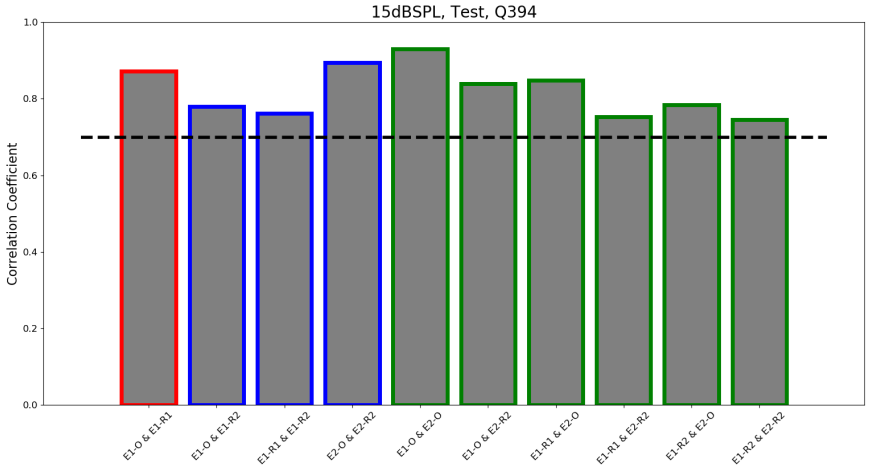
15dBSPL, Test, Q394
Correlation Coefficient
1.0
0.8
0.6
0.4
0.2
0.0
E1-O & E1-R1
E1-O & E1-R2
E1-R1 & E1-R2
E2-O & E2-R2
E1-O & E2-O
E1-O & E2-R2
E1-R1 & E2-O
E1-R1 & E2-R2
E1-R2 & E2-O
E1-R2 & E2-R2

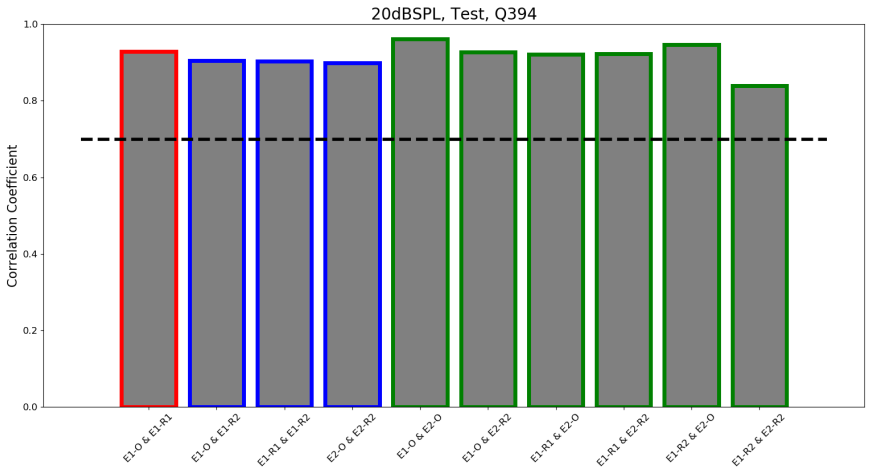
20dBSPL, Test, Q394
Correlation Coefficient
1.0
0.8
0.6
0.4
0.2
0.0
E1-O & E1-R1
E1-O & E1-R2
E1-R1 & E1-R2
E2-O & E2-R2
E1-O & E2-O
E1-O & E2-R2
E1-R1 & E2-O
E1-R1 & E2-R2
E1-R2 & E2-O
E1-R2 & E2-R2

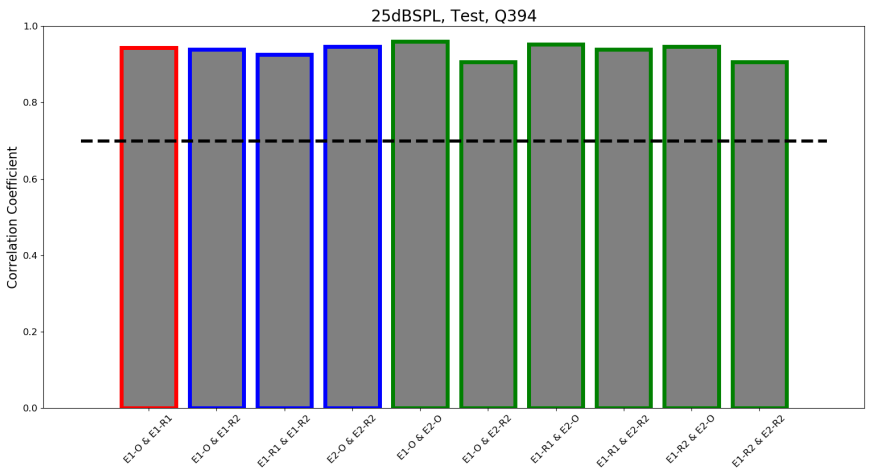
25dBSPL, Test, Q394
Correlation Coefficient
1.0
0.8
0.6
0.4
0.2
0.0
E1-O & E1-R1
E1-O & E1-R2
E1-R1 & E1-R2
E2-O & E2-R2
E1-O & E2-O
E1-O & E2-R2
E1-R1 & E2-O
E1-R1 & E2-R2
E1-R2 & E2-O
E1-R2 & E2-R2

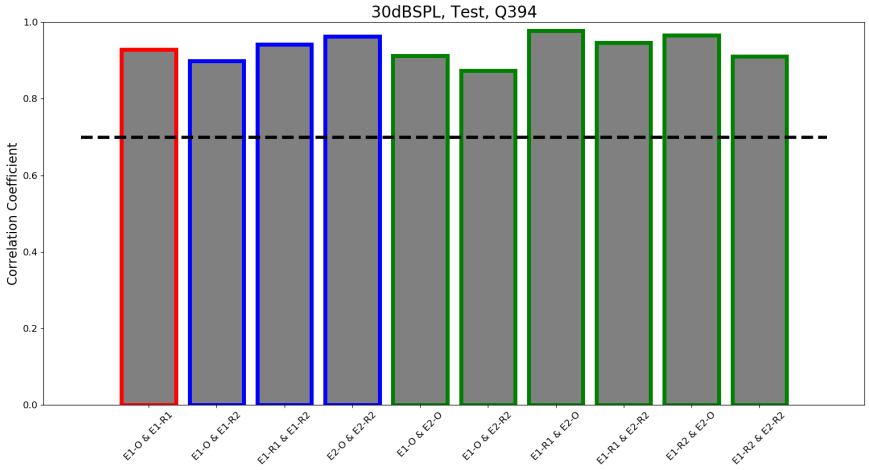
30dBSPL, Test, Q394
Correlation Coefficient
1.0
0.8
0.6
0.4
0.2
0.0
E1-O & E1-R1
E1-O & E1-R2
E1-R1 & E1-R2
E2-O & E2-R2
E1-O & E2-O
E1-O & E2-R2
E1-R1 & E2-O
E1-R1 & E2-R2
E1-R2 & E2-O
E1-R2 & E2-R2

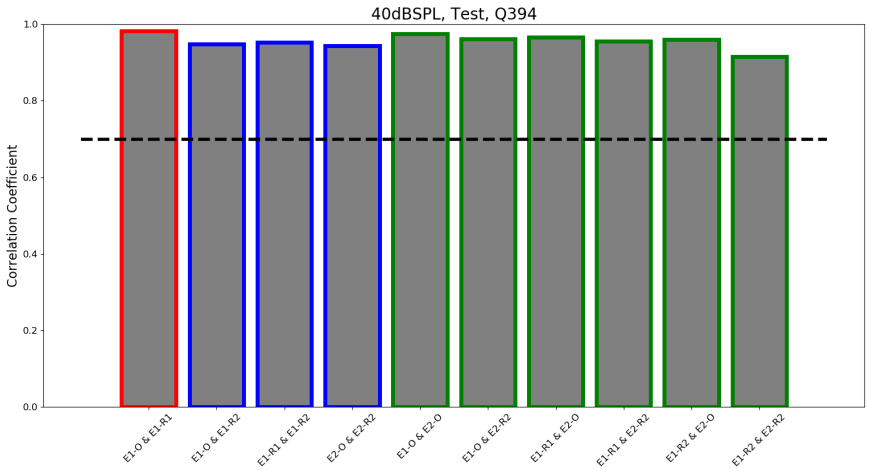
40dBSPL, Test, Q394
Correlation Coefficient
1.0
0.8
0.6
0.4
0.2
0.0
E1-O & E1-R1
E1-O & E1-R2
E1-R1 & E1-R2
E2-O & E2-R2
E1-O & E2-O
E1-O & E2-R2
E1-R1 & E2-O
E1-R1 & E2-R2
E1-R2 & E2-O
E1-R2 & E2-R2

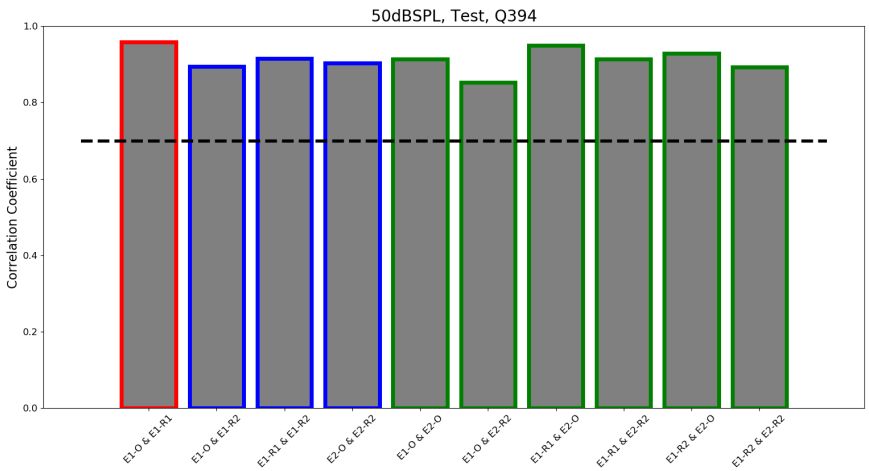
50dBSPL, Test, Q394
Correlation Coefficient
1.0
0.8
0.6
0.4
0.2
0.0
E1-O & E1-R1
E1-O & E1-R2
E1-R1 & E1-R2
E2-O & E2-R2
E1-O & E2-O
E1-O & E2-R2
E1-R1 & E2-O
E1-R1 & E2-R2
E1-R2 & E2-O
E1-R2 & E2-R2

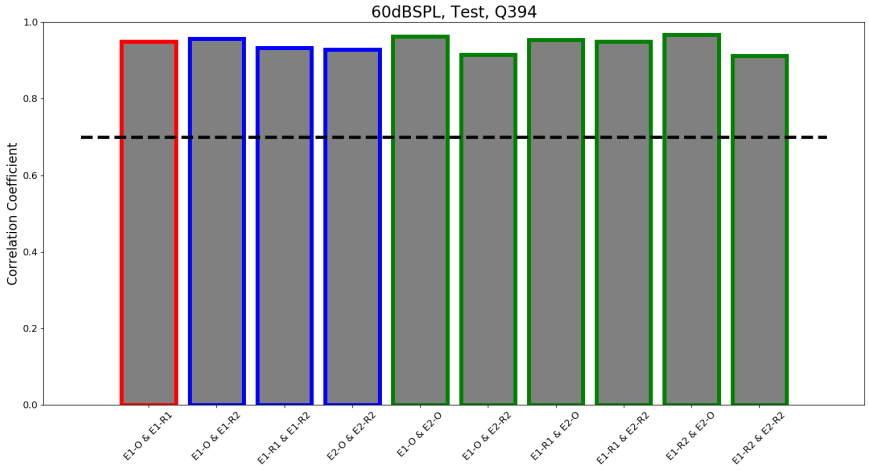
60dBSPL, Test, Q394
Correlation Coefficient
1.0
0.8
0.6
0.4
0.2
0.0
E1-O & E1-R1
E1-O & E1-R2
E1-R1 & E1-R2
E2-O & E2-R2
E1-O & E2-O
E1-O & E2-R2
E1-R1 & E2-O
E1-R1 & E2-R2
E1-R2 & E2-O
E1-R2 & E2-R2

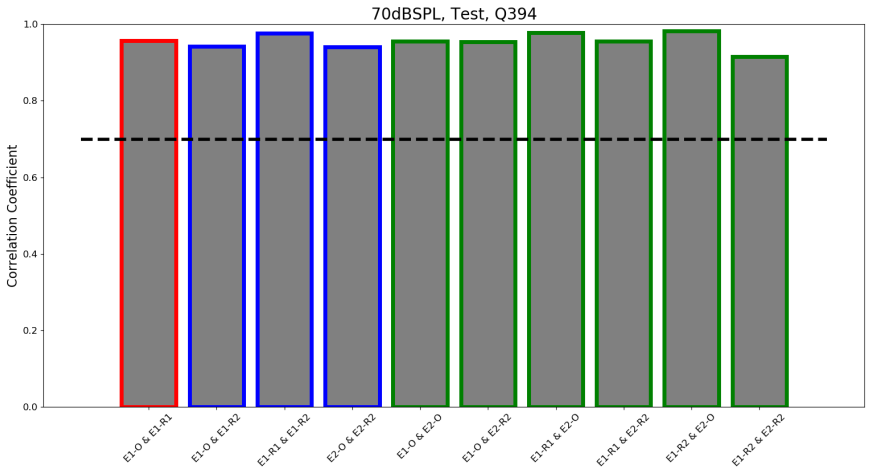
70dBSPL, Test, Q394
Correlation Coefficient
1.0
0.8
0.6
0.4
0.2
0.0
E1-O & E1-R1
E1-O & E1-R2
E1-R1 & E1-R2
E2-O & E2-R2
E1-O & E2-O
E1-O & E2-R2
E1-R1 & E2-O
E1-R1 & E2-R2
E1-R2 & E2-O
E1-R2 & E2-R2

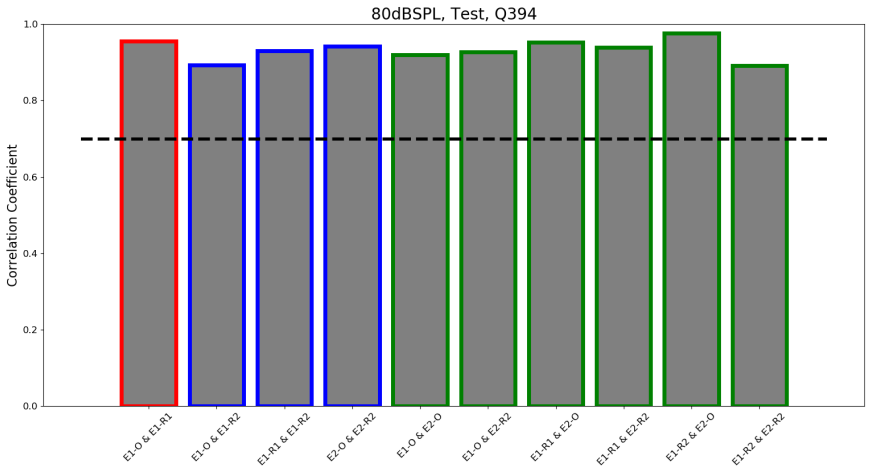
80dBSPL, Test, Q394
Correlation Coefficient
1.0
0.8
0.6
0.4
0.2
0.0
E1-O & E1-R1
E1-O & E1-R2
E1-R1 & E1-R2
E2-O & E2-R2
E1-O & E2-O
E1-O & E2-R2
E1-R1 & E2-O
E1-R1 & E2-R2
E1-R2 & E2-O
E1-R2 & E2-R2

Animal 3, Retest

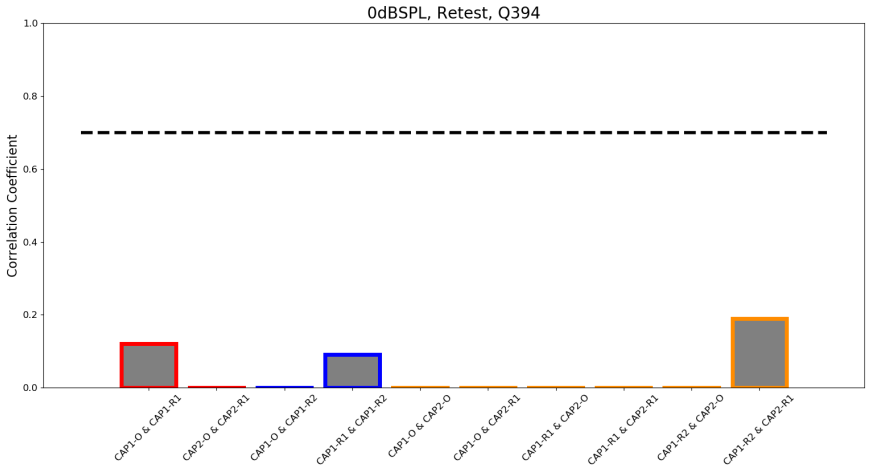

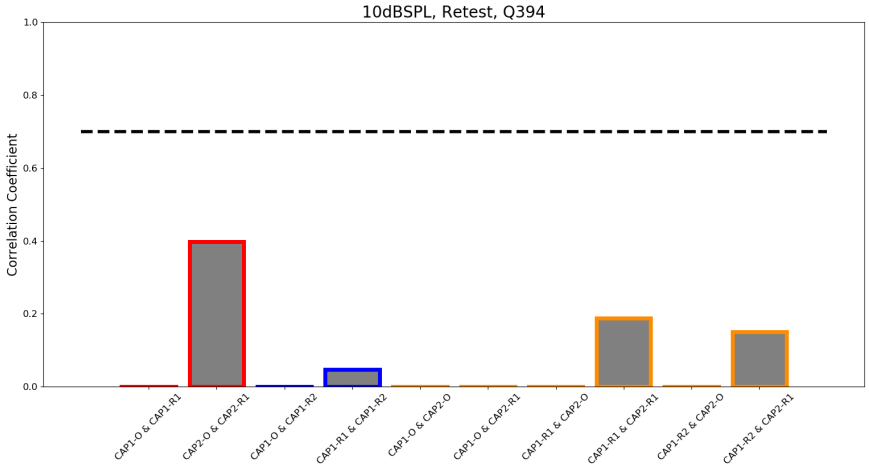

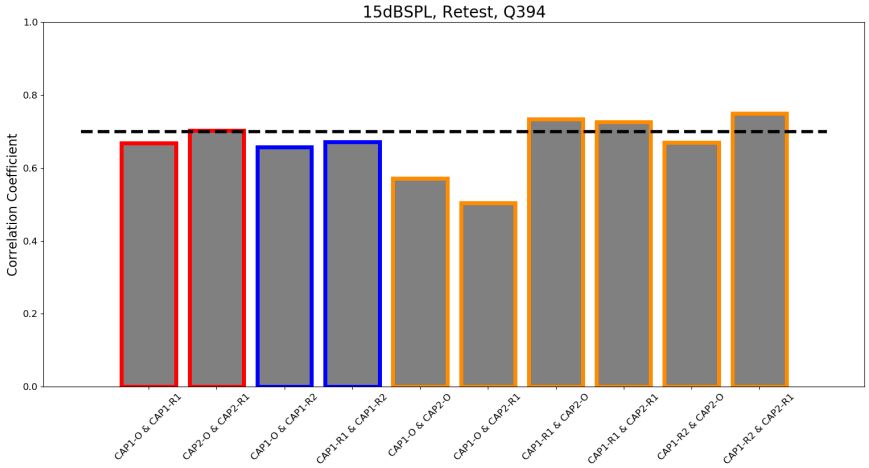
15dBSPL, Retest, Q394
Correlation Coefficient
1.0
0.8
0.6
0.4
0.2
0.0
CAP1-O & CAP1-R1
CAP2-O & CAP2-R1
CAP1-O & CAP1-R2
CAP1-R1 & CAP1-R2
CAP1-O & CAP2-O
CAP1-O & CAP2-R1
CAP1-R1 & CAP2-O
CAP1-R1 & CAP2-R1
CAP1-R2 & CAP2-O
CAP1-R2 & CAP2-R1

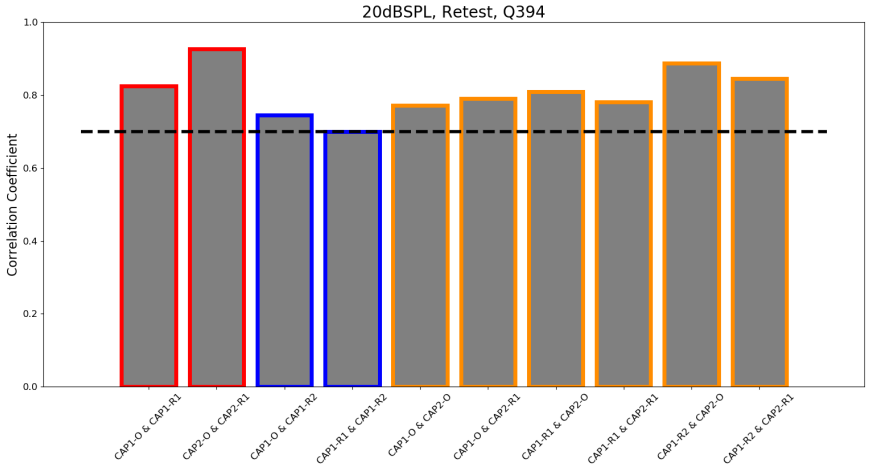
20dBSPL, Retest, Q394
Correlation Coefficient
1.0
0.8
0.6
0.4
0.2
0.0
CAP1-O & CAP1-R1
CAP2-O & CAP2-R1
CAP1-O & CAP1-R2
CAP1-R1 & CAP1-R2
CAP1-O & CAP2-O
CAP1-O & CAP2-R1
CAP1-R1 & CAP2-O
CAP1-R1 & CAP2-R1
CAP1-R2 & CAP2-O
CAP1-R2 & CAP2-R1

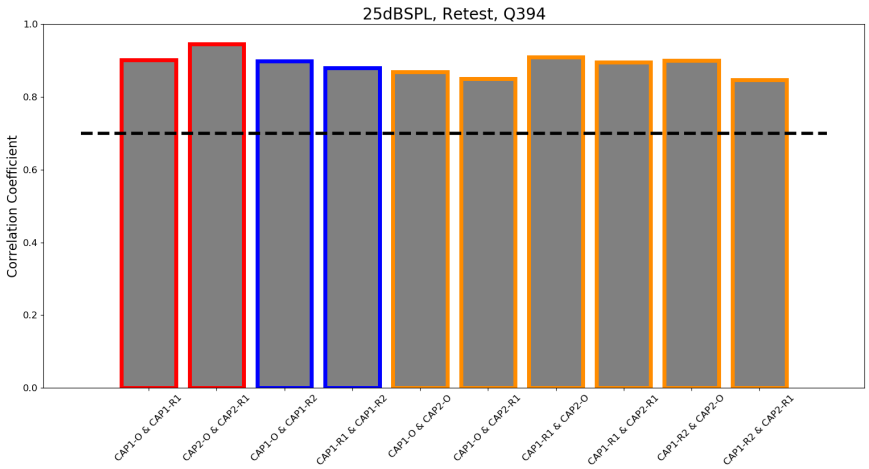
25dBSPL, Retest, Q394
Correlation Coefficient
1.0
0.8
0.6
0.4
0.2
0.0
CAP1-O & CAP1-R1
CAP2-O & CAP2-R1
CAP1-O & CAP1-R2
CAP1-R1 & CAP1-R2
CAP1-O & CAP2-O
CAP1-O & CAP2-R1
CAP1-R1 & CAP2-O
CAP1-R1 & CAP2-R1
CAP1-R2 & CAP2-O
CAP1-R2 & CAP2-R1

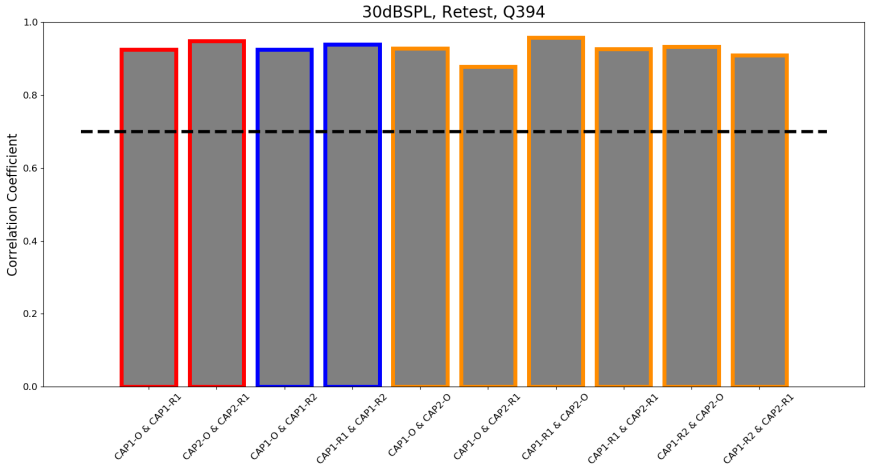
30dBSPL, Retest, Q394
Correlation Coefficient
1.0
0.8
0.6
0.4
0.2
0.0
CAP1-O & CAP1-R1
CAP2-O & CAP2-R1
CAP1-O & CAP1-R2
CAP1-R1 & CAP1-R2
CAP1-O & CAP2-O
CAP1-O & CAP2-R1
CAP1-R1 & CAP2-O
CAP1-R1 & CAP2-R1
CAP1-R2 & CAP2-O
CAP1-R2 & CAP2-R1

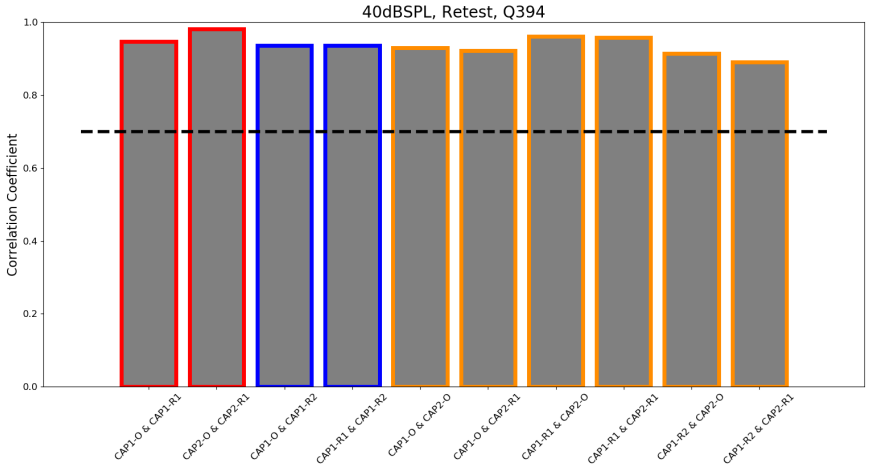
40dBSPL, Retest, Q394
Correlation Coefficient
1.0
0.8
0.6
0.4
0.2
0.0
CAP1-O & CAP1-R1
CAP2-O & CAP2-R1
CAP1-O & CAP1-R2
CAP1-R1 & CAP1-R2
CAP1-O & CAP2-O
CAP1-O & CAP2-R1
CAP1-R1 & CAP2-O
CAP1-R1 & CAP2-R1
CAP1-R2 & CAP2-O
CAP1-R2 & CAP2-R1

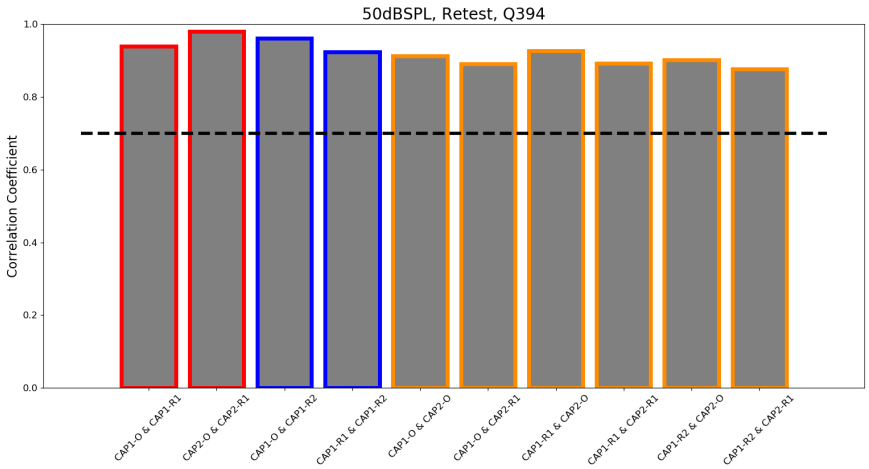
50dBSPL, Retest, Q394
Correlation Coefficient
1.0
0.8
0.6
0.4
0.2
0.0
CAP1-O & CAP1-R1
CAP2-O & CAP2-R1
CAP1-O & CAP1-R2
CAP1-R1 & CAP1-R2
CAP1-O & CAP2-O
CAP1-O & CAP2-R1
CAP1-R1 & CAP2-O
CAP1-R1 & CAP2-R1
CAP1-R2 & CAP2-O
CAP1-R2 & CAP2-R1

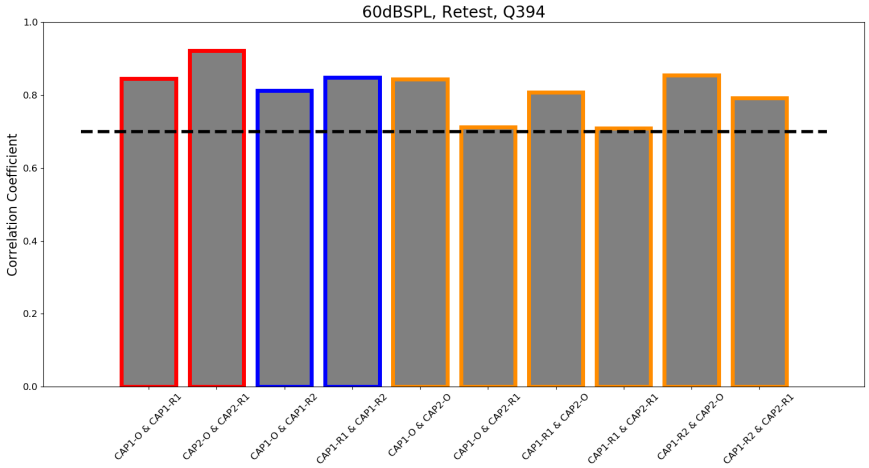
60dBSPL, Retest, Q394
Correlation Coefficient
1.0
0.8
0.6
0.4
0.2
0.0
CAP1-O & CAP1-R1
CAP2-O & CAP2-R1
CAP1-O & CAP1-R2
CAP1-R1 & CAP1-R2
CAP1-O & CAP2-O
CAP1-O & CAP2-R1
CAP1-R1 & CAP2-O
CAP1-R1 & CAP2-R1
CAP1-R2 & CAP2-O
CAP1-R2 & CAP2-R1

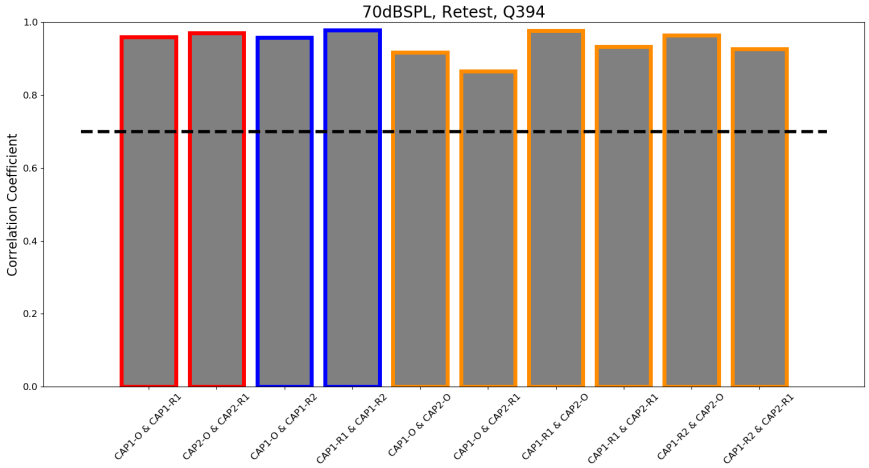
70dBSPL, Retest, Q394
Correlation Coefficient
1.0
0.8
0.6
0.4
0.2
0.0
CAP1-O & CAP1-R1
CAP2-O & CAP2-R1
CAP1-O & CAP1-R2
CAP1-R1 & CAP1-R2
CAP1-O & CAP2-O
CAP1-O & CAP2-R1
CAP1-R1 & CAP2-O
CAP1-R1 & CAP2-R1
CAP1-R2 & CAP2-O
CAP1-R2 & CAP2-R1

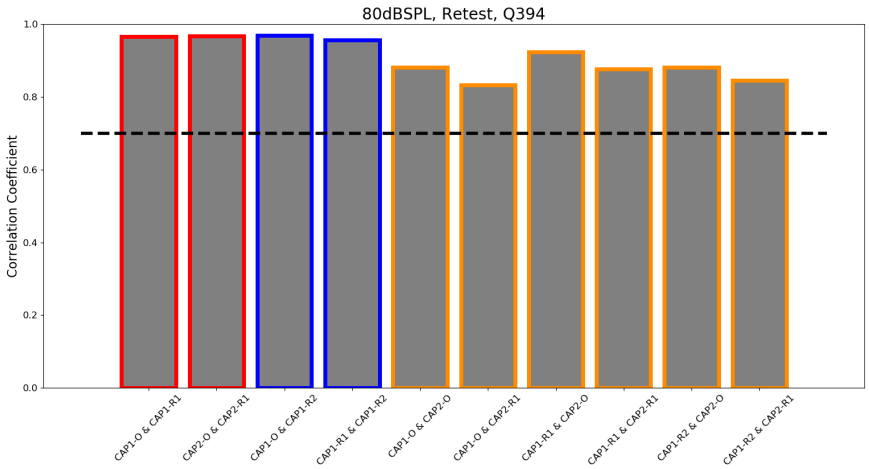
80dBSPL, Retest, Q394
Correlation Coefficient
1.0
0.8
0.6
0.4
0.2
0.0
CAP1-O & CAP1-R1
CAP2-O & CAP2-R1
CAP1-O & CAP1-R2
CAP1-R1 & CAP1-R2
CAP1-O & CAP2-O
CAP1-O & CAP2-R1
CAP1-R1 & CAP2-O
CAP1-R1 & CAP2-R1
CAP1-R2 & CAP2-O
CAP1-R2 & CAP2-R1

APPENDIX B. DETAILED INSTRUCTIONS, DATA COLLECTION

Pre-Experiment Preparation

Preparation of software

1. Ensure everything is properly connected for the experiment both inside and outside of the sound booth.
2. Turn all hardware on, then open NEL software via Matlab.
3. After opening NEL, create new directory when prompted.
4. Confirm ABR code is running and generating sound before anesthetizing the chinchilla.
5. Create a new experiment-specific folder to save bdf files into – "MMDDYY".

Preparation of animal

1. Anesthetize chinchilla with xylazine (SQ), followed by ketamine (SQ) about 5-10 min later.
2. After the chinchilla is effectively anesthetized, move animal into sound booth, placing it properly into bite bar.
3. Attach the pulse ox clip to chinchilla's paw.
4. Ensure oxygen is on and pumping; check the chinchilla's vitals.
5. Place the rectal probe of temperature-regulator in animal.
6. Check internal temperature of animal (should be around 37 degrees and increasing).
7. Apply ophthalmic ointment to the eyes.
8. Inject 6cc of Ringers solution (SQ), 3cc on each side of the body.

Preparation of mini cap

1. Fill a 3cc syringe, 20G needle with paste, ensuring there are no air bubbles.
    (a) From previous experiments, it appears that only about 1cc, at most, of paste is needed for injecting.
2. Fill in each of the 32 electrodes (+2 A&B electrodes) from the bottom up with the electrode paste without creating any air bubbles.
3. Ensure that all electrodes are properly filled with paste (i.e. no holes, should not be able to see metal electrode inside tube anymore).
4. Bring filled cap into sound booth.
    (a) Keep cap's bottom facing upward as animal is being prepared to ensure no paste leakage.
5. Attach all cap wiring to Biosemi wiring (3 channel connections, CMS/DRL)
    (a) Note: Do not turn on the Biosemi yet.

During the Experiment

1. Place yellow microphone tip into right ear canal of chinchilla; record calibration file using NEL.
    (a) If desired, collect a DPOAE response after recording the calibration file.
2. Next, open ABR collection on NEL (where you set ABR stimuli).
    (a) Note: You need a calibration file in the specific folder to open this with no errors.
3. After collecting the calibration file, remove microphone tip from ear.
4. Shave the chinchilla's head where the cap is going to be placed.
    (a) First, use the electronic razor (with narrow head) to remove coarse hair.

(b) Second, use Nair Hair Removal Lotion to remove remaining fine hair.

5. Rub the head with isopropyl alcohol to remove any debris and stimulate the blood vessels.

6. Place a saline-soaked cloth over the exposed scalp until the EEG mini-cap is properly attached and ready to be placed onto the chinchilla's head.

7. Place two gold-foiled tiptrodes, one into each of the chinchilla's ear canals.

   (a) Ensure each tiptrode is replaced at the start of every experiment.

8. Place three subdermal needle electrodes in proper places on the chinchilla skull.

9. Now, the mini cap is ready to be placed. Inject more paste into channels if necessary.

10. Remove saline-soaked cloth and place the prepared (i.e. filled-with-paste) EEG mini-cap on the exposed skin of the chinchilla.

11. Secure the cap onto the head with cap-securing device.

    (a) Ensure the cap is tightly secured to the chinchilla's head. Any looseness will result in noisy data.

12. Ensure tiptrodes and subdermal needle electrodes are still in proper place (i.e. haven't been moved or displaced during securing the cap).

13. Turn on Biosemi; observe "CM in range" LED.

    (a) An open circuit exists if the blue button is blinking at any capacity. This must be addressed and fixed before moving on. This may be caused by the cap not being properly secured to head, or a channel needs paste reinjected, etc.

    (b) You want to see a solid blue (i.e. no blinking). If there is no blinking, the circuit is closed and that signifies that the impedance of each electrode is good enough to continue.

14. Next, open Actiview software.

(a) Ensure you do not turn the Actiview software on until the Biosemi is turned on or you will get an error message.

15. Adjust settings as follows (from top-to-bottom order):

    (a) Set Y-scale. Determine the lowest value to effectively view the signal(s); ideal is 100 uV. If the signals appear noisy, try replacing the cap or reinjecting more paste.

    (b) Set Lowpass to 3000 Hz.

    (c) Set Highpass to 10 Hz.

    (d) Set Channels to A(32).

16. Press *Start* in top left corner to begin visually seeing data.

    (a) Review signal quality of each channel on *Monopolar Display*; note and record the noisy channels.

        i. If you see high 60 Hz on all channels, check the impedance at the reference and ground and ensure that both have suitably low contact impedance.

        ii. For example, normal noisy channels for cap include A25-A28.

    (b) Move to the *Electrode Offset* tab; view the offsets of each channel.

        i. If a channel offset is greater than the abs(40 millivolts), record the channel as having a bad offset (e.g. usually A28 has a bad offset).

        ii. If many channels have bad offsets, remove cap and try reinjecting paste into those channels. Also, ensure that the mini-cap is tightly secured on the chinchilla.

        iii. If only a couple electrodes have bad offsets, this may indicate contact problems for those specific electrodes, and/or polluted electrodes (i.e. corrosion).

    (c) After the impedance (and offset) checking, set parameters in Actiview software.

        i. Go to *Event Related Potential* Tab and adjust the following settings:

            A. Choose *Trig 1* (and *AND trigs*).

B. Set Sweep length to 20 ms.

C. Set Lowpass to 3000 Hz.

D. Set Highpass to 100 Hz.

E. Deselect *Autoscale*.

F. Set Rejection of all sweeps larger than 200 uV.

G. Set Rejection of difference with average more than 100 uV.

H. Set comparison of top panel to view mini cap ABRs: Midline channel (e.g., A8) versus reference EXG1.

I. Set comparison of bottom pannel to view subdermal ABRs: EXG4 versus EXG3.

ii. Once all settings set properly for both the Monopolar Display and Event Related Potential, you are ready to begin collecting data.

(d) To start collecting raw data (without triggers, set in next step), press Paused button (lower right) in bottom right corner to start saving data.

(e) Next, set desired stimuli on NEL to start sending trigger information to Biosemi.

i. To collect an unlimited number of repetitions for a single level/frequency combination, click *Start Trigger* after setting desired level and frequency.

A. This acts as auto-run and will continue sending triggers until *Stop Trigger* is pressed.

B. To start a new stimuli, after pressing *Stop Trigger* and setting the new desired level and frequency, re-press *Start Trigger*.

ii. To collect a set number of repetitions for a single level/frequency combination, click *Run Levels* after setting desired level and frequency.

A. This will collect 1000 repetitions for each particular condition.

iii. To collect a full waterfall, set desired frequency and move level down below 20 dBSPL. Then, press *Auto Levels* button.

A. This will collect 1000 repetitions for each level, from 0 dBSPL to 80 dBSPL in 10 dBSPL increments, adding 25 dBSPL condition as well.

iv. Note: NEL is controlling the triggers that are sent to Actiview. Each new level/condition initiates a new trigger code saved into each bdf file. Each time a new trigger code is created, the trigger number, frequency, and level information is saved into a triggers.txt file located in the NEL-specific data directory.

(f) When you are finished collecting data (i.e. NEL has stopped sending triggers), click Pause Save button (lower right), followed by *Stop* button (upper left) in Actiview.

(g) To start a new BDF file, press Stop button in upper left corner.

i. Triggers must be re-initiated in NEL as well.

(h) Continue saving new BDF files and re-initiating triggers for each desired stimuli.

(i) Once all data has been collected, you are ready to begin the post-experiment cleanup process below.

Post-Experiment Cleanup

1. Close Actiview software on computer.
2. Turn off Biosemi amplifier.
3. Remove cap from animal's head.
   (a) Clean any remaining paste residue from animal's head using kimwipe and ethanol; ensure animal's head is clean and no residue remains.
4. Unplug cap from Biosemi amplifier.
5. Remove rectal probe from animal.
6. Inject 6cc of Ringers solution (SQ), 3cc on each side of the body.
7. Inject appropriate amount of Atipam (IP) (i.e. reversal agent).
8. Move animal into cage placed on heater, with head placed upward using towel.

(a) Place Critical Care, along with a raisin, inside cage.

9. As animal is waking up, place EEG mini-cap into salt water to soak.

10. Clean sound booth, turn off oxygen, and turn off all hardware (inside and outside of sound booth).

11. Continue monitoring animal.

12. After 15-20 min of soaking cap, check cap and clean out remaining paste-filled channels using 22G, 1cc needle filled with salt water.

13. After all channels are effectively cleaned and no paste remains, store cap in dark place wrapped in kimwipe.

14. Return animal to LSA once the animal has recovered long enough.

Processing Setup

1. Install mne-python (see installing instructions here).
2. Install a Python IDE. I recommend installing Spyder.
3. Fork and then clone each of the following Github repositories onto your computer: mne-python and ANLffr
4. If using software like Spyder, other Python packages should already be installed. Ensure that the following directories are installed: matplotlib, os, scipy, and numpy.

Basic Processing in Python

1. Import relevant libraries: *numpy, os, mne, scipy, anlffr,* and *matplotlib.*
2. Load in bdf file using *bs.importbdf().*

   .Set reference channel to EXG1 for mini cap ABRs and EXG5 for replicated subdermal ABRs. This will result in two structures: raw and events.

3. Set channel types of external channels to EEG using *raw.set_channel_types().*
4. Filter raw data.
   (a) Set band pass filter from 300 to 3000 Hz using *raw_filter().*
   (b) Set 60 Hz notch filter with bands up to 600 Hz using *raw_notch_filter().*
5. Epoch the data.
   (a) Set start time to -4 ms and end time to 15 ms.
   (b) Set baseline correction from -2 ms to 0 ms.
   (c) Epoch the raw data using *epochs = mne.Epochs(raw,eves).*
6. For each epoch strcuture, average across all epochs (repetitions x channels x time).

(a) Average epochs to obtain abr structure using *abr = epochs.average()*.

(b) Initialize amplitude and time vectors in correct units of uV and ms.

i. Initialize x using *x = (-1)*abr.data * 1e6*.

ii. Initialize t using *t = abr.times * 1e3*.

7. For subdermal ABRs, average across repetitions for each of the three channels (reps x time per channel) and then average across each particular EXG channel (1 x time) to obtain response for each EXG channel.

(a) Subtract EXG4 response response from EXG3 response to obtain final replicated subdermal ABR response.

8. For mini cap ABRs, identify bad channels using the z-score deviation criterion (see description here), with a threshold of 2.0.

9. Average across all good channels (1 x time).

10. Demean averaged response from 0 to 1 ms to obtain final mini cap ABR response.

Including Trigger Codes

1. Identify which trigger codes refer to which stimuli by referring back to triggers.txt.

2. Initialize variables to equal the desired trigger code(s) into an array called *conds*.

3. Loop through each condition in *conds*.

(a) For each *cond* in *conds*, create a new epochs variable by using *mne.Epochs(raw,eves,cond)*.

4. Follow the same procedure for epoch analysis as described in *Basic Processing in Python*. This addition only groups relevant epochs together representative of each trigger code.

REFERENCES

[1] *Deafness and hearing loss*. [Online]. Available: https://www.who.int/news-room/fact-sheets/detail/deafness-and-hearing-loss.

[2] K. J. Cruickshanks, T. L. Wiley, T. S. Tweed, B. E. Klein, R. Klein, J. A. Mares-Perlman, and D. M. Nondahl, "Prevalence of hearing loss in older adults in Beaver Dam, Wisconsin. The Epidemiology of Hearing Loss Study," eng, *American Journal of Epidemiology*, vol. 148, no. 9, pp. 879–886, Nov. 1998.

[3] A. Davis, *Hearing in adults*. London, England: Whurr, 1995.

[4] D. Wilson, P. Walsh, L. Sanchez, and P. Reed, "Hearing impairment in an Australian population.," 1998.

[5] L. L. Cunningham and D. L. Tucci, "Hearing Loss in Adults," *The New England journal of medicine*, vol. 377, no. 25, pp. 2465–2473, Dec. 2017.

[6] *Age-Related Hearing Loss (Presbycusis) — Causes and Treatment*, Aug. 2015.

[7] CDC, *Preventing Noise-Induced Hearing Loss | CDC*, en-us, May 2020. [Online]. Available: https://www.cdc.gov/ncbddd/hearingloss/noise.html.

[8] *U.S. adults aged 20 to 69 years show signs of noise-induced hearing loss*, Feb. 2017. [Online]. Available: https://www.nidcd.nih.gov/news/2017/us-adults-aged-20-69-years-show-signs-noise-induced-hearing-loss.

[9] M. C. Brown and J. Santos-Sacchi, "Peripheral Auditory System - an overview," in *Fundamental Neuroscience*, 4th ed., 2013.

[10] H. J. White, M. Helwany, and D. C. Peterson, "Anatomy, Head and Neck, Ear Organ of Corti," eng, in *StatPearls*, Treasure Island (FL): StatPearls Publishing, 2020.

[11] L. Rüttiger, U. Zimmermann, and M. Knipper, "Biomarkers for Hearing Dysfunction: Facts and Outlook," *ORL*, vol. 79, pp. 93–111, Feb. 2017. DOI: 10.1159/000455705.

[12] R. Litovsky, "Development of the auditory system," *Handbook of clinical neurology*, vol. 129, pp. 55–72, 2015.

[13] H. Howard, *Central auditory pathway — Brain & language*, 2019. [Online]. Available: http://www.tulane.edu/~h0Ward/BrLg/CentralAudPathway.html.

[14] D. P. Rowe and S. J. O'Leary, "Auditory System, Peripheral," en, in *Encyclopedia of the Neurological Sciences (Second Edition)*, M. J. Aminoff and R. B. Daroff, Eds., Oxford: Academic Press, Jan. 2014, pp. 329–334.

[15] D. Peterson, V. Reddy, and R. Hamel, "Neuroanatomy, Auditory Pathway," *StatPearls*, Aug. 2020.

[16] M. Trevino, E. Lobarinas, A. C. Maulden, and M. G. Heinz, "The chinchilla animal model for hearing science and noise-induced hearing loss," *The Journal of the Acoustical Society of America*, vol. 146, no. 5, pp. 3710–3732, Nov. 2019.

[17] E. Brender, A. E. Burke, and R. M. Glass, "Audiometry," *JAMA*, vol. 295, no. 4, pp. 460–460, Jan. 2006.

[18] A. Bronkhorst, "The Cocktail Party Phenomenon: A Review of Research on Speech Intelligibility in Multiple-Talker Conditions," *Acta Acustica united with Acustica*, vol. 86, pp. 117–128, Jan. 2000.

[19] E. C. Cherry, "Some experiments on the recognition of speech, with one and with two ears," *Journal of the Acoustical Society of America*, vol. 25, pp. 975–979, 1953, Place: US Publisher: Acoustical Society of American.

[20] W. A. Yost, "The cocktail party problem: Forty years later," in *Binaural and spatial hearing in real and virtual environments*, Hillsdale, NJ, US: Lawrence Erlbaum Associates, Inc, 1997, pp. 329–347.

[21] S. G. Kujawa and M. C. Liberman, "Synaptopathy in the noise-exposed and aging cochlea: Primary neural degeneration in acquired sensorineural hearing loss," en, *Hearing Research*, Auditory Synaptology, vol. 330, pp. 191–199, Dec. 2015.

[22] M. C. Liberman and S. G. Kujawa, "Cochlear synaptopathy in acquired sensorineural hearing loss: Manifestations and mechanisms," *Hearing research*, vol. 349, pp. 138–147, Jun. 2017.

[23] H. F. Schuknecht and R. C. Woellner, "An experimental and clinical study of deafness from lesions of the cochlear nerve," *The Journal of Laryngology and Otology*, vol. 69, no. 2, pp. 75–97, Feb. 1955.

[24] R. Schaette and D. McAlpine, "Tinnitus with a normal audiogram: Physiological evidence for hidden hearing loss and computational model," eng, *The Journal of Neuroscience: The Official Journal of the Society for Neuroscience*, vol. 31, no. 38, pp. 13 452–13 457, Sep. 2011.

[25] J. H. Grose, E. Buss, and J. W. Hall, "Loud Music Exposure and Cochlear Synaptopathy in Young Adults: Isolated Auditory Brainstem Response Effects but No Perceptual Consequences," *Trends in Hearing*, vol. 21, Nov. 2017.

[26] S. G. Kujawa and M. C. Liberman, "Adding Insult to Injury: Cochlear Nerve Degeneration after "Temporary" Noise-Induced Hearing Loss," *The Journal of Neuroscience*, vol. 29, no. 45, pp. 14 077–14 085, Nov. 2009.

[27] A. F. Ryan, S. G. Kujawa, T. Hammill, C. Le Prell, and J. Kil, "Temporary and Permanent Noise-Induced Threshold Shifts: A Review of Basic and Clinical Observations," *Otology & neurotology : official publication of the American Otological Society, American Neurotology Society [and] European Academy of Otology and Neurotology*, vol. 37, no. 8, e271–e275, Sep. 2016.

[28] H. W. Lin, A. C. Furman, S. G. Kujawa, and M. C. Liberman, "Primary neural degeneration in the Guinea pig cochlea after reversible noise-induced threshold shift," eng, *Journal of the Association for Research in Otolaryngology: JARO*, vol. 12, no. 5, pp. 605–616, Oct. 2011.

[29] A. C. Furman, S. G. Kujawa, and M. C. Liberman, "Noise-induced cochlear neuropathy is selective for fibers with low spontaneous rates," *Journal of Neurophysiology*, vol. 110, no. 3, pp. 577–586, Aug. 2013.

[30] B. Shinn-Cunningham, "Cortical and Sensory Causes of Individual Differences in Selective Attention Ability Among Listeners With Normal Hearing Thresholds," *Journal of speech, language, and hearing research: JSLHR*, vol. 60, no. 10, pp. 2976–2988, 2017.

[31] M. D. Valero, J. A. Burton, S. N. Hauser, T. A. Hackett, R. Ramachandran, and M. C. Liberman, "Noise-induced cochlear synaptopathy in rhesus monkeys (Macaca mulatta)," *Hearing Research*, vol. 353, pp. 213–223, 2017.

[32] T. T. Hickman, C. Smalt, J. Bobrow, T. Quatieri, and M. C. Liberman, "Blast-induced cochlear synaptopathy in chinchillas," *Scientific Reports*, vol. 8, no. 1, p. 10 740, Jul. 2018, Number: 1 Publisher: Nature Publishing Group.

[33] A. E. Hickox, E. Larsen, M. G. Heinz, L. Shinobu, and J. P. Whitton, "Translational issues in cochlear synaptopathy," *Hearing Research*, vol. 349, pp. 164–171, 2017.

[34] L. M. Viana, J. T. O'Malley, B. J. Burgess, D. D. Jones, C. A. C. P. Oliveira, F. Santos, S. N. Merchant, L. D. Liberman, and M. C. Liberman, "Cochlear neuropathy in human presbycusis: Confocal analysis of hidden hearing loss in post-mortem tissue," eng, *Hearing Research*, vol. 327, pp. 78–88, Sep. 2015.

[35] G. Mehraei, A. P. Gallardo, B. G. Shinn-Cunningham, and T. Dau, "Auditory brainstem response latency in forward masking, a marker of sensory deficits in listeners with normal hearing thresholds," *Hearing Research*, vol. 346, pp. 34–44, 2017.

[36] H. M. Bharadwaj, S. Masud, G. Mehraei, S. Verhulst, and B. G. Shinn-Cunningham, "Individual Differences Reveal Correlates of Hidden Hearing Deficits," *Journal of Neuroscience*, vol. 35, no. 5, pp. 2161–2172, Feb. 2015, Publisher: Society for Neuroscience Section: Articles.

[37] B. T. Paul, I. C. Bruce, and L. E. Roberts, "Evidence that hidden hearing loss underlies amplitude modulation encoding deficits in individuals with and without tinnitus," eng, *Hearing Research*, vol. 344, pp. 170–182, 2017.

[38] D. Ruggles and B. Shinn-Cunningham, "Spatial selective auditory attention in the presence of reverberant energy: Individual differences in normal-hearing listeners," *Journal of the Association for Research in Otolaryngology: JARO*, vol. 12, no. 3, pp. 395–405, Jun. 2011.

[39] J. J. Eggermont, "Chapter 5 - Types of Hearing Loss," en, in *Hearing Loss*, J. J. Eggermont, Ed., Academic Press, Jan. 2017, pp. 129–173.

[40] J. J. Eggermont, "Chapter 30 - Auditory brainstem response," en, in *Handbook of Clinical Neurology*, ser. Clinical Neurophysiology: Basis and Technical Aspects, K. H. Levin and P. Chauvel, Eds., vol. 160, Jan. 2019, pp. 451–464.

[41] D. J. Creel, "Visual and Auditory Anomalies Associated with Albinism," en, Jun. 2015, Publisher: University of Utah Health Sciences Center.

[42] G. Zhou, B. Dornan, and W. Hinchion, "Clinical Experience of Auditory Brainstem Response Testing on Pediatric Patients in the Operating Room," *International Journal of Otolaryngology*, vol. 2012, 2012.

[43] S. Abadi, G. Khanbabaee, and K. Sheibani, "Auditory Brainstem Response Wave Amplitude Characteristics as a Diagnostic Tool in Children with Speech Delay with Unknown Causes," *Iranian Journal of Medical Sciences*, vol. 41, no. 5, pp. 415–421, Sep. 2016.

[44] R. D. Chambers, L. E. Rowan, M. L. Matthies, and M. A. Novak, "Auditory brain-stem responses in children with previous otitis media," *Archives of Otolaryngology–Head & Neck Surgery*, vol. 115, no. 4, pp. 452–457, Apr. 1989.

[45] E. A. Conijn, J. F. Van der Drift, M. P. Brocaar, and G. A. Van Zanten, "Conductive hearing loss assessment in children with otitis media with effusion. A comparison of pure tone and BERA results," eng, *Clinical Otolaryngology and Allied Sciences*, vol. 14, no. 2, pp. 115–120, Apr. 1989.

[46] O. Fjermedal and E. Laukli, "Paediatric auditory brainstem response and pure-tone audiometry: Threshold comparisons. A study of 142 difficult-to-test children," eng, *Scandinavian Audiology*, vol. 18, no. 2, pp. 105–111, 1989.

[47] R. Galambos and K. E. Hecox, "Clinical applications of the auditory brain stem response," eng, *Otolaryngologic Clinics of North America*, vol. 11, no. 3, pp. 709–722, Oct. 1978.

[48] M. P. Warren, "The auditory brainstem response in pediatrics," *Otolaryngologic Clinics of North America*, vol. 22, no. 3, pp. 473–500, Jun. 1989.

[49] K. Hill, "Evoked Potentials Part 1: Good Practice and Auditory Brainstem Response," p. 21,

[50] M. P. Gorga, T. A. Johnson, J. K. Kaminski, K. L. Beauchaine, C. A. Garner, and S. T. Neely, "Using a combination of click- and toneburst-evoked auditory brainstem response measurements to estimate pure-tone thresholds," *Ear and hearing*, vol. 27, no. 1, pp. 60–74, Feb. 2006.

[51] D. R. Stapells, "Threshold Estimation by the Tone-Evoked Auditory Brainstem Response: A Literature Meta-Analysis Evaluation du seuil de la surdite par la methode des potentiels evoques auditifs avec stimulus tonal: Meta-analyse de la litterature," p. 10,

[52] C. A. Navntoft, J. Marozeau, and T. R. Barkat, "Cochlear Implant Surgery and Electrically-evoked Auditory Brainstem Response Recordings in C57BL/6 Mice," *JoVE (Journal of Visualized Experiments)*, no. 143, e58073, Jan. 2019.

[53] M. P. Paulraj, K. Subramaniam, S. B. Yaccob, A. H. B. Adom, and C. R. Hema, "Auditory Evoked Potential Response and Hearing Loss: A Review," *The Open Biomedical Engineering Journal*, vol. 9, pp. 17–24, Feb. 2015.

[54] A. Bradley and W. Wilson, "Automated analysis of the auditory brainstem response," *Proceedings of the 2004 Intelligent Sensors, Sensor Networks and Information Processing Conference, 2004.*, 2004.

[55] K. S. Henry, S. Kale, R. E. Scheidt, and M. G. Heinz, "Auditory brainstem responses predict auditory nerve fiber thresholds and frequency selectivity in hearing impaired chinchillas," en, *Hearing Research*, vol. 280, no. 1, pp. 236–244, Oct. 2011.

[56] G. Mehraei, A. E. Hickox, H. M. Bharadwaj, H. Goldberg, S. Verhulst, M. C. Liberman, and B. G. Shinn-Cunningham, "Auditory Brainstem Response Latency in Noise as a Marker of Cochlear Synaptopathy," *The Journal of Neuroscience*, vol. 36, no. 13, pp. 3755–3764, Mar. 2016.

[57] S. Verhulst, A. Jagadeesh, M. Mauermann, and F. Ernst, "Individual Differences in Auditory Brainstem Response Wave Characteristics," *Trends in Hearing*, vol. 20, Nov. 2016.

[58] P. Ledwidge, J. Foust, and A. Ramsey, "Recommendations for Developing an EEG Laboratory at a Primarily Undergraduate Institution," *Journal of Undergraduate Neuroscience Education*, vol. 17, no. 1, A10–A19, Dec. 2018.

[59] J. W. Kam, S. Griffin, A. Shen, S. Patel, H. Hinrichs, H.-J. Heinze, L. Y. Deouell, and R. T. Knight, "Systematic comparison between a wireless EEG system with dry electrodes and a wired EEG system with wet electrodes," *NeuroImage*, vol. 184, pp. 119–129, Jan. 2019.

[60] K. Manzoor, A. Kumar, and M. J. Vidya, "Analysis of EEG Using 10:20 Electrode System," *International Journal of Innovative Research in Science, Engineering and Technology*, vol. 1, no. 2, 2012.

[61] J. Hang, W. Pan, A. Chang, S. Li, C. Li, M. Fu, and J. Tang, *Synchronized Progression of Prestin Expression and Auditory Brainstem Response during Postnatal Development in Rats*, en, Research Article, Dec. 2016.

[62] J. R. Swearengen, "Choosing the right animal model for infectious disease research," *Animal Models and Experimental Medicine*, vol. 1, no. 2, pp. 100–108, 2018, _eprint: https://onlinelibrary.wiley.com/doi/pdf/10.1002/ame2.12020.

[63] A. Lundt, J. Soos, C. Henseler, M. I. Arshaad, R. Müller, D. Ehninger, J. Hescheler, A. Sachinidis, K. Broich, C. Wormuth, A. Papazoglou, and M. Weiergräber, "Data Acquisition and Analysis In Brainstem Evoked Response Audiometry In Mice," *JoVE (Journal of Visualized Experiments)*, no. 147, e59200, May 2019.

[64] A. Sumiyoshi, J. J. Riera, T. Ogawa, and R. Kawashima, "A mini-cap for simultaneous EEG and fMRI recording in rodents," eng, *NeuroImage*, vol. 54, no. 3, pp. 1951–1965, Feb. 2011.

[65] P. Mégevand, C. Quairiaux, A. M. Lascano, J. Z. Kiss, and C. M. Michel, "A mouse model for studying large-scale neuronal networks using EEG mapping techniques," *NeuroImage*, vol. 42, no. 2, pp. 591–602, Aug. 2008.

[66] S. Brenner, M. Hawkins, L. Tell, W. Hornof, C. Plopper, and F. Verstraete, *Clinical anatomy, radiography, and computed tomography of the chinchilla skull*, en, 2005.

[67] J. Martinovic, J. Mordal, and S. M. Wuerger, "Event-related potentials reveal an early advantage for luminance contours in the processing of objects," *Journal of Vision*, vol. 11, no. 7, pp. 1–1, Jun. 2011.

[68] A. C. Metting van Rijn, A. Peper, and C. A. Grimbergen, "High-quality recording of bioelectric events. Part 1. Interference reduction, theory and practice," eng, *Medical & Biological Engineering & Computing*, vol. 28, no. 5, pp. 389–397, Sep. 1990.

[69] A. C. Metting van Rijn, A. Peper, and C. A. Grimbergen, "High-quality recording of bioelectric events. Part 2. Low-noise, low-power multichannel amplifier design," *Medical & Biological Engineering & Computing*, vol. 29, no. 4, pp. 433–440, Jul. 1991.

[70] X. Li, H. Wodlinger, and Y. Sokolov, *Vivography*. [Online]. Available: https://www.otoemissions.org/old/whitepapers/signal_proc/vivography.html.

[71] A. Gramfort, M. Luessi, E. Larson, D. A. Engemann, D. Strohmeier, C. Brodbeck, R. Goj, M. Jas, T. Brooks, L. Parkkonen, and M. Hämäläinen, "MEG and EEG data analysis with MNE-Python," English, *Frontiers in Neuroscience*, vol. 7, 2013, Publisher: Frontiers.

[72] N. Bigdely-Shamlo, T. Mullen, C. Kothe, K.-S. Su, and K. A. Robbins, "The PREP pipeline: Standardized preprocessing for large-scale EEG analysis," *Frontiers in Neuroinformatics*, 2015.

[73] K. Henry and J. Lucas, "Auditory sensitivity and the frequency selectivity of auditory filters in the Carolina chickadee, Poecile carolinensis," *Animal Behaviour*, vol. 80, pp. 497–507, Sep. 2010.

[74] X. Lei and K. Liao, "Understanding the Influences of EEG Reference: A Large-Scale Brain Network Perspective," *Frontiers in Neuroscience*, vol. 11, 2017, Publisher: Frontiers.

[75] N. P. Subramaniyam, *Effect of EEG Reference Choice on Outcomes*, Mar. 2019.

[76] "Variability, Measure of," in *Encyclopedia of Research Design*, SAGE Publications, Inc., 2010.

[77] P. Price, R. Jhangiani, and I.-C. A. Chiang, "Reliability and Validity of Measurement," *Research Methods in Psychology*,

[78] N. I. of Standards and Technology, "NIST TN 1297: Appendix D1. Terminology," en, text, Nov. 2015.

[79] J. C. for Guides and Metrology, *International vocabulary of metrology — Basic and general concepts and associated terms*, 2008.

[80] L. Ferrante and R. Cameriere, "Statistical methods to assess the reliability of measurements in procedures for forensic age estimation," *International journal of legal medicine*, vol. 123, pp. 277–83, Jun. 2009.

[81] A. Subasi and M. Ismail Gursoy, "EEG signal classification using PCA, ICA, LDA and support vector machines," *Expert Systems with Applications*, vol. 37, no. 12, pp. 8659–8666, Dec. 2010.

[82] F. Artoni, A. Delorme, and S. Makeig, "Applying dimension reduction to EEG data by Principal Component Analysis reduces the quality of its subsequent Independent Component decomposition," *NeuroImage*, vol. 175, pp. 176–187, Jul. 2018.

[83] D. Veilleux-Lemieux, A. Castel, D. Carrier, F. Beaudry, and P. Vachon, "Pharmacokinetics of Ketamine and Xylazine in Young and Old Sprague–Dawley Rats," *Journal of the American Association for Laboratory Animal Science : JAALAS*, vol. 52, no. 5, pp. 567–570, Sep. 2013.

[84] P. A. Valdés-Hernández, A. Sumiyoshi, H. Nonaka, R. Haga, E. Aubert-Vásquez, T. Ogawa, Y. Iturria-Medina, J. J. Riera, and R. Kawashima, "An in vivo mri template set for morphometry, tissue segmentation, and fmri localization in rats," *Frontiers in Neuroinformatics*, vol. 5, no. 26, Nov. 2011.

[85] A. Parthasarathya and E. Bartlett, "Two-channel recording of auditory-evoked potentials to detect age-related deficits in temporal processing," *Hearing Research*, vol. 289, pp. 52–62, Jul. 2012.

[86] B. N. Buran, S. Elkins, J. B. Kempton, E. V. Porsov, J. V. Brigande, and S. V. David, "Optimizing Auditory Brainstem Response Acquisition Using Interleaved Frequencies," *Journal of the Association for Research in Otolaryngology*, vol. 21, no. 3, pp. 225–242, Jun. 2020.

[87] M. J. Polonenko and R. K. Maddox, "The Parallel Auditory Brainstem Response," *Trends in Hearing*, vol. 23, Jan. 2019.

[88] H. M. Bharadwaj, A. R. Mai, J. M. Simpson, I. Choi, M. G. Heinz, and B. G. Shinn-Cunningham, "Non-Invasive Assays of Cochlear Synaptopathy - Candidates and Considerations," *Neuroscience*, vol. 407, pp. 53–66, May 2019.

[89] K. Dougherty, H. Ginsberg, A. Mai, S. Parida, J. M. Simpson, M. G. Heinz, and H. Bharadwaj, "Non-Invasive Assays of Cochlear Synaptopathy in Humans and Chinchillas," *Assoc. for Res. in Otolaryngology Abstracts*, vol. 42, pp. 382–383, 2019.